

A Reliability Physics Model for Aging of Cable Insulation Materials

Brookhaven National Laboratory

**U.S. Nuclear Regulatory Commission
Office of Nuclear Regulatory Research
Washington, DC 20555-0001**



AVAILABILITY OF REFERENCE MATERIALS IN NRC PUBLICATIONS

NRC Reference Material

As of November 1999, you may electronically access NUREG-series publications and other NRC records at NRC's Public Electronic Reading Room at <http://www.nrc.gov/reading-rm.html>. Publicly released records include, to name a few, NUREG-series publications; *Federal Register* notices; applicant, licensee, and vendor documents and correspondence; NRC correspondence and internal memoranda; bulletins and information notices; inspection and investigative reports; licensee event reports; and Commission papers and their attachments.

NRC publications in the NUREG series, NRC regulations, and *Title 10, Energy*, in the Code of *Federal Regulations* may also be purchased from one of these two sources.

1. The Superintendent of Documents
U.S. Government Printing Office
Mail Stop SSOP
Washington, DC 20402-0001
Internet: bookstore.gpo.gov
Telephone: 202-512-1800
Fax: 202-512-2250
2. The National Technical Information Service
Springfield, VA 22161-0002
www.ntis.gov
1-800-553-6847 or, locally, 703-605-6000

A single copy of each NRC draft report for comment is available free, to the extent of supply, upon written request as follows:

Address: Office of the Chief Information Officer,
Reproduction and Distribution
Services Section
U.S. Nuclear Regulatory Commission
Washington, DC 20555-0001
E-mail: DISTRIBUTION@nrc.gov
Facsimile: 301-415-2289

Some publications in the NUREG series that are posted at NRC's Web site address <http://www.nrc.gov/reading-rm/doc-collections/nuregs> are updated periodically and may differ from the last printed version. Although references to material found on a Web site bear the date the material was accessed, the material available on the date cited may subsequently be removed from the site.

Non-NRC Reference Material

Documents available from public and special technical libraries include all open literature items, such as books, journal articles, and transactions, *Federal Register* notices, Federal and State legislation, and congressional reports. Such documents as theses, dissertations, foreign reports and translations, and non-NRC conference proceedings may be purchased from their sponsoring organization.

Copies of industry codes and standards used in a substantive manner in the NRC regulatory process are maintained at—

The NRC Technical Library
Two White Flint North
11545 Rockville Pike
Rockville, MD 20852-2738

These standards are available in the library for reference use by the public. Codes and standards are usually copyrighted and may be purchased from the originating organization or, if they are American National Standards, from—

American National Standards Institute
11 West 42nd Street
New York, NY 10036-8002
www.ansi.org
212-642-4900

Legally binding regulatory requirements are stated only in laws; NRC regulations; licenses, including technical specifications; or orders, not in NUREG-series publications. The views expressed in contractor-prepared publications in this series are not necessarily those of the NRC.

The NUREG series comprises (1) technical and administrative reports and books prepared by the staff (NUREG-XXXX) or agency contractors (NUREG/CR-XXXX), (2) proceedings of conferences (NUREG/CP-XXXX), (3) reports resulting from international agreements (NUREG/IA-XXXX), (4) brochures (NUREG/BR-XXXX), and (5) compilations of legal decisions and orders of the Commission and Atomic and Safety Licensing Boards and of Directors' decisions under Section 2.206 of NRC's regulations (NUREG-0750).

DISCLAIMER: This report was prepared as an account of work sponsored by an agency of the U.S. Government. Neither the U.S. Government nor any agency thereof, nor any employee, makes any warranty, expressed or implied, or assumes any legal liability or responsibility for any third party's use, or the results of such use, of any information, apparatus, product, or process disclosed in this publication, or represents that its use by such third party would not infringe privately owned rights.

A Reliability Physics Model for Aging of Cable Insulation Materials

Manuscript Completed: February 2005
Date Published: March 2005

Prepared by
A.J. Buslik (NRC)
T.-L. Chu, M. Subudhi, and J. Lehner (BNL)

Energy Sciences and Technology Department
Brookhaven National Laboratory
Upton, NY 11973-5000

A.J. Buslik, NRC Project Manager

Prepared for
Division of Risk Analysis and Applications
Office of Nuclear Regulatory Research
U.S. Nuclear Regulatory Commission
Washington, DC 20555-0001
NRC Job Code Y6371



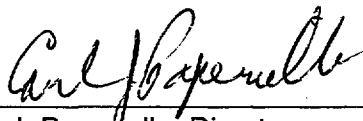
ABSTRACT

This report presents a method for predicting the probability that the insulation of an aged instrumentation or control cable inside of containment will reach a critical level of embrittlement. The critical level of embrittlement can be used to support an assessment of the probability that the cable will fail to perform its function if exposed to a loss of coolant accident (LOCA). However, there are instances where cables with severely embrittled insulation have performed their function, in tests. The method predicts the probability distribution for the time it takes for the insulation of a cable subjected to a constant dose rate and temperature to reach a critical level of embrittlement. The embrittlement level is measured by the elongation at break (EAB), a condition of the cable, the greater the EAB the less the embrittlement. In order to incorporate the results in a probabilistic risk assessment, it would be necessary to estimate the probability that a cable which has reached a critical level of embrittlement would fail to perform its intended function in a LOCA.

FOREWORD

This report was prepared jointly by the U.S. Nuclear Regulatory Commission (NRC) and Brookhaven National Laboratory under contract to the NRC. During the resolution of GSI-168, "Environmental Qualification of Low-Voltage Instrumentation and Control Cables", it was noted that the risk assessment methods for the risk due to cable aging were still evolving. This work was initiated to support the research effort that was undertaken to assess the aging of specific in-containment instrument and control (I&C) cables.

The report develops a method for estimating the probability that the insulation of an aged I&C cable inside containment would reach a critical level of embrittlement. The critical level of embrittlement can be used to support an assessment of the probability that the cable will fail to perform its function if exposed to a loss of coolant accident (LOCA). The primary failure mode of an I&C cable during a LOCA is the failure of the cable insulation, which could occur because of insulation embrittlement during normal operation, as a result of the temperature and radiation the cable is exposed to. The likelihood of this failure is reduced because of the requirements on environmental qualification of electrical equipment important to safety, as given in 10CFR50.49, "Environmental qualification of electric equipment important to safety for nuclear power plants." Moreover, there have been instances where cables that have been severely embrittled have performed their function, in tests. Note also that even if a cable fails during a LOCA, because of insulation embrittlement, the failure may have reduced risk significance if it occurs late in the LOCA. The model is applied to a number of different types of cable insulation. Before using the model in a probabilistic risk assessment (PRA), it would be necessary to estimate the probability that a cable which has reached a critical level of insulation embrittlement would fail to perform its intended function during a LOCA. The results of the PRA could then be used to identify which (if any) in-containment cable failures during LOCAs would contribute to plant risk, at a given time, because of insulation embrittlement. This requires plant operating data regarding the dose, dose rate, and temperature profile of I&C cables. Because this data is not readily available, no further work is planned at this time. Therefore, this report is issued to document the work that has been completed to date.



Carl J. Papenello, Director
Office of Nuclear Regulatory Research
United States Nuclear Regulatory Commission

CONTENTS

	Page
Abstract	iii
Foreword	v
List of Figures	viii
List of Tables	ix
Acknowledgments	xi
Acronyms	xii
1. INTRODUCTION	1
2. RELIABILITY PHYSICS METHODOLOGY	3
2.1 The Cable Resource or Capacity	3
2.2 Time-Temperature Dose Rate Shift Procedure	7
2.3 Use of IEC 1244-2 Formula for the Shift Factor	8
2.4 An Alternative Approach that Determines Parameters n, d without Interpolation	13
2.4.1 Use of Linear Regression to Estimate n and d	15
2.4.2 Use of Non-linear Regression to Estimate n and d	16
2.5 Probability Distribution of Time to Fixed Level of Degradation	17
2.6 Parameter Uncertainty	18
3. NUMERICAL RESULTS	19
3.1 Calculations Performed Using Reliability Physics Model	19
3.1.1 Calculations Performed for Different Materials	19
3.1.2 Determination of Probability Distribution of Time to a Specific Embrittlement Level for Kerite Hypalon Jacket	32
3.2 Results of No-interpolation Approach Using CPAD Data	34
3.2.1 Use of Thermal Aging Data	36
3.2.2 Combined Environment Data	38
3.2.3 Summary Discussion on No-interpolation Approach	47
3.3 Other Numerical Results Based on Reliability Physics Approach	48
3.3.1 Comparison of Different Fitting Methods	48
3.3.2 Manufacturer to Manufacturer Variability for CSPE	49
4. LIMITATIONS OF THE APPROACH	51
5. SUMMARY	53
6. REFERENCES	55
APPENDIX A: ADDITIONAL CALCULATIONS USING CPAD DATABASE	A-1
A.1 Aging Data Extracted from CPAD Database	A-6
A.2 Shifted Curves Using Temperature Superposition Method	A-32
A.3 Predictions of Reliability Physics Model	A-48
A.4 References	A-71

LIST OF FIGURES

Figure No.	Page
1 Comparison of Predictions of Reliability Physics Model of Sec. 2.3 with Test Data of Gillen for Hypalon B at a Degradation Level of 60% Relative EAB	12
2 Experimental values of log(DED) and fitted values of log(DED) vs. $-16+\log(\xi D)$, for CLPO-A ..	14
3 Experimental values of log(DED) and fitted values of log(DED) vs. $-19+\log(\xi D)$, for CLPO-B ..	14
4 Comparison of Predictions of Reliability Physics Model of Sec 2.3 with Test Data of Gillen for Hypalon B at a Degradation Level of 60% Relative EAB	23
5 Sensitivity Calculation with 22 C Data Excluded - Hypalon B (60 relative EAB)	23
6 Comparison of Predictions of Reliability Physics Model of Sec. 2.3 with Test Data of Gillen for Hypalon B at a Degradation Level of 100% Relative EAB	24
7 Comparison of Predictions of Reliability Physics Model of Sec. 2.3 with Test Data of Gillen for Hypalon C at a Degradation Level of 60% Relative EAB	24
8 Comparison of Predictions of Reliability Physics Model of Sec. 2.3 with Test Data of Gillen for Hypalon C at a Degradation Level of 100% Relative EAB	25
9 Comparison of Predictions of Reliability Physics Model of Sec. 2.3 with Test Data of Gillen for Silicone Rubber at a Degradation Level of 50% Relative EAB	25
10 Comparison of Predictions of Reliability Physics Model of Sec. 2.3 with Test Data of Gillen for Silicone Rubber at a Degradation Level of 100% EAB	26
11 Comparison of Predictions of Reliability Physics Model of Sec. 2.3 with Test Data of Gillen for ETFE at a Degradation Level of 100% EAB	26
12 Comparison of Predictions of Reliability Physics Model of Sec. 2.3 with Test Data of Gillen for EPR A at a Degradation Level of 100% EAB	27
13 Sensitivity Calculation with 22, 41, and 60 C Data Excluded-EPR A(100% EAB)	27
14 Comparison of Predictions of Reliability Physics Model of Sec. 2.3 with Test Data of Gillen for EPR B at a Degradation Level of 100% EAB	28
15 Sensitivity Calculation with 41, 60, 61, 80 C Data Excluded-EPR B (100% EAB)	28
16 Comparison of Predictions of Reliability Physics Model of Sec. 2.3 with Test Data of Gillen for CLPO A at a Degradation Level of 100% EAB	29
17 Sensitivity Calculation with 22, and 66C Data Excluded-CLPO A (100%)	29
18 Comparison of Predictions of Reliability Physics Model of Sec. 2.3 with Test Data of Gillen for CLPO B at a Degradation Level of 100% EAB	30
19 Sensitivity Calculation with 22, and 41 C Data Excluded-CLPO B (100%)	30
20 Comparison of Predictions of Reliability Physics Model of Sec. 2.3 with Test Data of Gillen for CLPO C at a Degradation Level of 100% EAB	31
21 Sensitivity Calculation with 41, and 60 C Data Excluded-CLPO B (100%)	31
22 Predicted DED to 100% EAB for Different Materials	32
23 Predicted DED vs D of Kerite CSPE Jacket (50% EAB)	33
24 Distribution of Time to 50% EAB of Kerite Hypalon Jacket C-6	34
25 Thermal Aging Data of Hypalon C	35
26 Combined Aging Data of Hypalon C	36
27 Determination of Activation Energy Using Time-Temperature Superposition	37
28 Comparison of Different Prediction Methods - 22 C and 13.7 Gy/hr	41
29 Comparison of Different Methods- 22 Degree C, 90 Gy/hr	41
30 Comparison of Different Methods- 24 Degree C, 490 Gy/hr	42
31 Comparison of Different Methods- 30 Degree C, 2140 Gy/hr	42
32 Comparison of Different Methods- 35 Degree C, 3680 Gy/hr	43

LIST OF FIGURES
(Continued)

Figure No.		Page
33	Comparison of Different Methods- 38 Degree C, 9550 Gy/hr	43
34	Comparison of Different Methods- 100 Degree C, 2140 Gy/hr	44
35	Comparison of Different Methods- 120 Degree C, 2180 Gy/hr	44
36	Comparison of Different Methods- 140 Degree C, 2120 Gy/hr	45
37	Comparison of Different Prediction Methods - DED vs D (Hypalon C)	46
38	Comparison of Different Fitting Methods	49
39	Comparison of Different CSPEs	50

LIST OF TABLES

Table No.		Page
1	Estimated Parameters of Different Materials at EAB of 60% Relative and 100% Absolute	20
2	Estimated Weibull Parameters of h_0 and Times to 50% EAB of Kerite Hypalon Jacket	34
3	Comparison of Predictions with Original Data	39
4	Estimated Parameters of Hypalon C Using Different Fitting Methods	49
5	Summary of Calculations of CSPEs of Different Manufacturers	50

ACKNOWLEDGMENTS

The authors wish to acknowledge helpful discussions with Dr. Mow Lin and Dr. Ming-Shih Lu. The authors also wish to thank J. Frejka and A. Seda for their excellence in the preparation of this report, and C. Conrad for preparing the figures.

ACRONYMS

BNL	Brookhaven National Laboratory
CLPO	Cross Linked Polyolefins
CPAD	Computerized Polymer Aging Database
CSPE	Chlorosulfonated Polyethylene
DED	Dose to Equivalent Degradation
DLO	Diffusion-Limited Oxidation
EAB	Elongation at Break
EPDM	Ethylene Propylene Diene Monomer
EPR	Ethylene Propylene Rubber
ETFE	Ethylene Tetrafluoroethylene Copolymer
IAEA	International Atomic Energy Agency
I&C	Instrumentation and Control
IEC	International Electrotechnical Commission
LOCA	Loss of Coolant Accident
PRA	Probabilistic Risk Assessment
PVC	Polyvinyl Chloride
Rsquare	Coefficient of Determination
SNL	Sandia National Laboratories

1. INTRODUCTION

This report develops a method for estimating the probability that the insulation of an aged instrumentation and control (I&C) cable inside containment would reach a critical level of embrittlement. The critical level of embrittlement can be used to support an assessment of the probability that the cable will fail to perform its function if exposed to a loss of coolant accident (LOCA). Note that there are instances where cables that have been severely embrittled have performed their function in tests (see pages 6-3 and 7-8 of Reference 1). The reason for focusing on cables inside of containment is that they are liable to a potential common mode failure mechanism, since cables associated with redundant trains of a system are exposed to the same or similar harsh environment after a LOCA. The reason for focusing on instrumentation and control cables as opposed to power cables is that instrumentation and control cables are more sensitive to leakage currents, which could cause misleading operation indications, and failure of automatic actuation of equipment. The method assumes that the predominant mode of failure of the cable is related to insulation embrittlement. The case of bonded jacket cables will not be discussed. The method explicitly takes into account the synergistic effects caused by temperature and dose rate. For those instrumentation cables that operate at high voltages (1000 volts or more), i.e., those for radiation and neutron monitoring, the voltage acts as an additional stressor, and the method may not be applicable. In addition, cables that operate at high voltages frequently have mineral insulation, and the method of this report is only valid for polymer insulation. Although it would have been desirable to consider the behavior of the cable during the LOCA, this is beyond the scope of this report, because of resource limitations. In addition, for multiconductor cables, failure modes associated with differential expansion of the jacket and insulation due to moisture absorption during a LOCA were not considered. The method predicts the probability distribution for the time it takes for the insulation of a cable subjected to a constant dose rate and temperature to reach a critical level of embrittlement. The embrittlement level is measured by the elongation at break (EAB) of the cable. Some of the basic ideas of the method are presented in Reference 2. Similar to the reliability physics model developed for flow-accelerated corrosion in Reference 3, the model developed in this study could be used to estimate the probability of cable failures as a function of age, which could be incorporated into a probabilistic risk assessment (PRA). However, it would first be necessary to estimate the probability a cable with a critical level of insulation embrittlement would fail, given a LOCA.

2. RELIABILITY PHYSICS METHODOLOGY

As noted in the introduction, we are going to use the EAB of the cable insulation as a measure of the embrittlement of the cable insulation. If the cable insulation is sufficiently embrittled, then the cable insulation may crack during a LOCA, and leakage currents, either between two conductors within the same cable, or between the conductors and ground, can occur with misleading instrument indications occurring if the cable is an instrumentation cable, and possible loss of actuation of controlled devices for a control cable. We note, however, that the cable insulation may not crack during a LOCA even if severely degraded, if forces on the cable do not physically move the cable during the LOCA.

The dominant chemical reactions which result in the aging of cable insulation are oxidation reactions. Free radicals are formed, either by thermal decomposition of the polymer comprising the cable insulation, or by the action of radiation. These free radicals initiate chain reactions in the polymer, which involve oxygen (for cables in an oxygen-containing atmosphere). These reactions lead to the production of degradation products and the change in material properties of the cable insulation. (If cable insulation polymers are not in an oxygen-containing environment their degradation is typically much less rapid.) For a cable in an oxygen-containing environment, the surface of the insulation will first react with the oxygen. In order for the oxygen to react with the polymer in deeper layers of the insulation, the oxygen must first diffuse into the polymer. If the radiation dose rate is sufficiently high the reaction rate in the interior of the cable insulation will be limited by the rate of oxygen diffusion. Thus a greater time, and therefore a greater dose, will be required to reach a given level of degradation in the interior of the cable than on the surface. This phenomenon is called diffusion-limited oxidation (DLO). Since EAB depends on the level of degradation throughout the entire cross-section of the cable insulation, the EAB for a given dose rate and total dose will be higher if DLO is present than it would be otherwise. During service conditions the dose rates are lower, and one does not expect DLO. Therefore, care must be taken when setting up experimental conditions where dose rates may be such that DLO is present. If DLO is present, it may not be possible to use the results of the experiment to infer the behavior of cable insulation during service conditions.

DLO represents one type of dose-rate effect. Even in the absence of DLO, the amount of degradation experienced by cable insulation may depend not only on the total dose, but also on the dose rate. If the rate limiting step in the chemical kinetics is not the initiation step but another step in the chain of chemical reactions, then dose rate effects will be present. These are known as chemical dose rate effects. References 4 and 5 provide more discussions on the DLO and chemical dose rate effects. In the methods given in this report, it will be assumed that the dose rate effects are due to chemical dose rate effects, and that any experimental points which are affected by DLO have been discarded. This increases the likelihood that the experimental data can be applied to service conditions inside the containment of the nuclear plant.

2.1 The Cable Resource Or Capacity

We are interested in determining the probability that a cable inside of containment will reach a critical level of embrittlement. This probability will depend primarily on the temperature T and dose rate D that the cable is exposed to during normal plant operation, and the time of exposure t to these conditions. If a LOCA occurs after the cable insulation reaches a critical level of embrittlement, as measured by the EAB of the cable, the cable may fail to perform its function, although, as already noted, cables with severely embrittled insulation have performed successfully in environmental qualification tests. The problem being dealt with then is estimating the probability distribution $P_A(t)$ that, at time t , the cable insulation has a level of embrittlement greater than or equal to a critical level of embrittlement. The particular model we are using is one in which the cable insulation is assumed to have an initial capacity (or resource) H_{00}

(corresponding to the unaged condition) which is degraded by the aging stressors T and D. If the rate of degradation is R (T, D), then at time t the capacity h is given by

$$h=H_{00}-tR(T,D) \quad (2.1-1)$$

All indices of degradation, such as EAB, are assumed to be functions of h, and uniquely determined by h.

The initial resource H_{00} is assumed to be a random variable. The randomness in H_{00} comes from variation in the properties of the unaged cable.

The model being used is equivalent to the simple wear model described by Carfagno and Gibson (Ref. 6) (see Section 8.2.1 of Reference 6). Carfagno and Gibson treat a vector of stressors S, and use the notation K(S) to represent the rate of degradation of resource. In our case the stressors are (T, D), the temperature and dose rate, and we use the notation R instead of K. According to Equation 8-17 of Reference 6, the probability density function for $h(t)+K(S)t$ is independent of t. By putting $t=0$, and denoting the resource h at time t by h_{00} , one obtains the result that the probability density function for $h(t)+K(S)t$ is the same as the probability density function for h_{00} . This means that for any questions involving probabilities, one can set $h(t)+K(S)t = h_{00}$. In other words, $h(t)=h_{00}-K(S)t$, which is equivalent to our Equation 2.1-1, since K(S) in our case is given by R(T,D).

We are interested in the time to reach some critical level of degradation h_{crit} . From

$$h_{crit} = H_{00} - tR(T,D), \quad (2.1-2)$$

we see that since H_{00} is a random variable, and h_{crit} and R(T,D) are non-random, that t is a random variable whose probability distribution is determined by that for H_{00} .

Let us consider the form of the probability distribution for H_{00} . We have defined the resource as applying to a particular cable length. However, we can think of the particular cable as made up of many small segments, each of which has a particular value of the resource. The resource varies randomly along the cable length, since the composition of the insulation has variability along the cable. What determines the resource, or resistance to degradation, of the particular cable length is the lowest value of the resource at any point along the cable, since this will determine the probability of a cable of specific age t reaching a critical resource level, and hence critical EAB, at some point along the cable. If the cable reaches a critical EAB at some point along the cable, then the cable insulation may crack at that point during a LOCA, and the cable may fail because of leakage currents. The problem of determining the probability distribution is then directly analogous to the problem of determining the probability distribution for the failure of a chain of links, where the chain fails if any of its links fails. The solution of this problem is that the probability distribution is a Weibull distribution, and consequently we assume a Weibull distribution for H_{00} .

This Weibull distribution for H_{00} will depend on the length of the cable. This is of some importance since EAB measurements are generally made on small samples of about 5.08 centimeters (two inches) in length, while the length of a cable which may be exposed to high temperature (or dose rate) and, therefore, be vulnerable to embrittlement, may be about 3.05 meters (10 feet) in length.

Consider the Weibull distribution for a cable of unit length. Denote by $H_{00}(1)$ the initial resource of this cable. Construct a cable N units in length from these cables of unit length, and denote by $H_{00}(N)$ the initial resource of this cable. The initial resource of this cable of N units in length is the least value of resource of any of the units making up its length. Each unit of length is assumed to be independent from

the other units, and all units have the same probability distribution for their resource capacity. The probability $G(h;1)$ that $H_{00}(1)$ exceeds some value h is given by a Weibull distribution. We denote by γ_h , η_h , and β_h the location, scale, and shape parameters of this distribution, respectively. Then

$$G(h;1) = \Pr\{H_{00}(1) > h\} = e^{-(h-\gamma_h)/\eta_h)^{\beta_h}} \text{ for } h \geq \gamma_h \text{ and unity otherwise.} \quad (2.1-3)$$

For the cable N units in length, the resource will exceed h if and only if all units making up the cable exceed h . Then

$$G(h;N) = G(h;1)^N = e^{-N(h-\gamma_h)/\eta_h)^{\beta_h}}, \text{ for } h \geq \gamma_h \text{ and unity otherwise.} \quad (2.1-4)$$

which shows that a cable N units in length has the same shape factor and location parameter as the cable of unit length, but that the scale factor for cable of length N (call it $\eta_h(N)$) is related to the scale factor for the cable of unit length by

$$\eta_h(N) = \frac{\eta_h}{N^{1/\beta_h}}, \quad (2.1-5)$$

so that as the cable becomes longer and longer the distribution becomes more and more peaked, and for very long cables the probability of a resource greater than γ_h is very small.

Let us now consider the probability distribution for $P_f(t)$. The cable will be liable to failure from insulation embrittlement if the resource h at time t is less than the value h_{crit} . Then

$$1 - P_f(t) = \Pr\{h > h_{crit}\} = \Pr\{H_{00} - t R(T,D) > h_{crit}\} = \Pr\{H_{00} > h_{crit} + t R(T,D)\}, \quad (2.1-6)$$

where Equation 2.1-1 has been used. From Equations 2.1-3 and 2.1-6, one has, for a cable of unit length,

$$1 - P_f(t) = \exp(-((h_{crit} + t R(T,D) - \gamma_h)/\eta_h)^{\beta_h}), \text{ for } h_{crit} + t R(T,D) - \gamma_h \geq 0 \text{ and unity otherwise.} \quad (2.1-7)$$

Some algebraic manipulations on the argument of the exponential function lead to

$$1 - P_f(t) = \exp(-(t - \gamma_t)/\eta_t)^{\beta_t}), \text{ for } t - \gamma_t \geq 0, \text{ and unity otherwise.} \quad (2.1-8)$$

where

$$\gamma_t = (\gamma_h - h_{crit})/R(T,D), \quad \eta_t = \eta_h/R(T,D), \text{ and } \beta_t = \beta_h. \quad (2.1-9)$$

Thus the parameters for the Weibull distribution for $P_f(t)$ are obtained. The scale parameter for the distribution $P_f(t)$ is the scale parameter for the resource h divided by $R(T,D)$. The shape parameter is the same as the shape parameter for the resource h . The location parameter has a translation and a scale factor applied to it.

Connection with the Constant Wearout Method of Gillen

The fact that the degradation is assumed to be of the form $tR(T,D)$ is equivalent to the constant wear out assumption of Reference 7. A more general form of the degradation in resource would be a general function $f(t,T,D)$ instead of the form $tR(T,D)$. If the form $tR(T,D)$ for the degradation in resource holds, then, if one exposes a cable to a temperature T_1 and dose rate D_1 for a time t_1 , and then exposes the cable to a temperature T_2 and dose rate D_2 for a time t_2 , the degradation in resource will be

$$t_1 R(T_1, D_1) + t_2 R(T_2, D_2) = \Delta h. \quad (2.1-10)$$

which is linear in t_1 and t_2 . Suppose furthermore that T_1, D_1 correspond to operating temperature and dose rate, and T_2, D_2 correspond to some accelerated temperature, and the dose rate used at this temperature. Choose Δh to correspond to the amount of degradation to reach some critical level of degradation (such as 50 percent absolute EAB), neglecting random variation in the initial value of the resource. (The treatment of the random variation will be made more precise later in this section.) We can solve Equation 2.1-10 for t_1 in terms of t_2 , obtaining

$$t_1 = a - b t_2, \text{ where } a = \Delta h / R(T_1, D_1) \text{ and } b = R(T_2, D_2) / R(T_1, D_1) \quad (2.1-11)$$

Therefore, if we obtain two sets of values of (t_1, t_2) by exposing a cable to plant conditions for two different times, and for each case finding the amount of time t_2 necessary to complete the aging to the given degree of degradation at the accelerated aging conditions, one has sufficient information to determine the constants a and b , and then to determine the time at plant conditions to reach the critical level of degradation, by using Equation 2.1-10 with $t_2 = 0$. In practice, several sets of values (t_1, t_2) are obtained and a line of best fit is obtained. By obtaining several sets of values of (t_1, t_2) , one can also test the hypothesis of constant wearout, by seeing how well the set of points (t_1, t_2) fit on a straight line. This is equivalent to Gillen's constant wearout procedure, although Gillen discusses explicitly only the case where the dose rates are equal to zero. Thus the assumption that the amount of degradation depends on t, T, D in the form $tR(T, D)$ implies Gillen's constant wearout procedure. Moreover, if we apply Gillen's constant wearout procedure and obtain values for a and b , then one obtains $R(T_1, D_1) = \Delta h / a$ and $R(T_2, D_2) = b R(T_1, D_1)$, so that, given Δh , one has the values of $R(T_1, D_1)$ and $R(T_2, D_2)$. The value of Δh can be chosen arbitrarily because the resource h is determined only up to a linear transformation. If h is a possible resource function, then we see that a linear function of h also satisfies Equation 2.1-1 and is a possible resource function.

Rudd (Ref. 8) calls this type of behavior type 1 superposition. As noted by Gillen (Ref. 7), not all materials exhibit constant wear out behavior.

So far, we have neglected the random variation in the initial resource of the polymer H_{00} , in describing the constant wear-out method. Let us now consider the random variation. The polymer is aged for a specific (non-random) time t_1 at T_1, D_1 , and then the aging is completed at T_2, D_2 until a specific degree of degradation h_{crit} is reached. The time t_2 needed to reach a specific degree of degradation will be a random variable, since the initial resource is a random variable. In fact, one has, from Equation 2.1-1, $h = H_{00} - t_1 R(T_1, D_1)$ and $h_{crit} = h - t_2 R(T_2, D_2)$, so that

$$H_{00} - \tau_1 R(T_1, D_1) - t_2 R(T_2, D_2) = h_{crit} \quad (2.1-12)$$

where τ_1 has been written for t_1 to emphasize that it is not a random variable in this discussion. The quantity h is a random variable, which plays the role of the initial value of the resource for the aging which occurs at T_2, D_2 .

If one takes expected values in Equation 2.1-12, denoting expected values by the brackets $\langle \dots \rangle$, then one obtains

$$\tau_1 R(T_1, D_1) + \langle t_2 \rangle R(T_2, D_2) = \langle H_{00} \rangle - h_{crit} = \Delta h. \quad (2.1-13)$$

Comparing Equation 2.1-10 to Equation 2.1-13, one sees that when random variation is considered the time t_2 in the constant wearout method is really the expected value of t_2 , and t_1 is a fixed number, determined by when the aging at normal service conditions is stopped.

In certain cases, the assumption of constant wearout behavior can be relaxed, and results for the probability distribution for the time to reach a critical level of embrittlement can still be obtained. In other words, the assumption that the rate of degradation of the resource is constant may be relaxed, and the amount of degradation in time t need not be assumed to be of the form $tR(T,D)$. This is discussed further in Section 2.3.

2.2 Time-Temperature Dose Rate Shift Procedure

Gillen & Clough (Ref. 9) have introduced a time-temperature dose rate procedure. When this procedure is valid for a given material, the dose to equivalent degradation (DED) for a dose rate D at a temperature T is equal to the DED for a dose rate D_0 (the shifted dose rate) at a reference temperature T_0 provided the relationship

$$\exp(\beta E) D = \exp(\beta_0 E) D_0, \quad (2.2-1)$$

holds, where $\beta=1/k_B T$, $\beta_0=1/k_B T_0$, k_B is the Boltzmann constant, and E is an activation energy. In other words, the dose to equivalent degradation is a function of temperature and dose rate only in the combination of $\exp(\beta E) D$. Rudd (Ref. 8) calls this type of behavior type 2 superposition. (Hopefully, the dual use of β as the shape parameter of the Weibull distribution and the reciprocal temperature (in energy units) will not occasion any confusion.)

The time temperature dose rate shift procedure can be derived from a dimensional analysis argument, on the assumption that the chemical kinetics is dominated by a single rate parameter, $k_R(T)$, with T being the temperature. Let P be the mass of degradation product produced, per unit mass of polymer. The degradation products are produced by chemical reactions initiated either thermally or by radiation. P is a measure of the degree of degradation of the polymer. Then P will be a function of the time t , the dose rate D , and the rate parameter $k_R(T)$, which is a function of temperature T . We, therefore, write

$$P = f(D, t, k_R(T)) \quad (2.2-2)$$

Let us take as our fundamental units the units of velocity, mass, and time. P is dimensionless. The dose rate D has units of energy per unit mass per unit time, or units of velocity squared per unit time. The rate constant $k_R(T)$ has units of inverse time. Hold the units of velocity and mass fixed, and consider how Equation 2.2-2 changes if the units of time are multiplied by a factor λ . The numerical value of P remains unchanged. The numerical values of D and $k_R(T)$ are each multiplied by a factor of λ , while the numerical value of t is divided by λ . If D' , P' , $k_R'(T)$, and t' represent the new numerical values of D , P , $k_R(T)$, and t after the units of time are multiplied by λ , then

$$D' = \lambda D \quad (2.2-3a)$$

$$P' = P \quad (2.2-3b)$$

$$k_R'(T) = \lambda k_R(T) \quad (2.2-3c)$$

$$t' = t/\lambda \quad (2.2-3d)$$

The form of Equation 2.2-2 cannot depend on the units used to represent the time and hence must remain valid with the primed variables substituted for the original variables. Then

$$P'=f(D',t',k_R'(T)) \quad (2.2-4)$$

or, using Equations 2.2-3,

$$P=f(\lambda D, t/\lambda, \lambda k_R(T)) \quad (2.2-5)$$

Choose $\lambda=1/k_R(T)$. Then

$$P=f(D/k_R(T), t k_R(T), 1) \quad (2.2-6)$$

Thus P is a function of only the two variables $D/k_R(T)$ and $t k_R(T)$. We can solve Equation 2.2-6 for $t k_R(T)$ in terms of $D/k_R(T)$ and P.

$$t k_R(T) = g(D/k_R(T), P) \quad (2.2-7)$$

For a fixed level of degradation P is a constant. Moreover, the dose to equivalent degradation corresponding to this fixed level of degradation is Dt . Then, multiplying Equation 2.2-7 by $D/k_R(T)$ one obtains

$$DED= (D/k_R(T)) g(D/k_R(T), P) \quad (2.2-8)$$

which shows that DED is a function of the single variable $D/k_R(T)$, for a fixed level of degradation (fixed P). If $k_R(T)$ has Arrhenius behavior, $k_R(T) \sim \exp(-\beta E)$, then DED is a function of $D \exp(-\beta E)$ only, for fixed degradation level, which gives the Gillen & Clough time-temperature-dose-rate superposition property. Note that one can have time-temperature-dose rate superposition even if the material exhibits non-Arrhenius behavior. In such cases, $k_R(T)$ would not have an Arrhenius form. One can always write

$$k_R(T)= A \exp(-\beta E(\beta)), \quad (2.2-9)$$

where A is a constant, and $E(\beta)$ is a temperature dependent effective activation energy. In certain cases, the effective activation energy changes smoothly between two asymptotes, the one asymptote being the value of the activation energy at high temperature and the other asymptote being the value of the activation energy at low temperature. Gillen et al. (Ref. 10) discuss this and show that such behavior occurs for an Ethylene Propylene Diene Monomer (EPDM) material, with a high temperature asymptote for the activation energy of 118 kJ/mol (1.22 eV/molecule), and a low temperature asymptote of 82 kJ/mol (0.85 eV/molecule).

2.3 Use of IEC 1244-2 Formula for the Shift Factor

The International Electrotechnical Commission (IEC) Technical Report IEC 1244-2 (Ref. 11) on the determination of long-term radiation aging in polymers gives a procedure for determining the time to a given damage level for a polymer from the temperature and dose rate it is subjected to. The procedure defines an empirical shift factor $a(T,D)$ which relates the time $t(T,D)$ to reach a given damage level at temperature T and dose rate D to the time $t(T_0, D=0)$ it would take to reach the given damage level at a reference temperature T_0 and a dose rate of zero. These times are related to each other, and to the shift factor $a(T,D)$, by

$$t(T,D) = t(T_0, D=0) / a(T,D). \quad (2.3-1)$$

The quantity $a(T,D)$ is called a shift factor because it represents a translation, or shift, if a logarithmic scale is used for the time to reach a given damage level. The times here are non-random, and correspond, as will be seen later, to expected values of the corresponding random times. In the IEC 1244-2 formulation, one is interested in obtaining a point estimate of the lifetime of the polymer under given conditions of temperature and dose rate, and one does not consider the random variations in the lifetime. In the notation we will be using the empirical formula for the shift factor (Equation 3 of Section 3.3 of IEC 1244-2) is given by

$$a(T,D) = e^{-(\beta-\beta_0)E} (1 + kD)^n e^{n(\beta-\beta_0)E} \quad (2.3-2)$$

Here n is used for the parameter x in IEC 1244-2, and, as before, we have used β for the reciprocal temperature in energy units; the subscript 0 refers to the reference conditions. The parameters n and k are determined from experimental data. The Arrhenius energy E is determined, according to IEC 1244-2 from pure thermal aging. It appears from IEC 1244-2, and the method used to determine the values of k and n there (see Figure 12 of IEC 1244-2, and the accompanying discussion on p. 19), that the constants k and n are assumed to be independent of the level of degradation.

In Equation 2.3-2, the constants k and n could depend on the reference temperature, but the form of Equation 2.3-2 cannot depend on the reference temperature, if the procedure is to be valid. Let us make use of this invariance of the form of the expression for $a(T,D)$ to the choice of the reference temperature to determine the dependence of k on the reference temperature, and to show that n is independent of the reference temperature. Define $a(T,D;T_1)$ as the shift factor if T_1 is used as the reference temperature, and $a(T,D;T_0)$ as the shift factor if T_0 is used as the reference temperature. Then, we have, on the one hand, from Equation 2.3-1, using T_1 as the reference temperature,

$$t(T_1, D) = t(T_1, 0) / a(T_1, D; T_1), \quad (2.3-3)$$

while, on the other hand, using T_0 as the reference temperature,

$$t(T_1, D) = t(T_0, 0) / a(T_1, D; T_0) \quad (2.3-4)$$

From Equations 2.3-1 and 2.3-2, one has for $T=T_1$ and $D=0$,

$$t(T_1, 0) = t(T_0, 0) / a(T_1, 0; T_0) = t(T_0, 0) / \exp(-(\beta_1 - \beta_0)E), \quad (2.3-5)$$

which is just the usual Arrhenius relation connecting times to reach the same level of degradation at two different temperatures. Using Equation 2.3-5 in Equation 2.3-3 and comparing to Equation 2.3-4, one sees that

$$\exp(-(\beta_1 - \beta_0)E) a(T_1, D; T_1) = a(T_1, D; T_0) \quad (2.3-6)$$

Use n_0, k_0 for the constants n, k corresponding to reference temperature T_0 , and n_1, k_1 for the constants corresponding to reference temperature T_1 . Then, using Equation 2.3-2 in Equation 2.3-6, one obtains

$$e^{-(\beta_1 - \beta_0)E} (1 + k_1 D)^{n_1} = e^{-(\beta_1 - \beta_0)E} (1 + k_0 D)^{n_0} e^{n_0(\beta_1 - \beta_0)E} \quad (2.3-7)$$

or, simplifying,

$$k_1 D^{n_1} = k_0 D^{n_0} e^{n_0(\beta_1 - \beta_0)E} \quad (2.3-8)$$

By taking logarithms of both sides of Equation 2.3-8, one obtains an equation of the form

$$(n_1 - n_0) \log(D) = \text{const}, \quad (2.3-9)$$

where const is independent of D. This can only be true for all D (or even for two distinct values of D) if $n_1 = n_0$. Putting the common value of n_1 and n_0 equal to n , one sees from Equation 2.3-8 that

$$k_1 e^{-n\beta_1 E} = k_0 e^{-n\beta_0 E} \quad (2.3-10)$$

Thus n and $d \equiv k_0 \exp(-n\beta_0 E)$ are independent of the reference temperature used. Using this in Equation 2.3-2 and substituting the result in Equation 2.3-1, one obtains

$$t(T, D) = \frac{t(T_0, 0) e^{-\beta_0 E}}{e^{-\beta E} (1 + d D^n e^{n\beta E})} \quad (2.3-11)$$

The numerator of the right hand side of Equation 2.3-11 is independent of T_0 by Equation 2.3-5 and is a measure of the amount of degradation of the polymer. Comparing Equation 2.3-11 with Equation 2.1-1, we see that the amount of degradation of the polymer (difference in the initial resource and the resource h) can be identified with $H_{00} - h$, for a fixed final level of degradation h , and one can identify $e^{-\beta E} (1 + d D^n e^{n\beta E})$ with $R(T, D)$, so that Equation 2.3-11 reads

$$t(T, D) R(T, D) = \Delta H, \quad (2.3-12)$$

where $\Delta H = H_{00} - h$, and

$$R(T, D) = e^{-\beta E} (1 + d D^n e^{n\beta E}) \quad (2.3-13)$$

which gives us an expression for $R(T, D)$ from the IEC 1244-2 approach described above. We note that the expression for $R(T, D)$ is consistent with Gillen's time-temperature dose rate superposition method, as can be seen as follows. From Equations 2.3-12 and 2.3-13, one has

$$DED = D t(T, D) = D_s \Delta H / (1 + d D_s^n), \text{ where } D_s = D \exp(\beta E), \quad (2.3-14)$$

which shows that the expression for DED is a function of D_s only, and, therefore, obeys Gillen's time temperature dose rate superposition rule. Note from Equation 2.3-13 that the rate of degradation is composed of the sum of two parts, a part representing thermal degradation, and a part representing degradation initiated by radiation. In the limit where the dose rate approaches zero, the formula for $R(T, D)$ approaches the formula for pure thermal degradation consistent with the Arrhenius law. The part representing the radiation aging corresponds to the power law of radiation aging, as described in IEC 1244-2 on page 13ff. The power law is valid only when thermal aging is negligible, or, in other words for sufficiently high dose rates. One sees from Equation 2.3-14 that for large values of the dose rate D that DED is proportional to $D^{(1-n)}$, which gives the power law (the notation in IEC-1244-2 uses n where we use $1-n$).

As we have defined $t(T, D)$, $t(T, D)$ is a random variable since H_{00} is a random variable, and hence ΔH is, so that, from Equation 2.3-12, $t(T, D)$ is a random variable. ($R(T, D)$ has no randomness, in our formulation, although the parameters d and n appearing in Equation 2.3-13 will be estimated from data

and will have state of knowledge uncertainties.) However, in the IEC 1244-2 formulation, t is thought of deterministically, in the same way we may talk of the lifetime of a cable deterministically. We can identify the expected value of t , $\langle t \rangle$, with the deterministic lifetime (to a fixed level of degradation) t , of IEC 1244-2.

Let us consider the limits on the values of the parameters n and d in Equation 2.3-13 for $R(T,D)$.

From IAEA-TECDOC-1188, vol. II, p. 73 (Ref. 12), the parameter $(1-n)$ (called n in the IAEA-TECDOC) usually takes values from 0 to 0.3, or, in other words, n usually takes values between 0.7 and 1.0. In general, when the chemical kinetics equations are dominated by unimolecular termination, then one would expect n to be close to unity, as Gillen & Clough found for Polyvinyl Chloride (PVC) (Ref. 13), but if bimolecular termination dominates, then n would be lower. For pure bimolecular termination one would expect, from the work of Bolland (Ref. 14), that n would equal 0.5, since the overall rate of degradation by oxidation is found by him to be proportional to the square root of the initiation rate, and the initiation rate would be proportional to the radiation dose rate. Thus one would expect n generally to be between 0.5 and 1. In practice, values of n that are empirically determined sometimes slightly exceed unity, although it is not clear what would happen at very high dose rates. As far as the parameter d is concerned, one sees from Equation 2.3-13 that negative values of d correspond to a decrease in aging with increase in dose rate, which is non-physical.

Note that the general formulation given in IEC 1244-2 implies that n and d are independent of the degree of degradation. However, empirically, one can allow n and d to depend on the level of degradation h . If then one was interested in a particular level of degradation, such as that which corresponds to a critical level of degradation, one could determine n and d for that level of degradation, provided experimental data existed for that level of degradation. If n and d depend on the level of degradation, or, equivalently, on the change ΔH of the resource, then ΔH is not expressible in the form $tR(T,D)$, with $R(T,D)$ independent of ΔH . If n and d are dependent on ΔH , then the Equation 2.3-13 for $R(T,D)$ depends on ΔH . If we denote this dependence explicitly by writing $R(T,D;\Delta H)$, then Equation 2.3-12 becomes

$$tR(T,D;\Delta H)=\Delta H. \quad (2.3-15)$$

We can in principle solve this equation for ΔH as a function of t , T , and D :

$$\Delta H= f(t, T, D), \quad (2.3-16)$$

and one does not in general have ΔH in the form $tR(T,D)$, with $R(T,D)$ independent of ΔH . This means that the rate of degradation (rate of increase of ΔH) is not independent of time, in a model where n and d depend on ΔH .

If data is available, one can use a model where E is not constant, but temperature dependent, if the material under study is non-Arrhenius, and there is a sufficient amount of data to determine the energy dependence of E . This is discussed further later in this section.

Numerical Estimation of the Parameters n and d from Data

Gillen & Clough (Ref. 9) have tested time-temperature-dose rate superposition on several materials, and it is possible to test how well the formula for $R(T,D)$ given in Equation 2.3-13 holds, for the cases where time temperature dose rate superposition holds. From Gillen's data, experimental values of t_i corresponding to particular dose rates and temperatures D_i , and T_i can be obtained. A least squares

procedure was used to estimate n and d. Here, for brevity, denote the expected value of the quantity ΔH in Equation 2.3-13 or Equation 2.3-14 by h_0 . Then the least squares procedure used was to minimize

$$S = \sum_i (h_0 - h_i)^2, \quad (2.3-17)$$

where

$$h_i = t_i R(T_i, D_i) = t_i e^{\beta_i E} (1 + d e^{n \beta_i E} D_i^n) \quad (2.3-18)$$

Inspection of Equations 2.3-17 and 2.3-18 show that for fixed n the parameters d and h_0 appear linearly. Therefore, a linear regression technique can be used, to minimize S for fixed n and then varying n to find the overall minimum. This procedure was followed for hypalon-B, using the 60% relative EAB data of Figure 6 of Gillen (Ref. 9). The results obtained are compared to the experimental data in Figure 1; the abscissa is the shifted dose rate, $D_0 = D \exp((\beta - \beta_0)E) = D_s \exp(-\beta_0 E)$, where β_0 corresponds to the reference temperature of 45 degrees C. For a cable environment temperature of 45 degrees C, the DED corresponding to a particular dose rate can be read directly from Figure 1. Of course, the DED corresponding to a given dose rate D, as given by Equation 2.3-14, is independent of the reference temperature used. If a reference temperature T_1 were used, with a corresponding $\beta_1 = 1/(k_B T_1)$, then the shifted dose rate $D_1 = D_s \exp(-\beta_1 E)$ is related to D_0 by

$$\ln(D_1) = \ln(D_0) + (\beta_0 - \beta_1)E. \quad (2.3-19)$$

Comparison to Gillen Data for Hypalon B, 60% Relative EAB

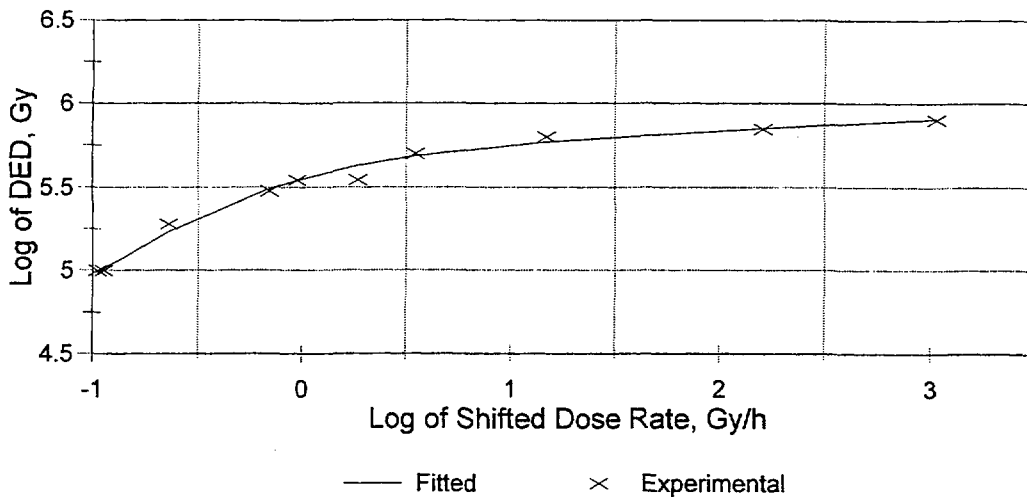


Figure 1 Comparison of Predictions of Reliability Physics Model of Sec 2.3 with Test Data of Gillen (Ref. 9) for Hypalon B at a degradation level of 60% relative EAB

Note: The values of the constants in Equation 2.3-14 are $n=9335$, $d=7.544E-14$, $h_0=\Delta H=4.187E-9$. Time-temperature dose rate superposition is assumed, with an activation energy of $E=0.912$ eV and a shifted temperature of 45 degrees C.

This means that, in Figure 1, the use of a reference temperature T_1 instead of T_0 corresponds to a horizontal translational shift of the prediction curve and the data by an amount proportional to $(\beta_0 - \beta_1)E$, since the horizontal axis is a log (to base 10) scale. As an example, if a reference temperature of 22 degrees C, instead of 45 degrees C, were used in Figure 1, then any abscissa point x should be relabeled $x - 1.1265$, since $(\beta_0 - \beta_1)E \log(e) = -1.1265$, for this case.

A Temperature-Dependent Activation Energy Approach for Modeling Non-Arrhenius Behavior

In certain cases, materials with non-Arrhenius behavior can be treated by using a modification of Equation 2.3-14 for DED as a function of D_s . In fact, the same formula holds with a different definition of D_s . In Section 2.2, we showed that time temperature dose rate superposition can hold, even for non-Arrhenius materials, and that in these cases DED was a function of the single parameter $D/k_R(T)$, with $k_R(T) = A \exp(-\beta E(\beta))$. One can, therefore, consider an extension of Equation 2.3-14 where D_s is replaced by $D/k_R(T)$, or, more simply, and equivalently, by $D \exp(\beta E(\beta))$. In cases where $E(\beta)$ varies smoothly with energy, having one asymptotic value at high temperature, and a lower asymptotic value at lower temperatures, one can try an effective activation energy of logistic form,

$$E(\beta) = E_B + (E - E_B) / (1 + \exp(K(\beta - \beta_m))) \quad (2.3-20)$$

Here E_B = the limiting value of $E(\beta)$ for large β (small T), E is the limiting value of $E(\beta)$ for small β (large T), K is a constant with dimensions of energy, and β_m is a midpoint value of β such that $E(\beta_m) = \frac{1}{2}(E + E_B)$.

This procedure was applied to the data for CLPO-A (Cross Linked Polyolefins) and CLPO-B given in Reference 15. Although the usual time temperature dose rate superposition method with a constant activation energy did not work well, the use of a temperature dependent activation energy, as described here, gave reasonable agreement. The results are given in Figures 2 and 3.

2.4 An Alternative Approach That Determines Parameters n , d without Interpolation

The approach described in Section 2.3 assumes that aging data for a specified level of degradation, i.e., EAB of 100% or 60% relative, is available, as is the case in many of Gillen's publications (Refs. 9 and 14). This form of data was obtained by interpolation of the original data that corresponds to different damage levels. The Cable Polymer Aging Database (CPAD) (Ref. 16) contains cable aging data from many different sources including the work of Gillen, and has the data in a rawer format. For each material, two types of aging data, thermal aging and combined environment aging, are tabulated separately. For each of the aging environments, the duration of aging and the material property at the end of the test, e.g., EAB and modulus, are also listed. Using the data in this format, an alternative approach for estimating the parameters of the aging model was developed.

In this approach, both thermal-only and combined aging data are used in estimating the parameters of Equation 2.3-12, i.e.,

$$h_0 = t R(T, D) = t \exp(-\beta E) [1 + d \exp(n\beta E) D^n], \quad (2.4-1)$$

where h_0 denotes the change in resource.

CPLO-A, Dose to Equiv. Degrad (DED)
Fitted as a Function of $\log(\xi \cdot D)$

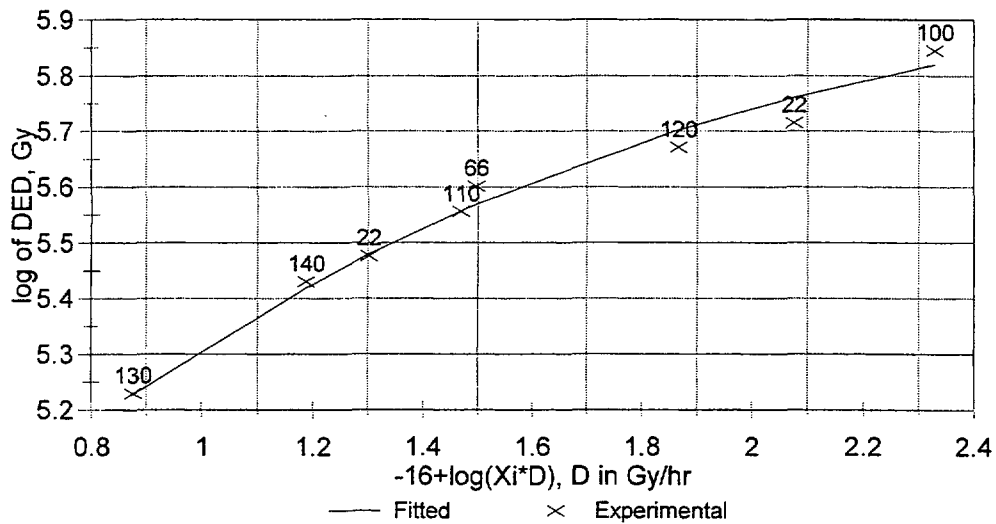


Figure 2 Experimental values of $\log(\text{DED})$ and fitted values of $\log(\text{DED})$ vs. $-16 + \log(\xi D)$ for CLPO-A

Note: Using Equation 2.3-14 for the fitted values of DED, with $\xi = \exp(\beta E(\beta))$, and $E(\beta)$ given by Equation 2.3-20, the values of the constants used in the fit were: $K=1$; $\beta_m=32.875$; $E=1.136$; $E_B=0.942$; $a=1.822E-15$; $h_0=3.580E-12$; $n=0.86$.

CLPO-B, Dose to Equiv. Degrad (DED)
Fitted as a Function of $\log(\xi \cdot D)$

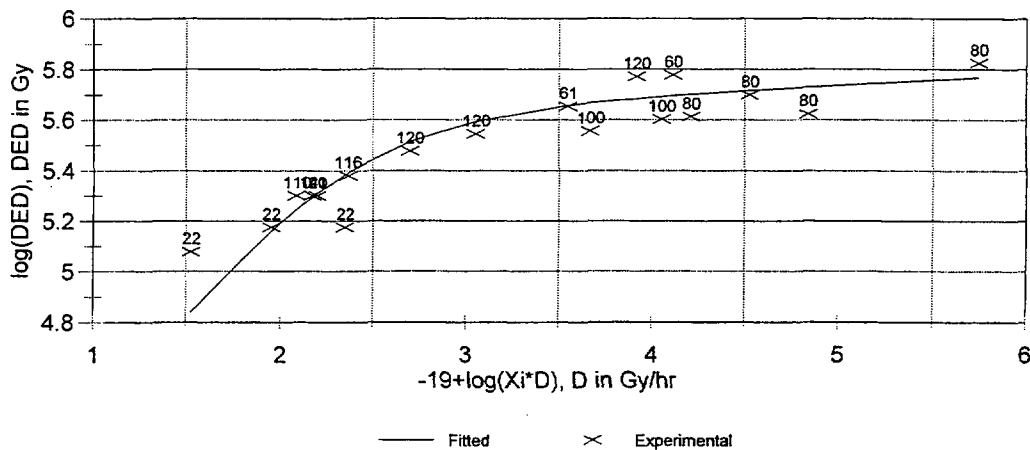


Figure 3 Experimental values of $\log(\text{DED})$ and fitted values of $\log(\text{DED})$ vs. $-19 + \log(\xi D)$ for CLPO-B

Note: Using Equation 2.3-14 for the fitted values of DED, with $\xi = \exp(\beta E(\beta))$, and $E(\beta)$ given by Equation 2.3-20. The values of the constants used in the fit were: $K=1$; $\beta_m=35.3/eV$; $E=1.50$; $E_B=1.15$; $a=4.143E-21$; $h_0=2.484E-16$; $n=0.96$.

The formula contains three parameters, h_0 , n and d , in addition to activation energy. It reduces to have a single parameter, h_0 , when thermal only aging is considered. Therefore, the h_0 for each damage level could be estimated using thermal aging data. The remaining two parameters are then estimated using combined aging data. The approach uses the same values of parameters n and d for all damage levels and all aging environments, as opposed to the approach discussed in Section 2.3 that uses different parameter values for different damage levels. The approach differs from the approach of Section 2.3 in that it does not use arbitrarily selected damage levels, and is generally applicable to all damage levels. It includes the following steps:

1. Estimation of activation energy using thermal aging data

Thermal aging data, designated as (T_i, t_i, EAB_i) , is used to determine the activation energy that gives the best time-temperature superposition results. This is typically done by plotting $\ln(EAB_i)$ against $\ln(t_{\text{shifted}_i})$ or t_{shifted_i} , where $t_{\text{shifted}_i} = t_i \exp(E/K_B * [1/(273+45) - 1/(273+T_i)])$, and identifying the activation energy that gives the least scattering. In this study, a linear regression of $\ln(EAB)$ and t_{shifted_i} is used to determine the activation energy that best fits the data.

2. Determination of the relationship between the change in resource and damage level using thermal aging data

The change in resource h_0 for thermal aging is $t_i \exp(-\beta_i E) = t_i \exp(-E/K_B / (273+T_i)) = t_{\text{shifted}_i} * \exp(E/K_B / (273+45))$. Note that the change in resource is simply the shifted time multiplied by a constant. A plot of EAB against h_0 shows that an exponential fit to the curve is reasonable. Therefore, a linear regression of h_0 and $\ln(EAB)$ was done to determine the relationship. That is,

$$\ln(EAB) = A + B h_0, \quad \text{or} \quad h_0 = (\ln(EAB) - A) / B \quad (2.4-2)$$

was used to determine the regression coefficients A and B . The equation can be used to determine the h_0 corresponding to any EAB , and vice versa, including those of combined aging environments.

3. Estimation of parameters n and d using combined aging data

The combined aging data can be represented as (T_j, D_j, t_j, EAB_j) with EAB_j related to h_{0j} by the exponential function determined above. Two different methods, based on a linear regression and a non-linear regression, are then used to estimate the parameters n and d of the $R(T,D)$ in Equation 2.4-1. They are discussed in more detail in the subsections below.

After the parameters are estimated, Equation 2.4-1 can be used to make predictions. For each aging environment, combined or thermal only, the change in resource is calculated as $t^*R(T,D)$, with the parameters n and d determined above. This change in resource is then used to calculate a predicted EAB using the exponential relationship between h_0 and EAB , i.e., Equation 2.4-2.

Section 3.2 documents the application of the no-interpolation approach to a Chlorosulfonated Polyethylene (CSPE) material made by Anaconda.

2.4.1 Use of Linear Regression to Estimate n and d

A linear regression relationship is derived below using Equation 2.4-1.

$$h_0 = t R(T,D) = t \exp(-\beta E) [1 + d \exp(n\beta E) D^n] \quad (2.4-3)$$

Moving $t \exp(-\beta E)$ to the left hand side, we get

$$h_0 - t \exp(-\beta E) = t \exp(-\beta E) d \exp(n\beta E) D^n. \quad (2.4-4)$$

Taking logarithm of both sides of the equation, we get

$$\begin{aligned} \ln[h_0 - t \exp(-\beta E)] &= \ln(t) - \beta E + \ln(d) + n\beta E + n \ln(D) \\ &= \ln(t) - \beta E + \ln(d) + n[\beta E + \ln(D)]. \end{aligned} \quad (2.4-5)$$

Moving $\ln(t) - \beta E$ to the left hand side, we get

$$\ln[h_0 - t \exp(-\beta E)] - \ln(t) + \beta E = \ln(d) + n [\beta E + \ln(D)]. \quad (2.4-6)$$

It is in the form of a linear regression line, i.e.,

$$y = \ln(d) + n x, \text{ where} \quad (2.4-7)$$

$$x = \beta E + \ln(D) = \ln(D \exp(\beta E)) \text{ and}$$

$$y = \ln[h_0 - t \exp(-\beta E)] - \ln(t) + \beta E = \ln\{ [h_0 - t \exp(-\beta E)] / [t \exp(-\beta E)] \}.$$

A linear regression using Equation 2.4-7 can be used to estimate parameters n and d .

Note that $t \exp(-\beta E)$ is the change h_0 in resource due to thermal aging. Then $h_0 - t \exp(-\beta E)$ is the additional change in resource due to radiation, and y is the logarithm of the ratio of the additional change in resource due to radiation to the change in resource due to thermal aging only.

Also, note that in this method the relation between EAB and h_0 was obtained from the thermal only data, and was treated as if it was a known physical relationship without any uncertainty, while, in reality there was scatter in the data about the line of best fit determining the relation of EAB and h_0 . The thermal only data is, therefore, not treated on exactly the same footing as the data when the cable is subject to radiation. The method of Section 2.3 would treat thermal only data on exactly the same footing as data where radiation was present.

Furthermore, note that x is the logarithm of the dose rate and becomes minus infinity as the dose rate becomes zero. This does not present a mathematical difficulty since the linear regression expression Equation 2.4-7 is only used for data points where the dose rate is not zero. However, for low values of the dose rate, one expects y to be large, and x to be large. The contribution to the sum of squares which is used in the linear regression analysis, for points with low dose rates, may therefore be large, and have an undue influence on the determination of the parameters n and d . For this reason, one might expect the nonlinear regression approach described in Section 2.4.2 to have better results.

2.4.2 Use of Non-linear Regression to Estimate n and d

The linear regression discussed above minimizes the additional change in resource due to radiation as a fraction of the change in resource due to thermal aging only. Since we are interested in making good predictions about EAB as a function of aging time, and the EAB is related to the change in resource by an exponential function, it is therefore desirable to minimize the errors in the estimated changes in resource, which in turn tends to minimize the errors in estimating EAB. Equation 2.4-1 is non-linear in parameter n . Therefore, a non-linear regression has to be done to estimate parameters n and d .

SigmaPlot (Ref. 17), a statistical software that is capable of doing the non-linear regression analysis, was used. Basically, Equation 2.4-1 was used as the formula for regression, and the input data, including T, D, t, and h₀, are based on the combined aging tests, where h₀ was calculated using the relationship between h₀ and EAB established with thermal aging.

2.5 Probability Distribution of Time to Fixed Level of Degradation

We now consider the problem of estimating the random variation in the time to a fixed level of degradation, for a fixed temperature and dose rate. We assume that our material obeys time-temperature-dose-rate superposition, and that the formula for R(T,D) given in Equation 2.3-13 is valid. The numerical example for Hypalon-B is an example where these assumptions are valid; good agreement between experiment and the predictions for the dose to equivalent degradation were obtained, as shown in Figure 1. According to our model, there is random variation in the initial capacity H₀₀ of the cable; therefore the time to a fixed level of degradation will be random, for a fixed temperature and dose rate, and, in fact, because of Equation 2.3-12 and because ΔH=H₀₀-h, where h is constant, corresponding to the fixed level of degradation we are considering, t is distributed according to a Weibull distribution if H₀₀ is. Moreover, from Equation 2.3-12, for all sets (t, T, D) corresponding to the same level of degradation, t R(T,D)= ΔH is distributed according to the same Weibull distribution. Therefore, from sets of (t, T, D) corresponding to a fixed level of degradation, it is possible to estimate the parameters for the Weibull distribution for ΔH, and consequently for t. If t_i, T_i, D_i are sample values, then the set of the sample values t_i R(T_i, D_i) can be used to estimate the parameters of the Weibull distribution. The cumulative distribution function of these sample values is an approximation to the cumulative distribution function of the parent distribution. If j represents the jth point after the sample values of t R(T, D) have been ordered, then a sample estimate of the cumulative distribution function value corresponding to ΔH_j is given by

$$f_j = (j-0.3)/(N+0.4), \quad (2.5-1)$$

where N is the number of sample points (see Ref. 18). A least squares procedure was used to fit a Weibull distribution to the sample distribution. Consider a Weibull distribution

$$F(u) = \text{pr}\{\Delta H < u\} = 1 - e^{-\left(\frac{u-\gamma}{\eta}\right)^\beta} \quad (2.5-2)$$

This equation is equivalent to

$$y = \beta x + c \quad (2.5-3)$$

where:

$$y = \ln(-\ln(1-F(u))), \quad x = \ln(u-\gamma), \quad \text{and } c = -\beta \ln \eta \quad (2.5-4)$$

The sample estimates of x_j are given by x_j=ln(ΔH_j - γ), and y_j=ln(-ln(1-f_j)). For fixed values of γ, one has a linear regression problem. Then γ is varied until the regression statistic r² is maximized.

Section 3.1.2 summarizes the application of the above approach to a Hypalon material made by Kerite.

2.6 Parameter Uncertainty

The approach described in Sections 2.3 and 2.5 gives a central estimate of the probability distribution for the time to reach a specified level of degradation. This probability distribution quantifies the aleatory, or random, uncertainty. It is desirable to obtain a family of these probability distributions, each with a degree-of-belief associated with it. Then, for a given temperature T and dose rate D , one would obtain not a single probability that a cable would reach the critical level of degradation after a specified time at (T, D) , but rather a degree of belief distribution for this (aleatory) probability. This degree-of-belief distribution quantifies what is sometimes called the epistemological uncertainty. An approach for doing this was developed in this project, but because of lack of resources the approach was not implemented. Basically, the method is that of the method of synthetic data sets, as described in Reference 19. The method there is used to obtain confidence intervals for parameters, but here we adopt a Bayesian point of view and use the method to obtain a joint degree of belief distribution for the parameters of the Weibull distribution discussed in Section 2.5.

The uncertainty in the Weibull distribution parameters comes ultimately from the fact that there are sample to sample variations in the material properties of the cable insulating material, so that the experimental results have scatter associated with them. Because of this scatter, the parameters obtained for the Weibull distribution of Section 2.5 are uncertain. For example, suppose our experiment had 10 data points. If we repeated the experiment with a different set of 10 samples then we would not have gotten exactly the same estimate of the Weibull parameters. In the method of synthetic data sets, we would use the Weibull distribution of Section 2.5, with the parameters obtained from the true data set, as if they were the true parameters without uncertainty, and use this Weibull distribution to generate synthetic data sets, each with the same number of data points as the true data set. Each synthetic data set would be for the same values of (T_i, D_i) as the true data set, where i runs over all the points in the experimental data set. One would pick a value of ΔH from the Weibull distribution of Equation 2.5-2 and divide by $R(T_i, D_i)$ to obtain a value for the time t_i to reach the critical level of degradation. This procedure would be repeated for all the data points (T_i, D_i) , obtaining in this way a synthetic data set. This synthetic data set would then be treated in the same way as the original data set. Numerical estimations of the parameters n , d , and h_0 would be obtained in the same way as in Section 2.3. The Weibull distribution parameters for this synthetic data set would be obtained as described in Section 2.5, in exactly the same way as the Weibull parameters for the true data set were obtained. By repeating this procedure many times one obtains a joint distribution for the Weibull parameters, and consequently, for any specified time one can obtain a distribution for the probability that the specified level of degradation is reached. For this procedure to be feasible, it must be automated.

3. NUMERICAL RESULTS

3.1 Calculations Performed Using Reliability Physics Model

In this section, the approach discussed in Sections 2.3 and 2.5 was applied to the aging data in Gillen's reports (Refs. 9 and 15), and the results are compared with the predictions made using Gillen's time-temperature-dose-rate superposition method. A reference temperature of 45 degree C was used in all calculations. Table 1 summarizes the calculations performed using Section 2.3. The detail of the calculations is presented in Section 3.1.1. Section 3.1.2 presents an example application of the method of Section 2.5 on the distribution of time to a specific embrittlement level, using a CSPE material made by Kerite in the CPAD data base.

3.1.1 Calculations Performed for Different Materials

In Gillen's reports, the time temperature-dose-rate superposition method was applied to combined aging test data for several different materials. Typically the data for two damage levels, 100% absolute and 60% relative EAB, were considered. They were obtained by interpolation of test data at various damage levels. The test data are typically plotted as data points in DED versus D figures, with each data point corresponding to a test environment. Each data point was shifted to an arbitrarily selected reference temperature, 45 degrees C unless otherwise specified, using time-temperature-dose-rate superposition method, and the results were presented in the form of fitted curves of DED versus the shifted dose rate D.

Gillen indicated that the data he obtained satisfied time-temperature-dose-rate superposition using a wide range of activation energies; typically the thermal activation energy was used in his calculations. Of course, if data were present for very low dose rates, then the results would be sensitive to the activation energy used, since the results must approach the thermal-only results in the limit that D approaches zero, and since the thermal-only results are sensitive to the activation energy used. In our calculations, the same activation energies as those used in Gillen's calculations were used.

The plotted test data in Gillen's reports were read and discretized into numeric values in the format of (T, D, DED), and for each such data point an aging time was calculated as DED/D. The data is then used as the input to the approach of Section 2.3 following the steps described below. QuattroPro software (Ref. 20) is the software tool used in the calculations.

1. Elimination of DLO data points – Gillen developed a criterion for identifying data points that are associated with DLO (Ref. 21), and used it to eliminate the DLO data points from being used in time-temperature-dose-rate superposition method. The DLO data points identified in Gillen's reports were also eliminated from our analysis.
2. Selection of an initial value of n for Equation 2.3-18 – According to IEC 1244-2 (Ref. 11), the value of n should be less than or equal to 1. According to Volume 2 of IAEA-TECDOC-1188 (Ref. 12), the value should be between 0.7 and 1.0. An initial guess of the value of n, e.g., n=1.0, is selected.
3. Linear regression – Perform a linear regression using Equation 2.3-18 to estimate the values of parameters d, and h_0 . The value of h_0 has to be positive, otherwise the resource would increase with age. The value of d has to be positive, because the radiation should enhance the degradation. The coefficient of variation, Rsquare, is used as the measure of goodness of fit.

Table 1 Estimated Parameters of Different Materials at EAB of 60% Relative and 100% Absolute

Material Abbreviation	Manufacturer Designation	Source of Data	Damage Level (EAB) (%)	Change in Resource h_0	n	d	Activation Energy (ev)	Notes
Hypalon-B	Kerite FR cable	SAND90-2009 (Ref. 9)	60% relative (164%)	4.187e-09	0.9335	7.544e-14	0.91168	88KJ/Mol of thermal activation energy was used. 75+/- 17 Kj/mol gives reasonable superposition.
			60% relative (164%)	4.350e-09	0.910	1.769e-13	0.91168	22 C data were excluded from regression.
			100%	7.872e-09	1.000	5.922e-15	0.91168	Reference 9 has no data at 22 degree C.
Hypalon-C	Anaconda Flameguard	SAND90-2009	60% relative (204%)	2.789e-12	0.910	4.449e-16	1.084128	105 KJ/Mol of thermal activation energy was used.
			100%	4.558e-12	0.931	1.100e-16	1.084128	
Silicone	Rockbestos SR cable	SAND90-2009	50% relative (210%)	8.792e-10	0.911	2.031e-13	0.91168	88KJ/Mol of thermal activation energy was used.
			100%	2.101e-09	0.960	4.808e-14	0.91168	
ETFE-A and B	Teledyne Thermatic cable, unknown	SAND90-2009	100%	$h_0/d=1.2E5$ Gray			0.91168	88KJ/Mol of thermal aging activation energy in air gives a shifted result of a horizontal line showing independence of dose rate and temperature.
EPR-A	Anaconda Flameguard FR-EP	SAND91-0822 (Ref. 15)	100%	4.142e-09	1.000	1.074e-14	0.91168	21 Kcal/Mol that worked for other material was used.
			100%	4.646e-09	0.990	1.705e-14	0.91168	22, 41, and 60 degree C data were excluded from regression.
EPR-B	Dekoron Elastoset	SAND91-0822	100%	3.920e-09	1.000	5.538e-15	0.91168	21 Kcal/Mol that worked for other material was used.
			100%	4.851e-09	1.000	7.026e-15	0.91168	41, 60, 61, and 80 degree C data were excluded from regression.
CLPO-A	ITT Suprenant	SAND91-0822	100%	1.989e-12	1.000	3.355e-18	1.13617	26.2Kcal/Mol of thermal activation energy was used.
			100%	3.663e-12	0.860	2.143e-15	1.13617	22 and 66 degree C data were excluded from regression.
CLPO-B	Brandex XLP	SAND91-0822	100%	2.935e-09	1.000	4.916e-15	0.91168	21Kcal/Mol of thermal activation energy was used.
			100%	8.248e-09	0.960	6.729e-14	0.91168	22 and 41 degree C excluded from regression.
CLOP-C	Dekron Polysat	SAND91-0822	100%	4.833e-09	1.000	4.768e-15	0.91168	21 Kcal/mol that gives reasonable results for other materials was assumed.
			100%	5.224e-09	0.980	1.051e-14	0.91168	41 and 60 degree C data were excluded from regression.

4. Iterations on value of n – The value of n is modified and step 3 is repeated until R_{square} is maximized.

With the values h_0 , n , and d determined, an estimated DED, DED_{calc} , is calculated using Equation 2.3-14.

Table 1 summarizes the calculations performed using the above procedure for different damage levels, and different cable materials. Figures 4 to 21 provide comparisons of the predictions made using the Section 2.3 approach with that of time-temperature-dose-rate superposition. The curves in the figures are the result of our approach and the data points marked by crosses are the result of time-temperature-dose-rate superposition. Note that for some of the materials, i.e., CLPO A, EPR A (Ethylene Propylene Rubber), and EPR B, Gillen fitted a S-shaped curve through the data points, representing chemical dose-rate effects that level out at low dose rates. The curves predicted using our approach can not take on such a shape, due to the use of simple empirical formula like Equation 2.3-13. The calculations are discussed in more detail below.

Hypalon B

Figure 4 shows the 60% EAB results of Hypalon B. Our predicted curve fits Gillen's results well. Figure 5 is a sensitivity calculation in which the 22 degree C data were excluded from the regression analysis of our approach. That is, the 22 degree C data were not used in our estimation of parameters. The resulting predictions at 22 degree C fit the data well, and represent a validation of our approach.

Gillen's report did not provide the test data for 100% EAB, and only showed the shifted results at the damage level. Figure 6 shows the 100% EAB results of our prediction which fits Gillen's results well.

Hypalon C

Figure 7 and 8 show the 60% and 100% EAB results of Hypalon C, respectively. Our predicted curves fit Gillen's results well.

Silicone Rubber

Figure 9 and 10 show the 50% relative and 100% EAB results of Silicone Rubber, respectively. Our predictions fit Gillen's results well.

ETFE A and B (Ethylene Tetrafluoroethylene Copolymer)

Gillen's analysis of 100% EAB data shows that the aging of the material does not have any dose rate effect. That is, the shifted data points fall on a horizontal line. Straight forward application of our approach did not lead to any meaningful results. In the case that n is set to one and the dose rate is high, Equation 2.3-14 reduces to $DED = h_0/d$, and an estimate for h_0/d is the mean of the DEDs of the applicable data points, i.e., $1.2E5$ Gray. Figure 11 shows the shifted data points and the constant DED line.

EPR A

Figure 12 shows the 100% EAB results of EPR A. Our predicted curve fits Gillen's shifted data reasonably well. In Gillen's analysis, it was pointed out that the S-shaped dose-rate effect, which levels out at low dose rates, is clearly indicated at the 120 C data, although the S-shapeness of his fitted curve is not very pronounced. Figure 13 shows the results of a sensitivity calculation in which the low

temperature data, i.e., at 22, 41, and 60 C, were not included in the estimation of the parameters. That is, the higher temperature data were used to make predictions about lower temperature conditions. The predictions appear reasonable.

EPR B

Figure 14 shows the 100% EAB results of EPR B. Our predicted curve fits Gillen's shifted data reasonably well, except for the singular anomalous result at 41 C that Gillen verified in his report. Similar to EPR A, EPR B shows S-shapeness in its 120 C data. Figure 15 shows the results of a sensitivity calculation in which the low temperature data, i.e., at 41, 60, 61, and 80 C, were not included in the estimation of the parameters. That is, the higher temperature data were used to make predictions about lower temperature conditions. The predictions appear reasonable.

CLPO A and B

Figure 16 shows the 100% EAB results of CLPO A. Our predicted curve does not fit the shifted lower temperature data very well. This implies that there is a change in the mechanism for the degradation in going from higher temperature to lower temperature. The anomalous aging phenomena was discussed in Reference 22. Section 2.3 presents an approach that allows activation energy to vary with aging temperature, and provides much better predictions at lower temperatures for CLPO A and B.

Figure 17 shows the results of a sensitivity calculation in which the lower temperature data points, i.e., at 22 and 66 C, were excluded from the parameter estimation procedure. The predictions for lower temperatures become worse.

Figures 18 and 19 shows the 100% EAB results of CLPO B. The results of our predictions are similar to Figures 16 and 17 for CLPO A.

CLPO C

Figure 20 shows the 100% EAB results of CLPO C. Our predicted curve fits Gillen's shifted data reasonable well. CLPO C is another material that Gillen found that a curve fitted to his shifted data would be S-shaped. Figure 21 shows the results of a sensitivity calculation in which lower temperature data, i.e., at 41 and 60 C, were not used in the parameter estimation. The predictions for the lower temperatures are good.

Summary of Point Estimate Calculations

Figure 22 summarizes the predicted dose to 100% EAB for different materials at 45 degrees C. Also shown in the figure are the lines for cumulated doses for 40 and 60 years of operation at 45 degrees C. These lines can be used to determine if a material would degrade below 100% in 40 or 60 years. If the curve of a material is above the 40-year line at a particular dose rate, then the material is not expected to reach 100% EAB if it is left in the environment for 40 year. For example, at 1 Gy/hr, only Silicone Rubber and EPR A are expected to degrade below 100% EAB in 40 years. Note that 100% EAB is not a critical embrittlement level. Typically, 50% EAB is used as a critical embrittlement criterion.

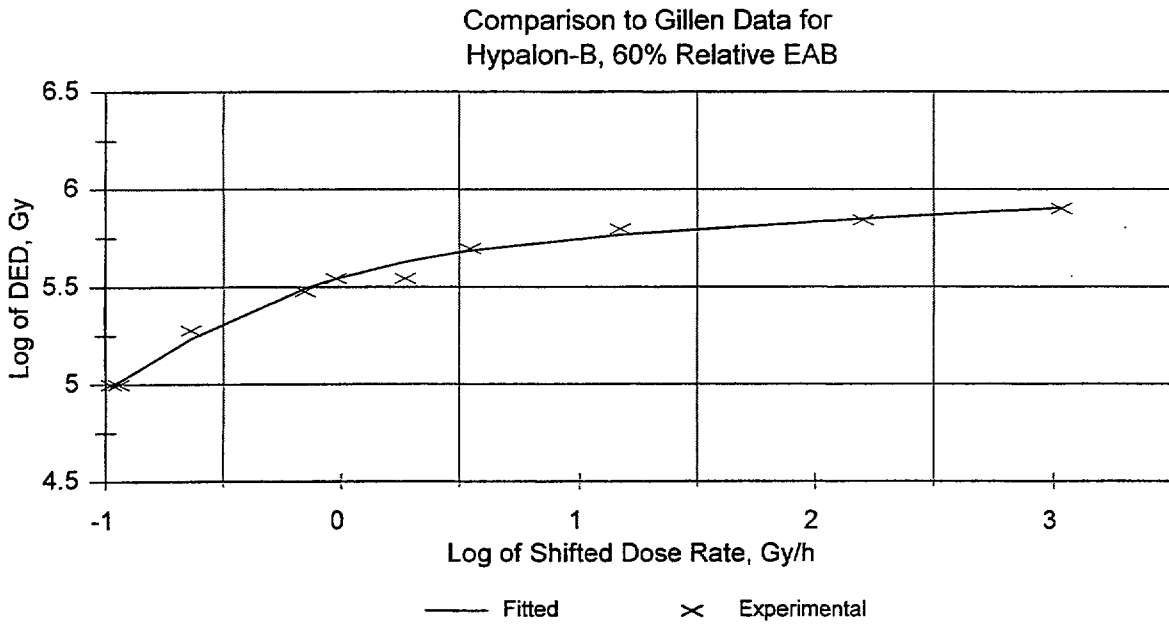


Figure 4 Comparison of Predictions of Reliability Physics Model of Sec 2.3 with Test Data of Gillen for Hypalon B at a degradation level of 60% relative EAB

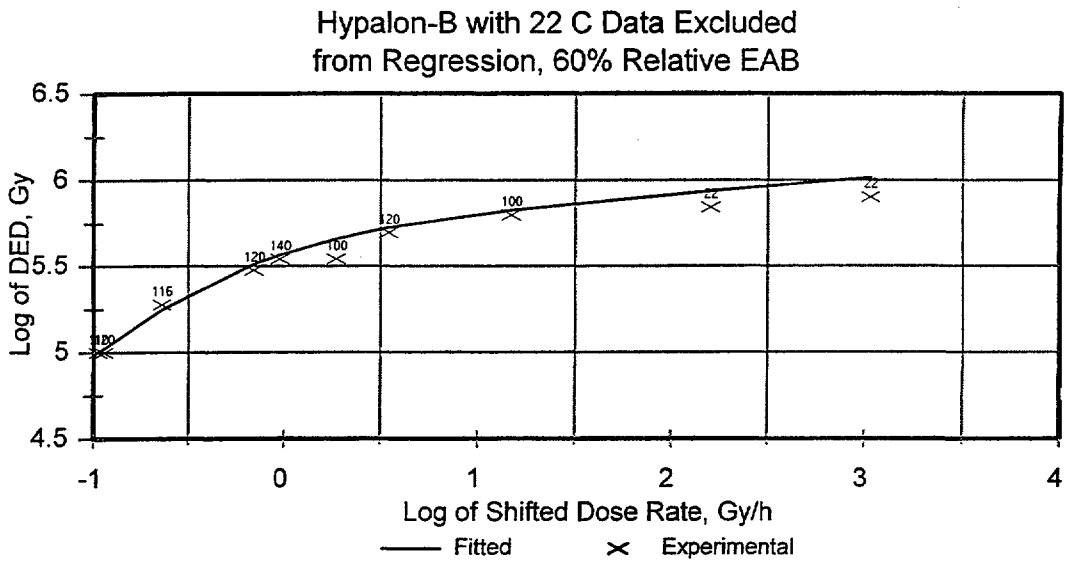


Figure 5 Sensitivity Calculation with 22 C Data Excluded - Hypalon B (60 relative EAB)

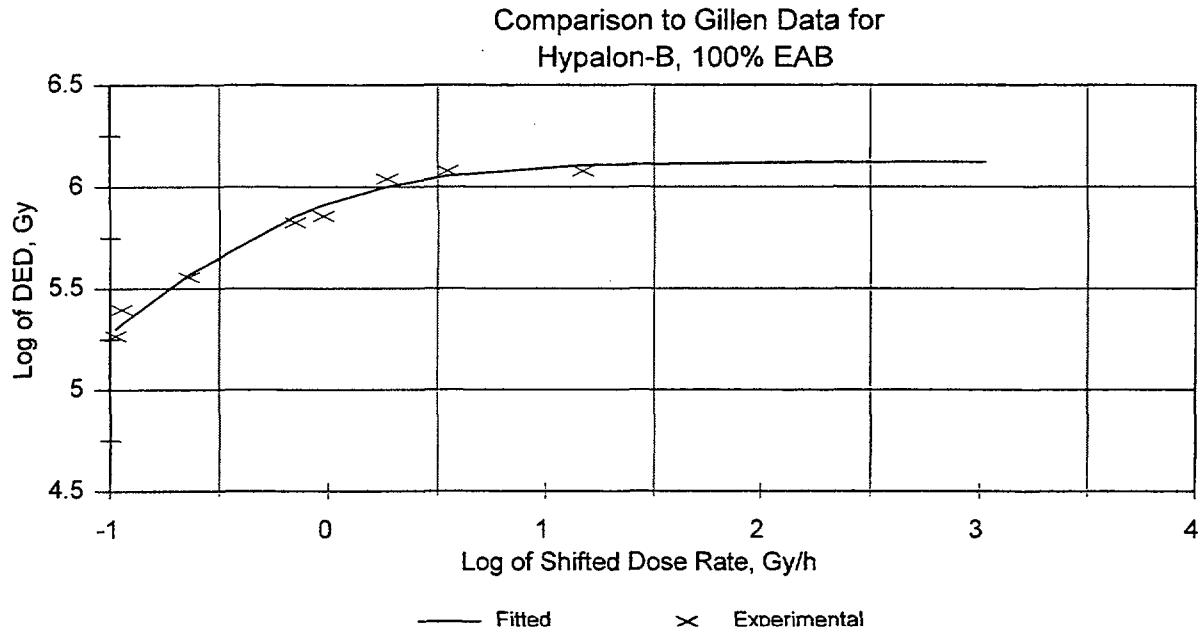


Figure 6 Comparison of Predictions of Reliability Physics Model of Sec 2.3 with Test Data of Gillen for Hypalon B at a degradation level of 100% EAB

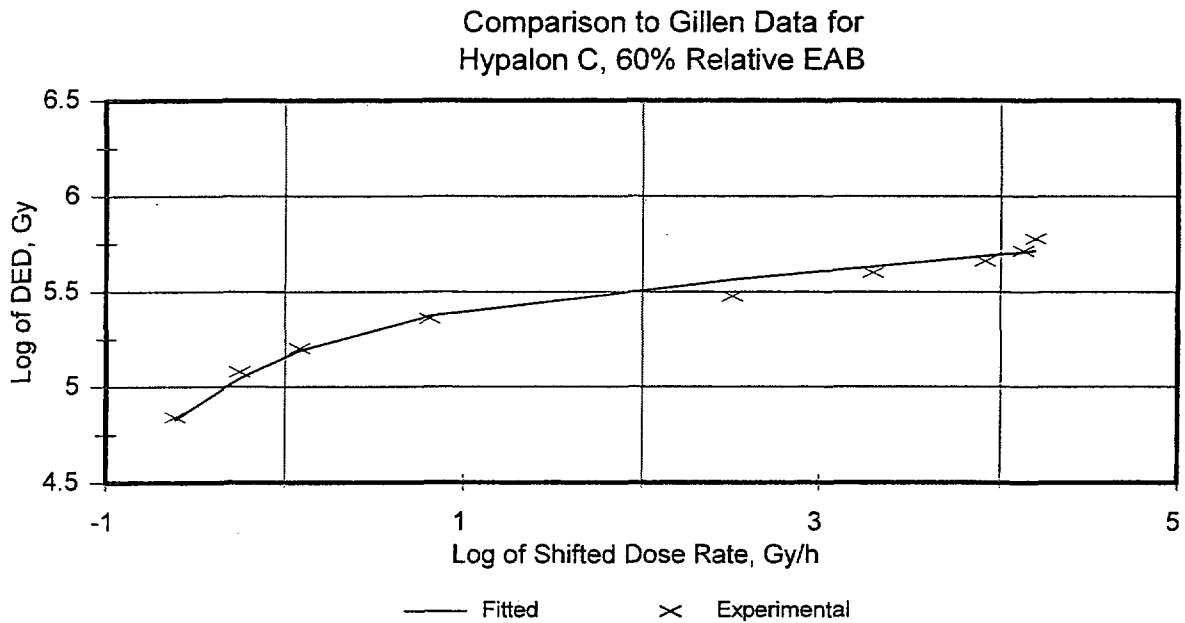


Figure 7 Comparison of Predictions of Reliability Physics Model of Sec 2.3 with Test Data of Gillen for Hypalon C at a degradation level of 60% relative EAB

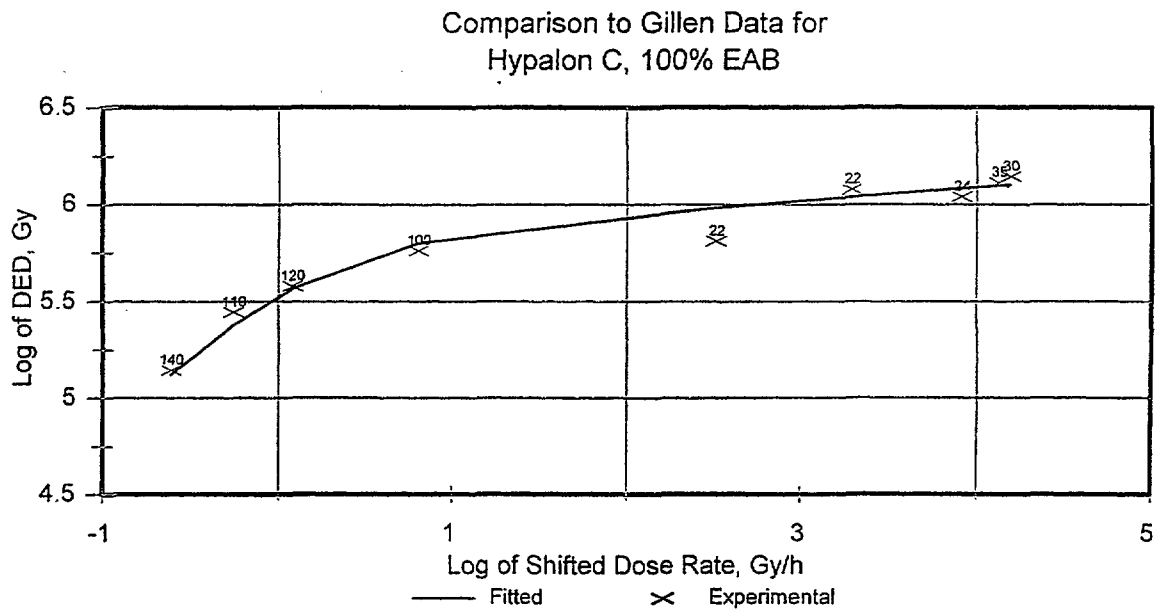


Figure 8 Comparison of Predictions of Reliability Physics Model of Sec 2.3 with Test Data of Gillen for Hypalon C at a degradation level of 100% EAB (100% EAB)

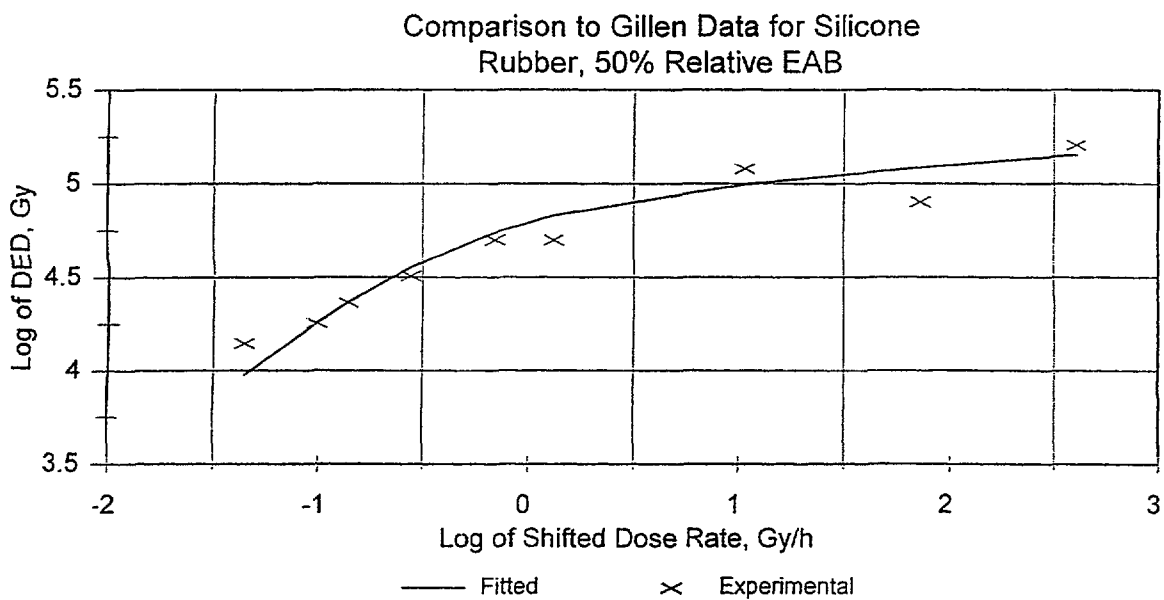


Figure 9 Comparison of Predictions of Reliability Physics Model of Sec 2.3 with Test Data of Gillen for Silicone Rubber at a degradation level of 50% relative EAB

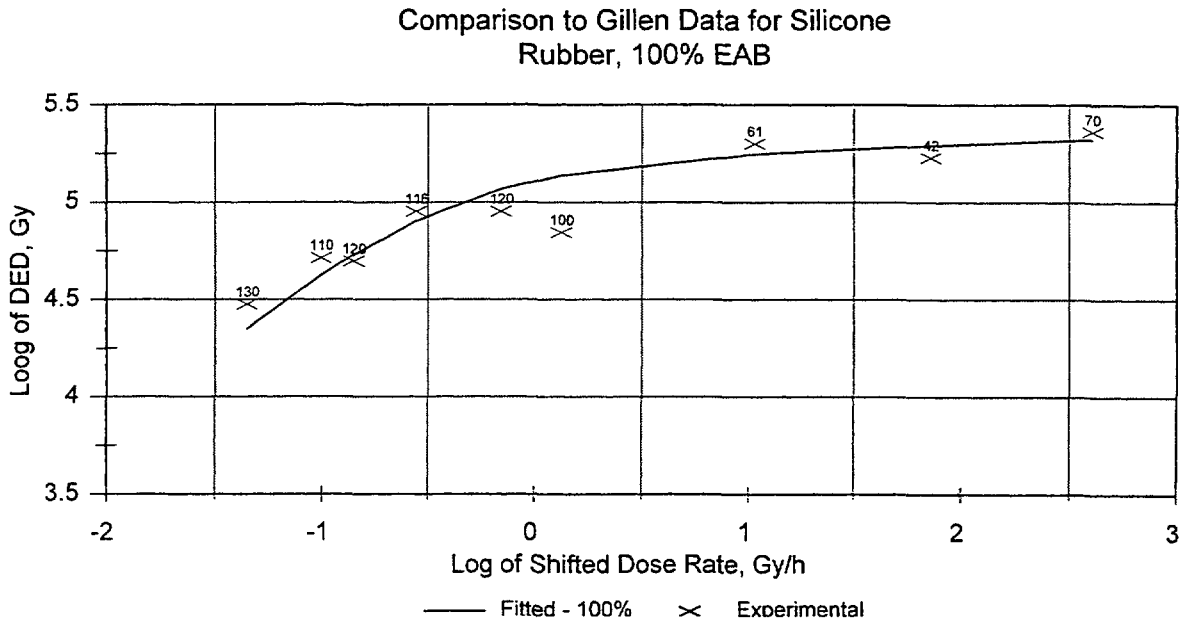


Figure 10 Comparison of Predictions of Reliability Physics Model of Sec 2.3 with Test Data of Gillen (Ref. 9) for Silicone Rubber at a degradation level of 100% EAB

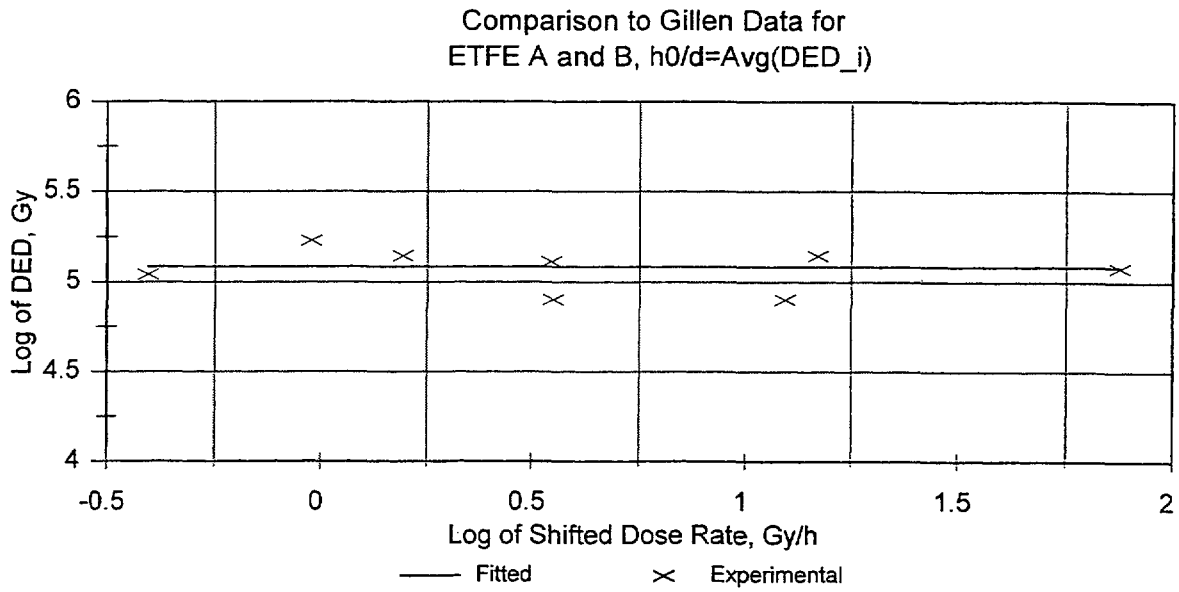


Figure 11 Comparison of Predictions of Reliability Physics Model of Sec 2.3 with Test Data of Gillen for ETFE at a degradation level of 100% EAB

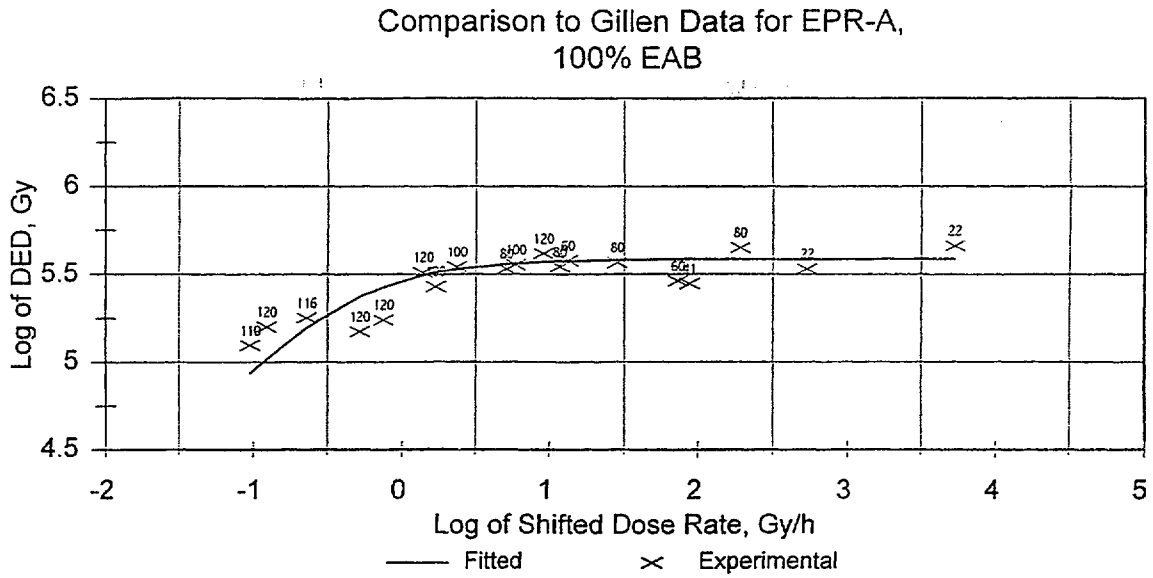


Figure 12 Comparison of Predictions of Reliability Physics Model of Sec 2.3 with Test Data of Gillen for EPR A at a degradation level of 100% EAB

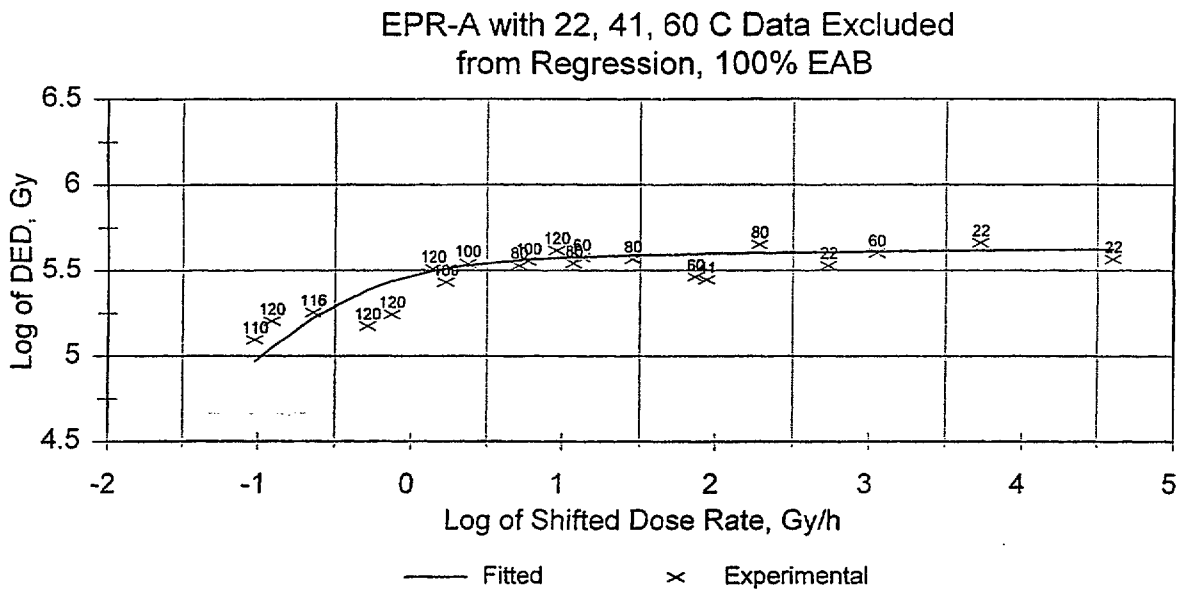


Figure 13 Sensitivity Calculation with 22, 41, and 60 C Data Excluded-EPR A(100% EAB)

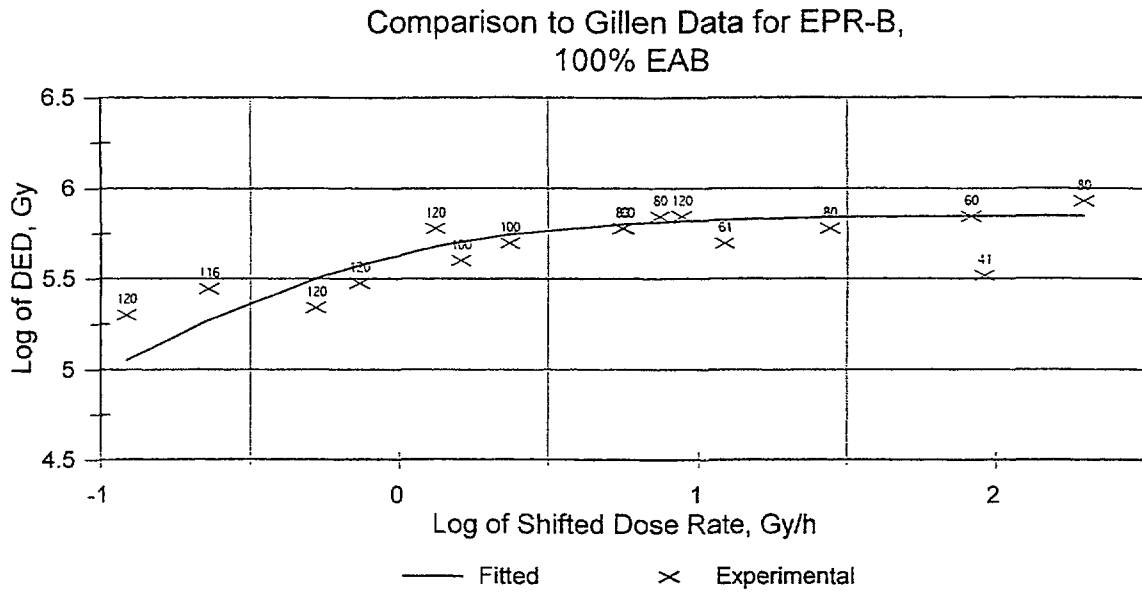


Figure 14 Comparison of Predictions of Reliability Physics Model of Sec 2.3 with Test Data of Gillen for EPR B at a degradation level of 100% EAB

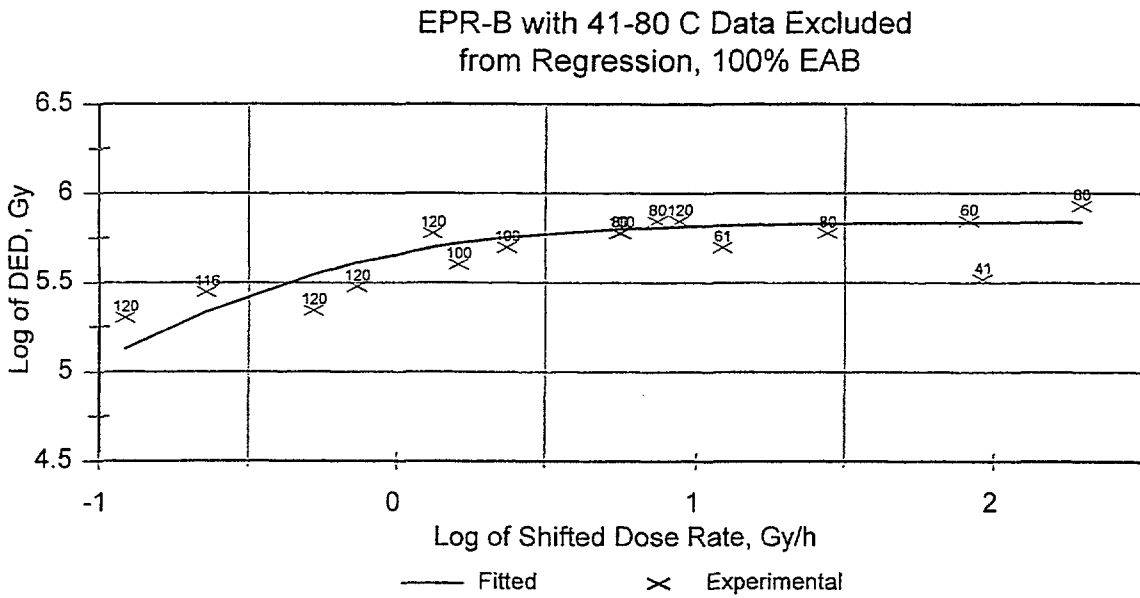


Figure 15 Sensitivity Calculation with 41, 60, 61, 80 C Data Excluded-EPR B (100% EAB)

Comparison to Gillen Data for CLPO-A,
100 EAB

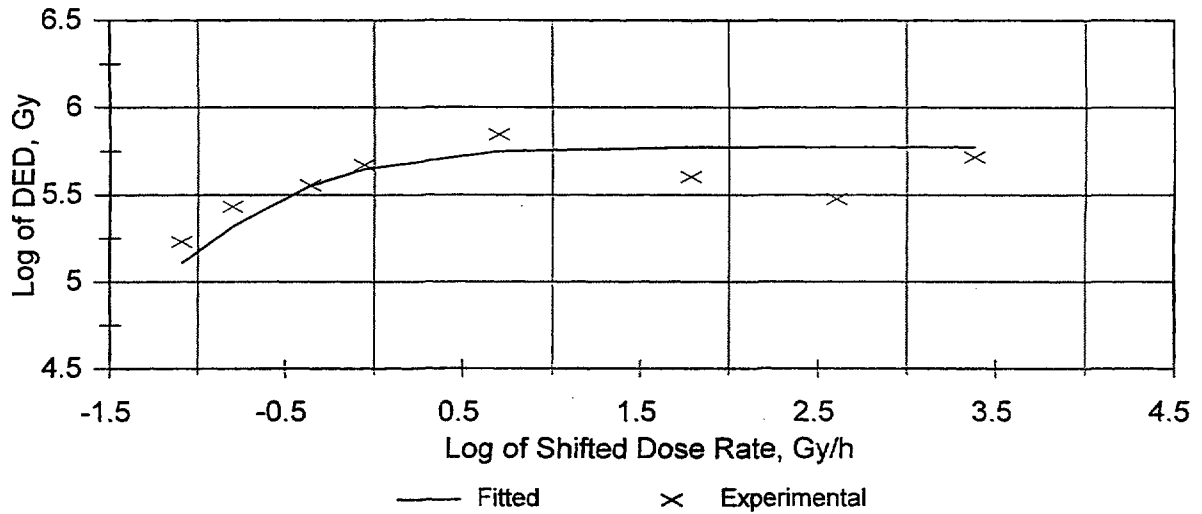


Figure 16 Comparison of Predictions of Reliability Physics Model of Sec 2.3 with Test Data of Gillen for CLPO A at a degradation level of 100% EAB.

Note that a better approach that uses a temperature dependent activation energy is discussed in Section 2.3 with its results shown in Figure 2.

CLPO-A with Data at 22 and 66C
Excluded from Regression

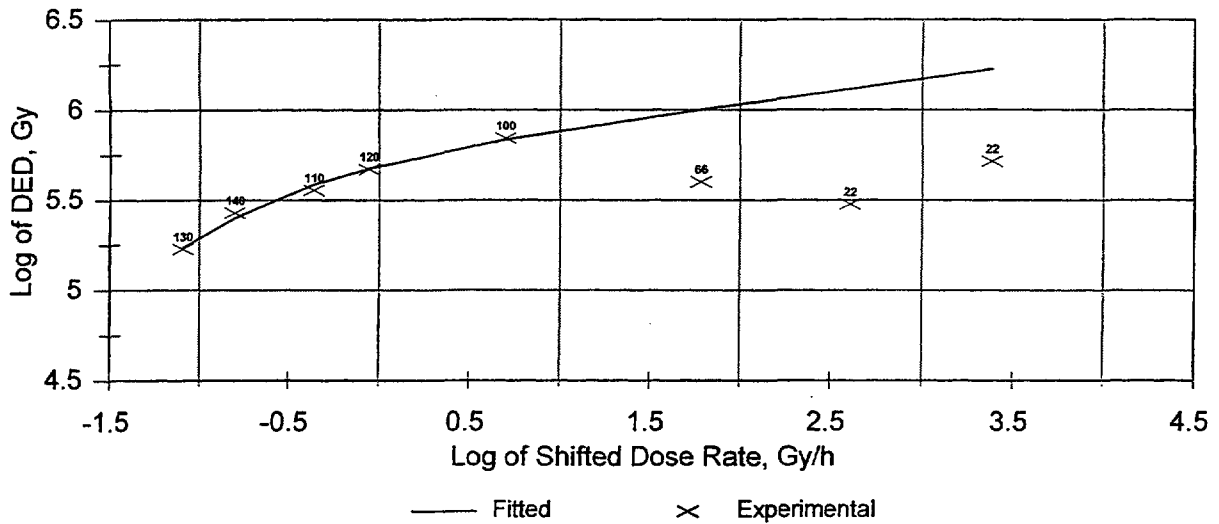


Figure 17 Sensitivity Calculation with 22, and 66C Data Excluded-CLPO A (100%)

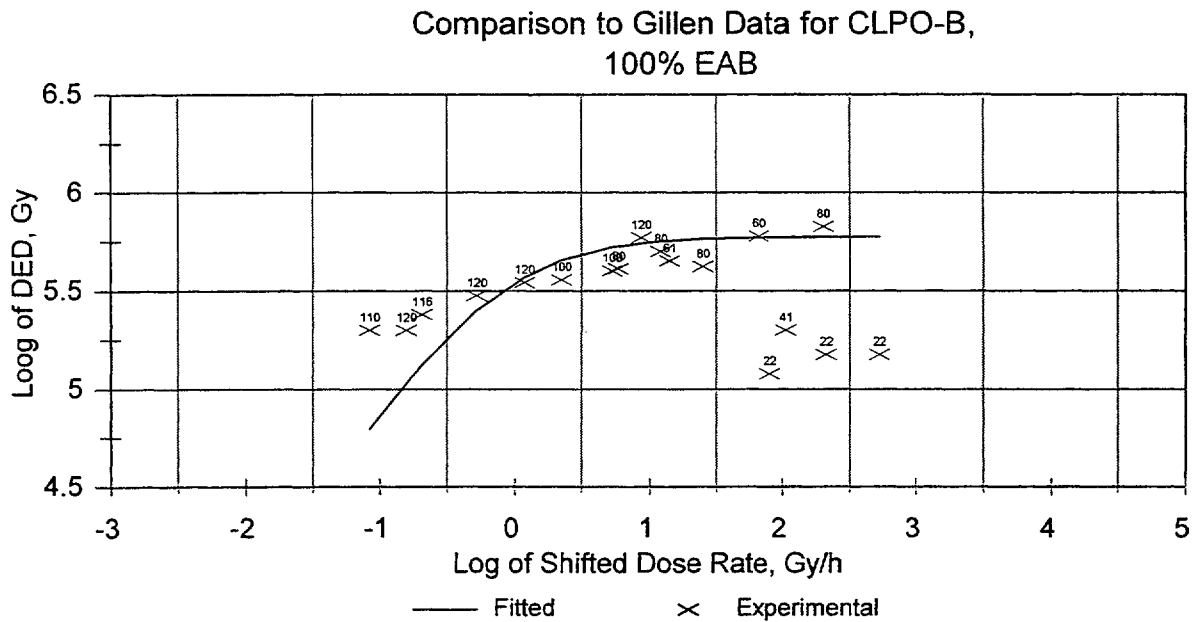


Figure 18 Comparison of Predictions of Reliability Physics Model of Sec 2.3 with Test Data of Gillen for CLPO B at a degradation level of 100% EAB.
 Note that a better approach that uses a temperature dependent activation energy is discussed in Section 2.3 with its results shown in Figure 3.

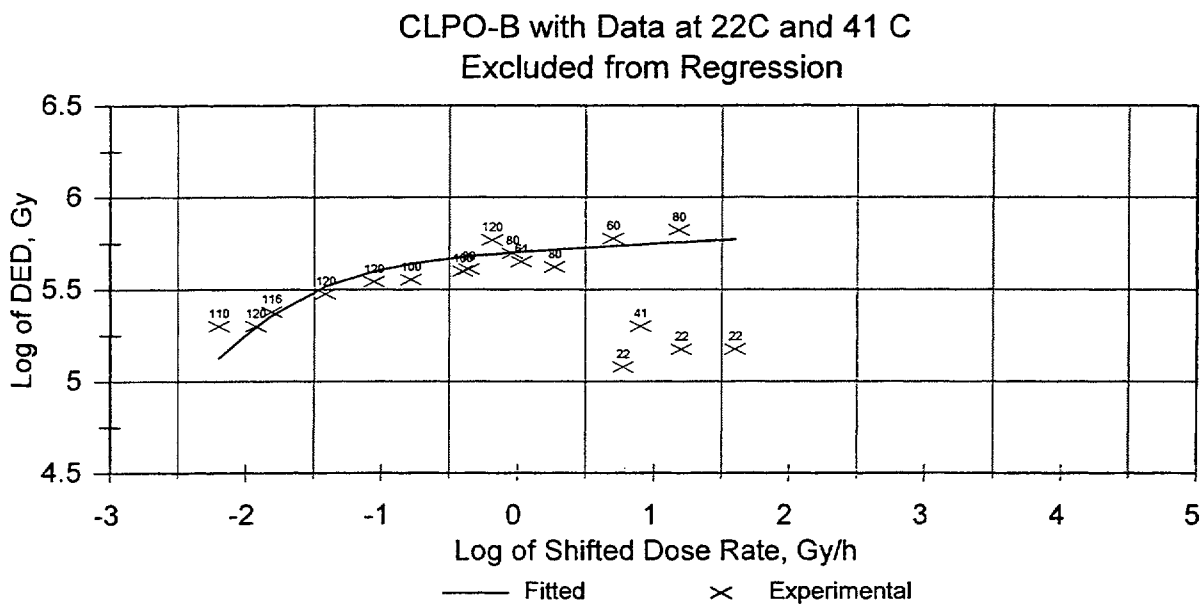


Figure 19 Sensitivity Calculation with 22, and 41C Data Excluded- CLPO B (100%)

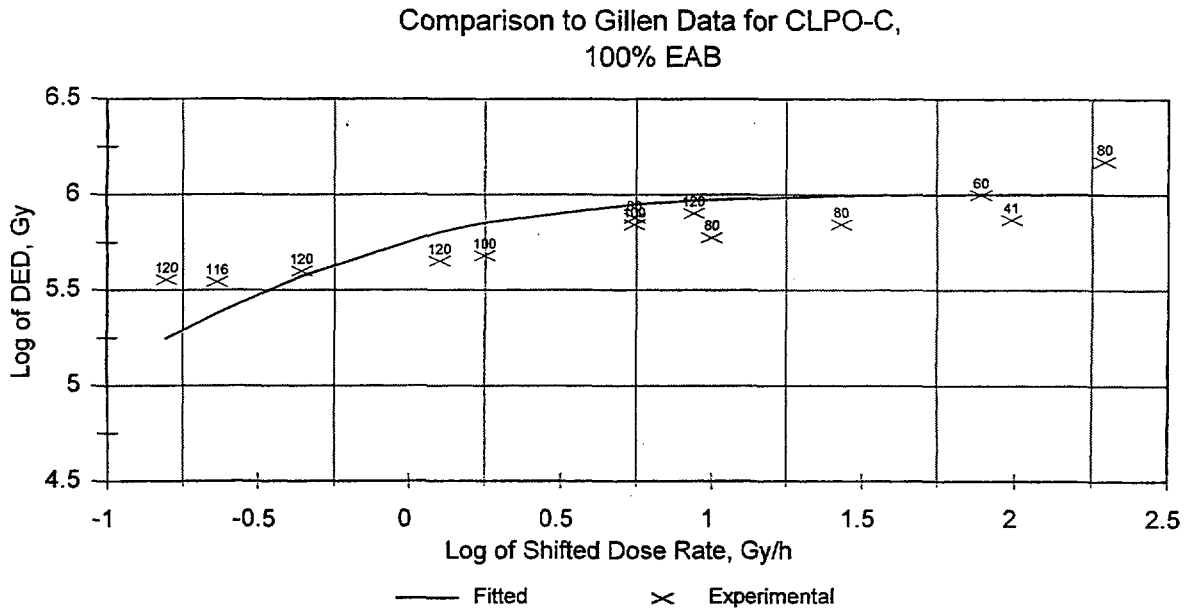


Figure 20 Comparison of Predictions of Reliability Physics Model of Sec 2.3 with Test Data of Gillen for CLPO C at a degradation level of 100% EAB

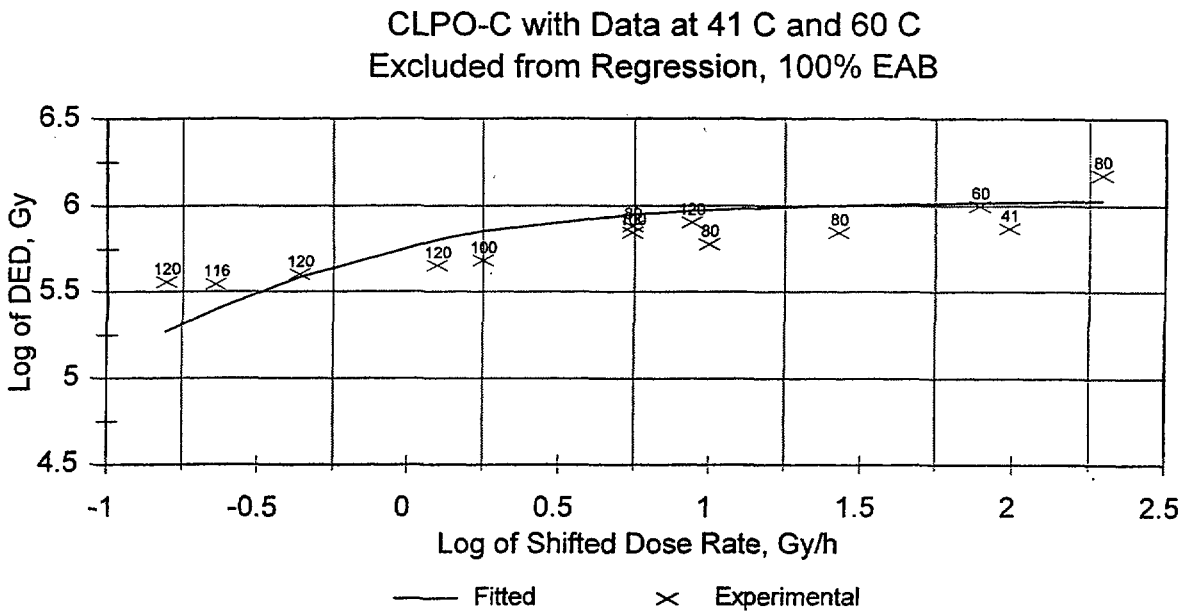


Figure 21 Sensitivity Calculation with 41, and 60 C Data Excluded- CLPO B (100%)

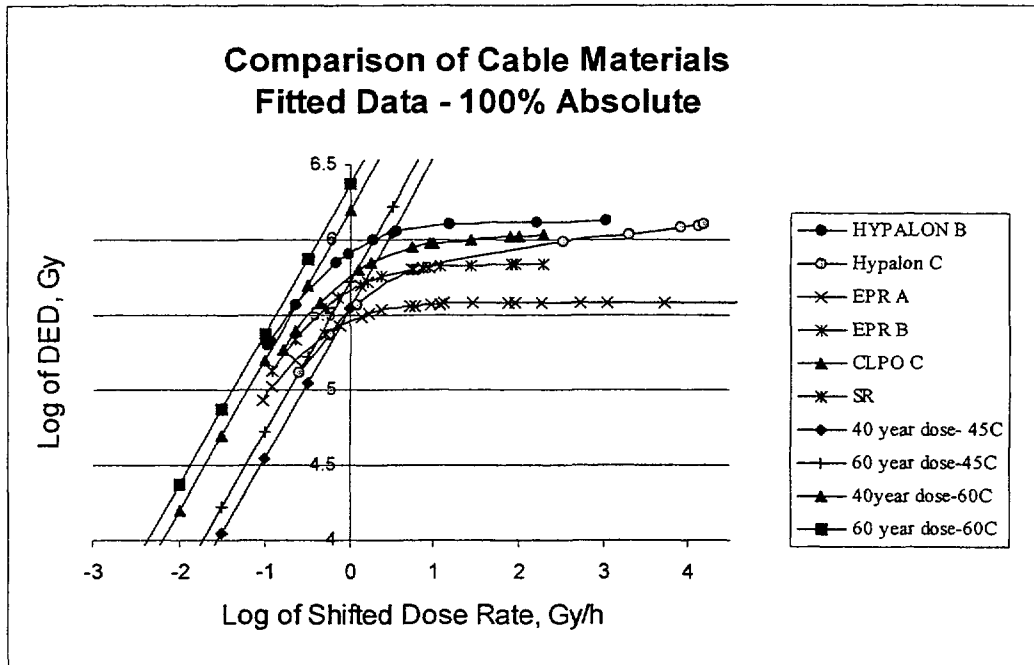


Figure 22 Predicted DED to 100% EAB for Different Materials

3.1.2 Determination of Probability Distribution of Time to a Specific Embrittlement Level for Kerite Hypalon Jacket

In this section, the approach described in Section 2.5 for determining the distribution of time to a fixed level of degradation of a cable material was applied to a 3.05 meter (10 foot) section of Hypalon cable jacket material in an environment of 45 degrees C and 1Gy/hr. As noted in Section 2.6, this distribution quantifies the aleatory uncertainty in the time to reach the fixed degradation level. One should also quantify the epistemological uncertainty in the manner indicated in Section 2.6, obtaining a family of such distributions. However, resources were insufficient to accomplish this. Fifty percent (50%) EAB was selected as the critical embrittlement level at which the cable may fail to perform its intended function (Ref. 23, p. 2 of the executive summary, and Ref. 24). The material considered is the Hypalon Jacket manufactured by Kerite and identified as C-6 in the CPAD database (Ref. 16). The CPAD database contains cable aging data from many different sources including the work of Gillen and has the data in a rawer format than that of Gillen's report. For each material, two types of aging data, thermal aging and combined environment aging, are tabulated separately. For each of the aging environments, the duration of aging and the material property at the end of the test, e.g., EAB and modulus, are also listed. Using the data in this format, the data needed in the reliability physics model at any damage level, e.g., 50% EAB, could be estimated by linear interpolation and extrapolation. The C-6 material is probably the same material as the Hypalon B in Gillen's report (Ref. 9). It is described in CPAD as a Hypalon jacket material of a cable made by Kerite with a trade name "FR." The Hypalon B of Gillen's report is a Hypalon insulation of a Kerite FR cable. Some of the test environments in the two sources of data are identical or close, with the CPAD data having significantly more test environments. Disagreements between the two sources include differences in initial EAB, and thicknesses of the materials.

Linear interpolation and extrapolation was done to obtain the 50% EAB data needed in our reliability physics model. It was assumed that the material is the same as the Hypalon B of Gillen's report and the thermal activation energy of Hypalon B was used. The parameters of our reliability physics model were estimated to be $n=0.94$, $d=4.845E-15$, and $h_0=9.1866E-10$. Figure 23 shows the results of the predicted dose to 50% EAB as a function of dose rate at 45 degrees C. For example, it takes approximately $2.0E5$ hours or 23 years for a 5.08-centimeter (2-inch) test sample of the jacket material to reach 50% EAB at a dose rate of 1 Gy/hr. Note that the material is used as a jacket material. Its reaching critical embrittlement level does not mean that the cable insulation material would reach critical embrittlement level also.

Due to the variability of material property along the length of a cable, it is more likely for a 3.05-meter (10-foot) long cable to reach the critical embrittlement level than a 5.08-centimeter (2-inch) cable. Section 2.5 provided a way to account for such a variability, i.e., the distribution of the predicted change in resource, h_0 , is used to characterize the variability. The predicted changes in resource of the data points follows a Weibull distribution. In this example, the parameters of the distribution were estimated, i.e., $\gamma=5.67E-10$, $\eta=3.967E-10$, and $\beta=1.329$. Time to damage is simply the change in resource ΔH divided by $R(T,D)$. Therefore, the (aleatory) distribution for the time to 50% EAB is also a Weibull distribution, with parameters simply related to those of the distribution of ΔH . That is the γ and η of time to 50% EAB are those of ΔH divided by $R(T,D)$, and β remains unchanged, where $R(T,D)$ is calculated using Equation 2.3-13, e.g., $R(T,D) = 4.2E-15$ for $T=45$ degrees C and dose rate of 1Gy/hour. Table 2 lists the estimated values of the parameters of h_0 and time to 50% EAB. For the example aging environment, the mean time to 50% EAB is approximately 25 years, close to the point estimate obtained in Figure 23.

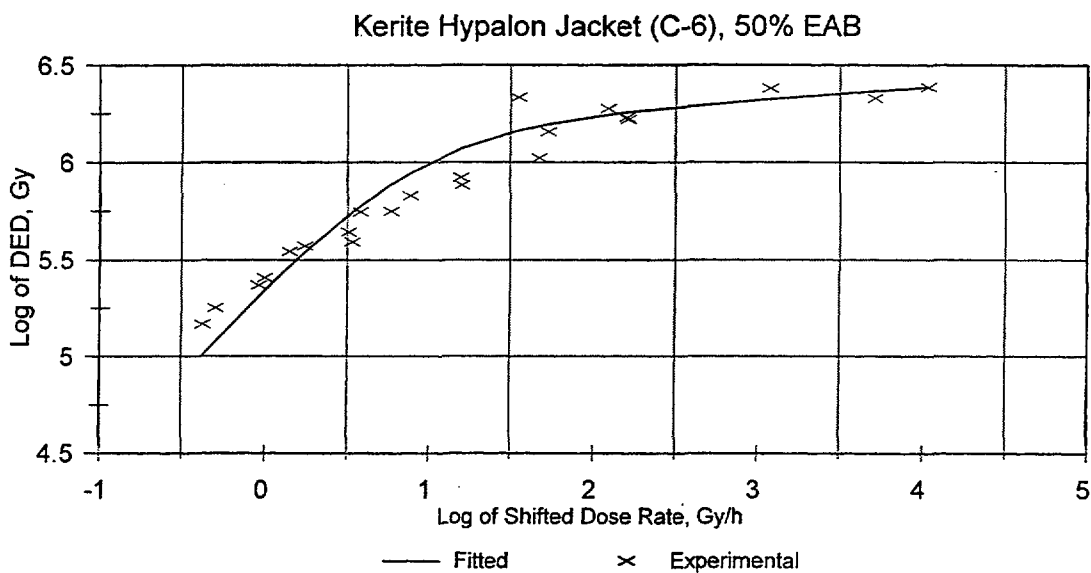


Figure 23 Predicted DED vs D of Kerite CSPE Jacket (50% EAB)

Table 2 Estimated Weibull Parameters of h_0 and Times to 50% EAB of Kerite Hypalon Jacket

Random Variable (hours)	γ (hour)	η (hour)	β	Mean
h_0	5.670e-10	3.967e-10	1.329	9.3E-10 hour
Time to 50% EAB (2")	1.346e+05	9.417e+04	1.329	25 years
Time to 50% EAB (10')	1.346e+05	4.328e+03	1.329	16 years

As derived in Section 2.1, the distribution of time to 50% EAB of a 3.05-meter (10-foot) cable is related to the distribution of time to 50% EAB of a 5.08-centimeter (2-inch) cable in a simple way. That is, the parameters γ and β remain the same, and the η of the 3.05-meter (10-foot) cable is the η of the 5.08-centimeter (2-inch) cable divided by $n^{(1/\beta)}$, where n is the ratio of 3.05 meters (10 feet) and 5.08 centimeters (2 inches), i.e., 60.

Figure 24 plots the distributions of time to 50% EAB for the jacket of a 5.08 centimeter (2-inch) cable and that of a 3.05 meter (10-foot) cable. As expected, the distribution for the 3.05-meter (10-foot) cable jacket is close to the location parameter γ , i.e., approximately 16 years.

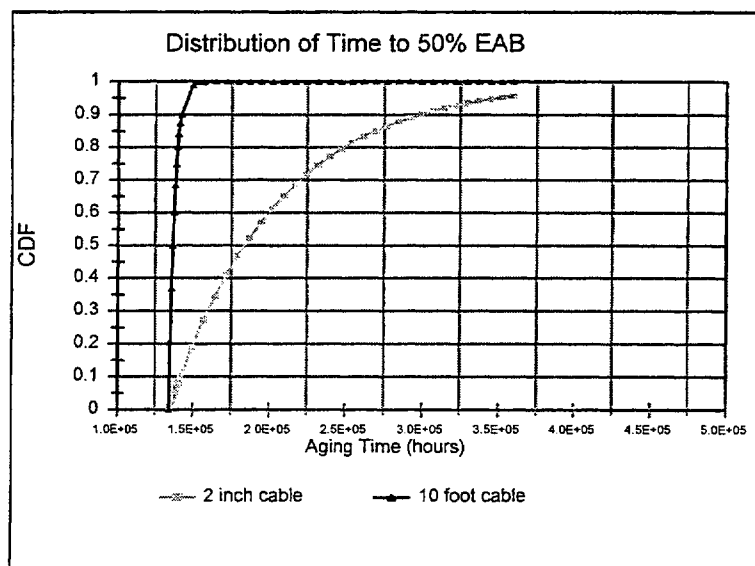


Figure 24 Distribution of Time to 50% EAB of Kerite Hypalon Jacket C-6

3.2 Results of No-interpolation Approach Using CPAD Data

In this section, the calculations performed using CPAD data are documented. The calculations of Hypalon C of Reference 9 are discussed in detail. Similar but more limited calculations were done for other materials, i.e., different CSPEs, EPRs, Neoprene, and Silicone rubber, and are documented in Appendix A. A reference temperature of 45 degree C was used in all calculations.

In this example, the CPAD data for Anaconda Flameguard CSPE of Sandia National Laboratories (SNL), was used. It is used as jacket insulation and designated as C-14 (thermal aging) and C-15 (combined environment aging). We believe this data is the same test data as those of the Hypalon C material in Gillen's report (Ref. 9). Figures 25 and 26 plot EAB as a function of aging time for pure thermal aging and combined thermal plus radiative aging, respectively. Note that in Figure 26, the curve for 22 degrees C and 13.7 Gy/hr has a weird turn, which is the cause of some inconsistency in the predicted results. It should also be pointed out that some inconsistencies exist in the two sources of Gillen's aging tests. The temperatures of the combined aging environments specified in the two sources are identical except that CPAD database has 38 degrees C data and Gillen's report (Ref. 9) does not, and Gillen's report has 110 degrees C data but not the CPAD database. For those temperatures that are identical for the two sources, their corresponding dose rates are close but not identical. This disagreement is probably due to the fact that the dose rate, and DED information of Gillen's report were obtained by manually discretizing the curves in his report.

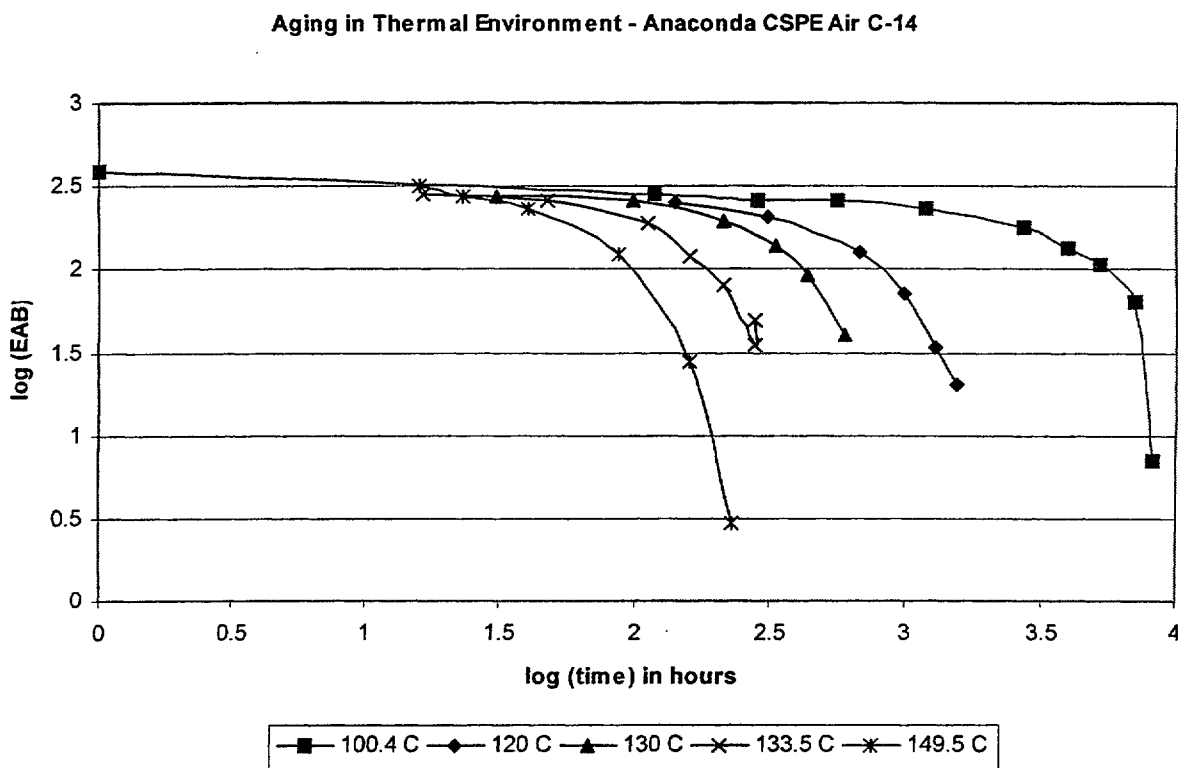


Figure 25 Thermal Aging Data of Hypalon C

Aging in Combined Environment - Anaconda CSPE Air C-15

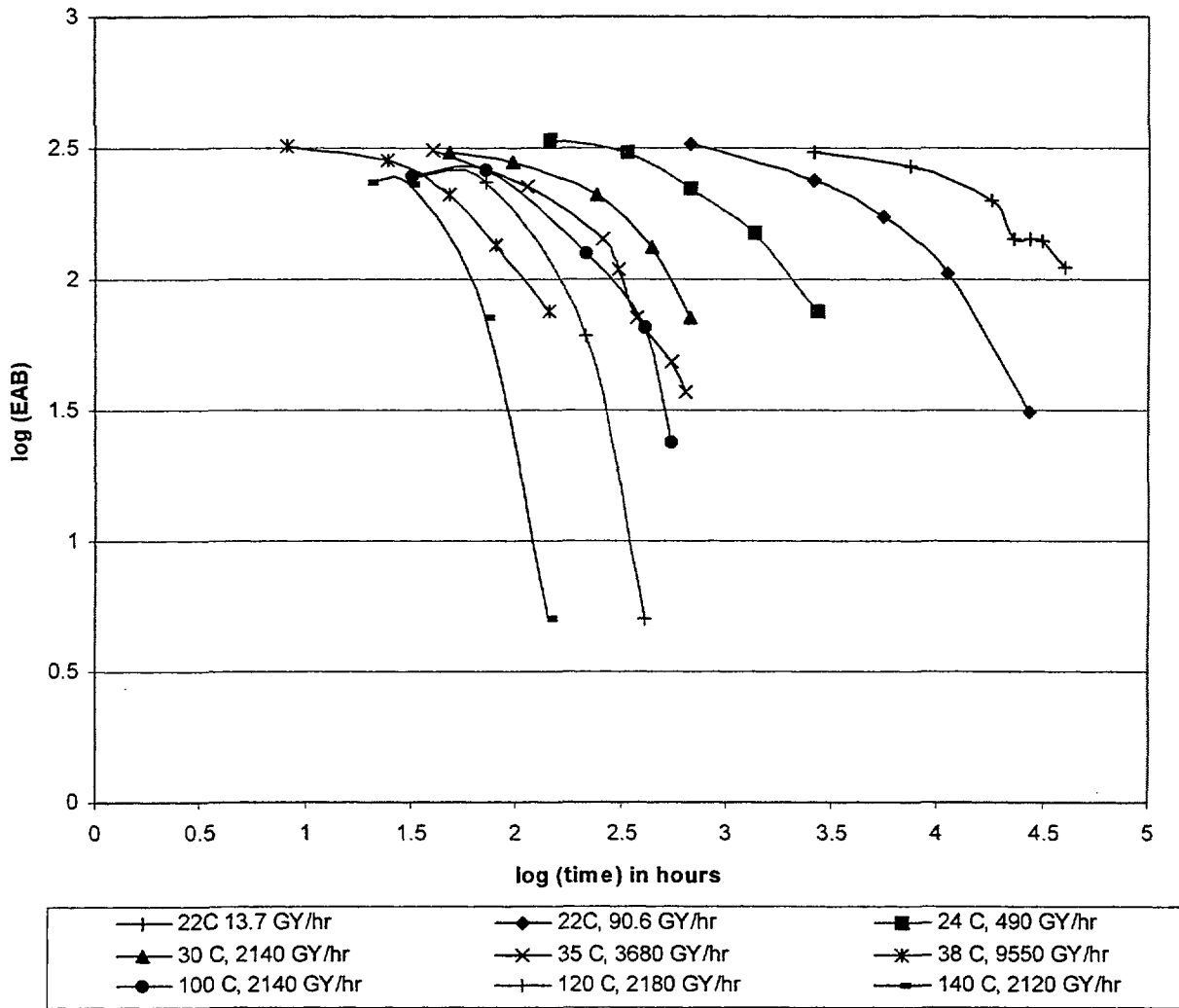


Figure 26 Combined Aging Data of Hypalon C

3.2.1 Use of Thermal Aging Data

Determination of Activation Energy

Activation energy was estimated by performing a linear regression analysis of $\ln(EAB_r)$ and t shifted using different values of activation energy, where EAB_r represents relative EAB. It was found that 1.09 eV provided the best fit in terms of Rsquare. Figure 27 plots the predicted curve and the original data. This result is close to but not exactly the same as the activation energy specified in Gillen's paper, i.e., 1.084 eV (25Kcal/mole).

Use of Time-Temperature Superposition to Determine Activation Energy (1.09 ev)

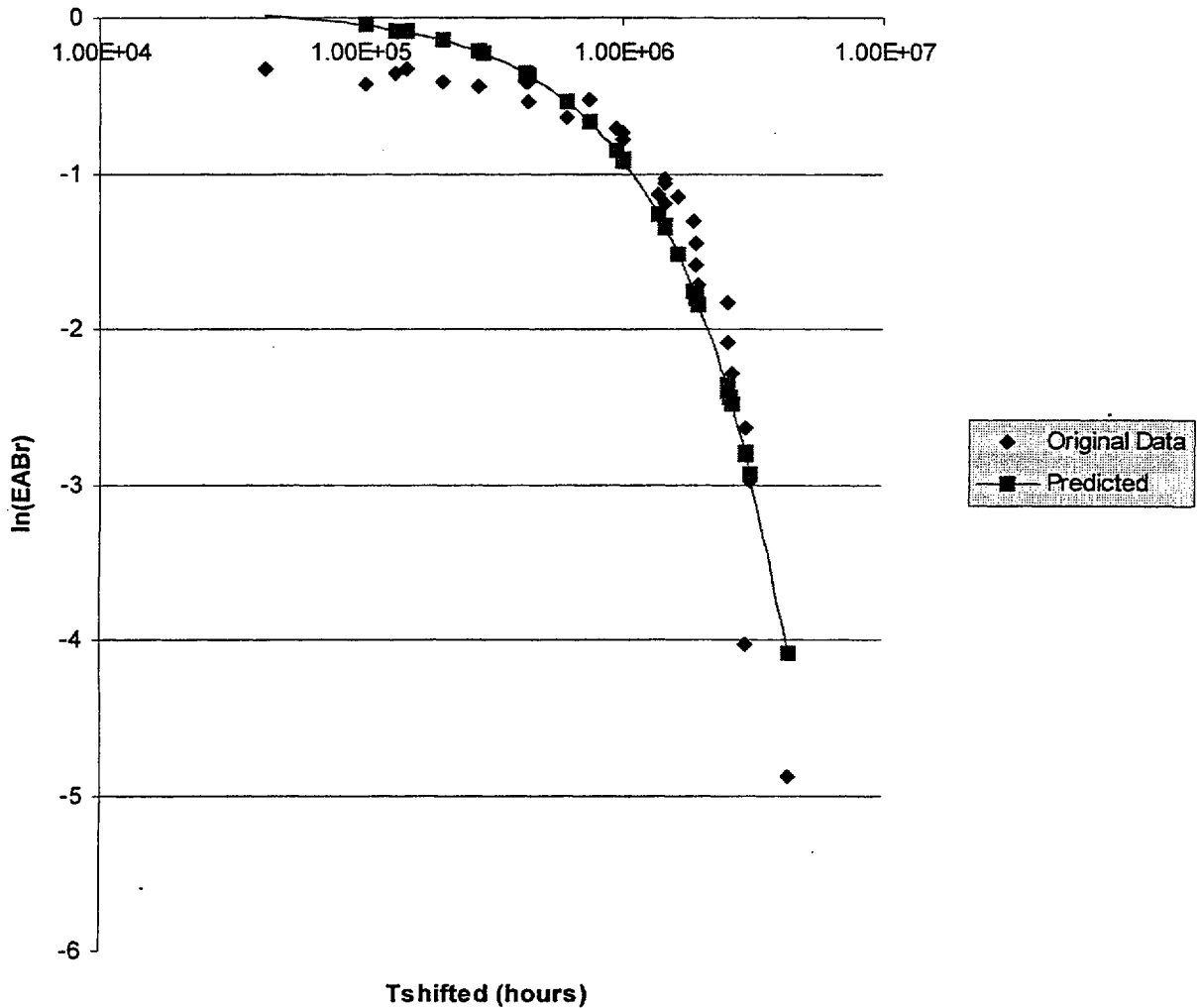


Figure 27 Determination of Activation Energy Using Time-Temperature Superposition

Relationship between EAB and h_0

A linear regression of $\ln(EAB)$ and h_0 was performed to determine the relationship between EAB and h_0 . The regression coefficients A and B are 6.02 and $-1.79E+11$, respectively. For example, for EAB of 100%, the corresponding h_0 is $7.905E-12$. Note that h_0 and t_{shifted} differ only by a multiplicative constant, i.e., $h_0 = t_{\text{shifted}} \exp[1/K_B/(273+45)]$. Therefore, the above two regression analyses are practically the same.

3.2.2 Combined Environment Data

The two different regression methods described in Section 2.4, linear and non-linear, were used with the original data of Figures 28-36 to estimate the values of parameters n and d . For the linear regression method, the values of n and d were estimated to be 0.883 and $2.831E-15$, respectively. SigmaPlot was used to minimize the error in h_0 of the no-interpolation approach. The resulting d and n were estimated to be $3.7115e-15$ and 0.8696 , respectively.

Table 3 compares the predictions of the linear regression method with the original data. Two comparisons are made, in terms of DED and EAB. The first five columns list the original data for each of the combined aging environments. The sixth column is the changes in resource h_0 predicted using the relationship between EAB and h_0 derived from thermal aging data, i.e., $\ln(\text{EAB}) = A + B * h_0$. The seventh column, the predicted DED (DED calc) for the given EAB or equivalently the corresponding predicted change in resource h_0 , was calculated as

$$D h_0/R(T,D) = D h_0 \exp(\beta E) / [1+d \exp(n\beta E)D^n]. \quad (3.2-1)$$

The eighth column, DEDcalc/DED, provides a measure of how good the prediction on DED is.

The ninth column lists the predicted change in resource for the aging time. It was calculated as

$$t R(T,D) = t \exp(-\beta E) [1+d \exp(n\beta E)D^n]. \quad (3.2-2)$$

The predicted change in resource was then used to calculate the predicted EAB in the tenth column, using $\ln(\text{EAB})=A+B*h_0$, again. Column eleven is the ratio of predicted EAB and EAB.

The comparison of Table 3 shows that the no-interpolation method consistently under-estimates the degradation for shorter aging times, and over-estimates for longer aging times.

Figures 28-36 plot the predicted aging curves of the two no-interpolation methods along with the original data, for different aging environments. To distinguish between the three types of curves, the points of the predicted curves using linear regression are marked by diamonds, the predicted curves using non-linear regression are marked by dots, and those of original data are marked by squares. They were plotted using Excel spreadsheet software which fits a smooth curve through the data points. The trending of the linear regression predictions shown in Table 3 can also be observed in the figures. That is, the predicted curves pass the curves of original data from above as time increases, with the exception that the 140 degrees C curve (Figure 36) actually crosses the curve of original data twice. This is due to the fact that the first two data points at 140 degrees C have approximately the same EAB. The curves predicted by the non-linear regression approach do not always cross the curves of the original data. For those that do, the crossing is from above. The curves of non-linear regression approach are always above those of the linear regression approach.

Table 3 Comparison of Predictions with Original Data

T _i (C)	D _i (Gy/hr)	(DED) _I (Gy)	t _i	EAB	h ₀ predicted from thermal	DEDcalc	DEDcalc/ DED	h ₀ predicted from t*R(T,D)	EAB(h ₀) from thermal	Ratio of predicted EAB and EAB
22.00	1.37e+01	3.6e+04	2592.00	306.00	1.658e-12	1.18e+05	3.33	4.979e-13	376.655	1.230899
22.00	1.37e+01	1.0e+05	7392.00	272.00	2.316e-12	1.65e+05	1.63	1.420e-12	319.3346	1.174024
22.00	1.37e+01	2.4e+05	17664.00	201.00	4.006e-12	2.86e+05	1.18	3.393e-12	224.2914	1.115878
22.00	1.37e+01	3.1e+05	22704.00	143.00	5.907e-12	4.21e+05	1.35	4.361e-12	188.5949	1.318846
22.00	1.37e+01	3.7e+05	26928.00	143.00	5.907e-12	4.21e+05	1.14	5.173e-12	163.0932	1.140512
22.00	1.37e+01	4.3e+05	31392.00	139.00	6.066e-12	4.33e+05	1.00	6.030e-12	139.8804	1.006334
22.00	1.37e+01	5.5e+05	40128.00	112.00	7.272e-12	5.19e+05	0.94	7.708e-12	103.5779	0.924802
22.00	9.06e+01	6.1e+04	672.00	326.00	1.305e-12	1.16e+05	1.91	6.841e-13	364.3052	1.117501
22.00	9.06e+01	2.3e+05	2592.00	238.00	3.062e-12	2.72e+05	1.16	2.639e-12	256.7316	1.078704
22.00	9.06e+01	5.0e+05	5520.00	173.00	4.843e-12	4.31e+05	0.86	5.619e-12	150.5569	0.870271
22.00	9.06e+01	1.0e+06	11064.00	105.00	7.632e-12	6.79e+05	0.68	1.126e-11	54.80759	0.521977
22.00	9.06e+01	2.4e+06	26928.00	31.00	1.445e-11	1.29e+06	0.53	2.741e-11	3.041275	0.09811
24.00	4.90e+02	7.1e+04	144.00	337.00	1.119e-12	1.17e+05	1.66	6.733e-13	365.0111	1.083119
24.00	4.90e+02	1.6e+05	336.00	303.00	1.713e-12	1.80e+05	1.09	1.571e-12	310.8137	1.025788
24.00	4.90e+02	3.3e+05	672.00	221.00	3.476e-12	3.64e+05	1.11	3.142e-12	234.6063	1.061567
24.00	4.90e+02	6.6e+05	1344.00	150.00	5.640e-12	5.91e+05	0.90	6.284e-12	133.6654	0.891103
24.00	4.90e+02	1.3e+06	2688.00	75.00	9.512e-12	9.97e+05	0.76	1.257e-11	43.38878	0.578517
30.00	2.14e+03	1.0e+05	48.00	303.00	1.713e-12	1.93e+05	1.88	9.106e-13	349.8278	1.154547
30.00	2.14e+03	2.1e+05	96.00	279.00	2.174e-12	2.45e+05	1.19	1.821e-12	297.1995	1.065231
30.00	2.14e+03	5.1e+05	240.00	211.00	3.734e-12	4.21e+05	0.82	4.553e-12	182.2339	0.863668
30.00	2.14e+03	9.3e+05	433.00	133.00	6.312e-12	7.12e+05	0.77	8.21e-12	94.60827	0.71134
30.00	2.14e+03	1.4e+06	671.00	71.00	9.818e-12	1.11e+06	0.77	1.273e-11	42.1549	0.593731
35.00	3.68e+03	1.4e+05	39.30	309.00	1.604e-12	1.78e+05	1.23	1.303e-12	326.121	1.055408
35.00	3.68e+03	4.1e+05	111.00	224.00	3.400e-12	3.78e+05	0.92	3.679e-12	213.1069	0.95137
35.00	3.68e+03	9.4e+05	255.00	143.00	5.907e-12	6.56e+05	0.70	8.452e-12	90.67523	0.634093
35.00	3.68e+03	1.1e+06	303.00	109.00	7.423e-12	8.24e+05	0.74	1.004e-11	68.20021	0.62569
35.00	3.68e+03	1.4e+06	375.00	71.00	9.818e-12	1.09e+06	0.79	1.243e-11	44.48682	0.626575
35.00	3.68e+03	2.0e+06	543.00	48.00	1.200e-11	1.33e+06	0.67	1.800e-11	16.41614	0.342003

Table 3 (Continued)

T _i (C)	D _i (Gy/hr)	(DED) _I (Gy)	t _i	EAB	h ₀ predicted from thermal	DEDcalc	DEDcalc/ DED	h ₀ predicted from t*R(T,D)	EAB(h ₀) from thermal	Ratio of predicted EAB and EAB
35.00	3.68e+03	2.4e+06	639.00	37.00	1.346e-11	1.49e+06	0.64	2.118e-11	9.286787	0.250994
38.00	9.55e+03	7.6e+04	8.00	320.00	1.408e-12	1.67e+05	2.18	6.447e-13	366.8827	1.146508
38.00	9.55e+03	2.3e+05	24.00	282.00	2.114e-12	2.51e+05	1.09	1.934e-12	291.2464	1.032789
38.00	9.55e+03	4.6e+05	47.80	211.00	3.734e-12	4.43e+05	0.97	3.852e-12	206.5922	0.97911
38.00	9.55e+03	7.6e+05	79.60	136.00	6.187e-12	7.33e+05	0.96	6.415e-12	130.5671	0.960052
38.00	9.55e+03	1.4e+06	143.50	75.00	9.512e-12	1.13e+06	0.82	1.156e-11	51.92707	0.692361
100.00	2.14e+03	6.7e+04	31.50	248.00	2.832e-12	1.23e+05	1.83	1.550e-12	312.0036	1.258079
100.00	2.14e+03	1.5e+05	71.25	258.00	2.611e-12	1.14e+05	0.74	3.505e-12	219.8361	0.852078
100.00	2.14e+03	4.6e+05	214.00	126.00	6.614e-12	2.88e+05	0.63	1.053e-11	62.52007	0.496191
100.00	2.14e+03	8.7e+05	405.70	65.00	1.031e-11	4.49e+05	0.52	1.996e-11	11.55275	0.177735
100.00	2.14e+03	1.2e+06	549.50	24.00	1.588e-11	6.91e+05	0.59	2.703e-11	3.255287	0.135637
120.00	2.18e+03	7.0e+04	32.00	248.00	2.832e-12	8.90e+04	1.28	2.219e-12	276.7653	1.115989
120.00	2.18e+03	1.5e+05	71.00	235.00	3.133e-12	9.85e+04	0.64	4.924e-12	170.5367	0.725688
120.00	2.18e+03	4.7e+05	214.00	61.00	1.067e-11	3.35e+05	0.72	1.484e-11	28.8895	0.473598
120.00	2.18e+03	8.8e+05	405.00	5.00	2.464e-11	7.74e+05	0.88	2.808e-11	2.69674	0.539348
140.00	2.12e+03	4.2e+04	20.00	235.00	3.133e-12	5.59e+04	1.32	2.376e-12	269.1071	1.145136
140.00	2.12e+03	6.6e+04	31.00	231.00	3.229e-12	5.76e+04	0.88	3.682e-12	212.9711	0.921953
140.00	2.12e+03	1.5e+05	71.00	71.00	9.818e-12	1.75e+05	1.16	8.434e-12	90.95985	1.281125
140.00	2.12e+03	3.0e+05	142.00	5.00	2.464e-11	4.40e+05	1.46	1.687e-11	20.09273	4.0185

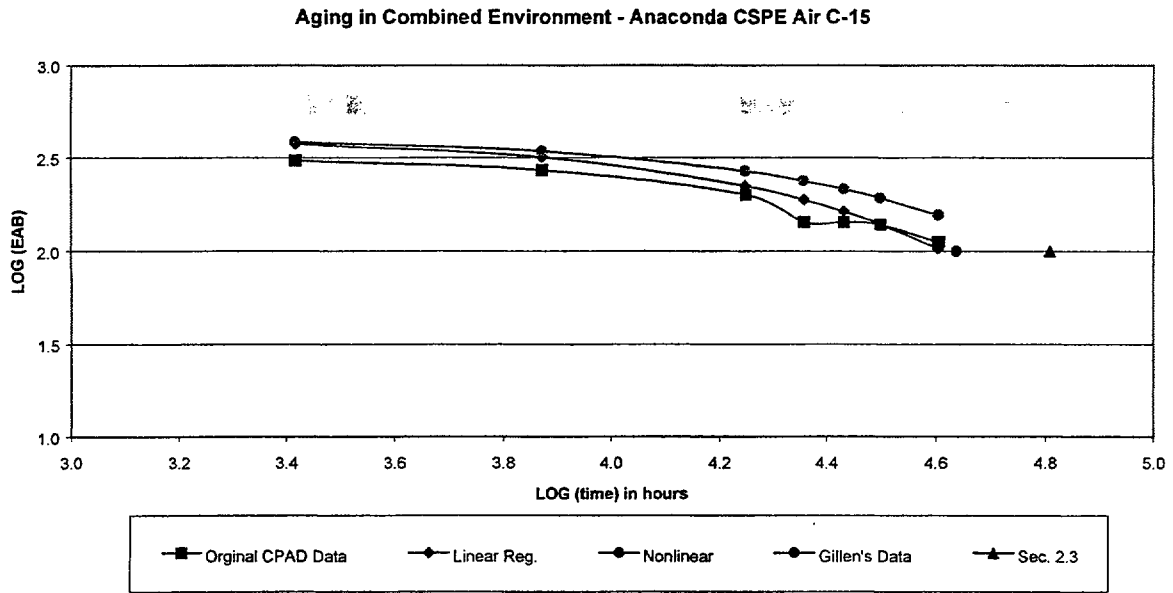


Figure 28 Comparison of Different Prediction Methods - 22 C and 13.7 Gy/hr

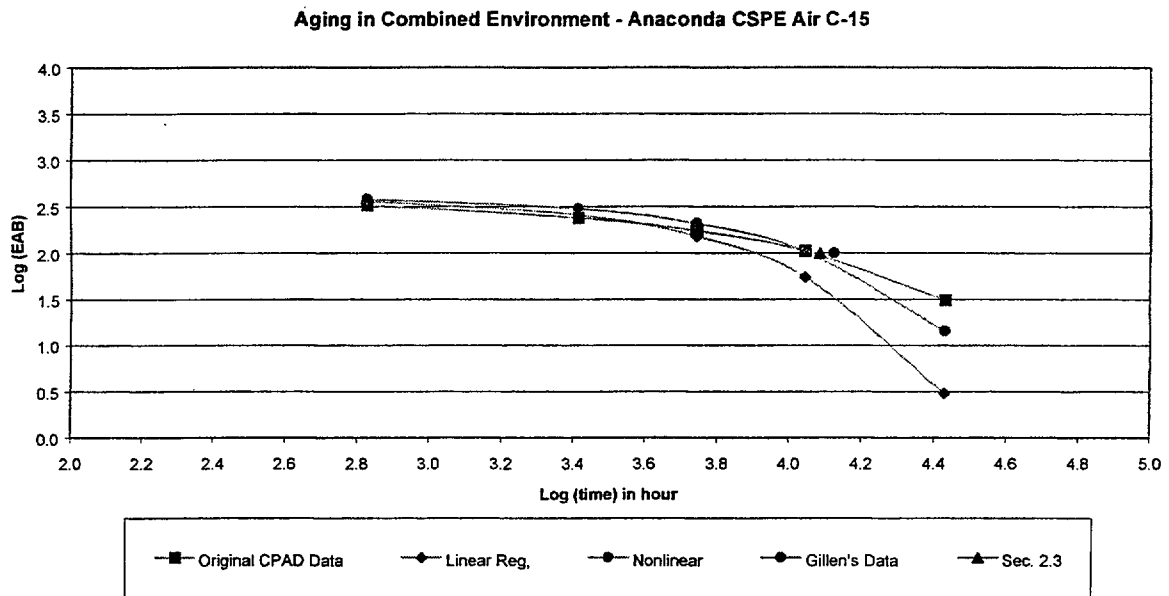


Figure 29 Comparison of Different Methods- 22 Degree C, 90 Gy/hr

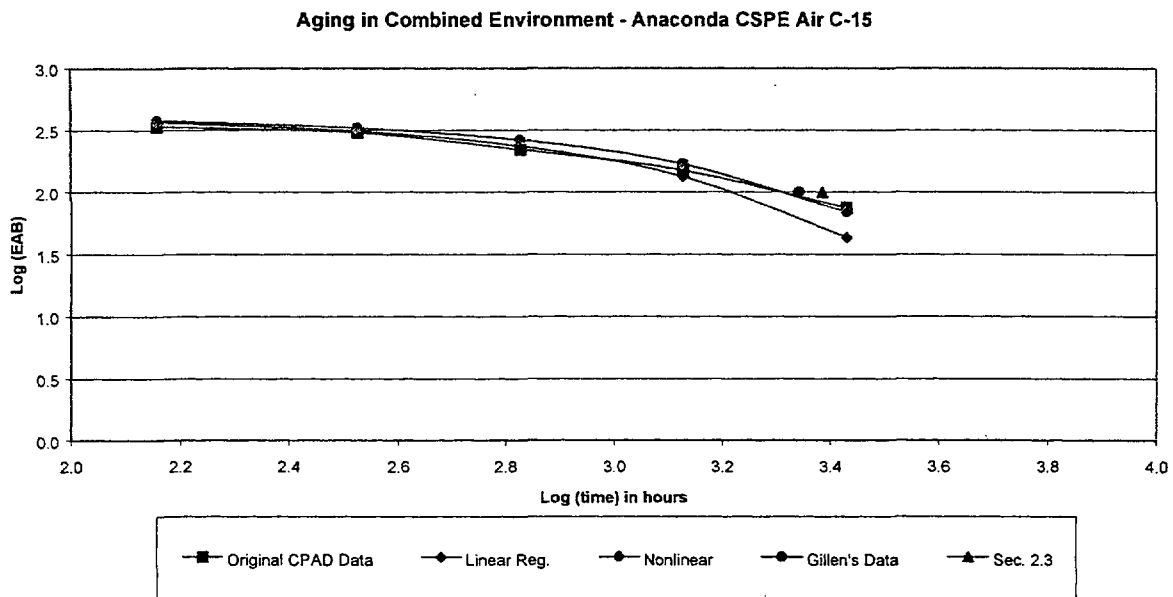


Figure 30 Comparison of Different Methods- 24 Degree C, 490 Gy/hr

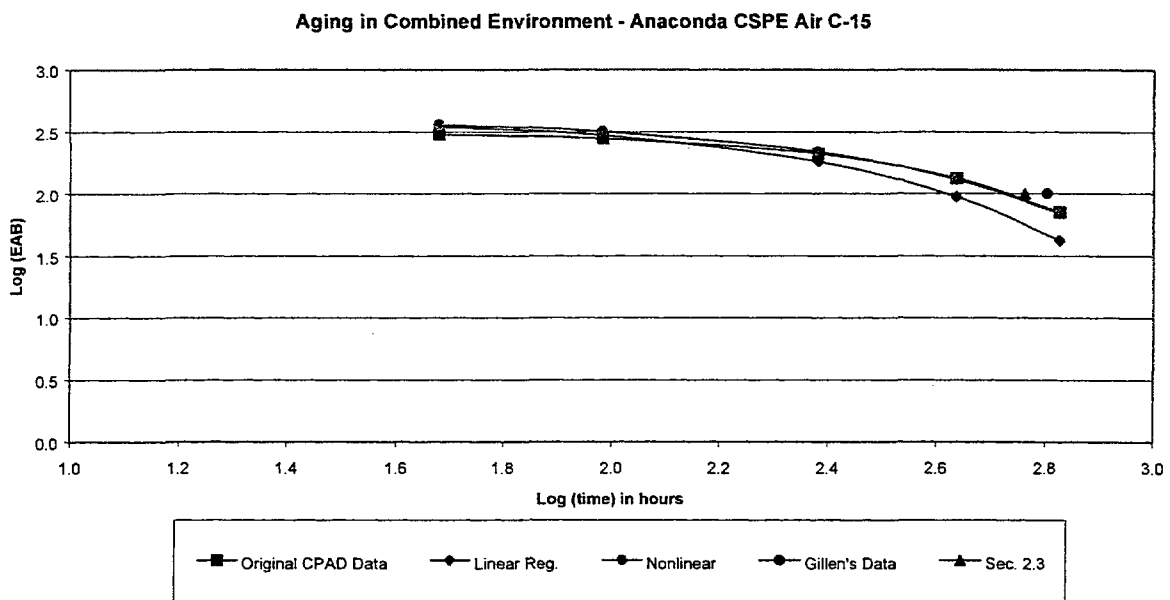


Figure 31 Comparison of Different Methods- 30 Degree C, 2140 Gy/hr

Aging in Combined Environment - Anaconda CSPE Air C-15

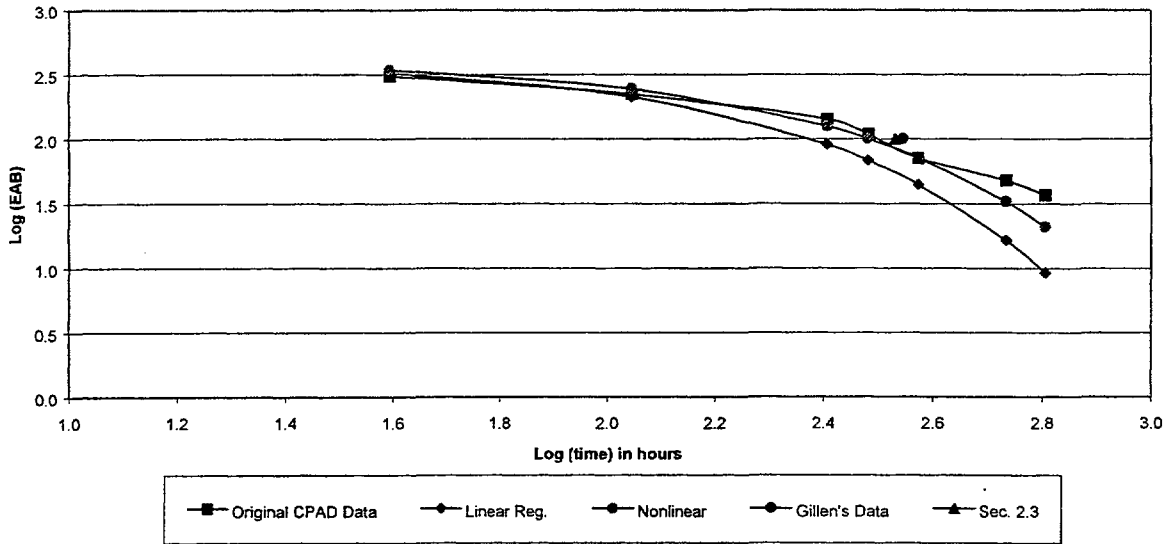


Figure 32 Comparison of Different Methods- 35 Degree C, 3680 Gy/hr

Aging in Combined Environment - Anaconda CSPE Air C-15

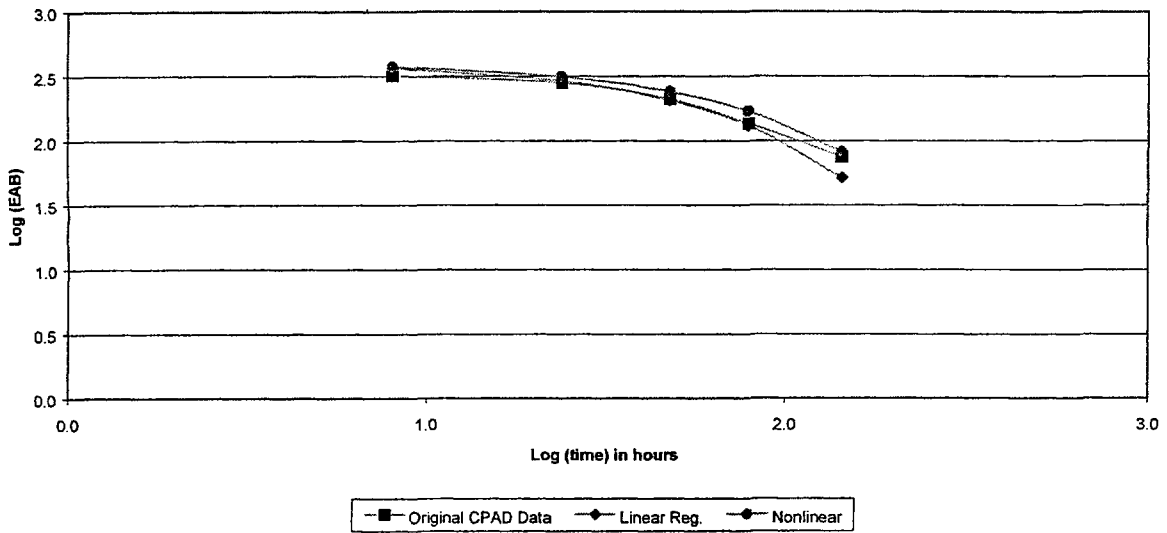


Figure 33 Comparison of Different Methods- 38 Degree C, 9550 Gy/hr

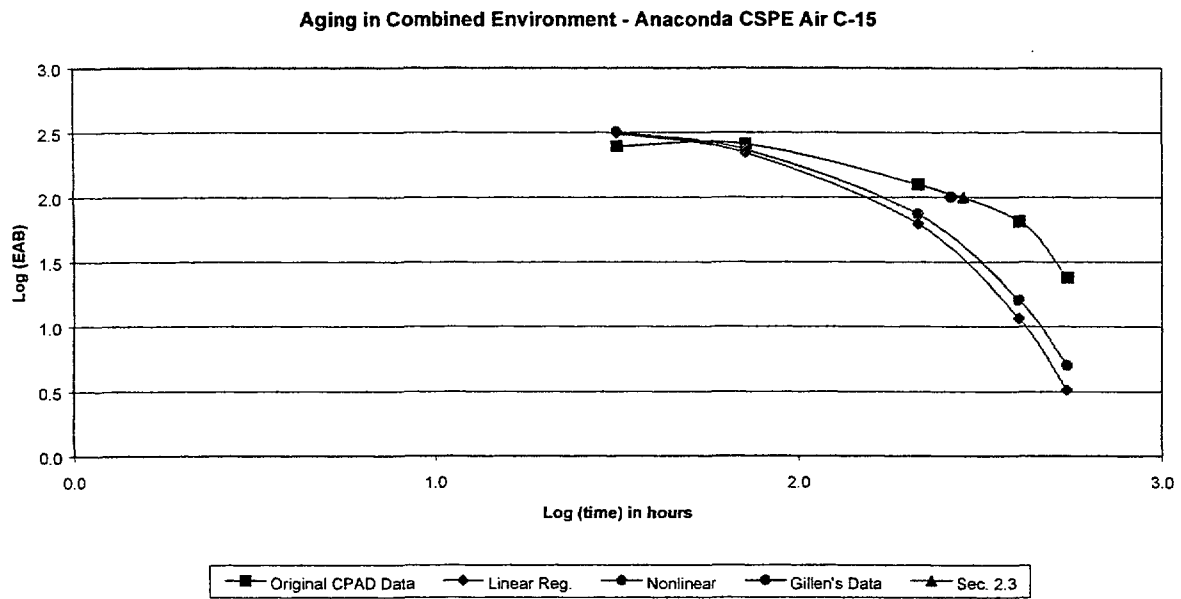


Figure 34 Comparison of Different Methods- 100 Degree C, 2140 Gy/hr

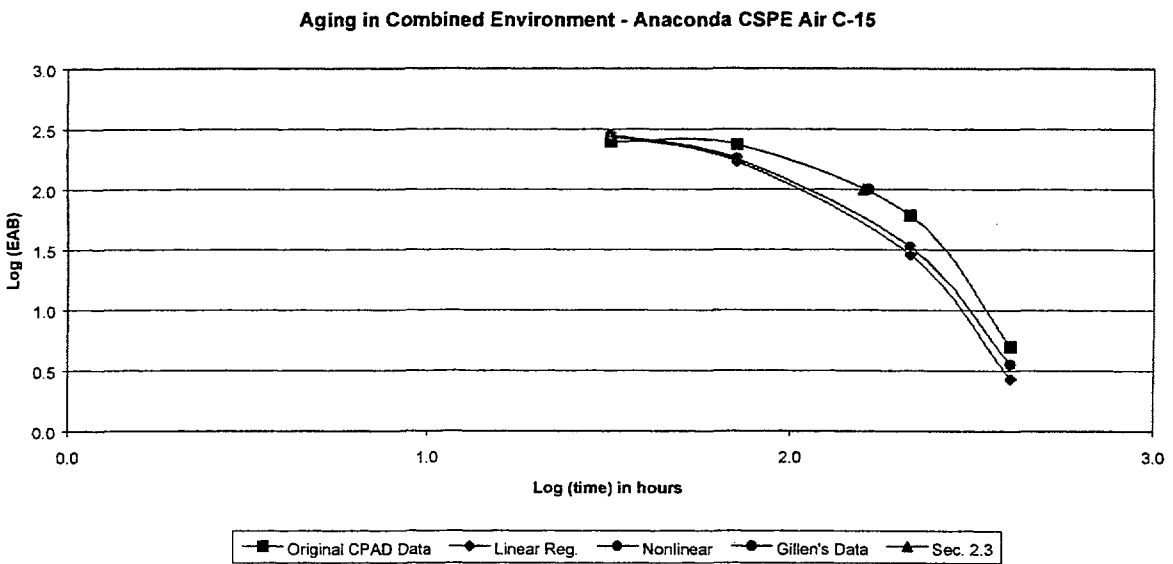


Figure 35 Comparison of Different Methods- 120 Degree C, 2180 Gy/hr

Aging in Combined Environment - Anaconda CSPE Air C-15

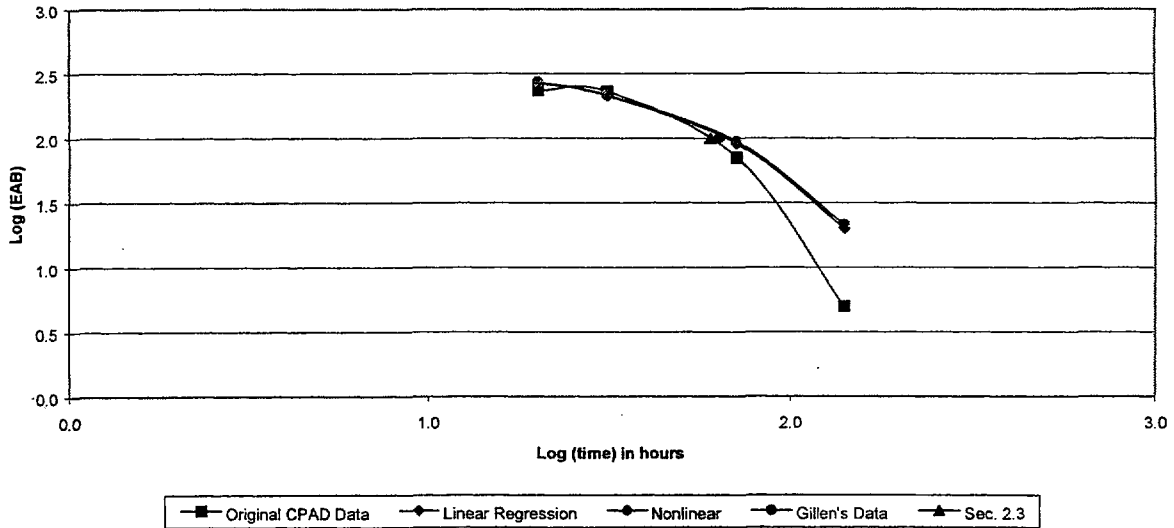


Figure 36 Comparison of Different Methods- 140 Degree C, 2120 Gy/hr

Also included in the figures are the 100% EAB data of Gillen's report and the predictions made using the approach of Section 2.3. The two data points of the same aging environment are marked by a dot and a triangle, respectively, at Log(EAB) of 2.0, i.e., EAB=100%. The distance between the two data points represents the error of the approach of Section 2.3 as compared to Gillen's data. Note that Gillen obtained his data by interpolation, and the Excel curves of the original data also use interpolation. The two approximations are not identical but always pretty close. It can be seen that the linear regression approach, as compared to the approach of Section 2.3, fits the 100% EAB data better at (22 degrees C, 13.7 Gy/hr) (Figure 28), and worse for all other environments. The non-linear regression approach gives better predictions than those of the linear regression approach, except for (22 degrees C, 13.7 Gy/h) and (140 degrees C, 2120 Gy/h) (Figure 36). At lower temperatures, i.e., 22 to 35 degrees C, the non-linear regression approach gives predictions that are as good as those of Section 2.3 approach, if not better. At higher temperatures, the predictions are not as good.

Figure 37 is a plot of the predicted DED versus dose rate curves at 45 degrees C for an EAB of 100% using different methods. The curves and their comparison are discussed below.

The first two methods and their results have been discussed in Section 3.1.1.

1. Gillen's Shifting Method

This is commonly known as the time-temperature-dose-rate superposition method. That is, the dose rates that would produce the same damage in different environments are related by Equation 2.2-1. If the method holds, it can be used to make predictions about lower temperature and lower dose rate environments, once the activation energy is determined. The predictions of this method are considered the original test data, for the purpose of comparing the predictions of different methods. Figure 37 plots the DED of accelerated aging environments versus the dose rate shifted to 45 degrees C. All other methods use Equation 2.3-14 for making predictions, and use the same activation energy derived by Gillen. They differ in the way the parameters n and d is estimated.

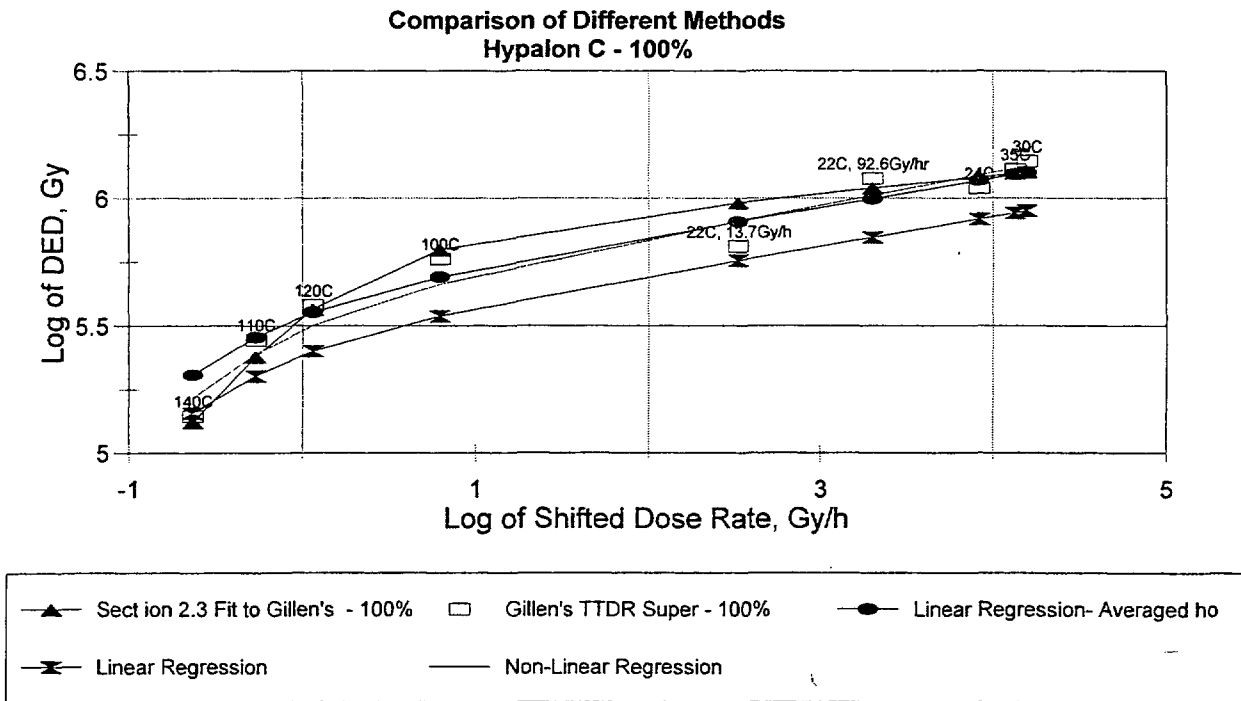


Figure 37 Comparison of Different Prediction Methods - DED VS D (Hypalon C)

2. Section 2.3 Approach

This is the basic approach of this study. As discussed in Section 3.1, it fits the results of time-temperature-dose-rate superposition method well, with the exception of the data at 22 degrees C and 13.7 Gy/hr.

The next three methods are based on the no-interpolation approach discussed in Section 2.4. They estimate the values of parameters h_0 , n , and d differently using the CPAD database, and are used to make predictions about time to 100% EAB for the aging environments of Gillen's report.

Since the CPAD database does not have data at 110 degrees C, the prediction at 110 degrees is a true prediction that does not appear in Figures 28 to 36. At other temperatures, the predictions are more like a fit to the results of time-temperature-dose-rate superposition method.

3. Linear Regression

In this approach, the predicted DED for each aging environment is calculated as

$$D \cdot t_{\text{Predicted}} = D h_0 / R(T,D) = D h_0 \exp(\beta E) / [1 + d \exp(\beta E n) D^n], \quad (3.2-3)$$

where $t_{\text{Predicted}}$ is the predicted time to 100% EAB; h_0 is the change in resource corresponding to the damage level and was estimated using the relationship between change in resource and EAB, i.e., $\text{Log}(EAB) = A + B \cdot h_0$, to be $7.905E-12$; and the values of n and d were estimated by the linear regression analysis discussed in Section 2.4.1. This value of h_0 differs from the h_0 's predicted by $t^* R(T,D)$ for different test environments, where t is the time to 100% EAB estimated in Gillen's report (Ref. 9) by

interpolation of the original test data. The next approach is an attempt to address this difference. Similar to Figures 28 to 36, Figure 37 shows that the linear regression approach, in comparison with the method of Section 2.3, gives better results at (22 degrees C, 13.7 Gy/hr) and (140 degrees C, 2120 Gy/hr), and worse results at all other aging environments, including the 110 degrees C data point which was not predicted in Figures 36. Note that the (22 degrees C, 13.7 Gy/hr) data shown in Figure 28 has a weird turn. This may be the cause of the inconsistent results of the method of Section 2.3.

4. Linear Regression with Averaged h_0

This approach is a modification of the linear regression approach. Instead of the h_0 determined using the relationship between h_0 and EAB derived from thermal aging data, the mean of the predicted h_0 's calculated using $t * R(T,D)$, i.e., 1.122E-11, was used. Therefore, the predicted curve of this approach differs from the predicted curve using the linear regression approach by a multiplicative factor which is equal to ratio of the two values of h_0 . This factor is approximately 1.42. Comparing to the linear regression approach, this approach makes better predictions at all environments except for (140 degrees C and 2120 Gy/hr).

5. Non-linear Regression

This approach, as compared with the linear regression approach, uses a different method for estimating n and d , and is identical otherwise. In comparison with the linear regression approach, its prediction is worse at (140 degrees C, 2120 Gy/hr), and better at all other data points.

3.2.3 Summary Discussion on No-interpolation Approach

In general, the predictions obtained without interpolation are not as good as those obtained using the method of Section 2.3 which has been applied at selected damage levels only. You simply can not use a simple formula to fit a wide range of environments and damage levels, and expect good fit everywhere. One may consider the three no-interpolation methods as different modeling assumptions. Maybe the results obtained from the no interpolation approach is a more realistic reflection of the variability of the data. If the uncertainties are properly accounted for, i.e., parameter and modeling uncertainty, the results of the approach may be able to envelop the original data.

In the approach of Section 2.3 as well as Gillen's time-temperature-dose-rate superposition approach, data for a selected damage level are required. Actual test data such as those reported in the CPAD database are not of the required format. Gillen has to use interpolation of the original data to determine a point estimate of the time to a specific damage level. The interpolated data was then used for the rest of the analysis. When the uncertainty associated with interpolation and extrapolation is properly accounted for, wider scattering in the predictions as compared with the original data is expected.

As a result of the way the no interpolation approach was developed, the prediction of the approach reproduces exactly the thermal only aging data that was used in estimating the relationship between h_0 and EAB.

3.3 Other Numerical Results Based of Reliability Physics Approach

3.3.1 Comparison of Different Fitting Methods

This section provides a comparison of the different fitting methods used in preparing the data needed in our reliability physics model. The Hypalon C material of Gillen's report was selected in the evaluation. It is a jacket material trade named "Flameguard" made by Anaconda. As discussed in Section 3.2, this material should be the same CSPE jacket material designated as C-14 and C-15 in the CPAD data base. One hundred percent (100%) EAB was used as the damage level.

The following three methods were used in the comparison.

1. Gillen's Method

Gillen's report (Ref. 9) only presented processed data in the form of DED as a function of test environment and damage level. Often, damage levels of 100% EAB and 60% relative EAB were used. Due to the understanding that the raw test data is unlikely to yield results exactly equal to these damage level, we believe that interpolation was done on the raw data. The exact method of interpolation is not known. In this study, the data in the report was discretized manually and used in the reliability physics calculations.

2. Linear Interpolation of CPAD Data

The data reported in CPAD is in the form of EAB as a function of test environment and aging time. Besides the minor discrepancy discussed in Section 3.2, the test environments of the material agree with those of Gillen's report. In Reference 25, Gillen stated that typically three or more samples were tested and the data averaged to obtain the results. This is probably how the data reported in CPAD was arrived at. In this method, for each aging environment, a linear interpolation using the table of $\ln(\text{EAB})$ versus $\ln(\text{aging time})$ was performed to obtain the data at 100% EAB.

3. Regression Fit of CPAD Data

In this method, for each test environment, a linear regression was performed on the natural logarithm of EAB and aging time to obtain the time when 100% EAB is reached.

The data obtained from the above three fitting methods agree reasonably well. Table 4 lists the parameters of the reliability physics model, estimated using the data of the three fitting methods. Figure 38 plots the predictions of the three methods. It can be seen that the three curves are close to each other. In the high dose rate range where most of the original data are located, i.e., above 1 Gy/hr, the curves match separately the original data well, and as a result, agree with each other well. In the low dose rate range, i.e., dose rates below $1\text{E-}2$ Gy/hr, the curves become straight lines representing that radiation contributes little to the degradation, and the difference between the lines are driven by the difference in the estimated h_0 which is not very large. In the transition range, i.e., dose rate between $1\text{E-}2$ and 1 Gy/hr, which is probably the most interesting range because it represents the range likely seen inside the containment, the difference between the curves are bounded by the differences of the two other ranges.

Table 4 Estimated Parameters of Hypalon C Using Different Fitting Methods

Material	h_0 (hour)	d	n	Activation Energy (ev)
Gillen's Report	4.558e-12	1.100e-16	0.9305	1.084
Regression Fit to CPAD Data	3.183e-12	6.179e-17	9.37	1.084
Linear Fit to CPAD Data	4.123e-12	4.055e-17	0.951	1.084

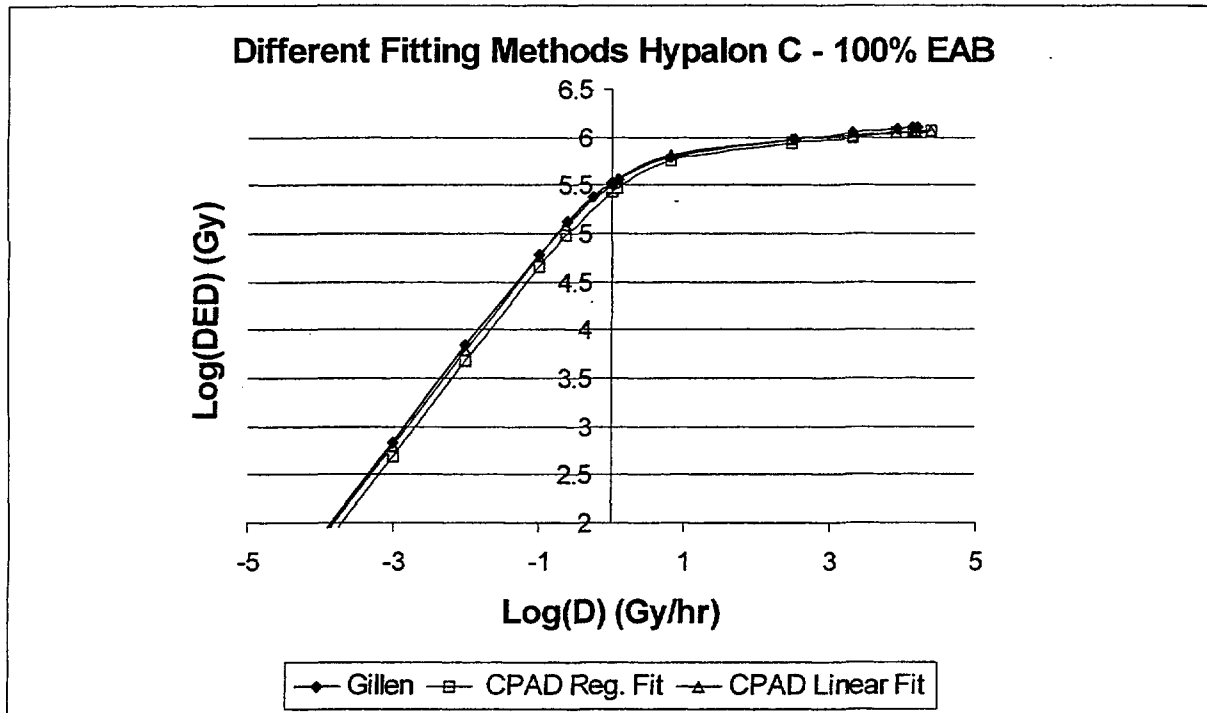


Figure 38 Comparison of Different Fitting Methods

3.3.2 Manufacturer to Manufacturer Variability for CSPE

It is well known that the same generic materials made by different manufacturers may have very different chemical compositions and additives, and age differently. This is demonstrated in the wide ranges of the reported thermal activation energies (Ref. 26). Therefore, it is not appropriate to use the aging data of one manufacturer for the material of a different manufacturer.

In this study, it was recognized that five of the CSPEs analyzed by SNL and reported in the CPAD data base have approximately the same activation energy, i.e., 1.08ev of the Hypalon C in Gillen's report (Ref. 9). The five CSPEs are listed in Table 5. The activation energy of a material was determined by using thermal aging data with the method of time-temperature superposition. That is, visual observation of the shifted data was made, and the value of activation energy that gives the least scattering is the correct value. The visual observation is a crude way of estimating activation energy. Using this

activation energy in our analysis of the five CSPEs, we obtained reasonably good results comparing with those of the time-temperature-dose-rate superposition approach. Appendix A has the comparisons plotted.

Table 5 summarizes the calculations with the estimated parameters of the materials. Figure 39 plots the DED vs. D curves of them. In the higher dose rate range, i.e., dose rate larger than 10 Gy/hr, the predictions diverge indicating the materials do behave differently. Another reason for the divergence could be because four out of five materials have no more than four data points each and do not have shifted dose rates above 1E2 Gy/hr. In the range of dose rate that is typically observed inside the containment, i.e., below 1 Gy/hr, the curves form a pretty closed band. At 1Gy/hr, the DEDs differ by no more than 50%. This observation seems to indicate that if we use the aging data of a different manufacturer of the same CSPE, the largest error is approximately 50%.

Table 5 Summary of Calculations of CSPEs of Different Manufacturers

Material	h_0 (hour)	d	n
Anaconda CSPE C-14, C-15	4.123e-12	4.055e-17	0.951
Samuel CSPE C-9	5.520e-12	7.233e-18	1
Anaconda CSPES jacket C-10	5.230e-12	1.421e-17	0.991
Rockesbestos CSPES C-11 100	7.368e-12	9.720e-18	1
Eaton CSPES C-5	5.698e-12	2.427e-14	0.807

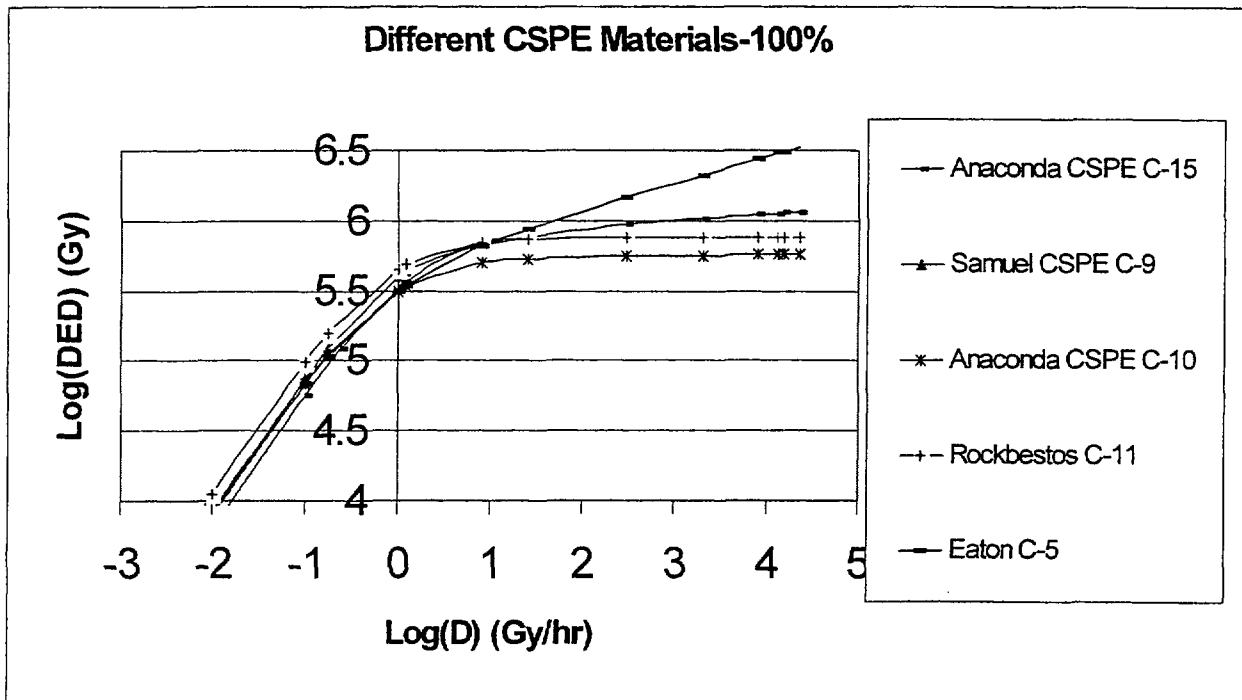


Figure 39 Comparison of Different CSPEs

4. LIMITATIONS OF THE APPROACH

Aging Only During Normal Operation Considered.

Our method only considers the degradation during normal operation and not during the LOCA. This means that it cannot be used to estimate the degradation level of the cable insulation as a function of the time during the LOCA. One cannot, for LOCA conditions, merely use the same formula with time varying temperature and dose rate. One problem with doing this is that initially during the LOCA the intermediate degradation products that have been built up during normal operation decay into the final degradation products. This means that initially during the LOCA, and perhaps for some days after the LOCA begins, the degradation depends on the dose rate before the LOCA, as well as the temperature during the LOCA. The effect here is similar to the effect that the amount of aging that occurs in a cable polymer depends on the order in which radiation aging and thermal aging are applied. The aging is generally greater when radiation aging is applied before thermal aging than in the opposite order, or if both thermal and radiation aging are applied simultaneously.

Estimates of Time to Failure Depend Only on Physical Condition of Cable.

Our estimates of time to critical embrittlement level depend only on the selection of a critical level of embrittlement of the cable. However, a cable which is embrittled to any selected embrittlement level may not fail if it is not subject to much handling during normal operation, and is not subject to appreciable forces during the LOCA.

Requirement of Validity of Time-temperature-dose-rate Superposition Method.

Our reliability physics model depends heavily on the validity of the time-temperature-dose-rate superposition method. Gillen found that some materials obey time-temperature-dose-rate superposition, and others do not. In some cases, the use of a temperature dependent activation energy results in good agreement with experimental data, while use of temperature independent activation energy does not. As noted in Section 2.2, the validity of time-temperature-dose-rate superposition does not depend on the validity of the Arrhenius law with a constant activation energy. It is possible that more basic research on the kinetics of aging phenomena will assist in the development of models where time-temperature-dose-rate superposition does not hold.

Variability in Material Composition and Additives.

The reliability physics model is capable of accounting for the variability of material property along the length of a cable, as discussed in Section 2.5, but its applicability is limited to the specific cable material made by the specific manufacturer for which accelerated aging data is available. It is desirable to develop a model that is capable of making predictions about a different material of the same generic class, e.g., CSPES, made by the same manufacturer or a different manufacturer. Section 3.3.2 represents an attempt in this direction.

S-shaped Curves.

According to Gillen's analysis, some materials, i.e., EPR A and B, and CLPO C, do have S-shaped DED vs. D curves. The form of the empirical formula of our model, i.e., Equation 2.3-13, does not take on a S-shape. Therefore, our model is not able to model the S-shapeness well. However, as discussed in Section 3.1, our models still is able to approximately fit the data of these materials. Nevertheless, there is a region of low shifted dose rate where there is little or no experimental data, and it is not clear whether

our model fits this range well, or, indeed how an empirically developed time temperature dose rate superposition curve should be extrapolated to this low shifted dose rate region. It is possible that the use of data for thermal only aging would help here, in developing an approximation.

Annealing Effect That Improves Mechanical Properties.

The Arrhenius equation is a widely accepted method for making life predictions in thermal only environments. Depending on the temperature, the governing aging mechanism may not be the same. For example, CSPES has a change in activation energy at approximately 120 degree C (Ref. 12). A similar issue arises in the case of aging in a combined environment. Gillen indicated that there is a change in degradation mechanism between 100 and 70 degree C for CLPO A of his analysis (Ref. 9). Section 2.2 showed that time-temperature-dose-rate superposition did not depend on a constant activation energy, and Section 2.3 showed that a particular form for the temperature dependence of the activation energy resulted in a good fit to the data, for CLPO-A and CLPO-B. The underlying phenomena appear to be associated with annealing effects in which the mechanical property of the material actually improved (Ref. 22). As noted above, our method does not handle cases where the dose rate and temperature change abruptly, as during a LOCA, and could not handle the annealing effects which may occur during a LOCA.

5. SUMMARY

This report presented a method for predicting the probability the insulation of an aged instrumentation or control cable inside of containment would reach a given level of embrittlement in a given time, which depends on the dose rate and temperature which the cable is exposed to during service conditions. The embrittlement of the cable is measured by the EAB of the cable insulation, and the greater the EAB of the cable, the less embrittled the cable insulation is. The failure mechanism of the cable being considered is that of the embrittled cable insulation cracking and resulting in leakage currents, either between two conductors within the same cable or between the conductors and ground. Typically, if the absolute EAB of the cable insulation is greater than 50%, it is assumed that the cable will perform its function in a LOCA. However, cables with severely embrittled insulation have successfully passed LOCA tests, so it cannot be assumed that cables with insulation EAB less than 50% (absolute) will fail in a LOCA. Note also that even if a cable fails to perform its function during a LOCA, it may fail late in the LOCA, when its failure may be less risk significant.

The reason for focusing on cables inside of containment is that they are liable to a potential common mode failure mechanism, since cables associated with redundant trains of a system are exposed to the same or similar harsh environment after a LOCA. The reason for focusing on instrumentation and control cables as opposed to power cables is that instrumentation and control cables are more sensitive to leakage currents, which could cause misleading operation indications, and failure of automatic actuation of equipment.

The concept of cable resource or capacity, discussed by Carfagno & Gibson (Ref. 6), is chosen as the starting point of the method. The connection with the constant wearout method of Gillen is shown. (The method of degradation of the cable resource applies to degradation by both temperature and radiation; although Gillen discusses the constant wearout method for pure thermal aging only, the method of extension is clear.) The time-temperature-dose-rate method of Gillen was reviewed, and a formula based on a formula in IEC-1244-2, was used to predict a central estimate of the time to a given level of degradation of cable insulation (or jacket material) subjected to a given temperature and dose rate during inservice conditions. The method used obeys time-temperature-dose-rate superposition. When time-temperature-dose-rate superposition holds, the dose to equivalent degradation is a function of dose rate and temperature only in a combination called the shifted dose rate. (Of course, a constant times the shifted dose rate can also be used.) The constants in the formula used for the rate of change of resource $R(T,D)$ (Equation 2.3-13) were obtained by fitting to data of Gillen, by different methods. In some cases, where the conventional time-temperature-dose-rate method failed to give good results with data, good agreement could be obtained (see Figures 2 and 3), by use of a temperature dependent activation energy. The use of a temperature dependent activation energy is within the framework of time-temperature-dose-rate superposition and was derived from dimensional considerations, under the assumption of a single rate-determining constant in the degradation of the polymer.

In some cases, time-temperature-dose-rate superposition holds, but the dose to equivalent degradation vs. shifted dose-rate curve is S-shaped. It was found that even here reasonable estimates of a central estimate of the time to a given level of degradation could be obtained, for a certain range of shifted dose rates, even basing the method on Equation 2.3-13, which cannot describe an S-shaped curve. However, it would be difficult to make a prediction for low dose rates, for such materials, without modification of Equation 2.3-13.

Up to this point, only a method for predicting a central estimate of the time for a cable polymer to reach a given level of degradation has been given. It is still necessary to obtain a probability distribution for the time to reach this given level of degradation. One would expect, based on extreme value theory, that this

probability distribution would be a Weibull distribution, whose parameters would depend on the length of the cable. In an example case (see Section 3.1.2), the Weibull distribution was found to fit the data well. The dependence of the parameters of the Weibull distribution on the length of the cable being studied was investigated, so that the probability distribution for a length of cable of interest, perhaps 3.05 meters (10 feet), could be obtained from the experimental measurements on 5.08-centimeter (two-inch) cable lengths (see Section 2.1). A method for treating the (state-of-knowledge) uncertainty in the parameters of the Weibull distribution was briefly discussed, but not implemented because of resource limitations.

Section 3 and the Appendix present various numerical results. Section 4 discusses limitations of the method.

This work only considered models for determining the time when instrumentation and control cables would reach a critical level of embrittlement. The critical level of embrittlement can be used to support an assessment of the probability that the cable will fail to perform its function if exposed to a loss of coolant accident (LOCA). It would be desirable to continue this work, to estimate the probabilities that the cables with a critical level of insulation embrittlement would fail given a LOCA, and use the failure probabilities as a function of time in a probabilistic risk assessment to estimate the contributions to the core damage frequency of the failure of these cables.

6. REFERENCES

1. Subudhi, M., "Literature Review of Environmental Qualification of Safety-Related Electric Cables," NUREG/CR-6384, BNL-NUREG-52480, Vol. 1, p. 6-3, and p. 7-8 (1996).
2. Buslik, Arthur, "Inclusion of Cable Aging in Probabilistic Risk Assessment with the Use of Reliability Physics Modeling," PSAM6, 6th International Conference on Safety Assessment and Management, San Juan, Puerto Rico, June 23-28, 2002.
3. Smith, C. L., Shah, V. N., Kao, T., and Apostolakis, G., "Incorporating Aging Effects into Probabilistic Risk Assessment - A Feasibility Study Utilizing Reliability Physics Models," NUREG/CR-5632, Idaho National Engineering and Environmental Laboratory, August 2001.
4. Gillen, K. T., and Clough, R. L., "Quantitative Confirmation of Simple Theoretical Models for Diffusion-Limited Oxidation," Radiation Effects on Polymers, R.L. Clough and S. Shalaby, Editors, ACS Symposium Series, Oxford University Press, May 1991.
5. Reynolds, A.B., Bell, R.M., Bryson, N.M., et al., "Dose-Rate Effects on the Radiation-Induced Oxidation of Electric Cable Used in Nuclear Power Plants," Radiation Physics and Chemistry, 45 (1) pp. 103-110, 1995.
6. Carfagno, S.P., and Gibson, R.J., "A Review of Equipment Aging Theory and Technology," Franklin Research Center, EPRI NP-1558, September 1980.
7. Gillen, K.T., and Celina, M., "The Wear-out Approach for Predicting the Remaining Lifetime of Materials," Polym. Degrad. Stabil., 71, 15 (2001).
8. Rudd, H.J., "Time Temperature Dose-Rate Superposition Behavior in Irradiated Polymers," Material Development Division, Harwell Laboratory, AERE-R13746, 1990.
9. Gillen, K.T, and Clough, R.L., "Predictive Aging Results for Cable Materials in Nuclear Power Plants," Sandia National Laboratories, SAND90-2009, November 1990.
10. Gillen, K.T, Celina, M., and Clough R.L., "Limitations of the Arrhenius Methodology," Water Reactor Safety Information Meeting, 1998.
11. "Determination of Long-Term Radiation Aging in Polymers-, Part 2: Procedures for Predicting Aging at Low Dose Rates," International Electrotechnical Commission, IEC 1244-2, First Edition, 1996-02.
12. "Assessment and Management of Aging of Major Nuclear Power Plant Components Important to Safety: In-Containment Instrumentation and Control Cables," LAEA-TECDOC-1188, Volumes 1 and 2, December 2000.
13. Gillen, K.T., and Clough, R.L., "Time-Temperature-Dose Rate Superposition: A Methodology for Extrapolating Accelerated Radiation Aging Data to Low Dose Rate Conditions," Polymer Degradation and Stability 24 (1989) 137-168.
14. Bolland, J.L., Proc. Roy. Soc., A186(1946) 218.

15. Gillen, K.T., and Clough, R. L., "Aging Predictions in Nuclear Power Plants- Crosslinked Polyolefin and EPR Cable Insulation Materials," Sandia National Laboratories, SAND91-0822, June 1991.
16. Cable Polymer Aging Database, EPRI Palo Alto, CA, and U.S. Department of Energy: 2002. 1001001.
17. SigmaPlot 2002 for Windows, Version 8, Copyright© 1986-2001, SPSS Inc.
18. See, for example, http://www.weibull.com/AccelTestWeb/graphical_method.htm.
19. Press, W.H., Teukolsky, S.A., Vetterling, W.T., Flannery, B.P., Numerical Recipes in Fortran 77, The Art of Scientific Computing, Section 15.6, Second Edition, Copyright ©) 1986-1992 by Cambridge University Press.
20. QuattroPro, Version 8.0, Corel Corporation and Corporation Limited, 1997.
21. Gillen, K.T., and Clough, R.L., "Techniques for Monitoring Heterogeneous Oxidation of Polymers", in Handbook of Polymer Science and Technology, Vol. 2, Performance Properties of Plastics and Elastomers, Cheremisinoff, N.P., Ed., Marcel Dekker, New York, 1989.
22. Celina, M., Gillen, K.T., Wise, J., and Clough, R.L., "Anomalous Aging Phenomena in a Crosslinked Polyolefin Cable Insulation," Radiat. Phys. Chem. Vol. 48, No. 5, pp. 613-626, 1996.
23. Jacobus, M.J., "Aging, Condition Monitoring, and Loss-of Coolant Accident (LOCA) Tests of Class 1E Electrical Cables," NUREG/CR-5772, SAND91-1766/2, Vol. 2, November 1992.
24. Pinel, B., and Boutaud, B., "A methodology to predict the life duration of polymers used in nuclear power stations. Industrial needs and their approach," Nuclear Instruments and Methods in Physics Research Section B: Beam Interactions with Materials and Atoms Volume: 151, Issue: 1-4 May 2, 1999, pp. 471-476.
25. Gillen, K.T., and Clough, R.L., "Predictive Aging Results in Radiation Environments," Radiative Physics and Chemistry, Vol. 41, No. 6, pp. 803-815, 1993.
26. Holzman, P.M., and Sliter, G.E., "Nuclear Power Plant : Equipment Qualification Reference Manual," EPRI TR-100516, 1992.

APPENDIX A

ADDITIONAL CALCULATIONS USING CPAD DATABASE

In this appendix, the calculations that were not documented in detail in the main report are documented. Section A.1 plots the original data extracted from CPAD, in the format of EAB as a function of aging time. The SNL data of the CPAD data base was used. It consists of two types of data--thermal aging and combined environment aging. The thermal aging data was used in the time-temperature superposition analysis of Section A.2. In the analysis, different values of activation energy were used in the shifting, and visual observation of the shifted data points was used to determine the appropriate value of activation energy. The combined environment data was used to estimate the times to 60% relative EAB and 100% EAB that were used in the reliability physics model calculations of Section A.3. The data was obtained by linear interpolation of $\ln(\text{EAB})$ and $\ln(\text{aging time})$. Note that some of the data points for some of the materials may be affected by diffusion-limited oxidation. The data points in the CPAD database were not reviewed to see which data points might be affected by DLO. Table A-1 summarizes the calculations of Section A.3.

The calculations performed are discussed in the notes below for each material.

Kerite CSPE

The Kerite CSPE jack material was analyzed. It should be the same material as the Hypalon B in Gillen's report (Ref. A1).

Thermal activation energy of 0.91186 ev was used according to Gillen's report. It gives reasonable time-temperature superposition results. The method is not very sensitive to activation energy. Using 0.75 and 1.2 ev would make the curve somewhat more scattered. However, 1.1 ev may give a better curve than 0.91168 ev.

A data point at 120 degrees 2180 ry/hr has a 6000% EAB. It was changed to 60% EAB. The curve appears reasonable. There is a very large difference between what we extracted from Gillen's report and what is in CPAD for Kerite FR CSPE. For example, our time to 60% at 100 degree and 2000 gy/hr is 315 hours, while CPAD's time to 60% at 100 degree and 2140 gr/hr is 132 hours.

The CPAD data of Kerite CSPE C-6 air contains more testing environments than what Gillen presented in his report. Linear interpolation of $\ln(\text{EAB})$ and $\ln(\text{time})$ was used on CPAD data to obtain time to 60% and 100%. For 60% EAB, out of the four testing environments that agree between the two sources of data, two have times to damage that are more than a factor of 2 apart. As indicated above, this probably can not be caused only by discretization errors and methods of interpolation. Such errors caused significant difference in the results of our approach.

Anaconda CSPE C-14 and C-15

Anaconda Flameguard CSPE insulation jacket (material Hyp-01B, cable C-15) was the material analyzed. It appears to be the same as the Hypalon C material from Gillen's reports, except that it has 38 degrees data but not 110 degrees data.

Thermal activation energy of 1.084 ev was used according to Gillen's report. It gives reasonable time-temperature superposition results. In a sensitivity calculation, the data on relative EAB as a function of shifted aging time was copied to SigmaPlot to fit an exponential function and determine the activation

energy that gives the best Rsquare. 1.052 ev was found instead of 1.084 that was used in the calculations. This is probably a better way to estimate activation energy than visual observation.

In a sensitivity calculation, a linear least squares fit of $\ln(EAB)$ against t for each (D,T) pair to get the time corresponding to $EAB=100\%$. The predicted DED vs D curve using this data is shown in Figure A.3.2.

Samuel Moore CSPE

This material is a Samuel Moore CSPE jacket material. The data at 80 degrees C and 60 gy/hr appears to be an anomaly.

The activation energy of 1.08 ev was taken from Hypalon C. It gives less scattering in time-temperature superposition than 1.2 and 0.9 ev.

Anaconda CSPE Jacket C-10

Anaconda Flameguard CSPE Jacket (material Hyp-04, cable C-10) was the material analyzed.

The activation energy of 1.084 was taken from Hypalon C. It gives less scattering than 1.2 and 0.9 ev in time-temperature superposition.

Rockbestos CSPE C-11

This material is the CSPE jacket material of Rockbestos Firewall III cable, C-11.

The activation energy of 1.08 ev was taken from Hypalon C. It gives less scattering than 1.2 and 0.9 ev in time-temperature superposition.

Eaton CSPE C-5

The material is the CSPE jacket of the Eaton Decron Elastoset cable, C-5.

The activation energy of 1.08 ev was taken from Hypalon C. It gives less scattering than 0.9 ev in time-temperature superposition. The comparison with 1.2 ev is close.

Anaconda EPR C-14 air

This material represents the EPR insulation material of Anaconda cable trade named "Anaconda Flameguard 1kv."

The C-14 thermal aging data was used in time-temperature superposition and produced scattered data that is hard to judge which activation energy gives better results. The widely scattered data is due to rapid drop in EAB near the end of the tests. This is probably the "induction time behavior" that Gillen discussed in his wire aging conference paper (Ref. A2). In Brookhaven National Laboratory's (BNL) work on condition monitoring techniques, BNL experimentally calculated (Ref. A3) the activation energy of the induction time behavior for an AIW EPR. In this study, we decided to divide the degradation process into two stages, during and after the induction time, and applied time-temperature superposition approach to the induction-time behavior stage only, not the rapid degrading stage afterwards. We probably have to assume that after induction time, the material becomes critically embrittled, because we do not have a separate model for the rapid degrading after induction-time behavior. The induction time

behavior ends around 150% EAB. That is, we truncated the thermal aging test data with EAB lower than 150%. The activation energy of EPR A was used. With the truncation, the data points became less scattered, and it is possible to fit a curve through the time-temperature superposition data and the EAB vs h0 data.

The combined aging data was linearly interpolated at 100% and 150%, and used in our approach.

Anaconda EPR FR-EP C-2

This EPR material is the conductor insulation of an Anaconda cable trade named "Flameguard FR-EP." It should be the same as Gillen's EPR A (Ref. A4).

Similar to the C-14 EPR, time-temperature superposition of the thermal aging data of this material is scattered due to oxidation induction time behavior. Truncated the data at 150% and the curves are still too scattered. The activation energy of EPR A was used in the calculations.

The time-temperature dose rate superposition was reasonably close to the EPR A results. At high dose rates, it agrees with EPR A very well. At lower dose rates, it gives more conservative results, due to its lower n and d values.

Eaton EPR C-5

This material is the conductor insulation of a Eaton cable trade named "Dekorun Elastoset." It should be the same as the EPR B of Gillen's report.

It has thermal aging data for two temperatures only. The activation energy of EPR B was used in the calculations.

The interpolated data at 100% does not give a good fit to our model. It is worse than our original work which did not give a very good fit either, even though the two data sets are close, probably within 20%. Similar to other EPRs of CPAD, oxidation induction time is a problem.

Rockbestos SIL C-7

This material is the silicone rubber insulation of a Rockbestos cable trade named "Firewall III." It should be the same material as the silicone in Gillen's report.

It has no thermal only data. The combined aging environments are close to those of Gillen's report.

The time to damage data is close to what is in Gillen's report, i.e., within discretization errors. Applying it to our approach, the fit is not as good because some of the data are not consistent, i.e., 100 degrees 176 gr/hr vs. 120 degrees 176 gr/hr. Gillen's work seems to have eliminated the inconsistent data. The fitted curves actually do not differ too much. Instead of 60% relative EAB, 50% relative EAB was used.

Eaton XLPO C-4

This material is the conductor insulation of a Eaton cable trade named "Kekoron Polyset." It should be the same as the CLPO C of Gillen's report. The activation energy of CLPO C was used in the calculations.

CPAD has only one temperature of thermal only data. Time-temperature superposition can not be performed.

The curve of our approach is close to the curve of CLPO C, except at lower dose rates it is higher. Note that the 60 degree data of CLPO C was diffusion limited. It probably corresponds to the 60.1 degree data of XLPO C-4, judging from the dose rate. In the XLPO analysis, the 60.1 degree data was not removed. It is interesting that the 60.1 data is right on the curve, indicating that the fact that it is diffusion limited does not affect the results.

Okonite Neo C-17 Air

This material is the jacket material of a Okonite cable trade named "3-conductor." It should be the same Neoprene material as in Gillen's report.

The 0.954 ev that Gillen used gives less scattering in time temperature superposition than 1.1 and 0.7 ev. However, one may argue that 0.9 ev gives even better results. Use of the combined environment data in our approach gives pretty good results.

Kerite Proprietary C-6 Air

This is a proprietary material used as the insulation of a Kerite cable trade named "FR." Its generic material type is not known. Gillen does have a Kerite FR cable jacket, which he calls Hypalon A. The two are probably not the same.

The activation energy of Hypalon B, 0.91168 ev, was used in the calculations. It gives less scattering than 1.2 and 0.75 ev.

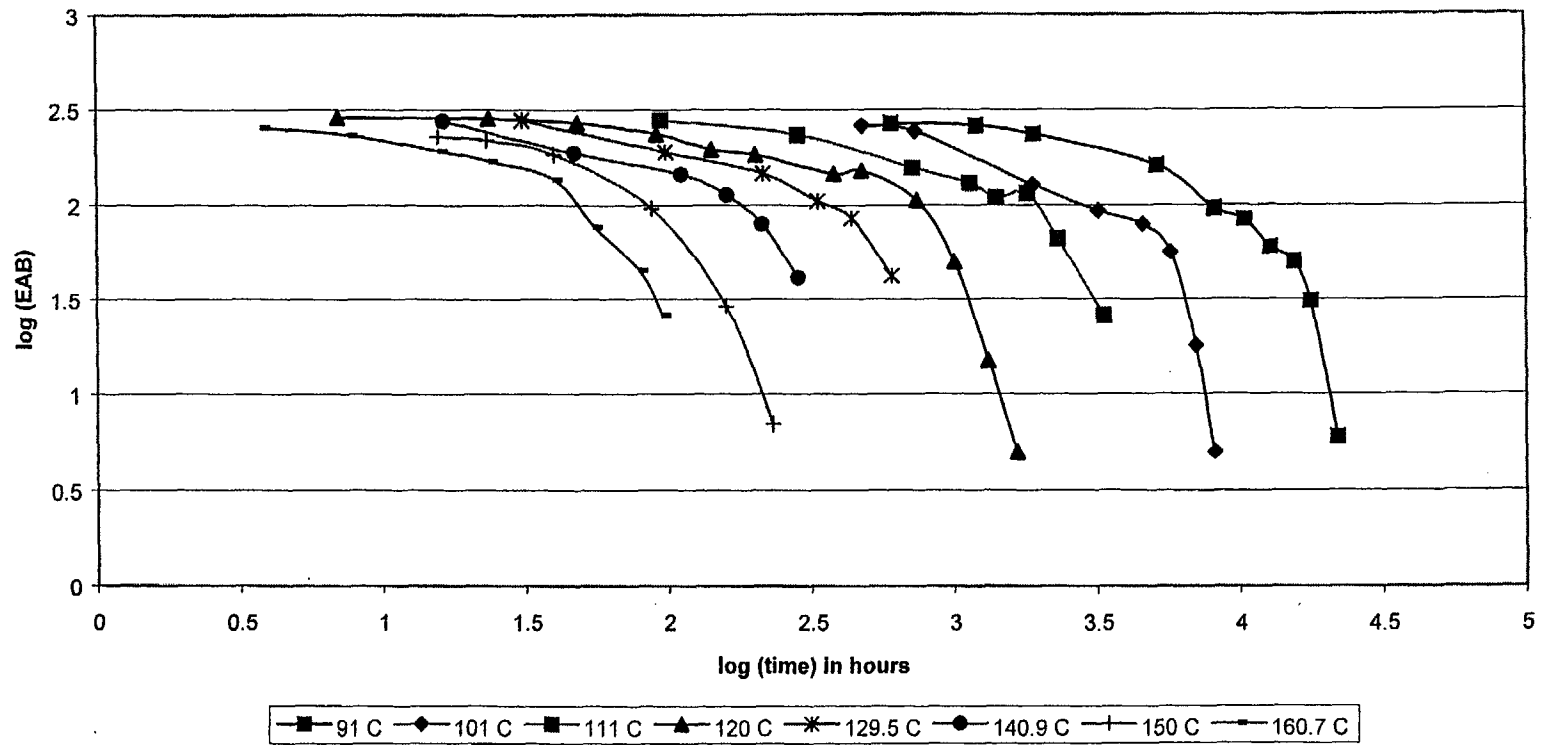
The combined environment data requires extrapolation to obtain 100% EAB data which turned out to be inconsistent at 22 degrees. As a result the fitted curve is not good.

Table A-1 Summary of Calculations of CPAD Materials

CPAD Material	Activation Energy (ev)	h0	d	n	Damage Level	Notes
	0.91168	3.389e-10	1.303e-14	0.918	60	
Kerite CSPE (C-6)	0.91168	6.859e-10	2.101e-14	0.911	100	Hypalon B
	1.084128	2.121e-12	2.388e-17	0.966	60	
Anaconda CSPE Insulation Jacket (C-14)	1.084128	4.123e-12	4.055e-17	0.951	100	Hypalon C
	1.084128	3.184e-12	6.179e-17	0.937	100	Hypalon C, Regression fit
	1.084128	2.687e-12	8.872e-17	0.949	60	
Samuel CSPE (C-9)	1.084128	5.520e-12	7.233e-18	1	100	Activation energy of Hypalon C was used.
Aanaconda CSPE Jacket (C-10)	1.084128	2.420e-12	7.893e-18	1	60	
	1.084128	5.230e-12	1.421e-17	0.991	100	Activation energy of Hypalon C was used.
	1.084128	2.703e-12	5.269e-18	1	60	
Rockesbestos CSPE (C-11)	1.084128	7.368e-12	9.720e-18	1	100	Activation energy of Hypalon C was used.
	1.084128	3.066e-12	6.368e-16	0.897	60	
Eaton CSPE C-5	1.084128	5.698e-12	2.427e-14	0.807	100	Activation energy of Hypalon C was used.
	0.91168	1.734e-09	9.869e-15	0.954	100	Activation energy of EPR A was used.
Anaconda EPR (C-14)	0.91168	1.769e-09	3.347e-15	1	150	Activation energy of EPR A was used.
						EPR A, 21 Kcal/Mol that worked for other material was used
Anaconda EPR (FR-EP C-2)	0.91168	3.131e-09	8.382e-15	0.999	100	material was used
Eaton EPR (C-5)	0.91168	2.902e-09	1.191e-15	1	100	EPR B, activation energy of EPR A was used.
	0.91168	1.714e-09	1.017e-14	0.996	100	Activation energy of Gillen's silicone rubber
Rockbestos SIL C-7	0.91168	7.012e-10	1.469e-14	0.977	50	was used.
Eaton XLPO C-4	0.91168	6.478e-09	6.494e-15	1	100	Activation energy of CLPO C was used.
Okonite Neo C-17	0.954	3.049e-11	2.247e-15	0.924	100	Aactivation energy from Gillen
Kerite Proprietary C-6 Air	0.91168	8.967e-10	2.000e-16	1	100	CPAD only

A.1 Aging Data Extracted from CPAD Data

Aging in Thermal Environment - Kerite CSPE Air C-6



-A7-

Figure A.1.1a Aging Data for Kerite CSPE C-6 - Thermal Aging.

Aging in Combined Environment - Kerite CSPE Air C-6

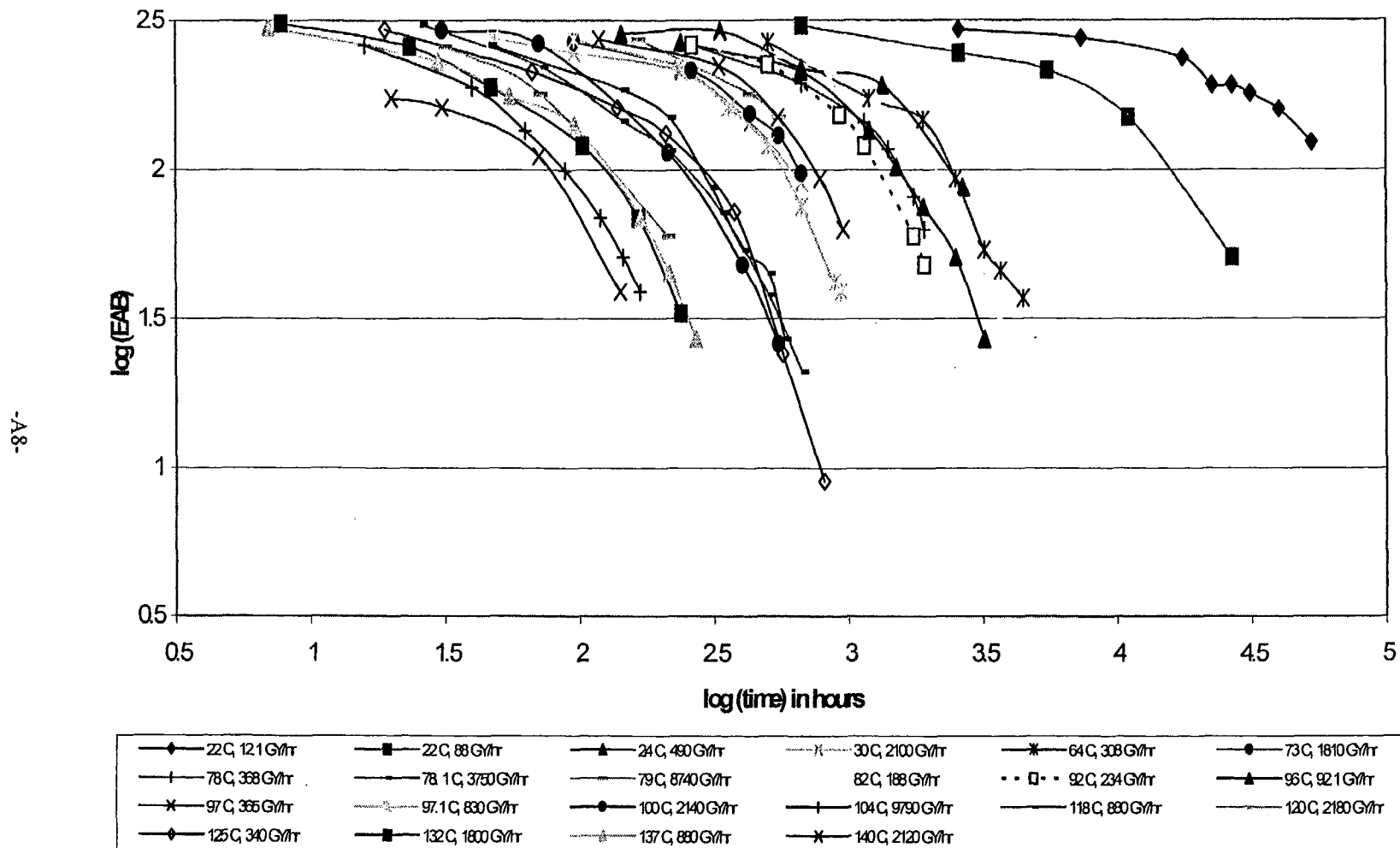


Figure A.1.1b Aging Data for Kerite CSPE C-6 - Combined Aging.

Aging in Thermal Environment - Anaconda CSPE Air C-14

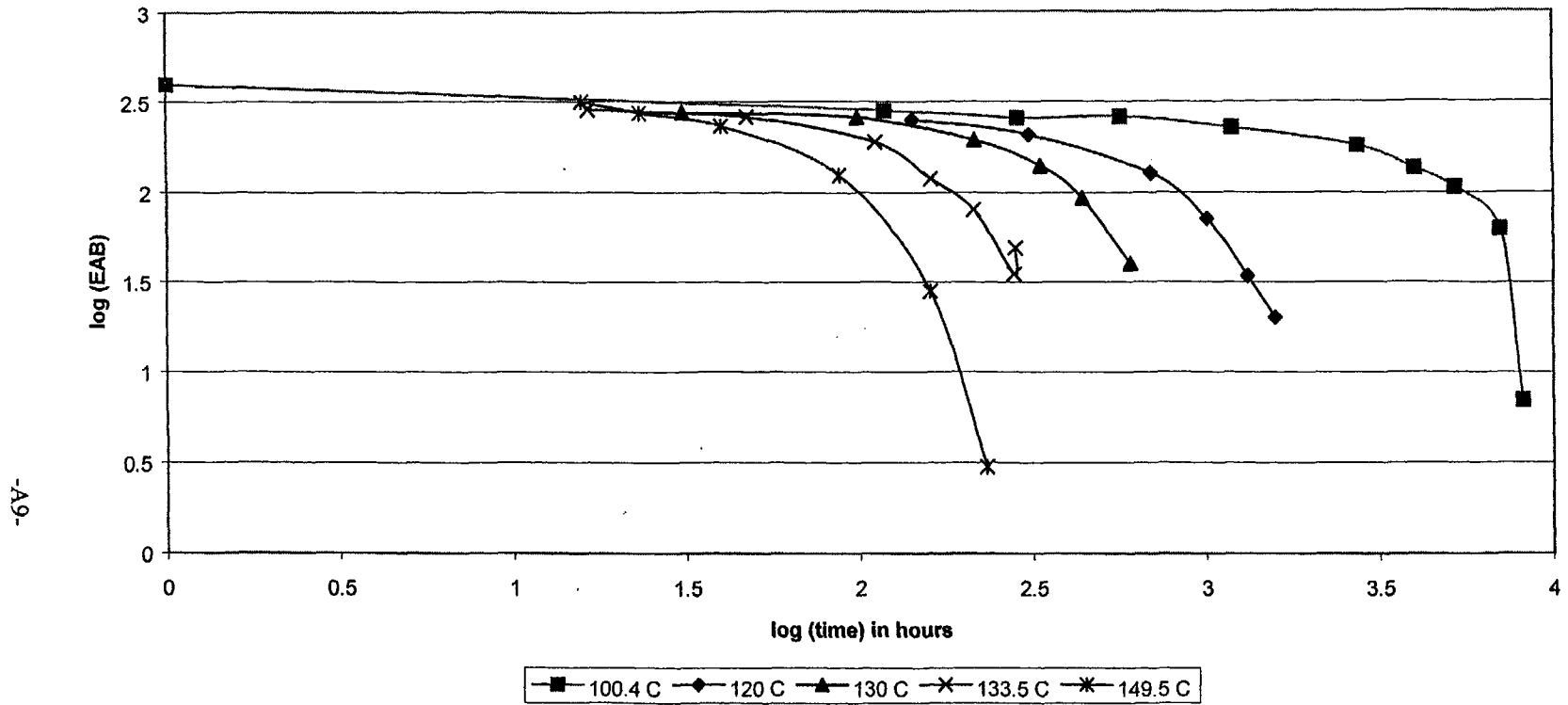


Figure A.1.2a Aging Data for Anaconda CSPE C-14 Thermal Aging

Aging in Combined Environment - Anaconda CSPE Air C-15

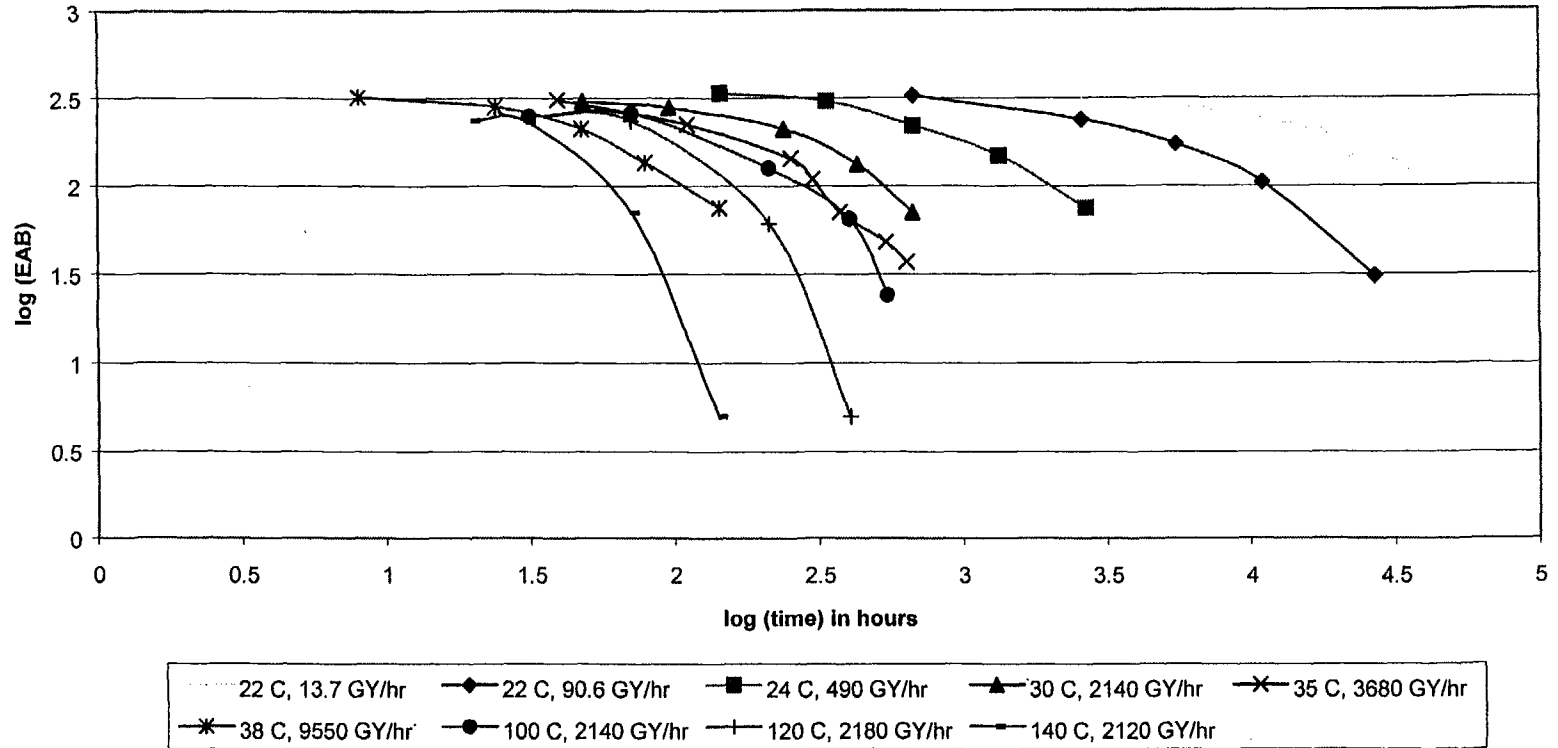


Figure A.1.2b Aging Data for Anaconda CSPE C-15 - Combined Aging.

Aging in Thermal Environment - Samuel Moore CSPE C-9

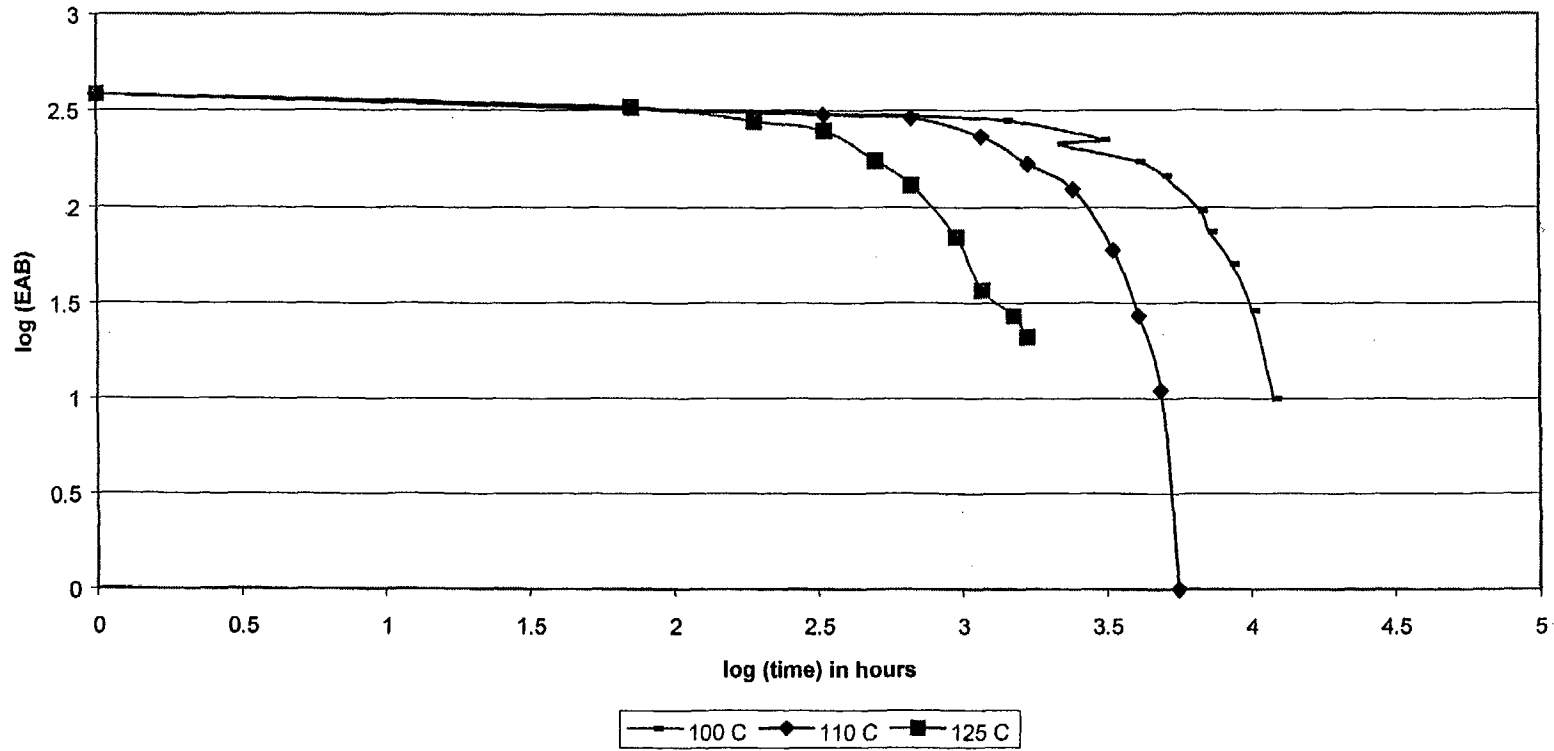


Figure A.1.3a Aging Data for Samuel Moore CSPE C-9 Thermal Aging.

Aging in Combined Environment - Samuel Moore CPSE C-9

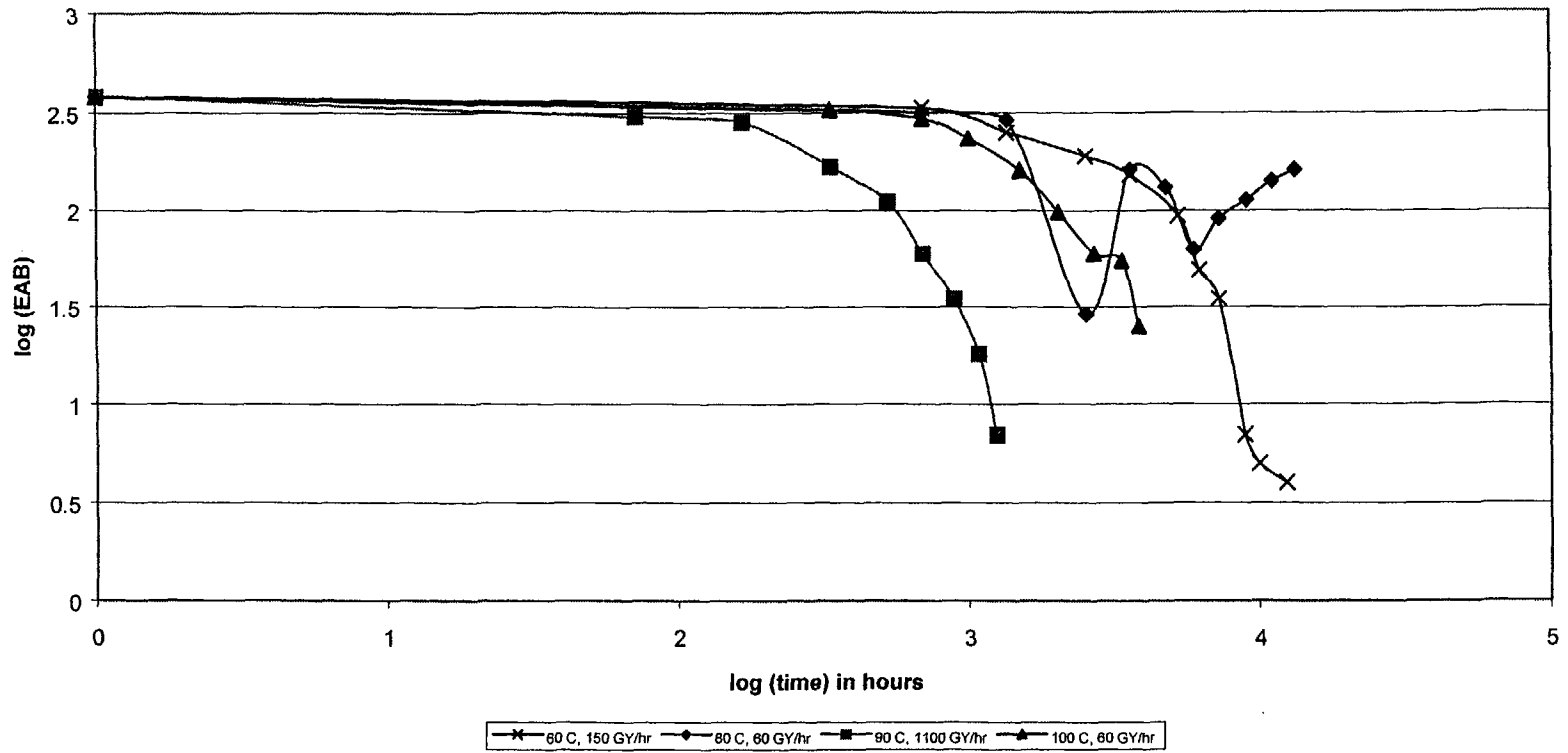


Figure A.1.3b Aging Data for Samuel Moore CSPE C-9 - Combined Aging.

Aging in Thermal Environment - Anaconda CPSE Jacket C-10

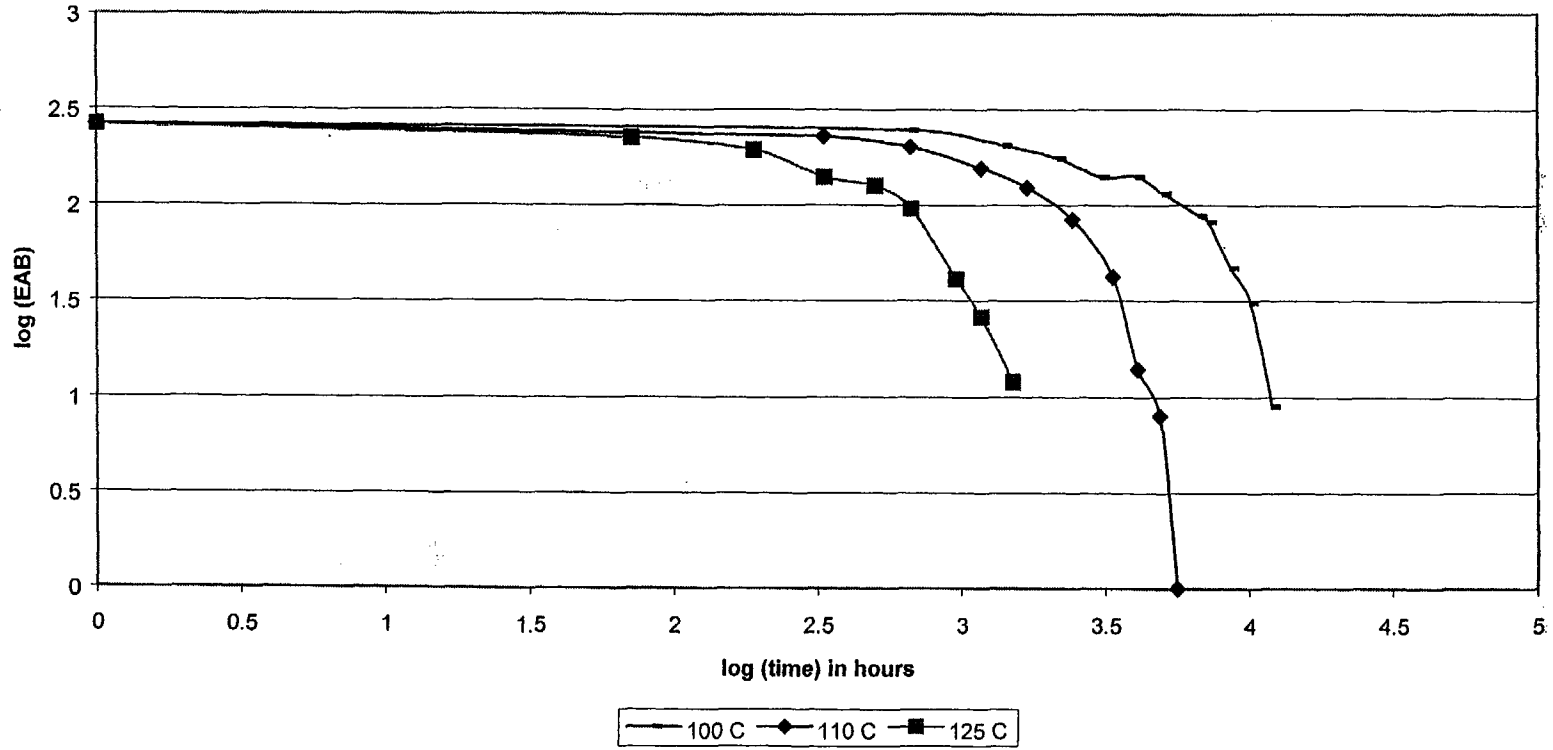


Figure A.1.4a Aging Data for Anaconda CSPE Jacket C-10 - Thermal Aging.

Aging in Combined Environment - Anaconda CPSE Jacket C-10

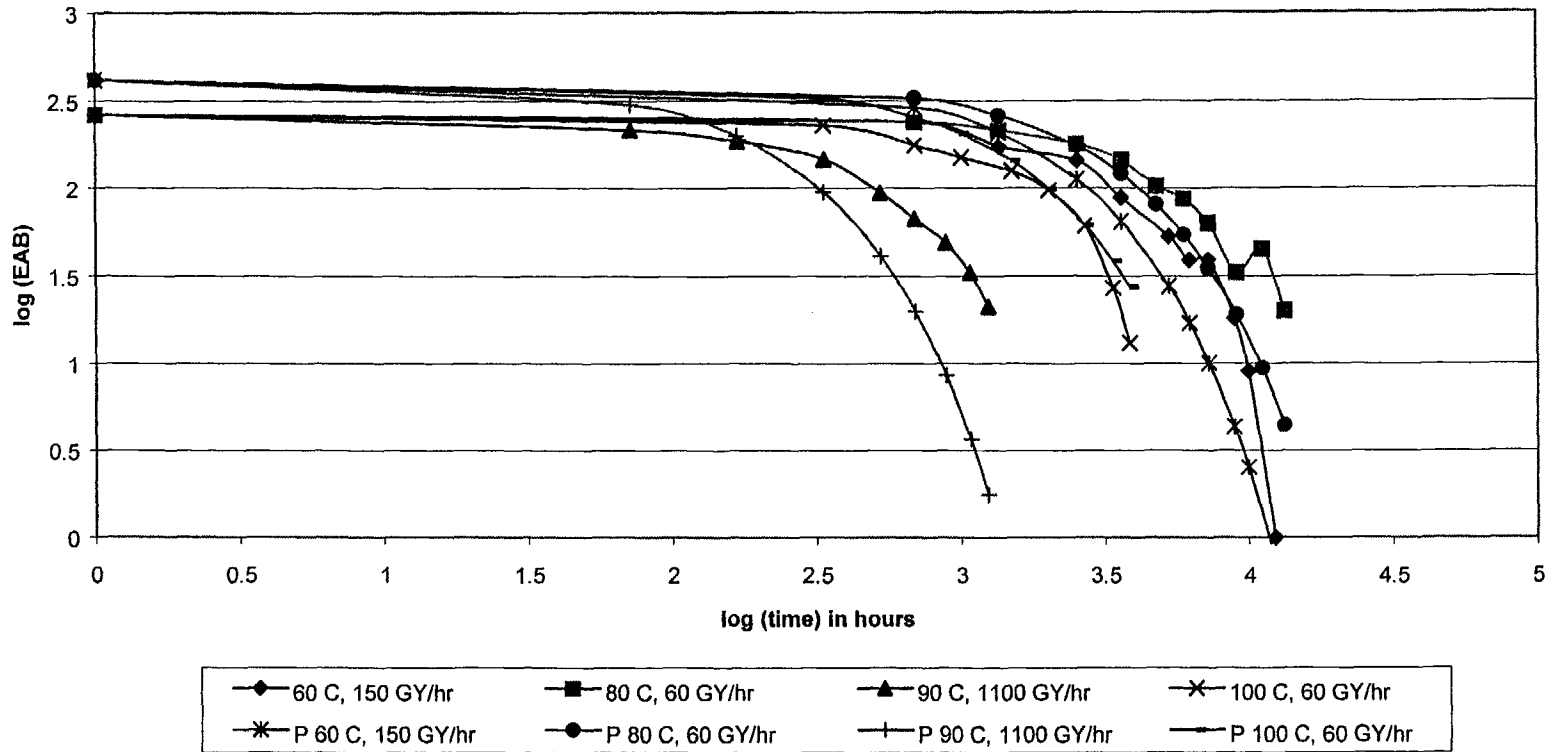


Figure A.1.4b Aging Data for Anaconda CSPE Jacket C-10 - Combined Aging.

Aging in Thermal Environment - Rockbestos CSPE C-11

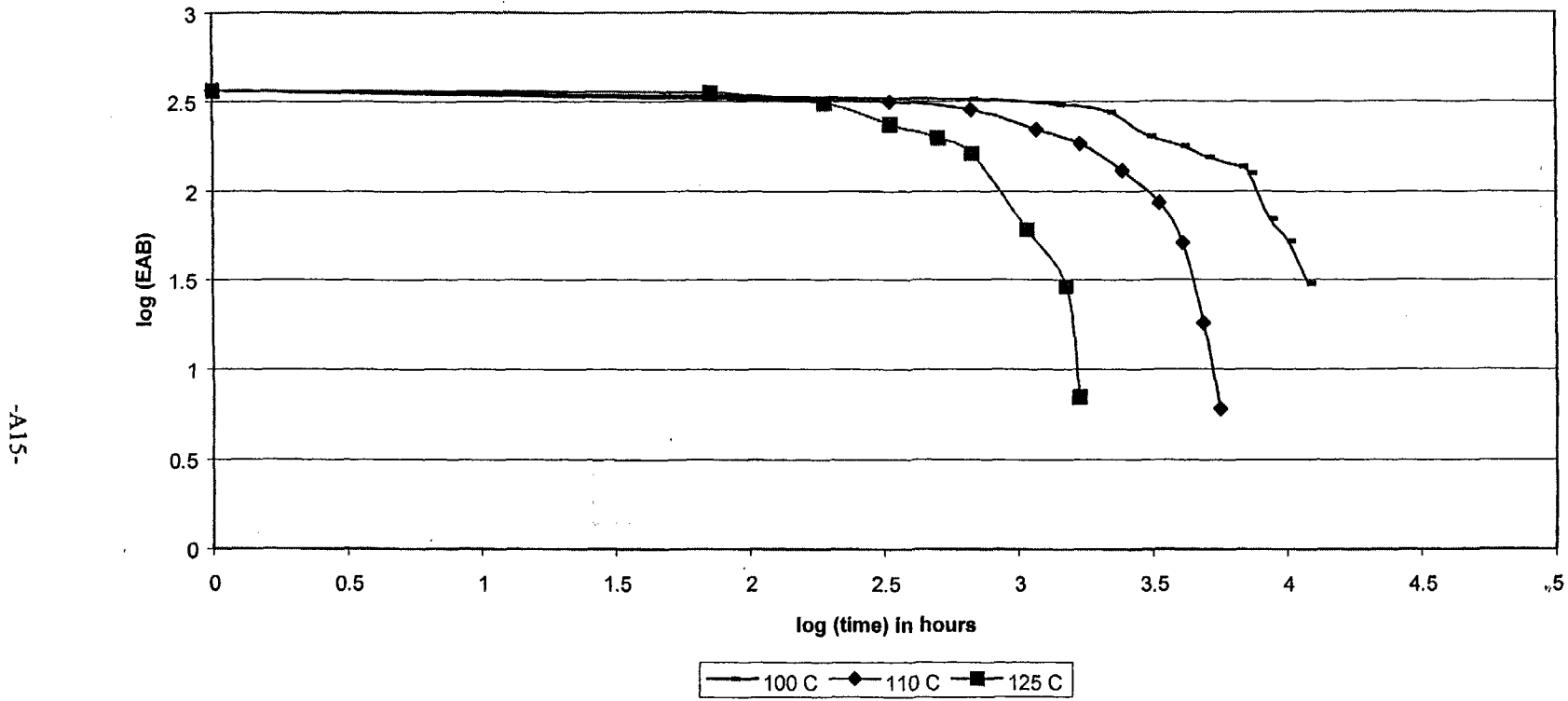
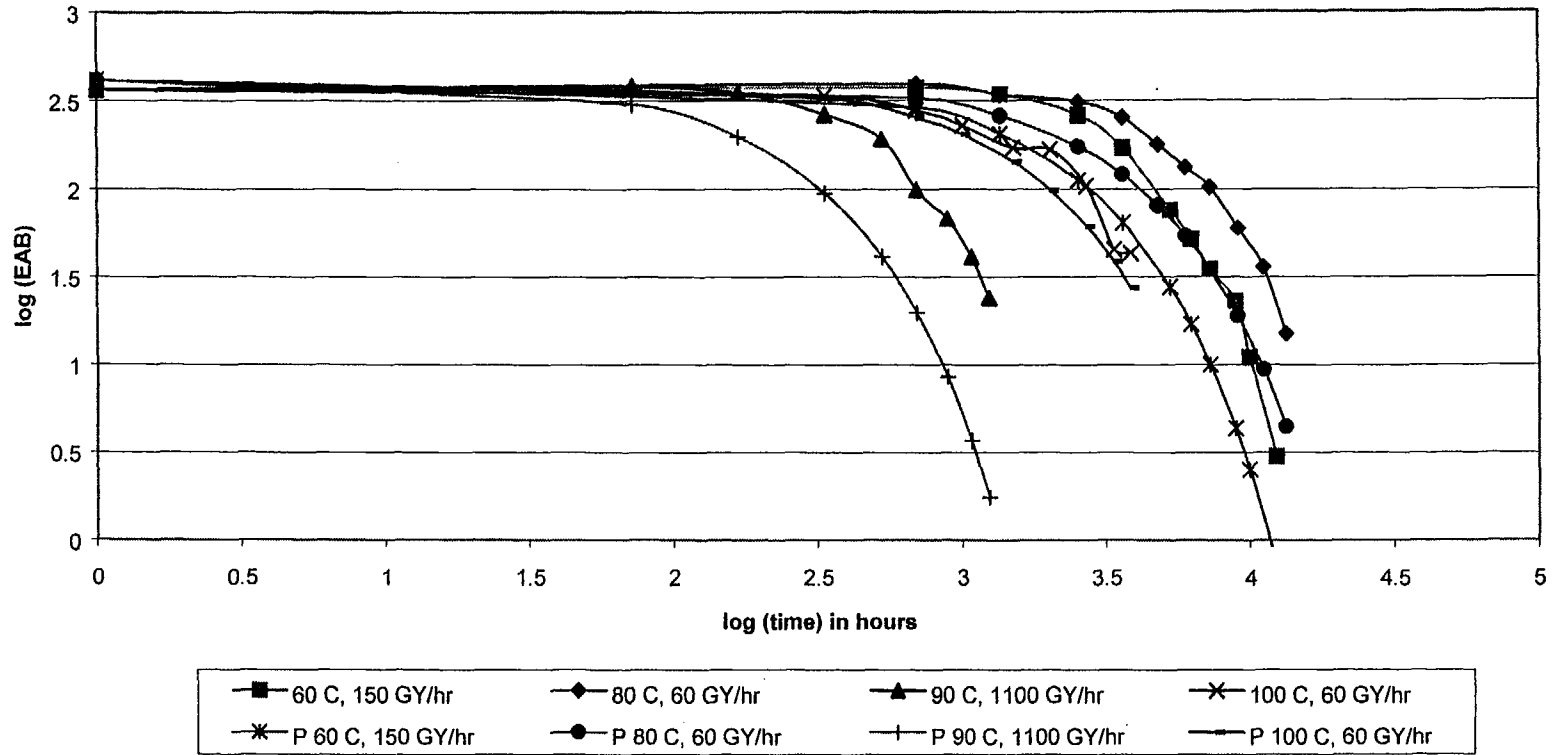


Figure A.1.5a Aging Data for Rockbestos CSPE C-11 - Thermal Aging.

Aging in Combined Environment - Rockbestos CSPE C-11



-A16-

Figure A.1.5b Aging Data for Rockbestos CSPE C-11 - Combined Aging.

Aging in Thermal Environment - Eaton CSPE C-5

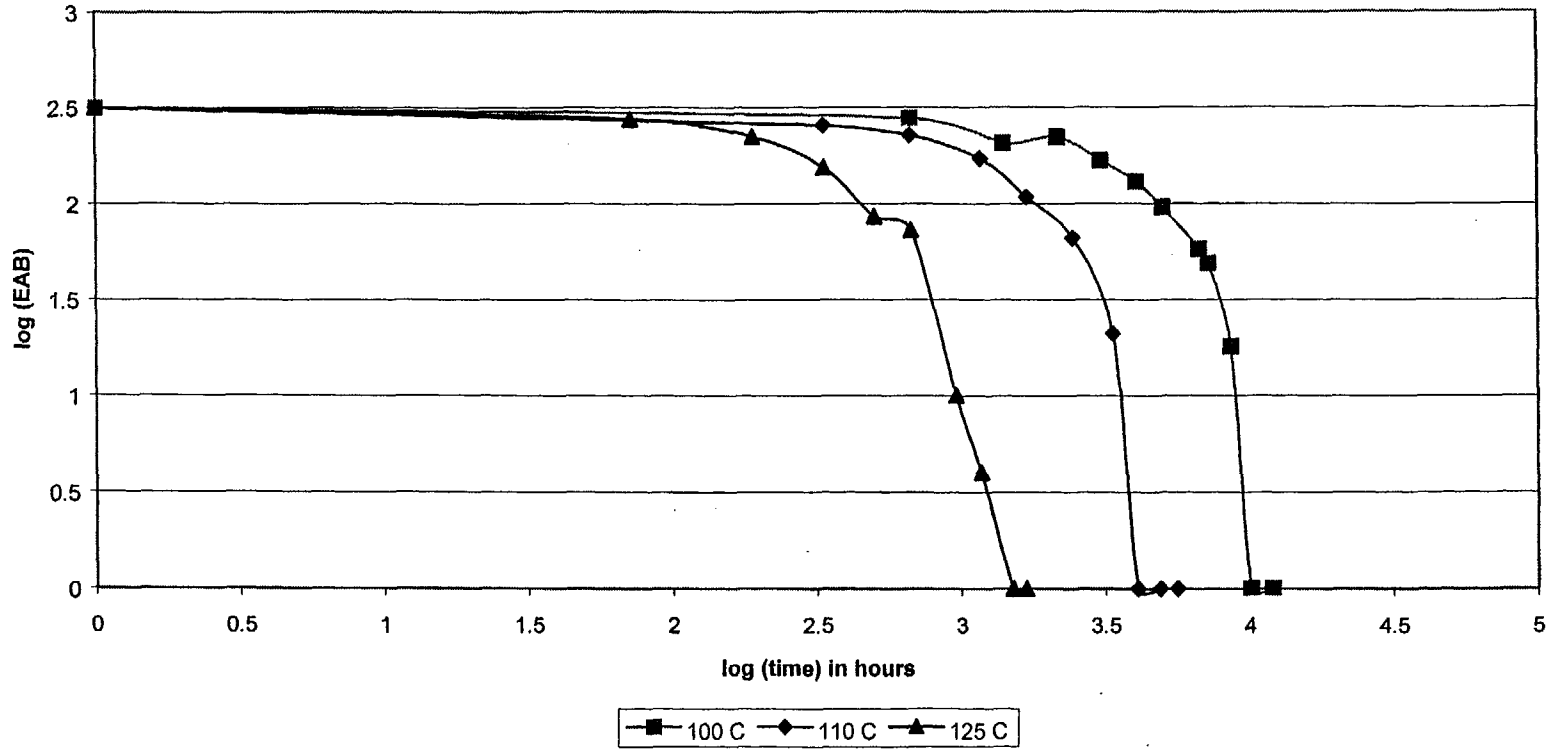


Figure A.1.6a Aging Data for Eaton CSPE C-5 - Thermal Aging.

Aging in Combined Environment - Eaton CSPE C-5

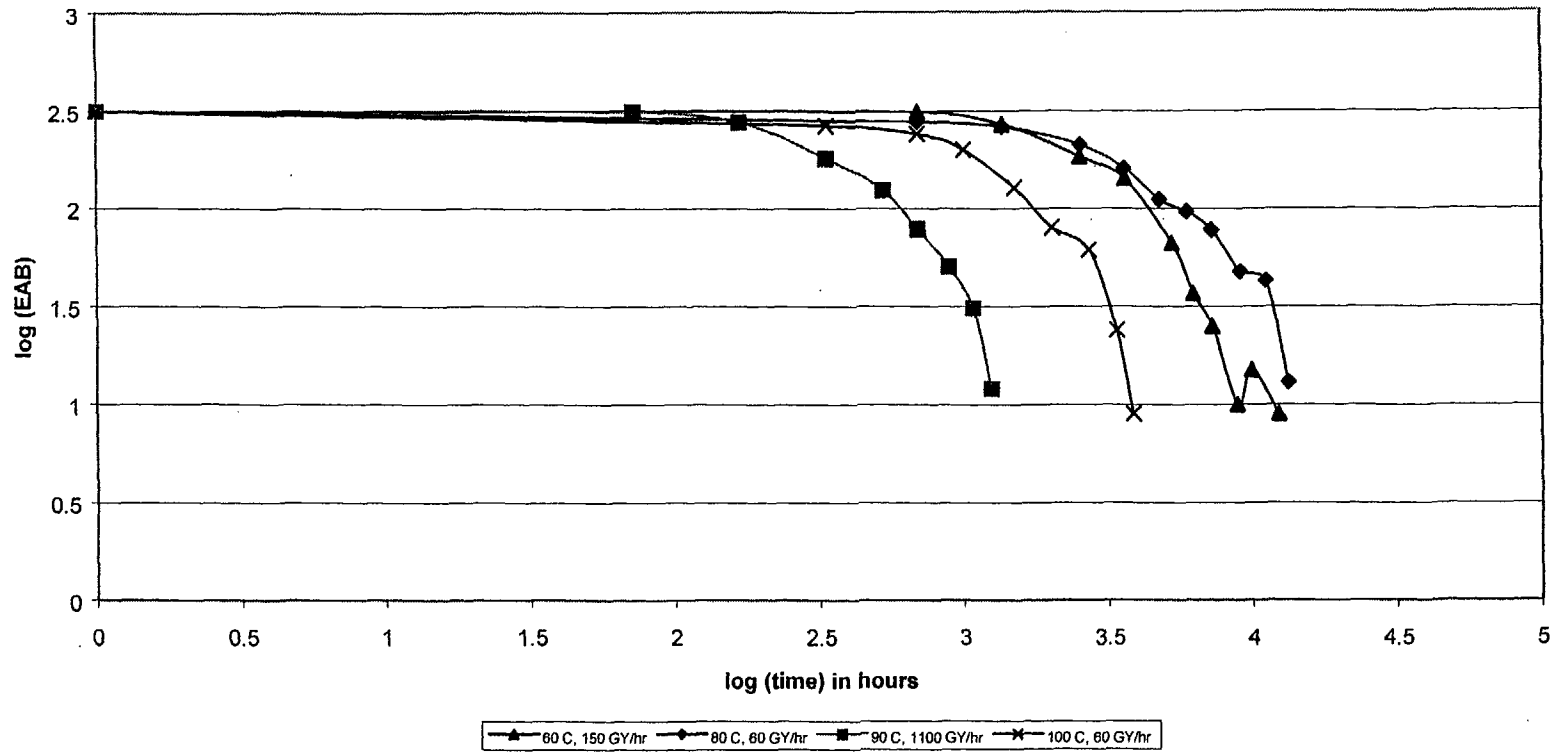
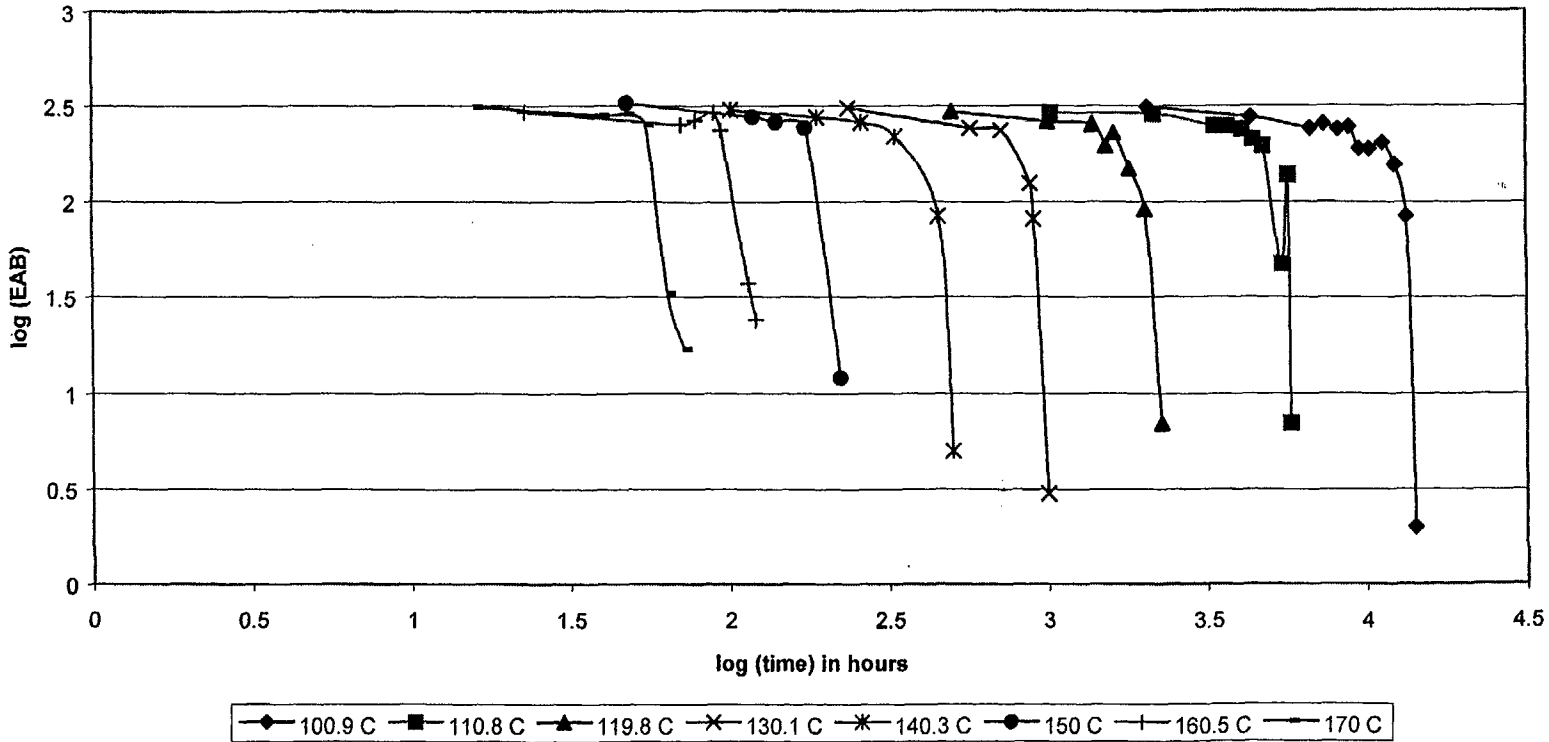


Figure A.1.6b Aging Data for Eaton CSPE C-5 - Combined Aging.

Aging in Thermal Environment - Anaconda EPR



-A19-

Figure A.1.7a Aging Data for Anaconda EPR C-14 - Thermal Aging.

Aging in Combined Environment - Anaconda EPR

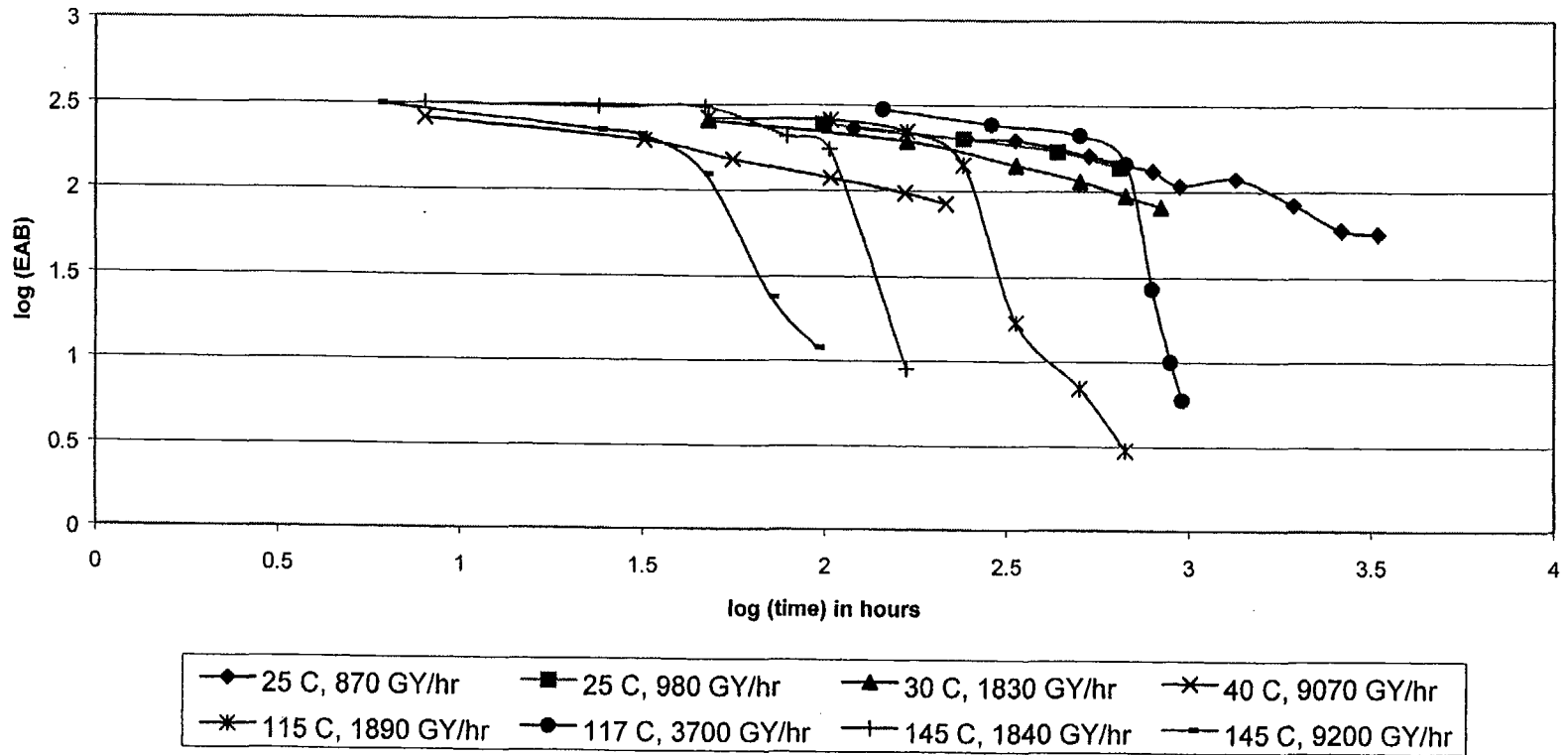
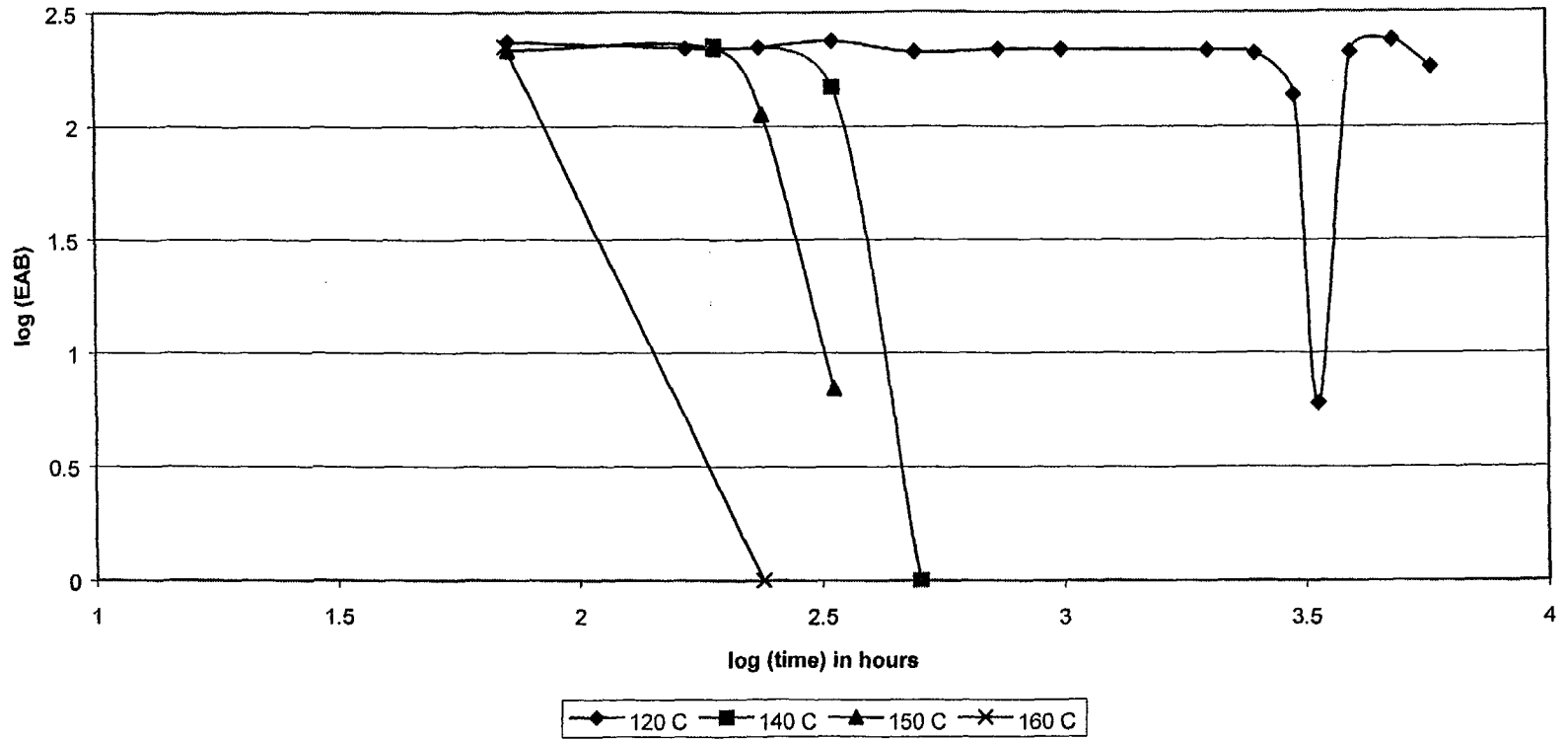


Figure A.1.7b Aging Data for Anaconda EPR C-14 - Combined Environment.

Aging in Thermal Environment - Anaconda EPR FR-EP C-2



-A21-

Figure A.1.8a Aging Data for Anaconda EPR FR-EP C-2 - Thermal Aging.

Aging in Combined Environment - Anaconda EPR FR-EP C-2

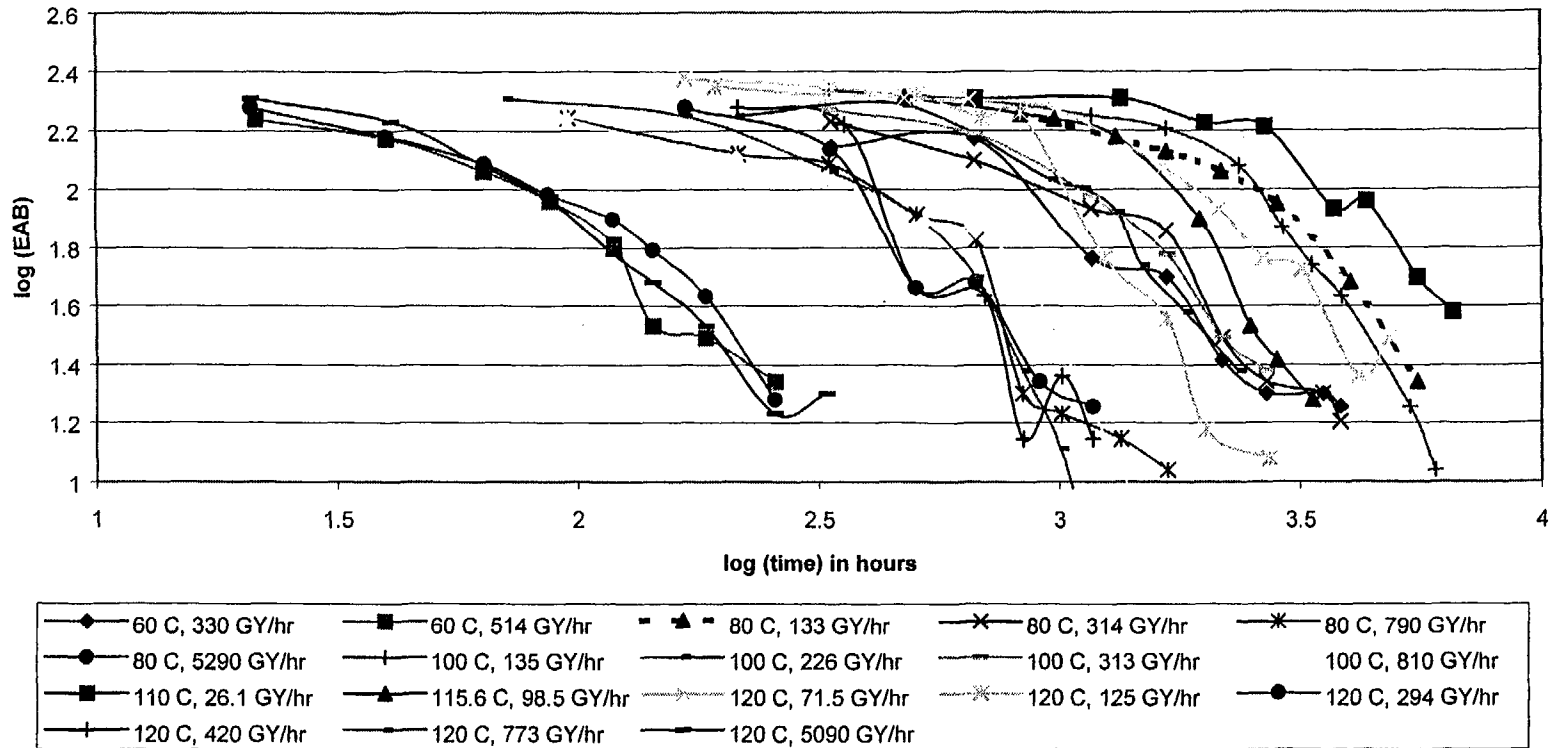
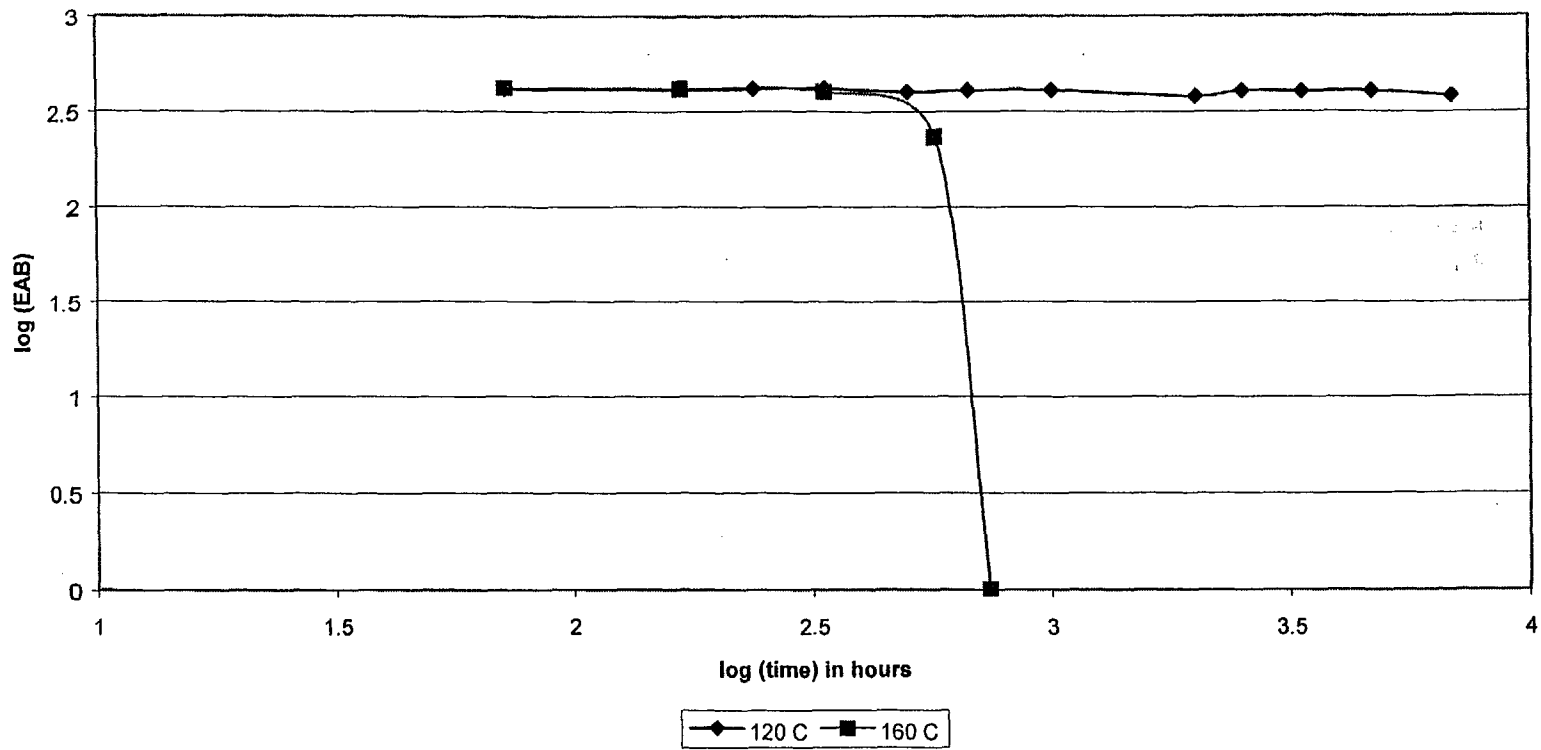


Figure A.1.8b Aging Data for Anaconda EPR FR-EP C-2 - Combined Environment.

Aging in Thermal Environment - Eaton EPR C-5



-A23-

Figure A.1.9a Aging Data for Eaton EPR C-5 - Thermal Aging.

Aging in Combined Environment - Eaton EPR C-5

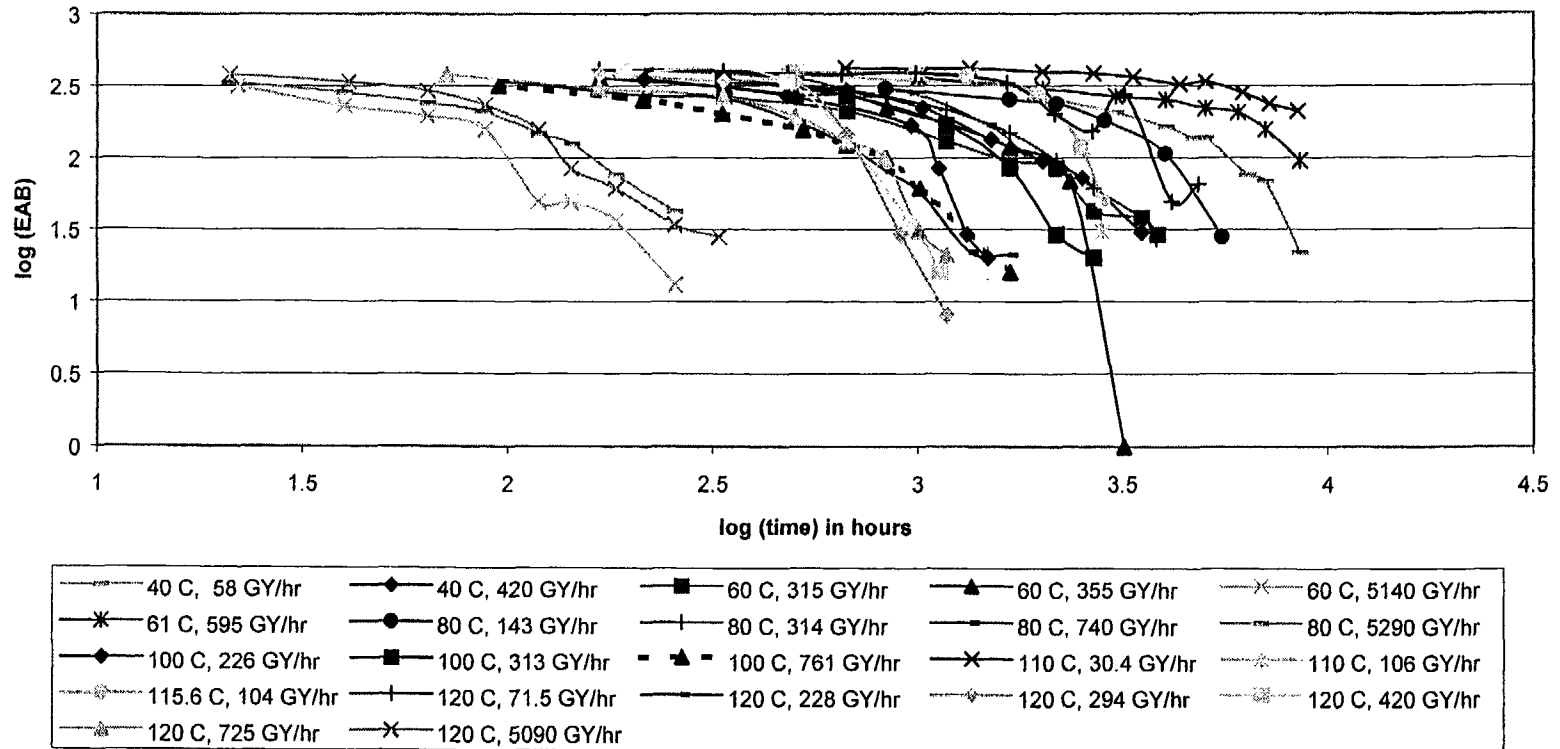


Figure A.1.9b Aging Data for Eaton EPR C-5 - Combined Environment.

Aging in Combined Environment - Rockbestos SIL C-7

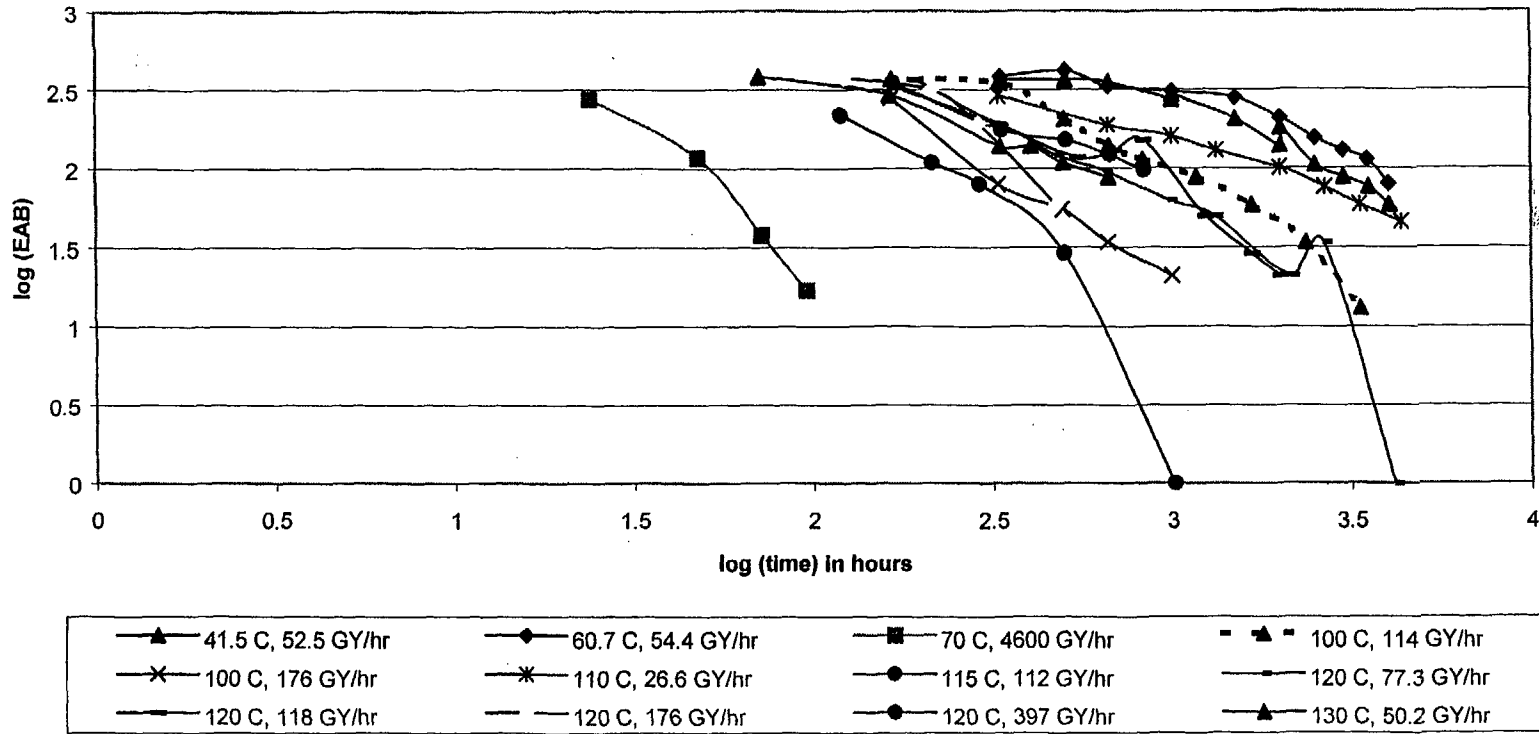
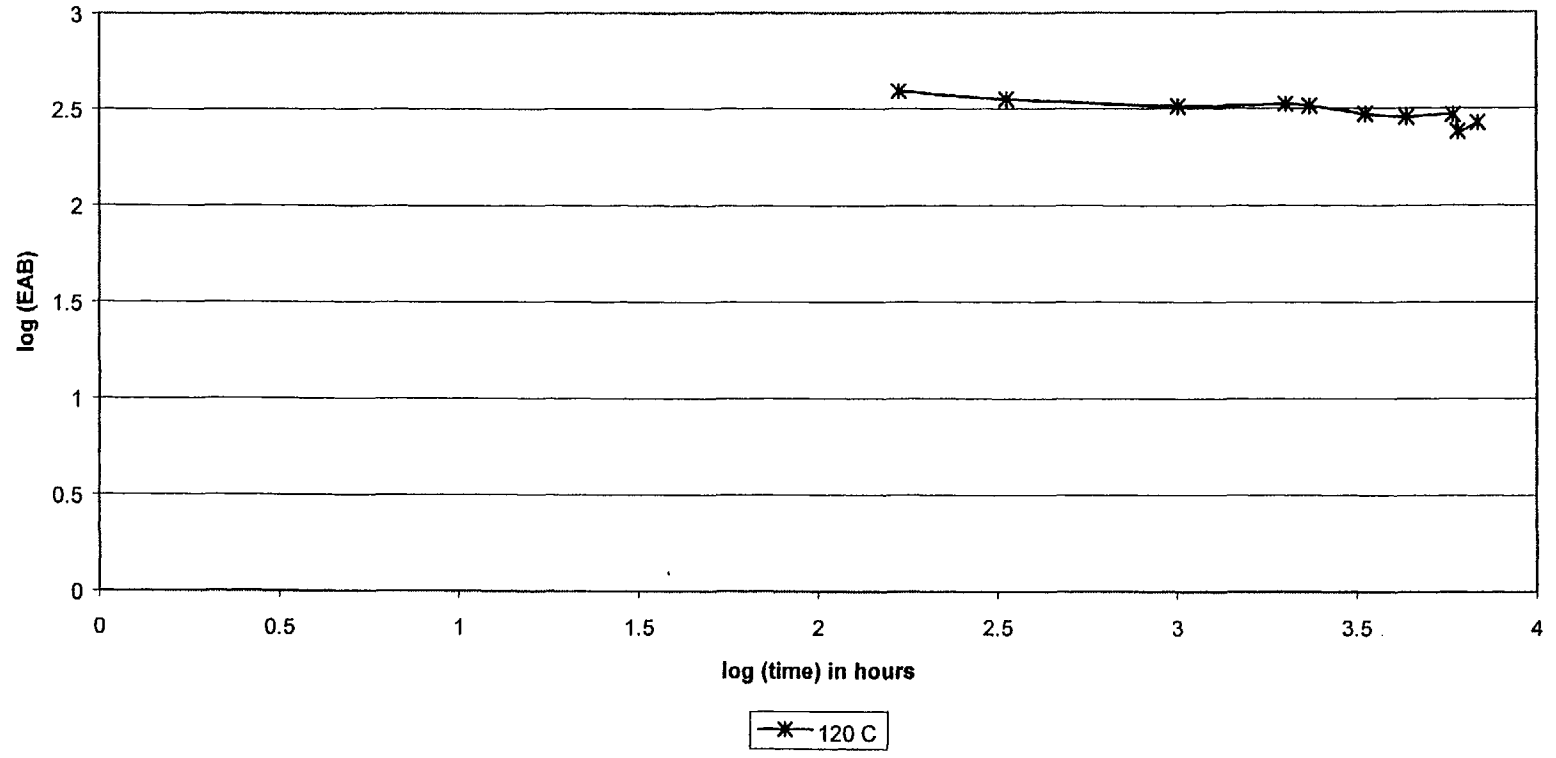


Figure A.1.10 Aging Data for Rockbestos Silicone Rubber C-7 - Combined Environment.

Aging in Thermal Environment - Eaton XLPO C-4



-A26-

Figure A.1.11a Aging Data for Eaton XLPO C-4 - Thermal Aging.

Aging in Combined Environment - Eaton XLPO C-4

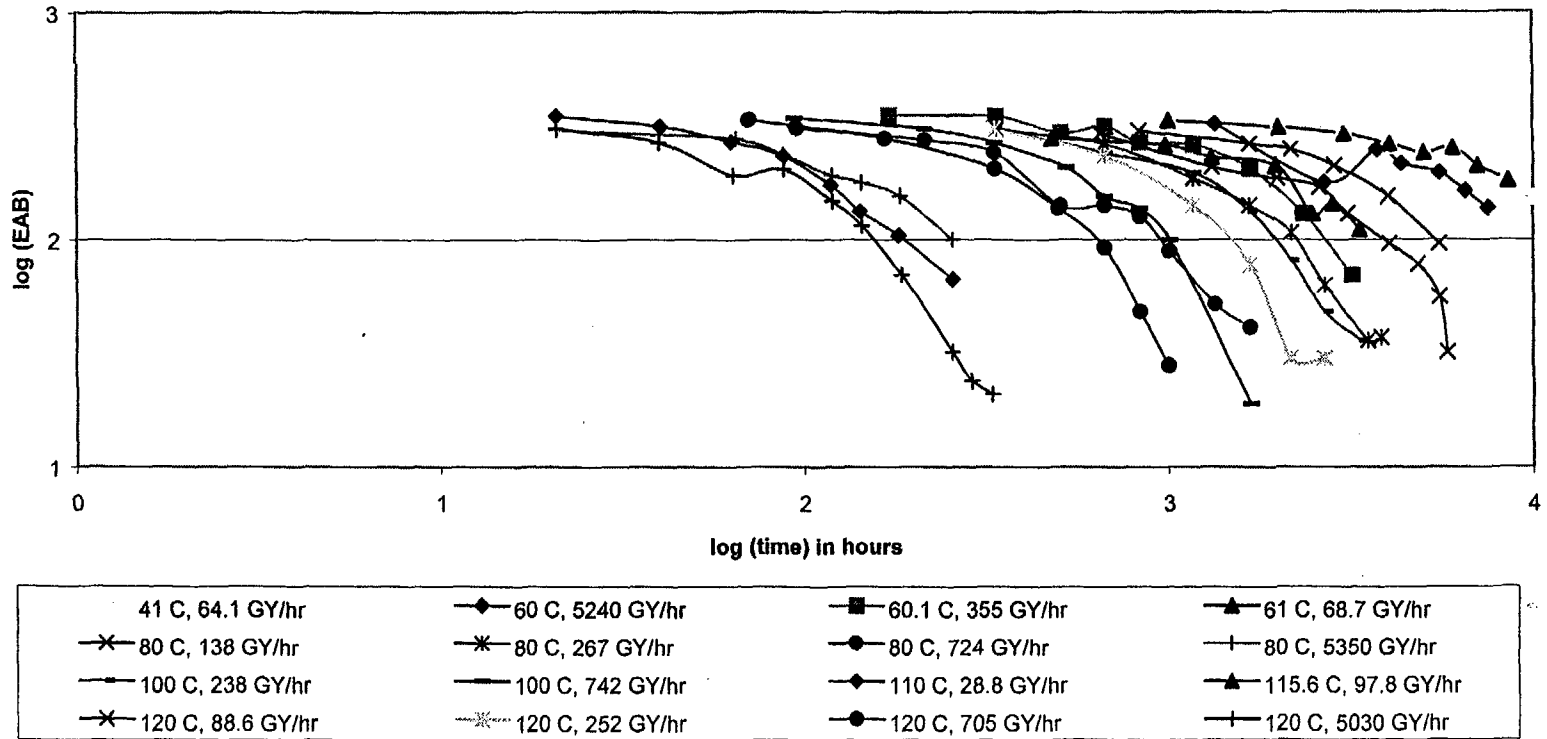


Figure A.1.11b Aging Data for Eaton XLPO C-4 - Combined Environment.

Aging in Thermal Environment - Okonite Neo C-17 Air

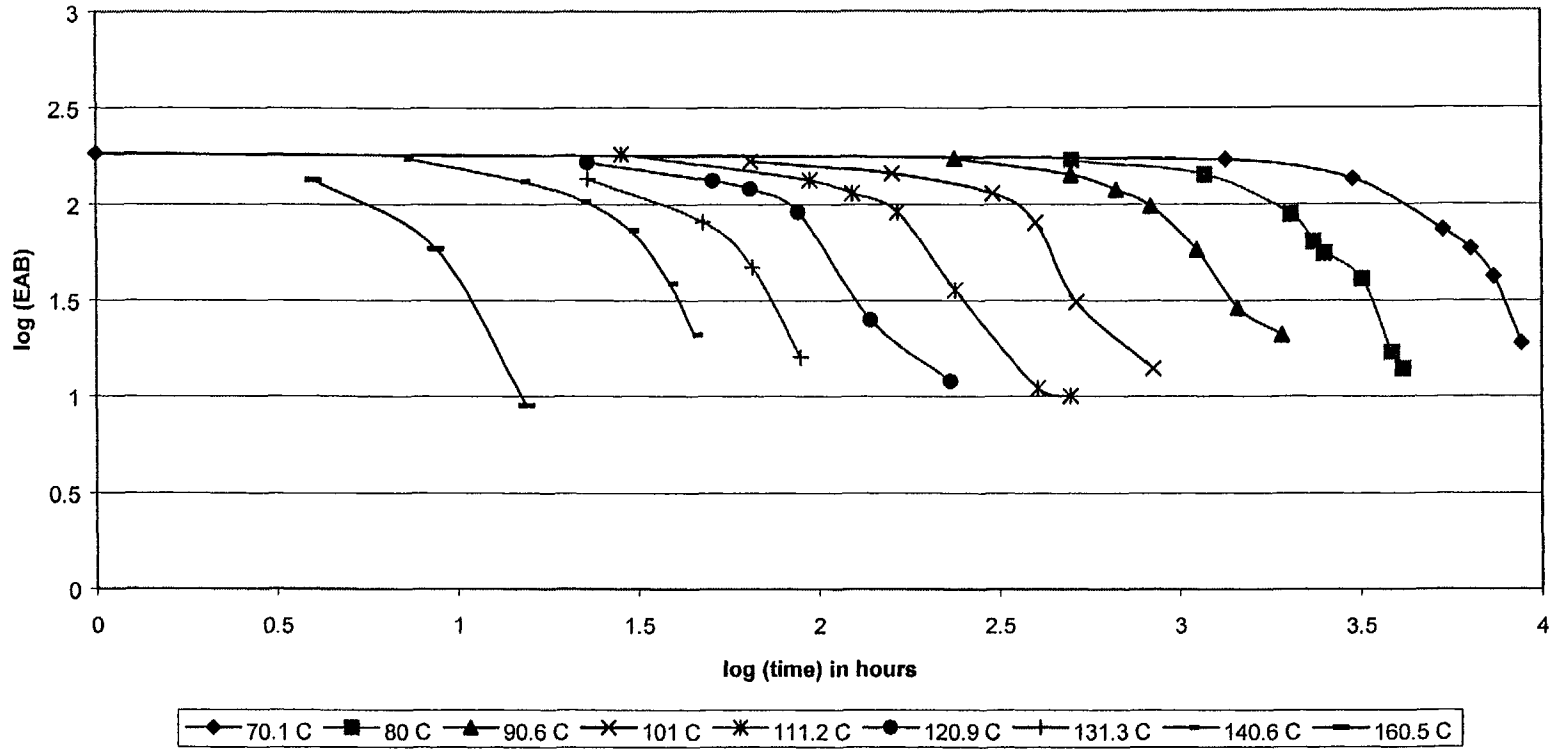


Figure A.1.12a Aging Data for Okonite Neoprene - Thermal Aging.

Aging in Combined Environment - Okonite Neo C-17 Air

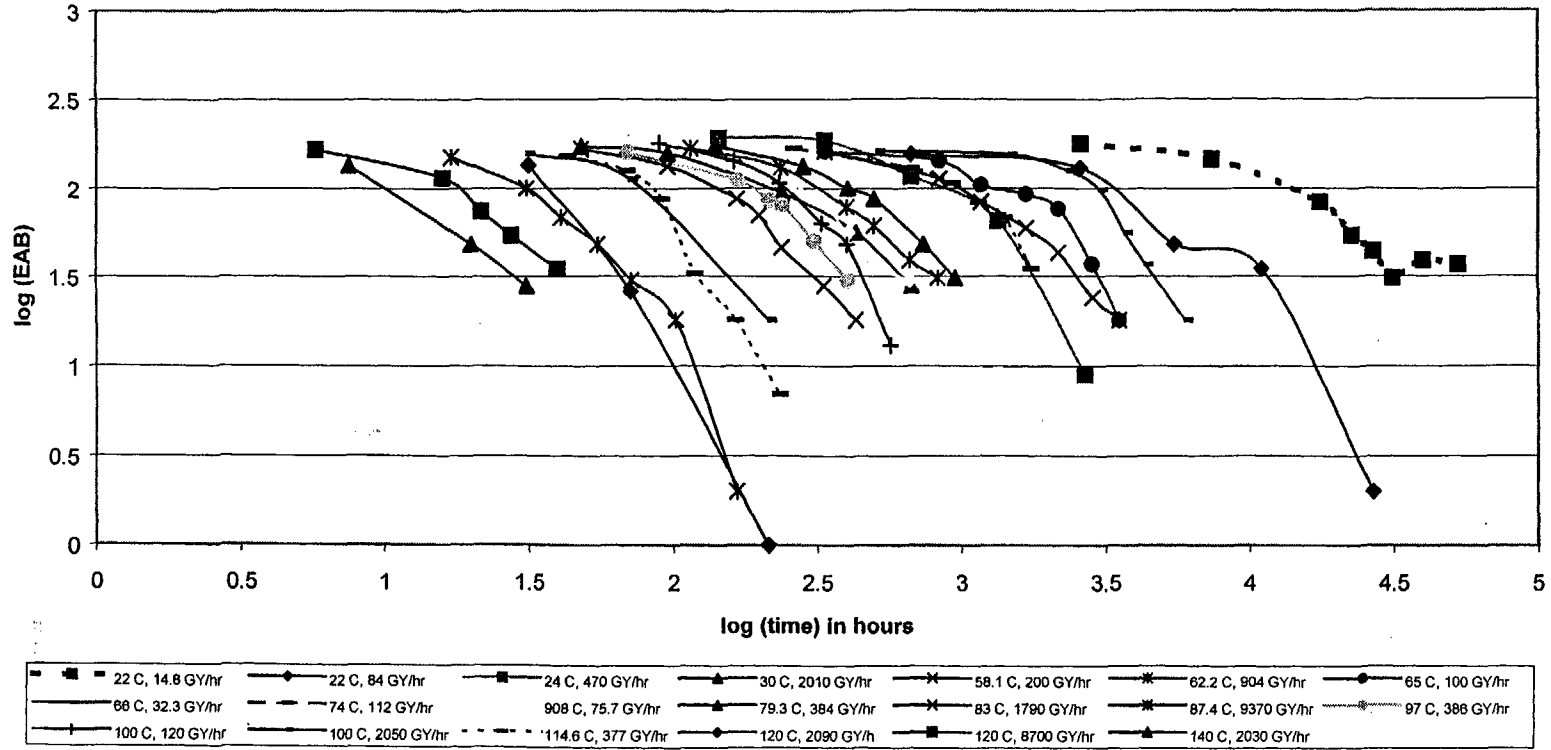
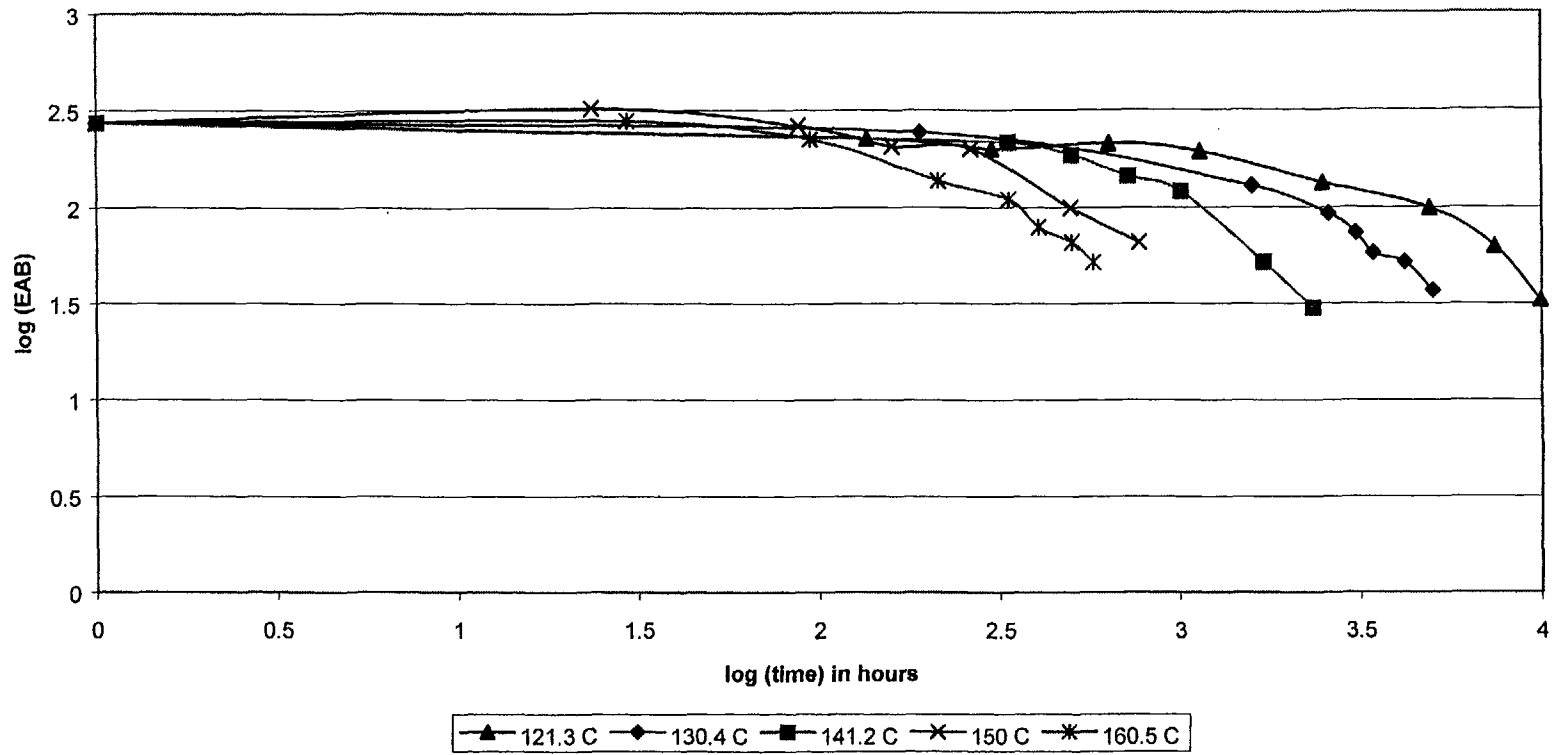


Figure A.1.12b Aging Data for Okonite Neoprene - Combined Environment.

Aging in Thermal Environment - Kerite Proprietary C-6 Air



-A30-

Figure A.1.13a Aging Data for Kerite Proprietary Insulation C-6 - Thermal Aging.

Aging in Combined Environment - Kerite Proprietary C-6 Air

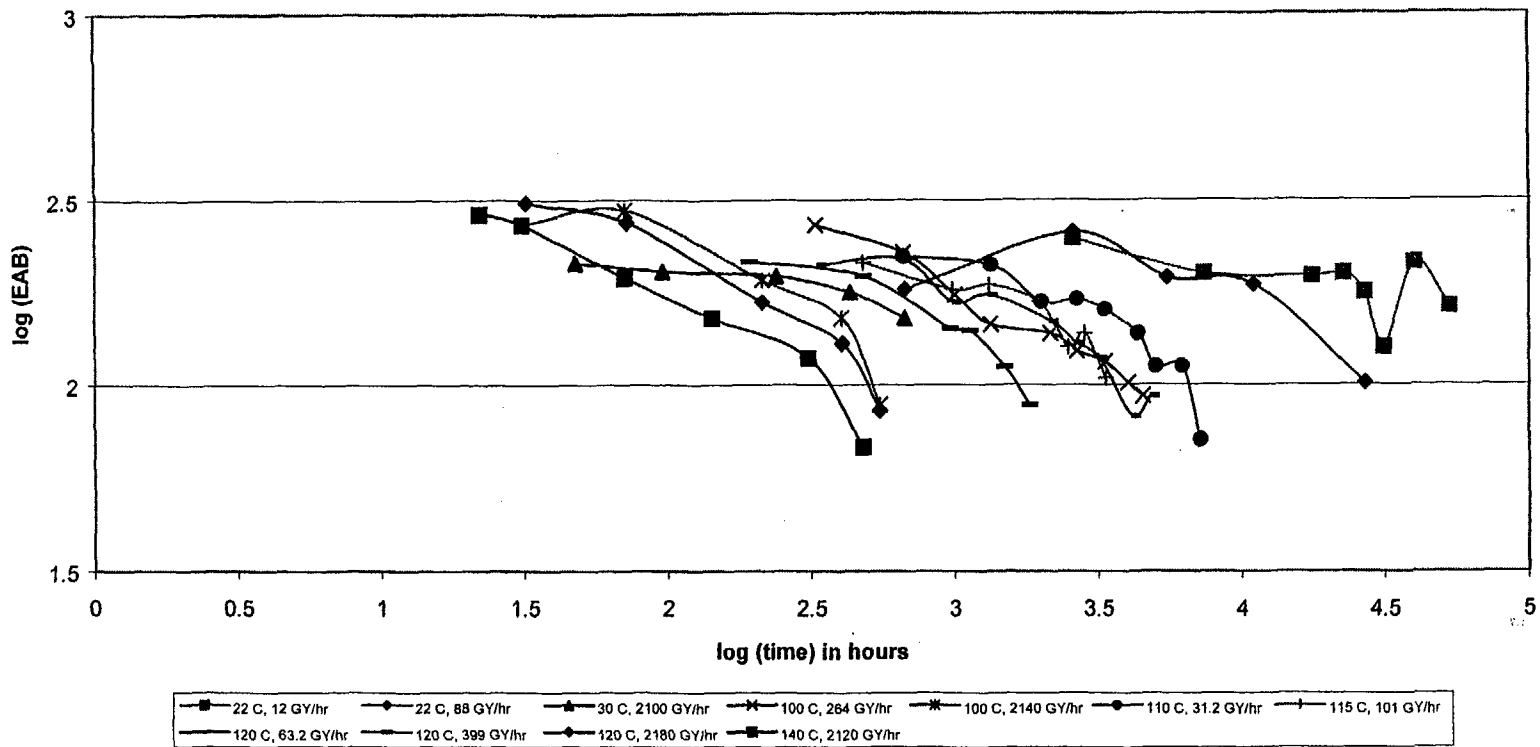
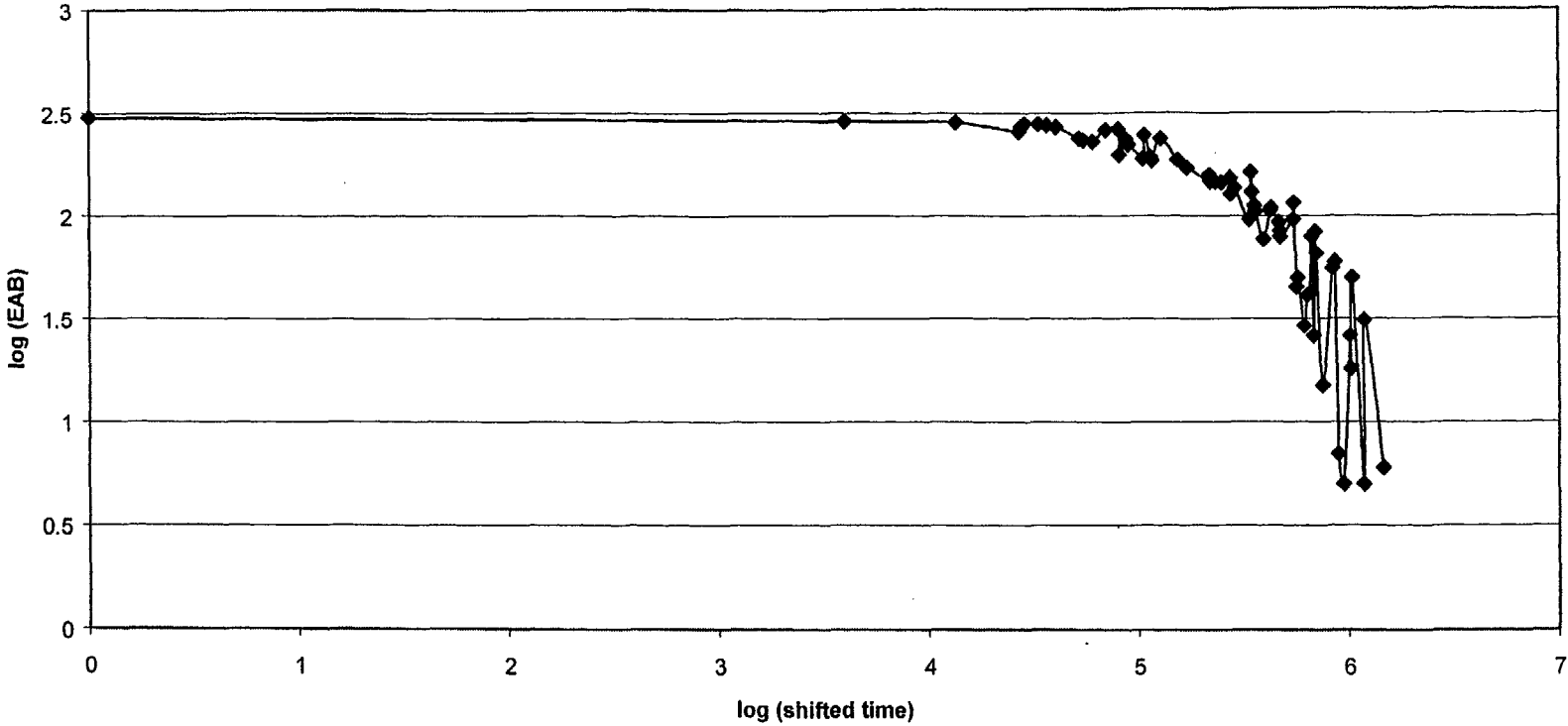


Figure A.1.13b Aging Data for Kerite Proprietary Insulation C-6 - Combined Environment

A.2 Shifted Curves Using Temperature Superposition Method

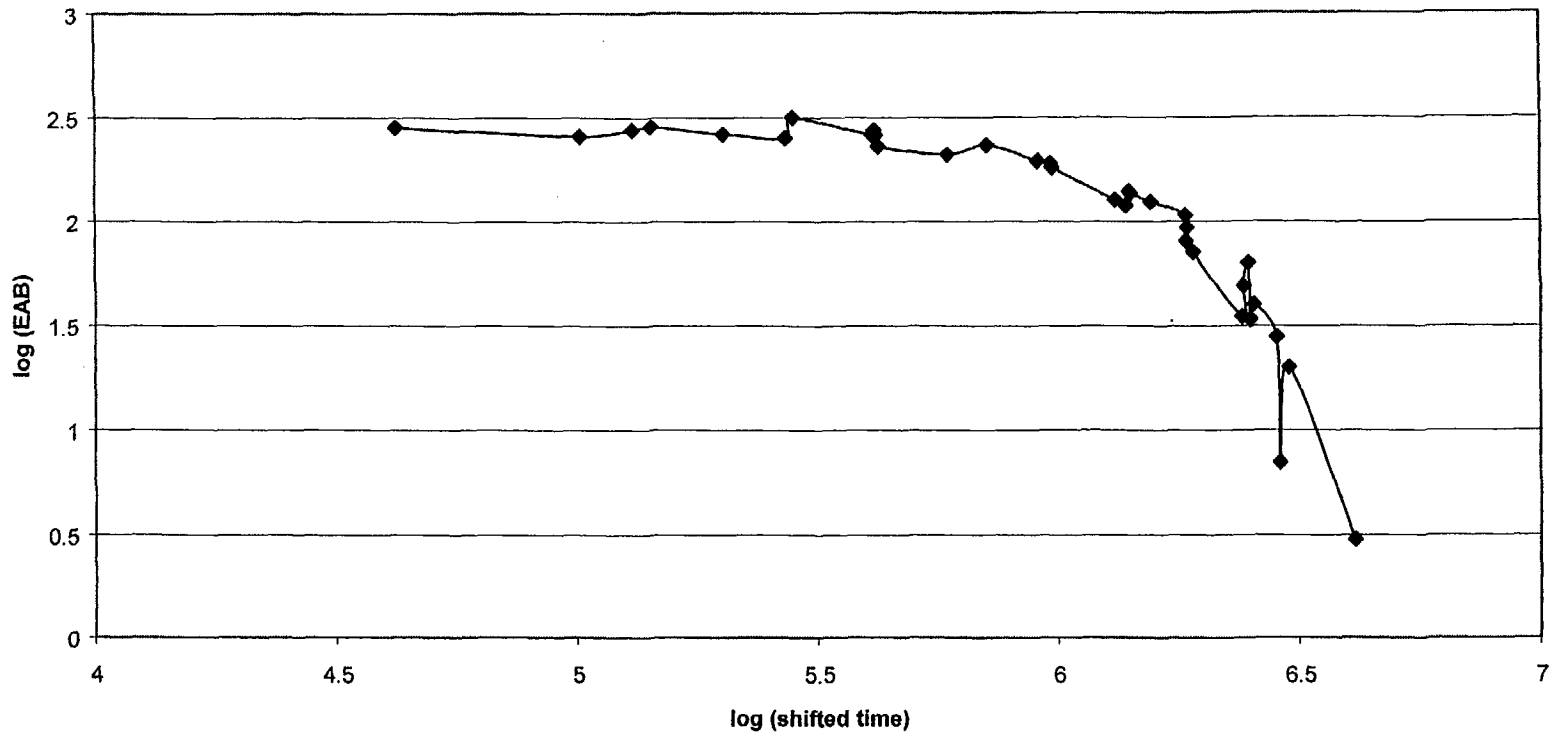
Time Temperature Superposition Using .91168 EV- Kerite CSPE Air C-6



-A33-

Figure A.2.1 Time-Temperature Superposition - Kerite CSPE C-6.

Time Temperature Superposition Using 1.084128 EV - Anaconda CSPE Air C-14



-A34-

Figure A.2.2 Time-Temperature Superposition - Anaconda CSPE C-14.

Time Temperature Superposition Using 1.084128 EV - Samuel Moore CPSE C-9

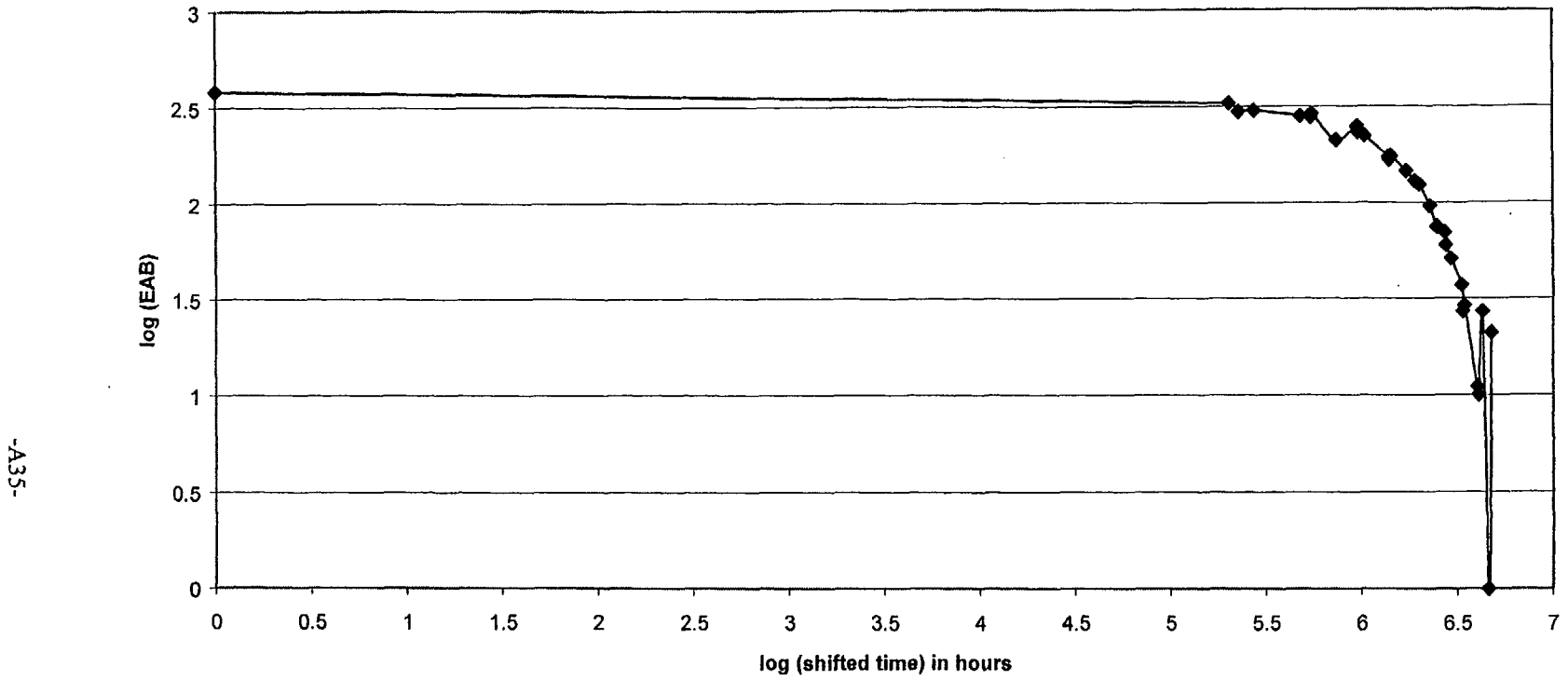
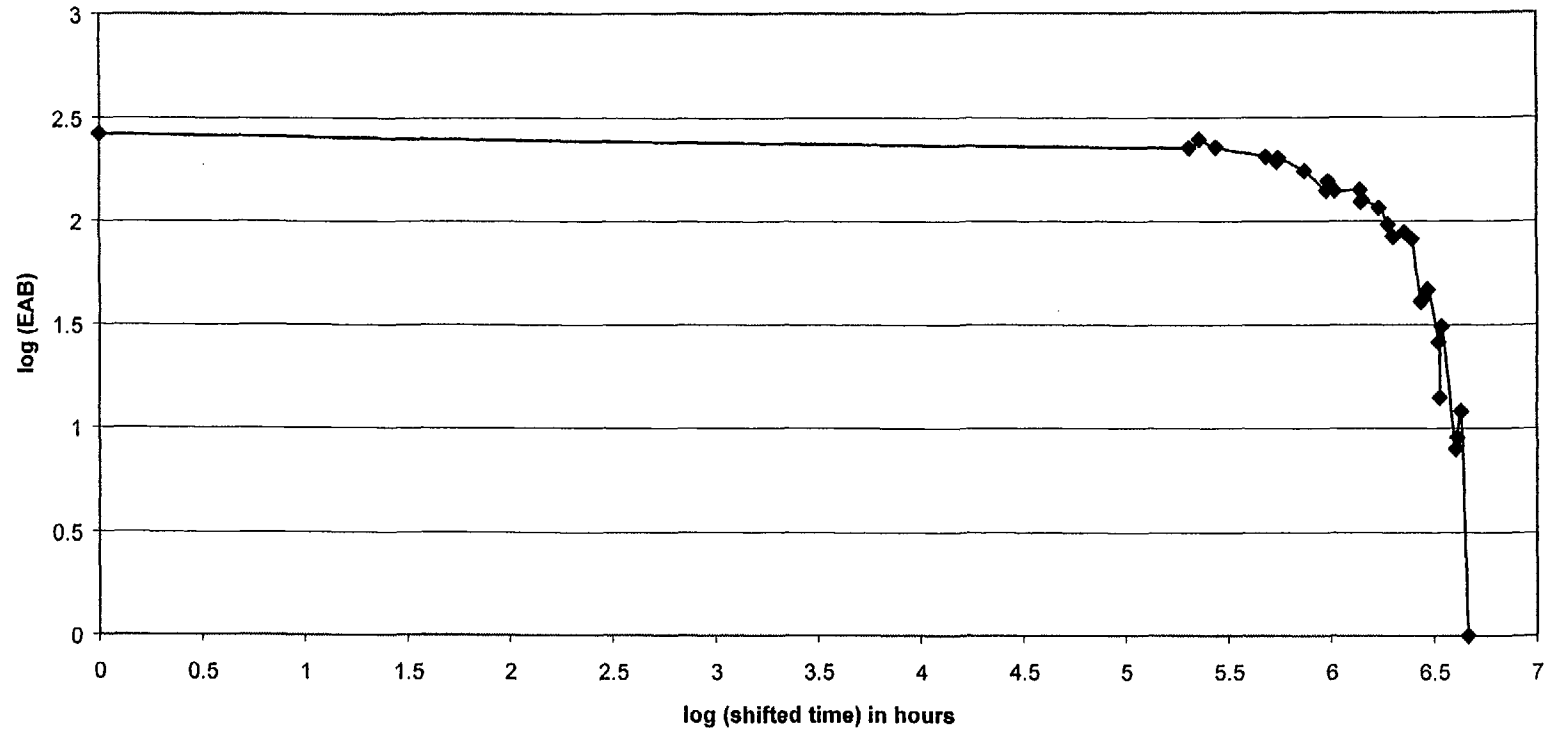


Figure A.2.3 Time-Temperature Superposition - Samuel Moore CSPE C-9

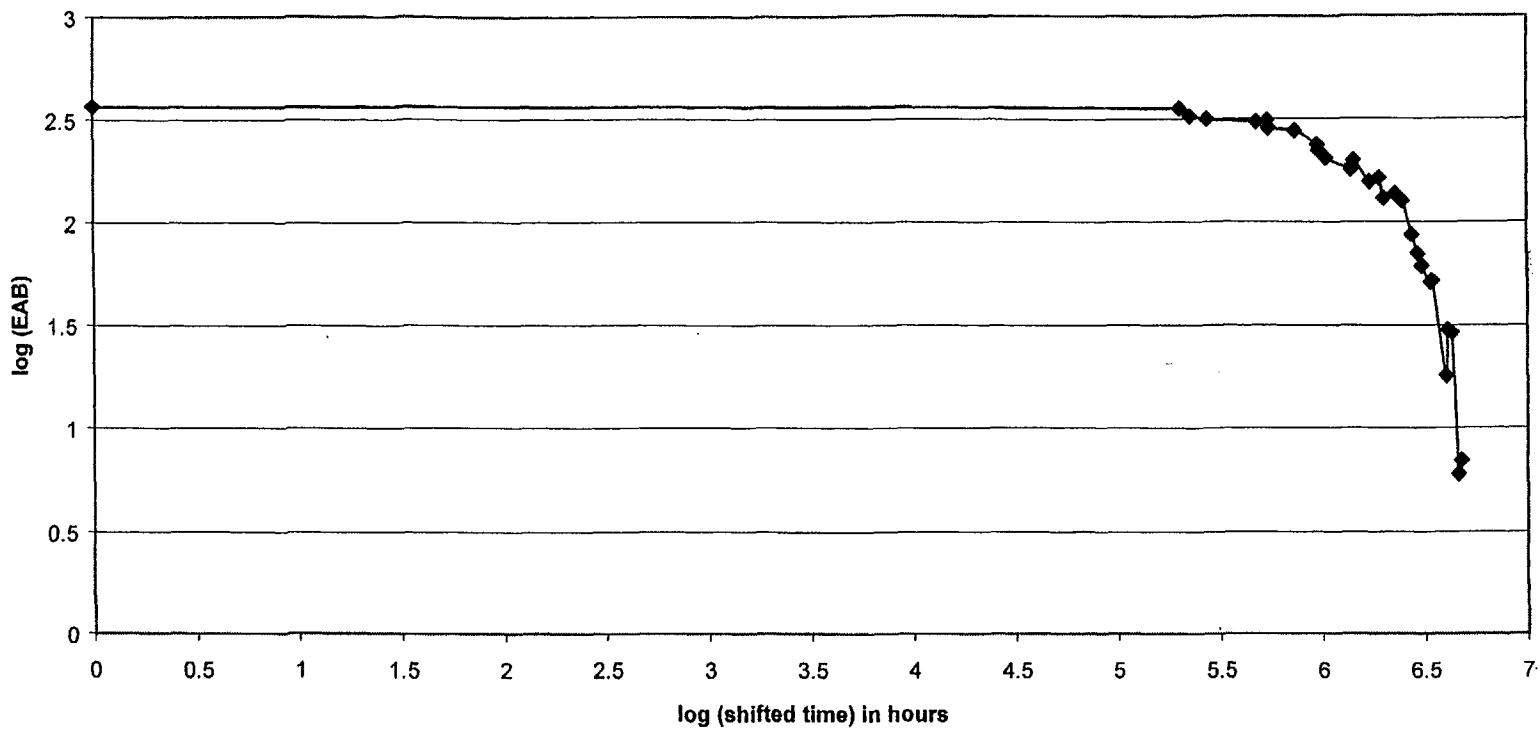
Time Temperature Superposition Using 1.084128 EV - Anaconda CPSE Jacket C-10



-A36-

Figure A.2.4 Time-Temperature Superposition - Anaconda CSPE Jacket C-10.

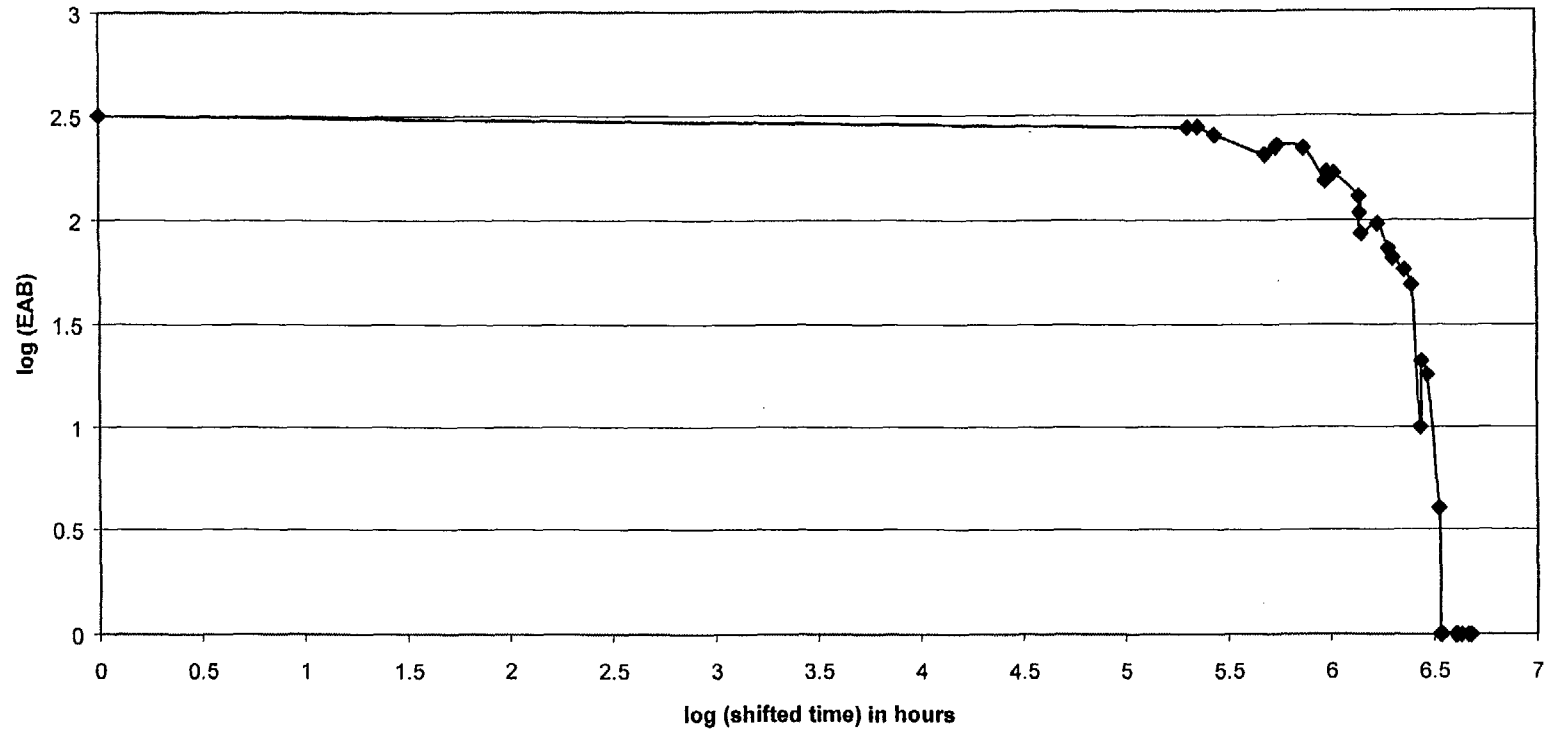
Time Temperature Superposition Using 1.084128 EV - Rockbestos CSPE C-11



-A37-

Figure A.2.5 Time-Temperature Superposition - Rockbestos CSPE C-11.

Time Temperature Superposition Using 1.084128 EV - Eaton CSPE C-5



-A38-

Figure A.2.6 Time-Temperature superposition- Eaton CSPE C-5.

Time Temperature Superposition Using .91168 EV - Anaconda EPR

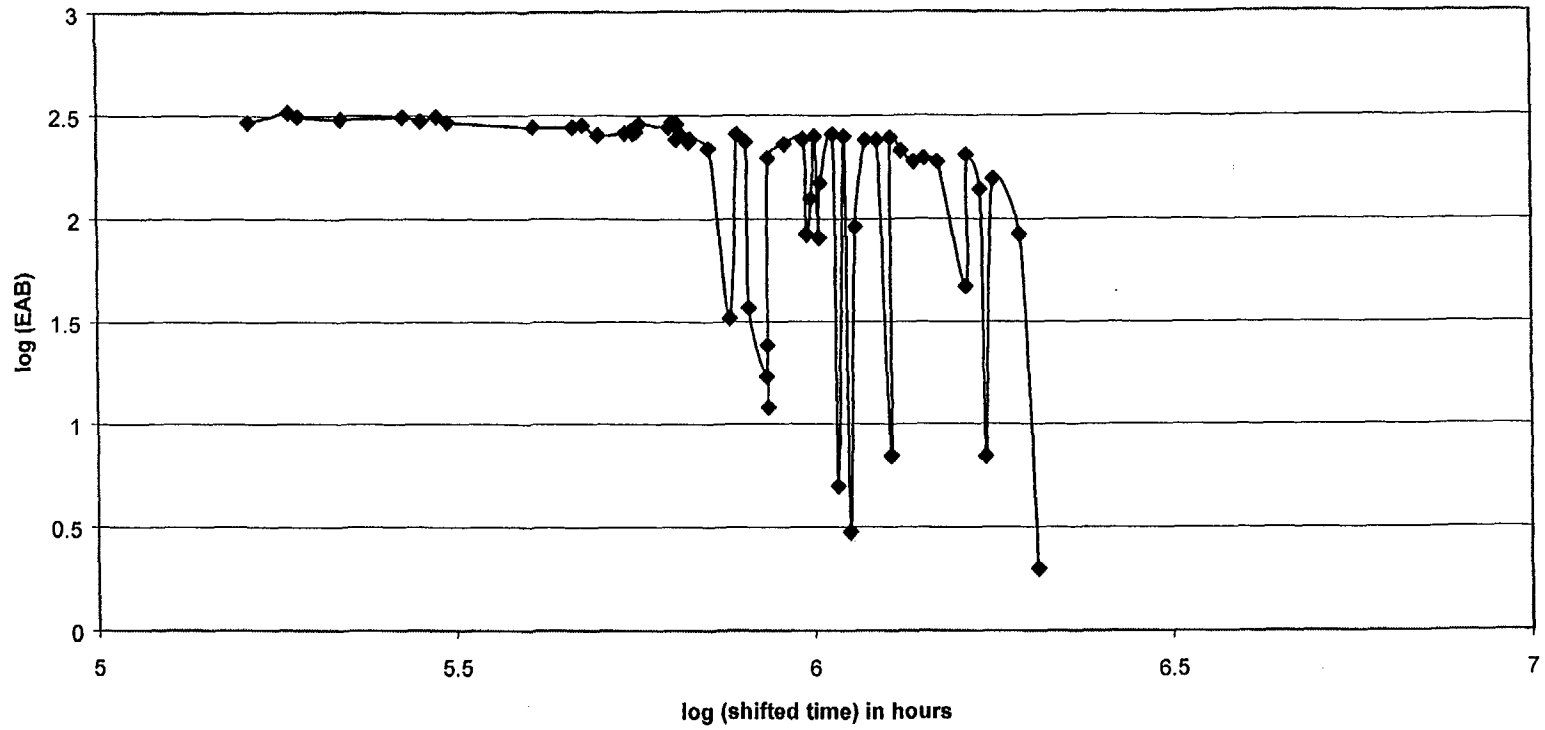
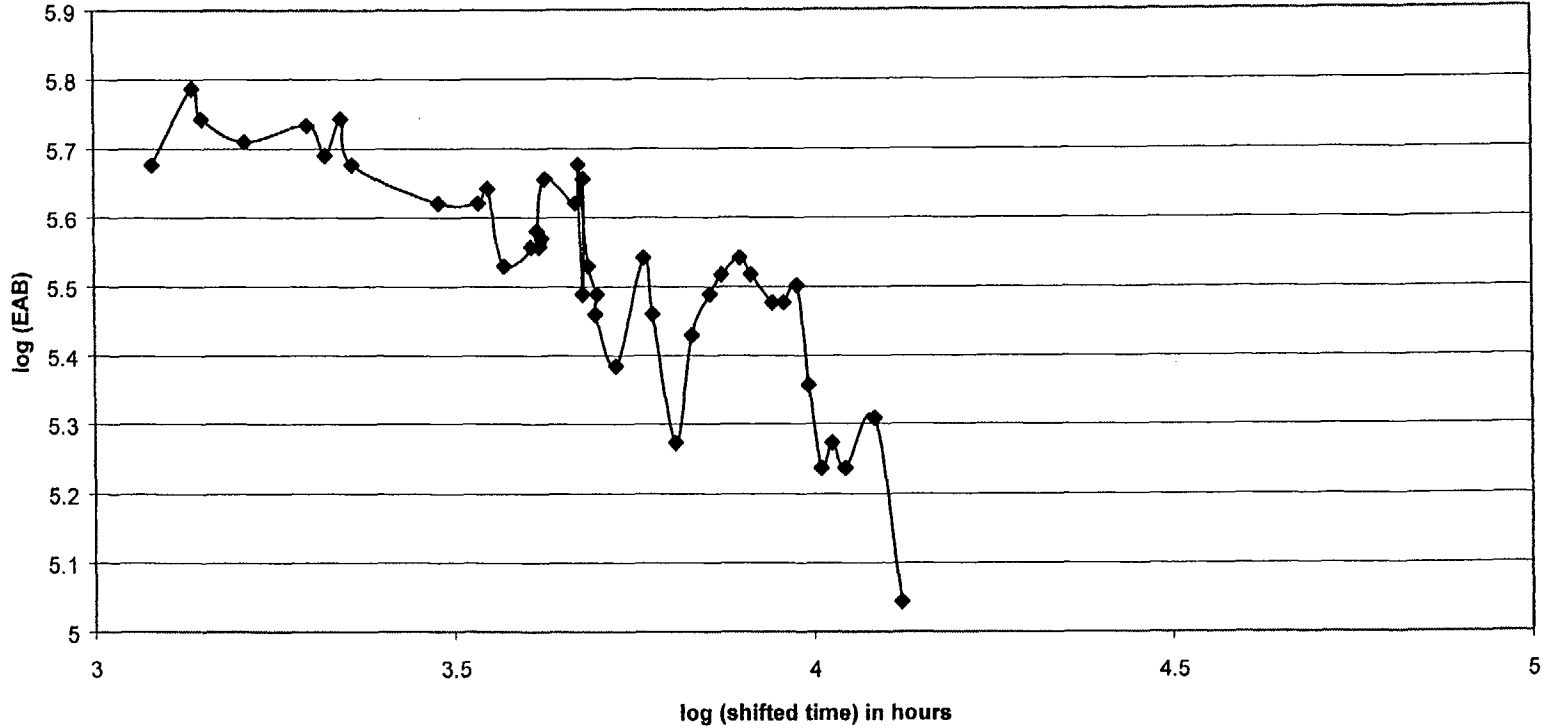


Figure A.2.7a Time-Temperature Superposition - Anaconda EPR C-14 (without truncation).

Time Temperature Superposition Using .91168 EV - Anaconda EPR



-A40-

Figure A.2.7b Time-Temperature Superposition - Anaconda EPR C-14 (with truncation).

Time Temperature Superposition Using .91168 EV- Anaconda EPR FR-EP C-2

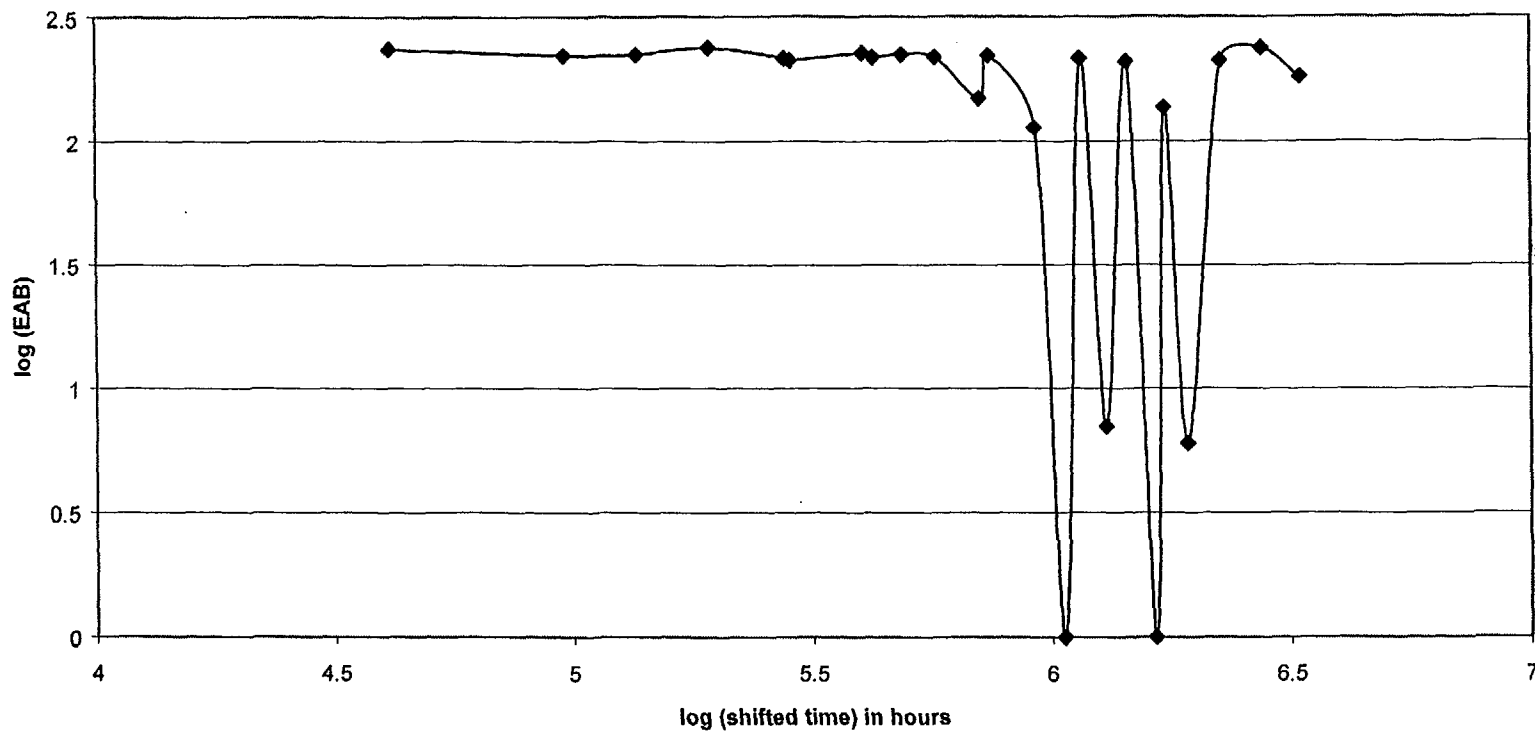


Figure A.2.8a Time-Temperature Superposition - Anaconda EPR FR-EP C-2 (without truncation).

Time Temperature Superposition Using .91168 EV- Anaconda EPR FR-EP C-2

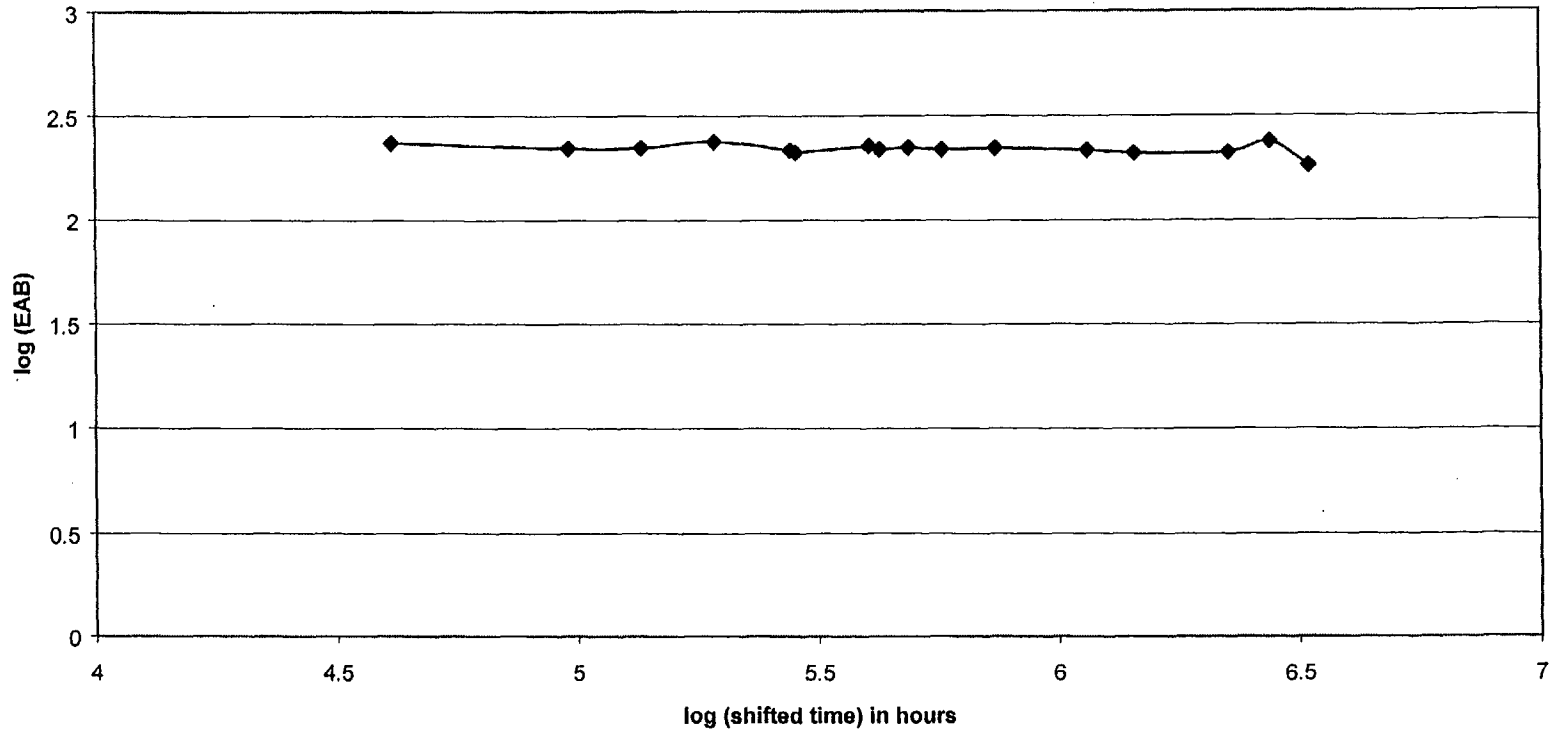
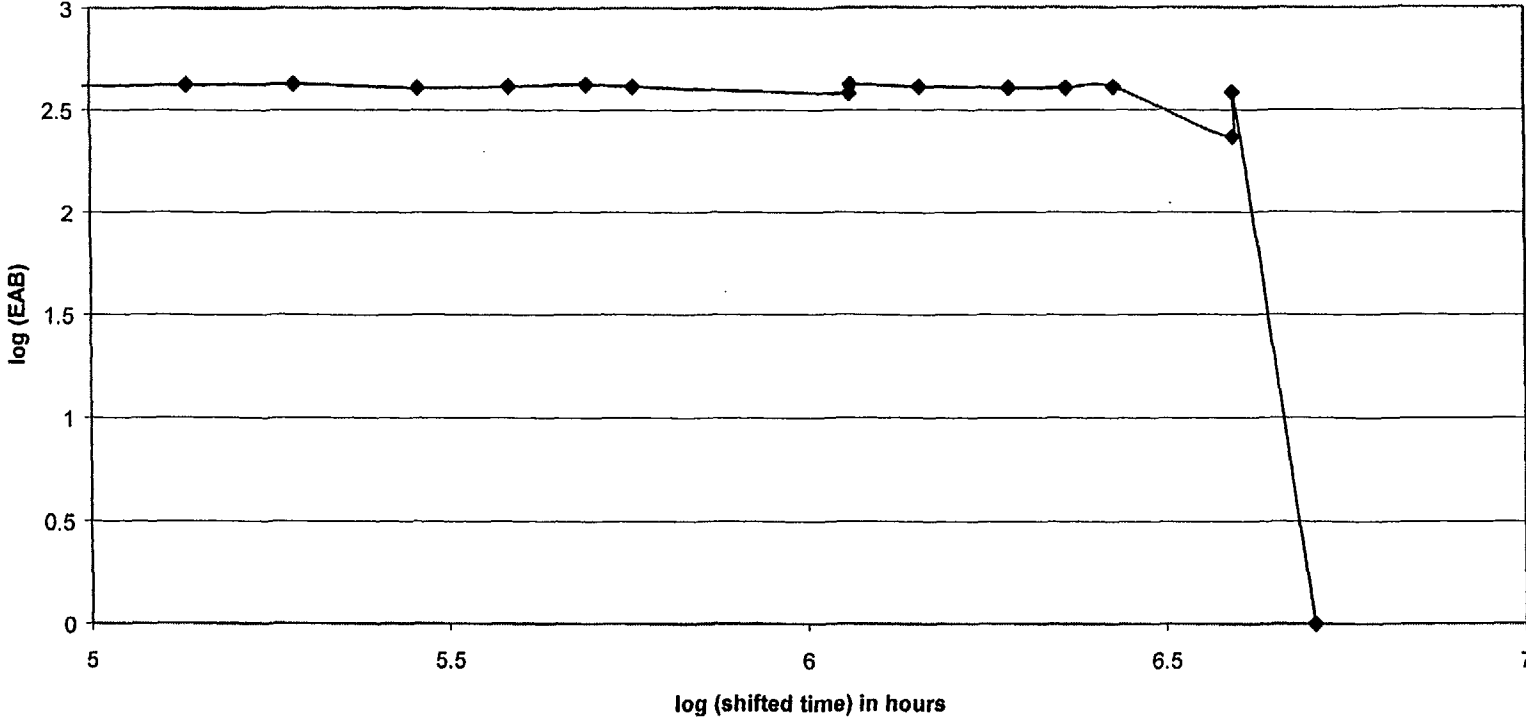


Figure A.2.8b Time-Temperature Superposition - Anaconda EPR FR-EP C-2 (with truncation).

Time Temperature Superposition Using .91168 EV- Eaton EPR C-5



-A43-

Figure A.2.9 Time-Temperature Superposition - Eaton EPR C-5.

Figure A.2.10 Time-Temperature Superposition - Rockbestos Silicone Rubber C-7.

(No thermal aging data is available in CPAD.)

Time Temperature Superposition Using 0.91168 EV - Eaton XLPO C-4

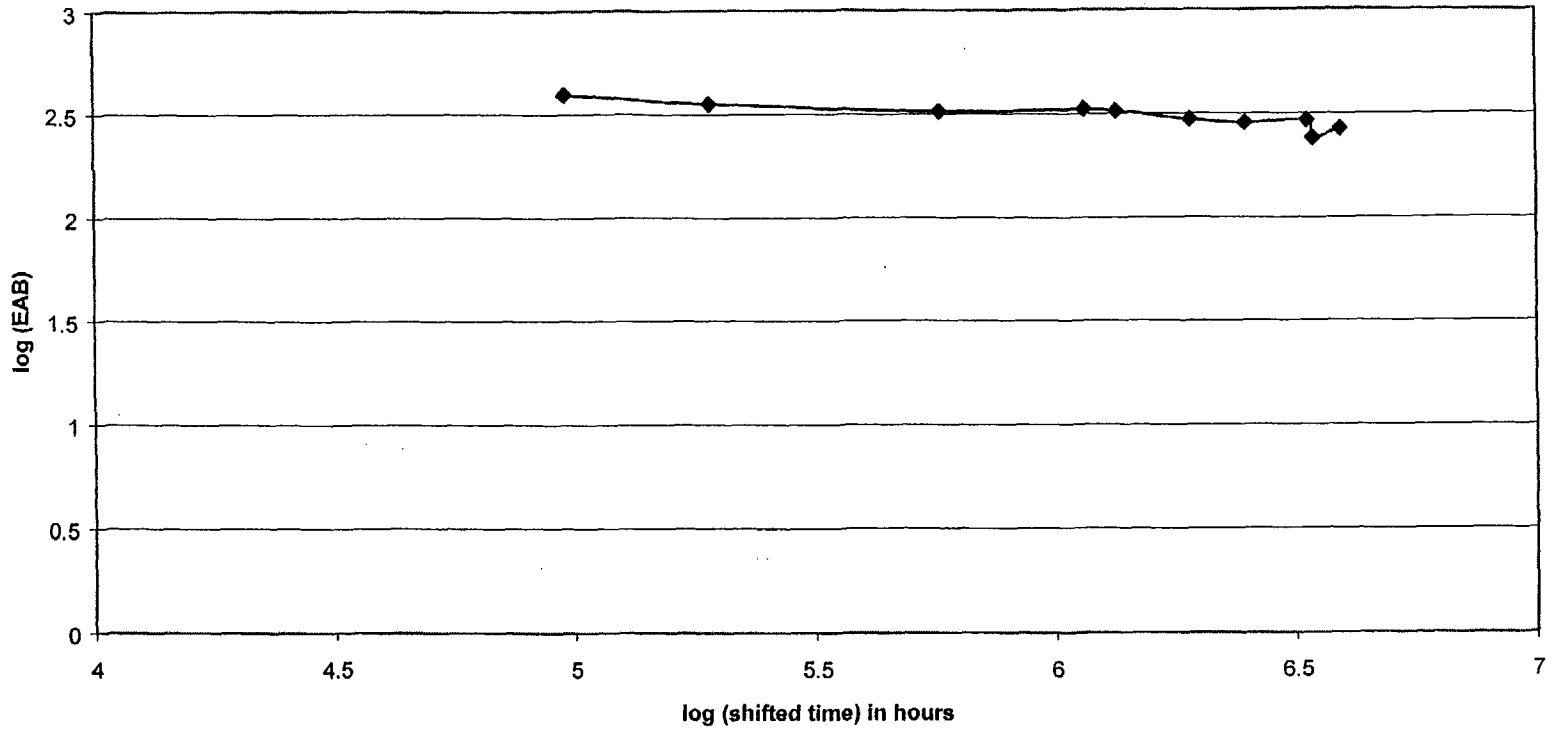
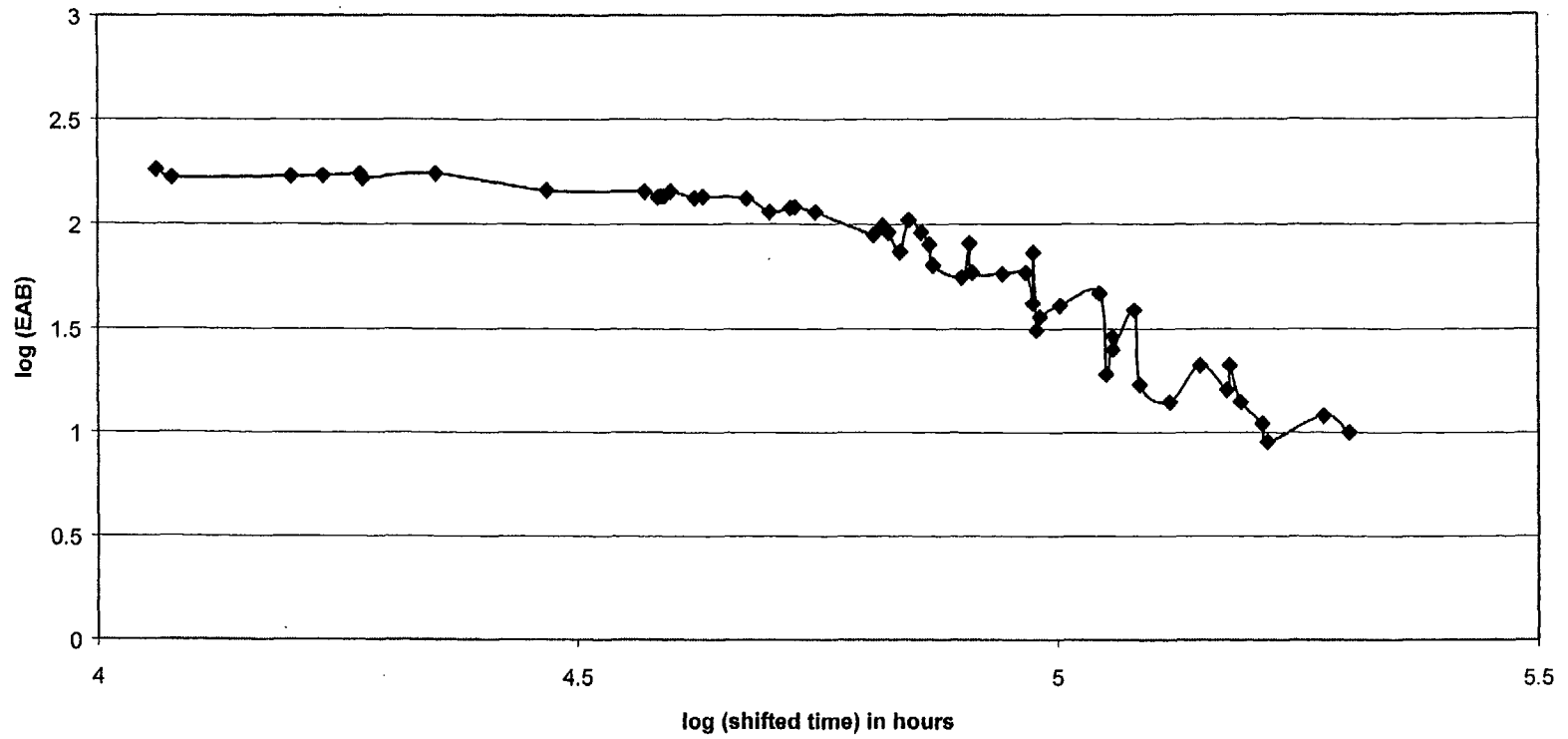


Figure A.2.11 Time-Temperature Superposition - Eaton XLPO C-4.

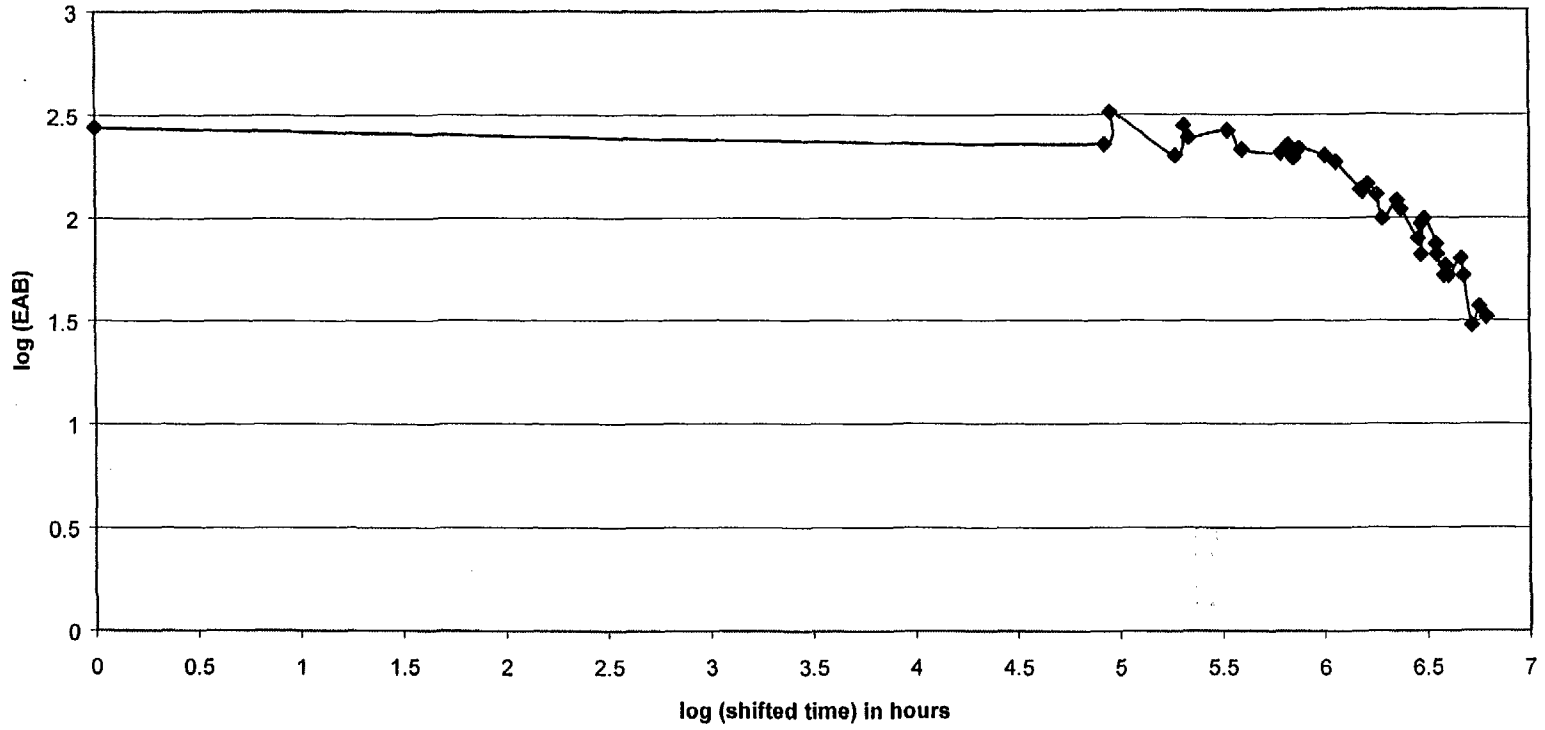
Time Temperature Superposition Using 0.954 EV - Okonite Neo C-17 Air



-A46-

Figure A.2.12 Time-Temperature Superposition - Okonite Neoprene C-17.

Time Temperature Superposition Using 0.91168 EV -Kerite Proprietary C-6 Air



-A47-

Figure A.2.13 Time-Temperature Superposition - Kerite Proprietary Insulation C-6.

A.3 Predictions of Reliability Physics Model

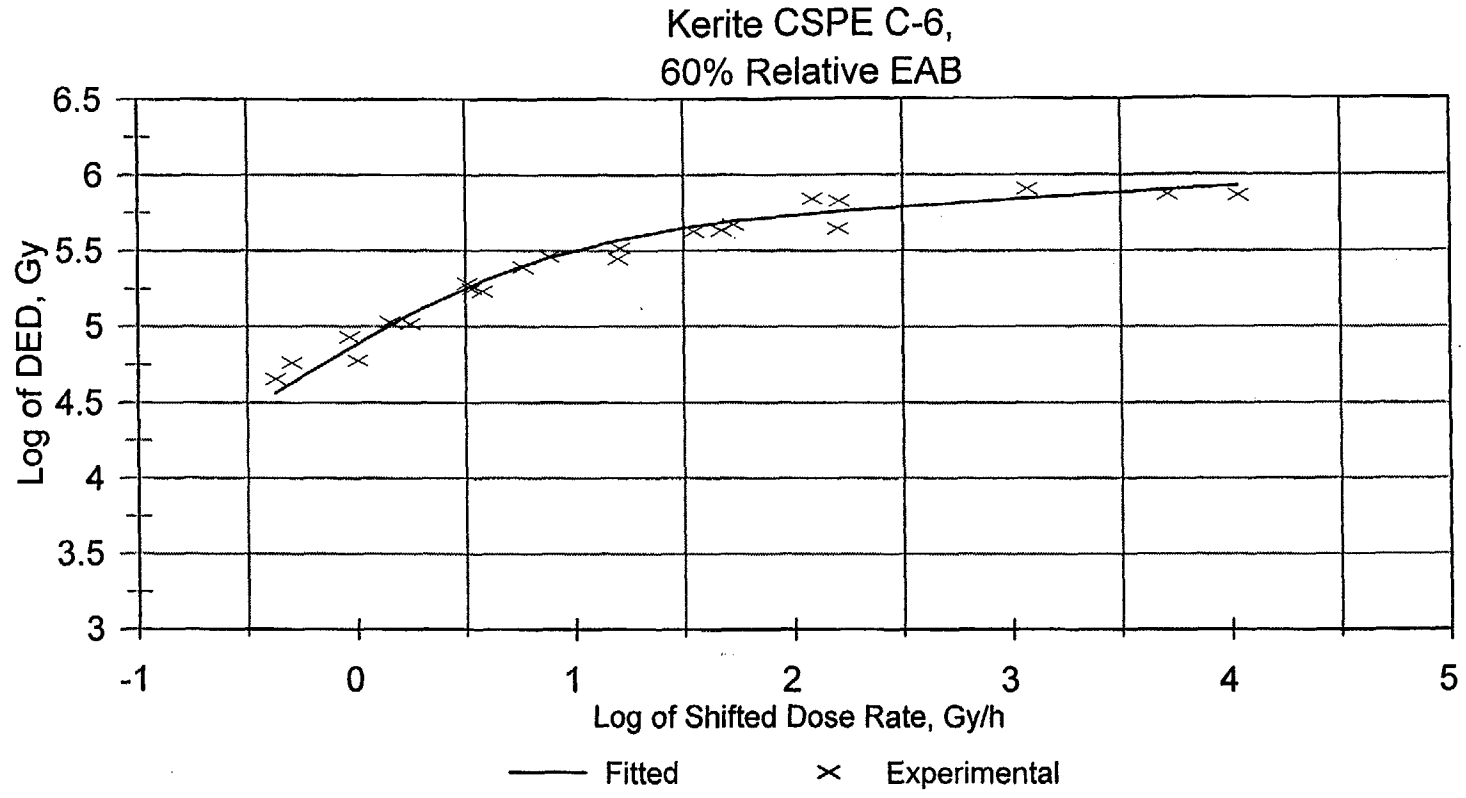


Figure A.3.1a Predicted DED vs D Curve - Kerite CSPE C-6 (60% Relative EAB)

Kerite CSPE C-6, 100% EAB

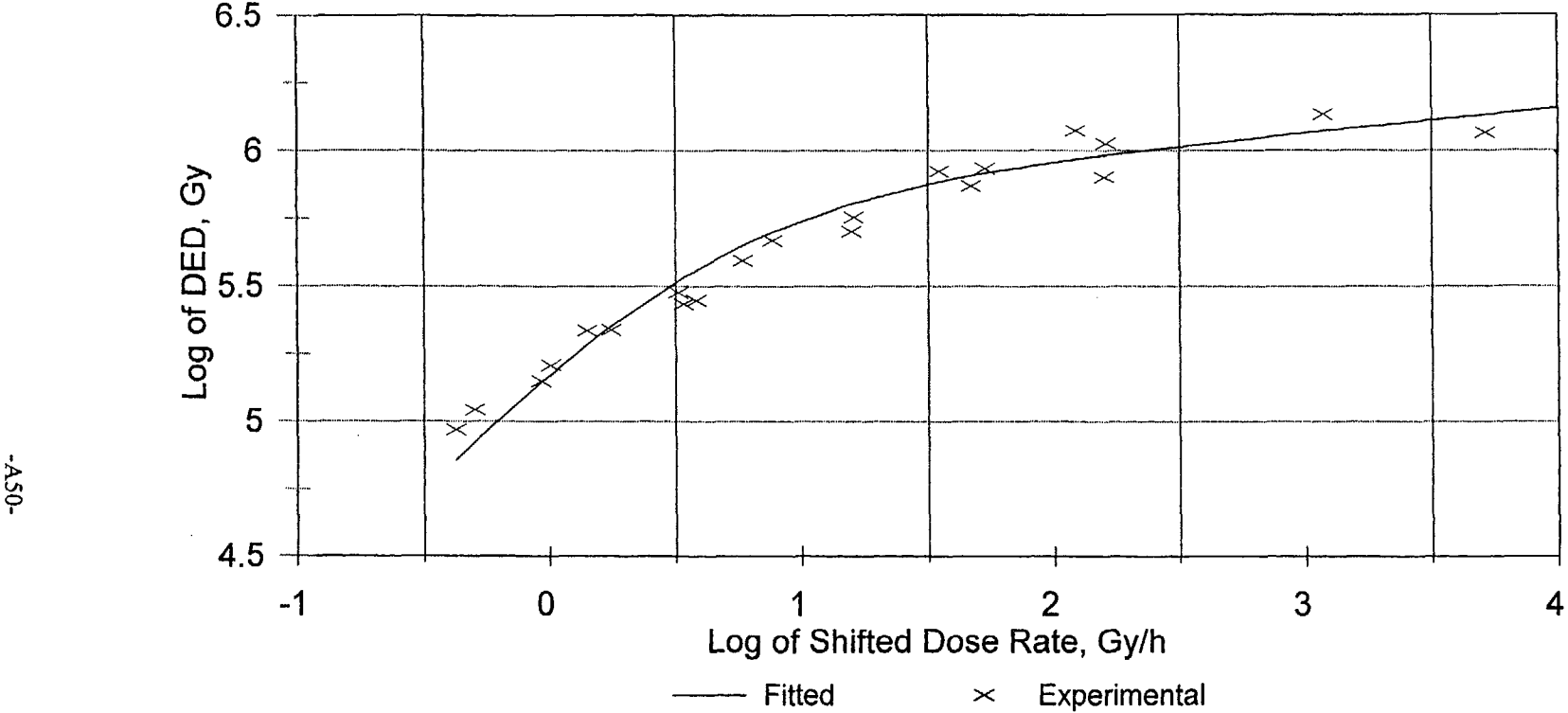


Figure A.3.1b Predicted DED vs D Curve - Kerite CSPE C-6 (100% EAB)

Anaconda CSPE C-15,
60% Relative EAB

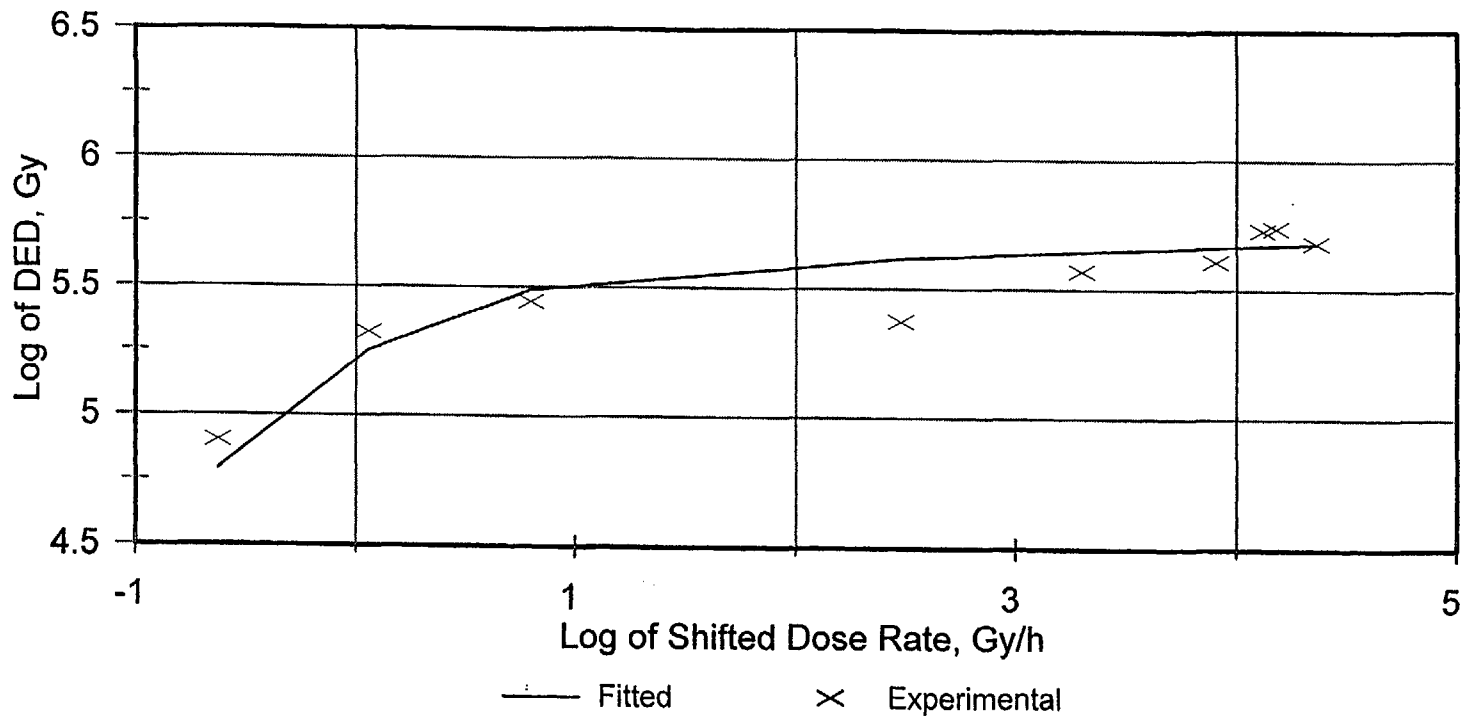


Figure A.3.2a Predicted DED vs D Curve - Anaconda CSPE C-15 (60% Relative EAB)

Anaconda CSPE C-15, 100% EAB

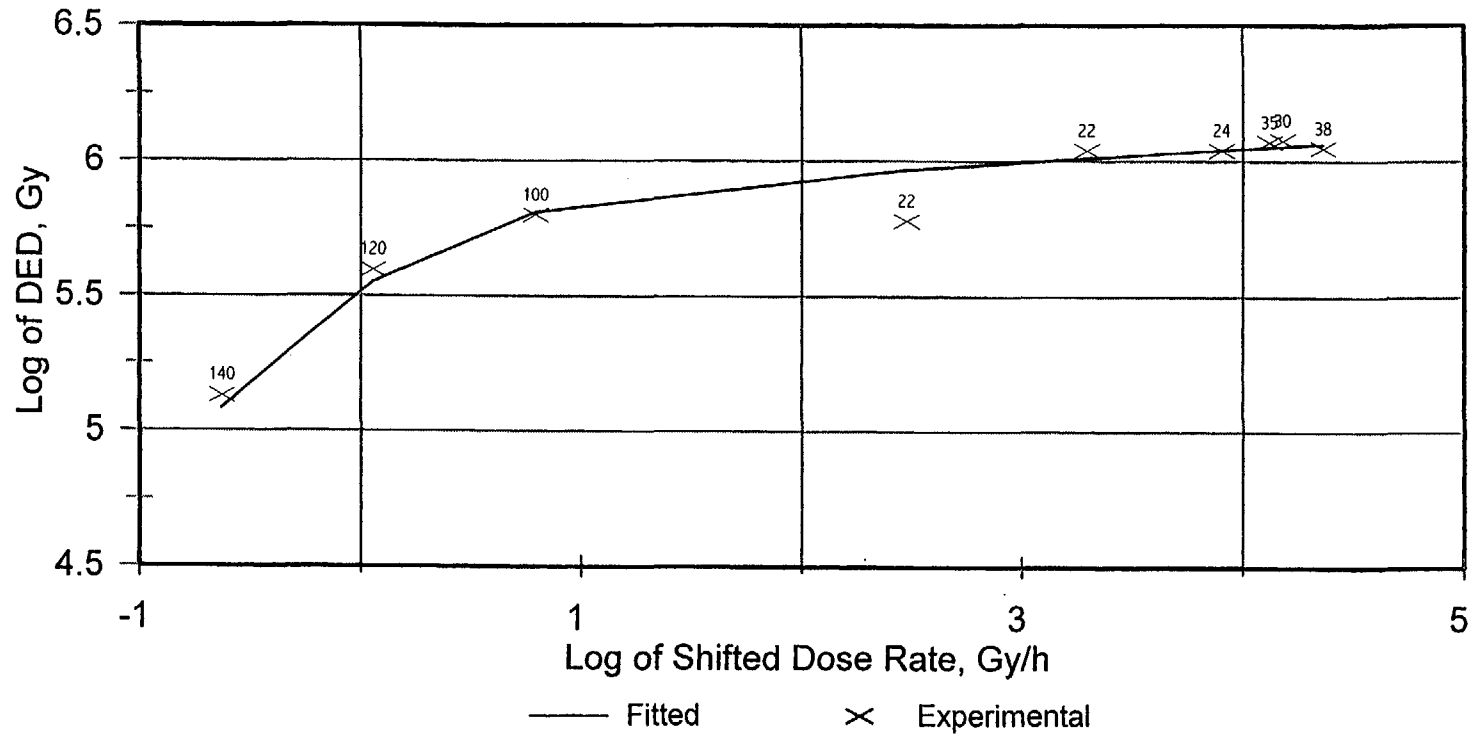


Figure A.3.2b Predicted DED vs D Curve - Anaconda CSPE C-15 (100% EAB)

Anaconda CSPE C-15, 100% EAB,
Regression Fit

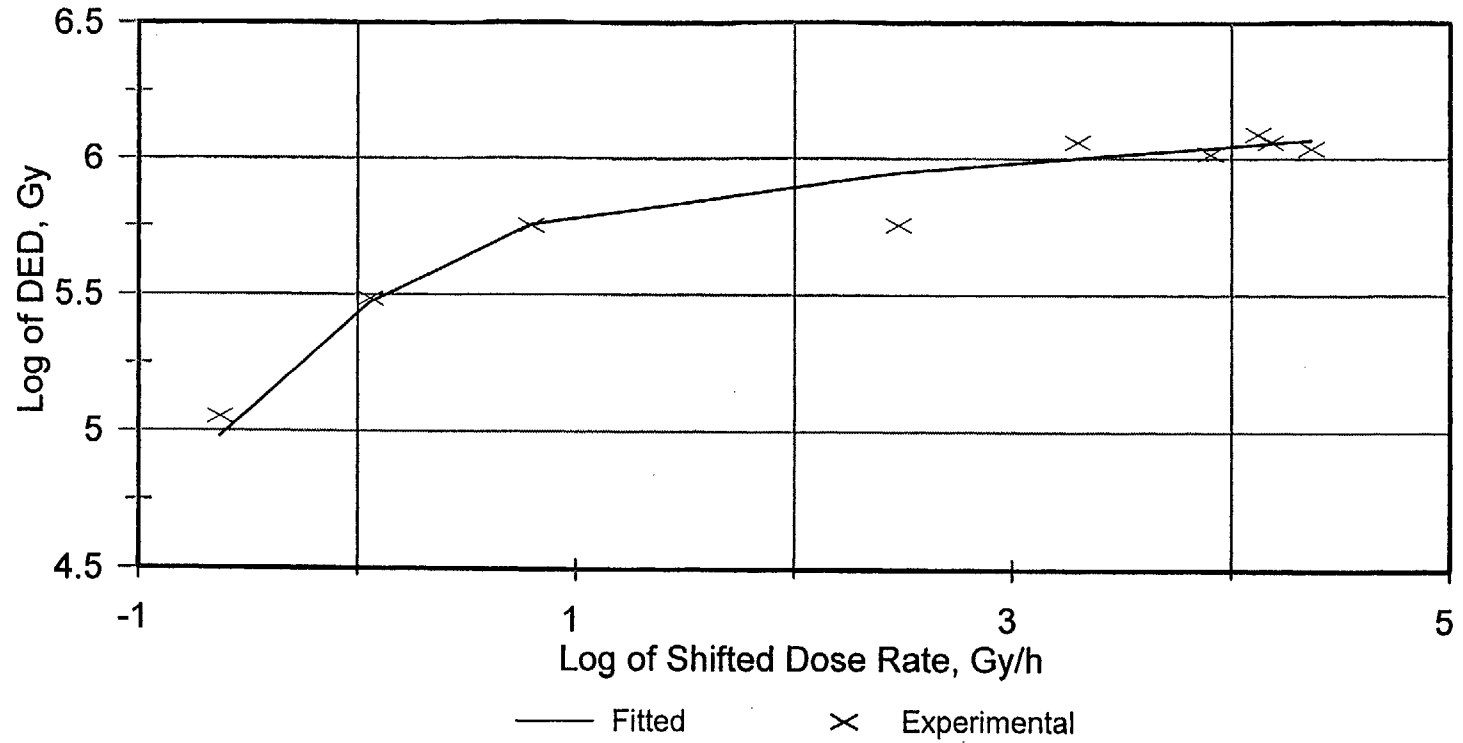


Figure A.3.2c Predicted DED vs D Curve - Anaconda CSPE C-15 (100% EAB), Regression Fit

Samuel Moore CSPE C-9,
60% Relative EAB

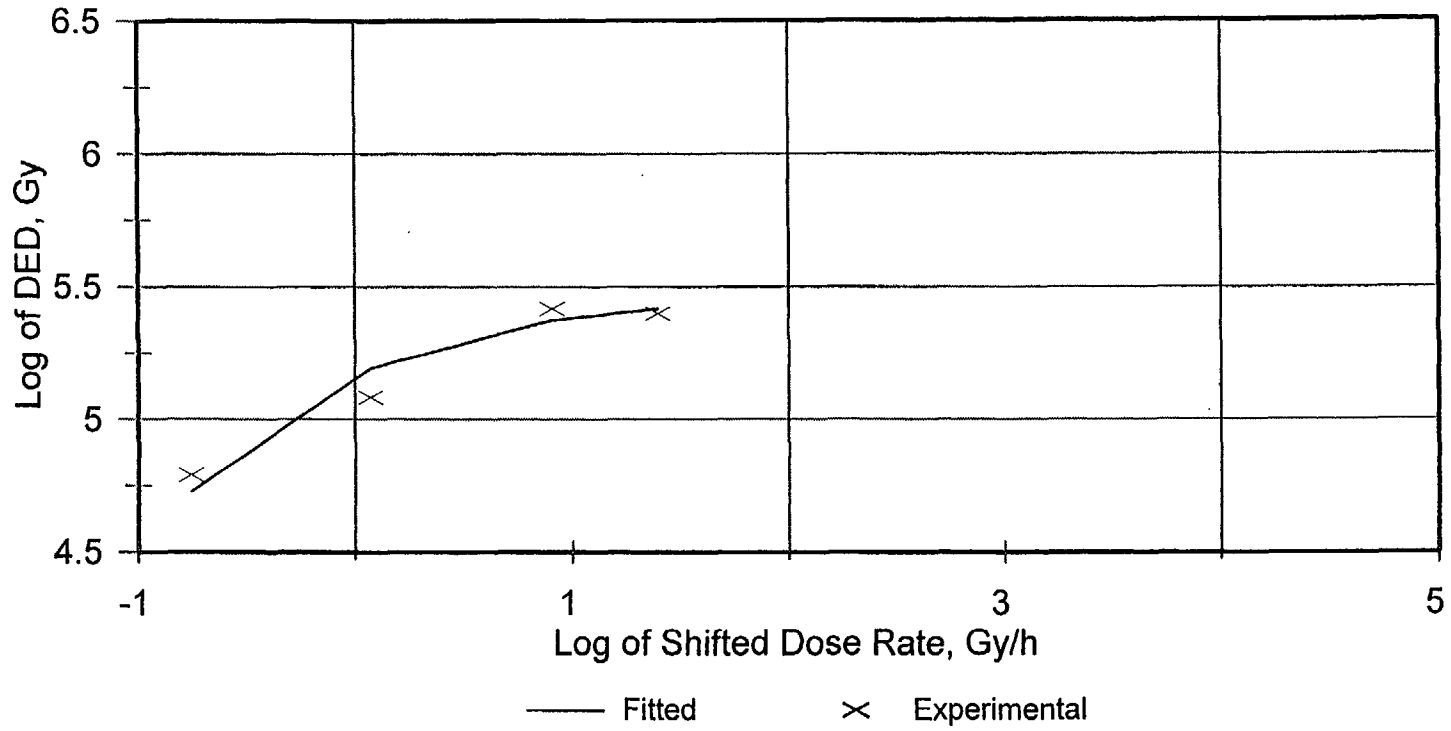


Figure A.3.3a Predicted DED vs D Curve - Samuel Moore CSPE C-9 (60% Relative EAB)

Samuel Moore CSPE C-9, 100% EAB

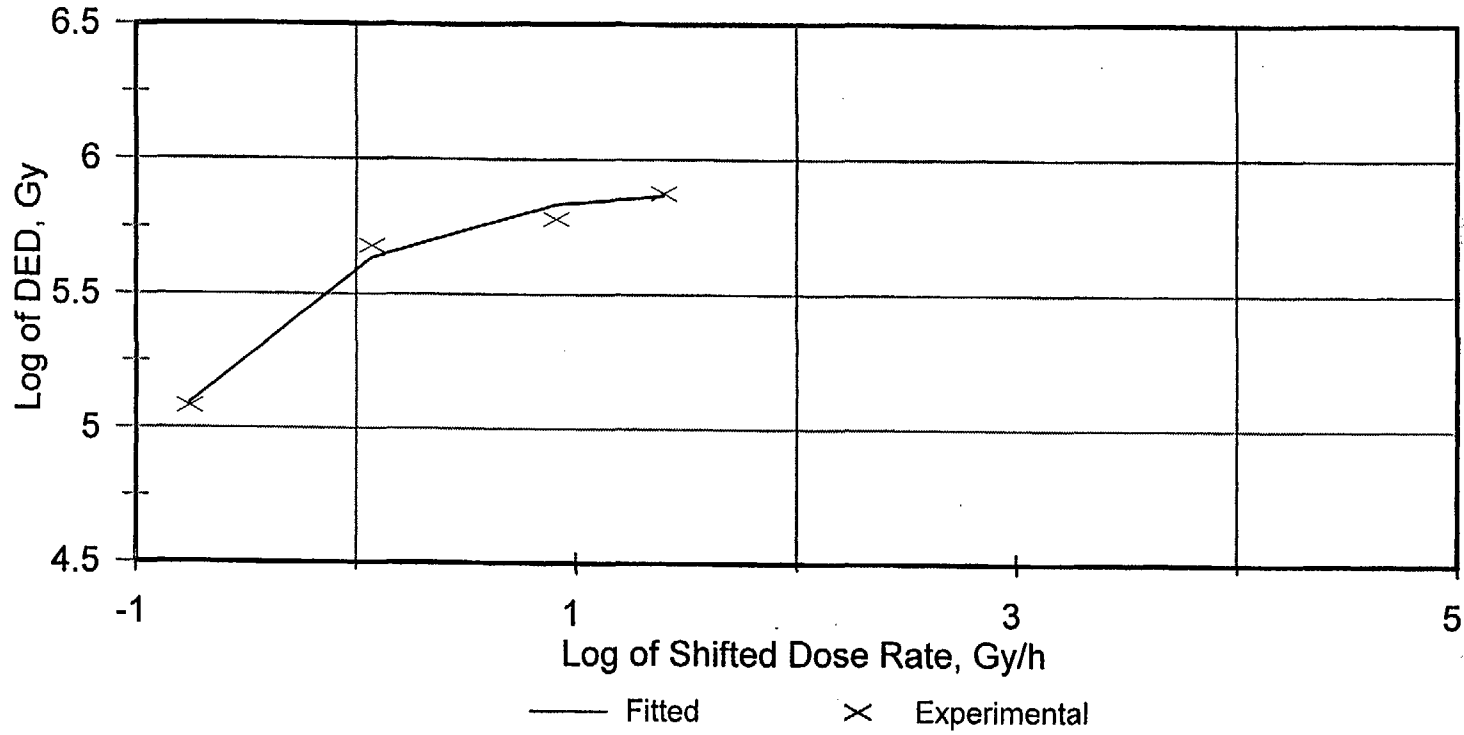


Figure A.3.3b Predicted DED vs D Curve - Samuel Moore CSPE C-9 (100% EAB)

-ASS-

Anaconda CSPE Jacket C-10,
60% Relative EAB

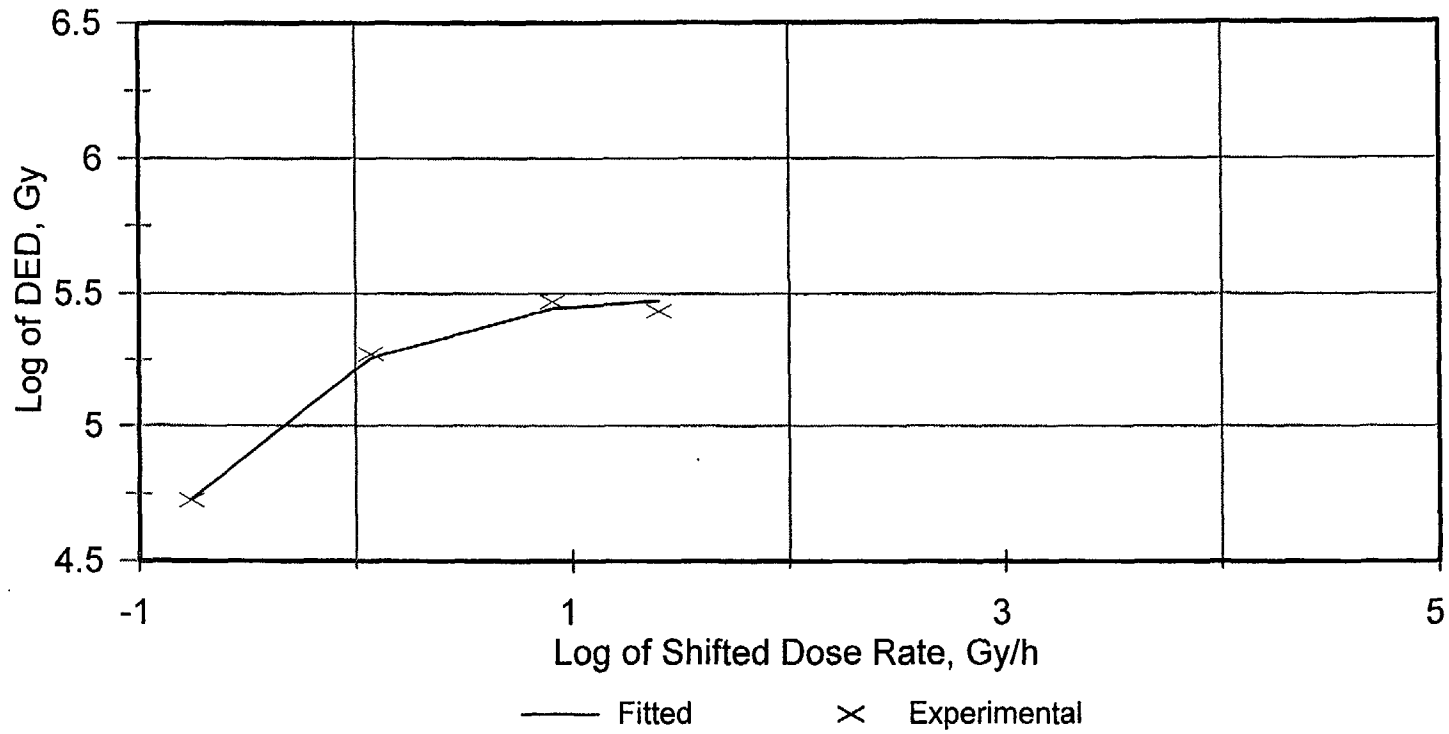


Figure A.3.4a Predicted DED vs D curve - Anaconda CSPE Jacket C-10 (60% Relative EAB)

Anaconda CSPE Jacket C-10, 100% EAB

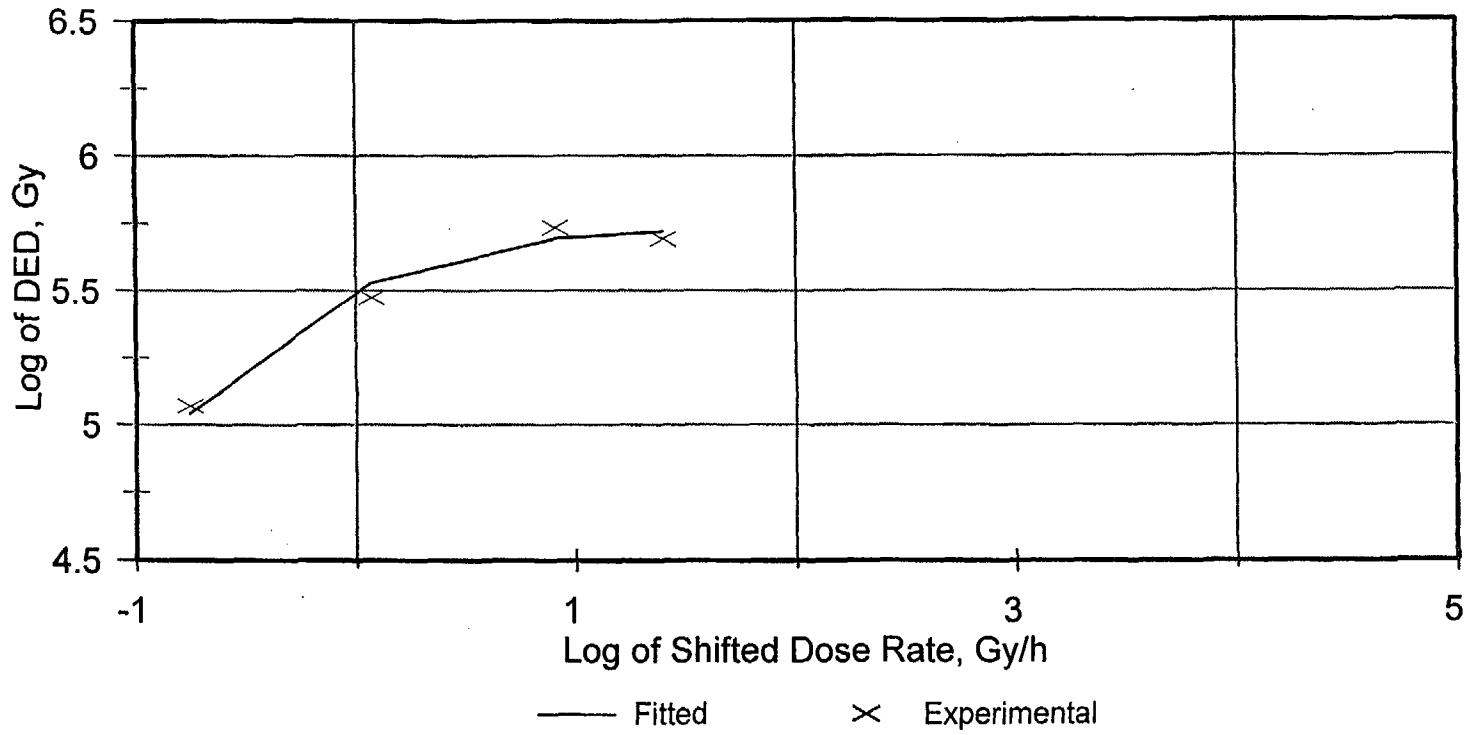


Figure A.3.4b Predicted DED vs D Curve - Anaconda CSPE Jacket C-10 (100% EAB)

Rockbestos CSPE Jacket C-11,
60% Relative EAB

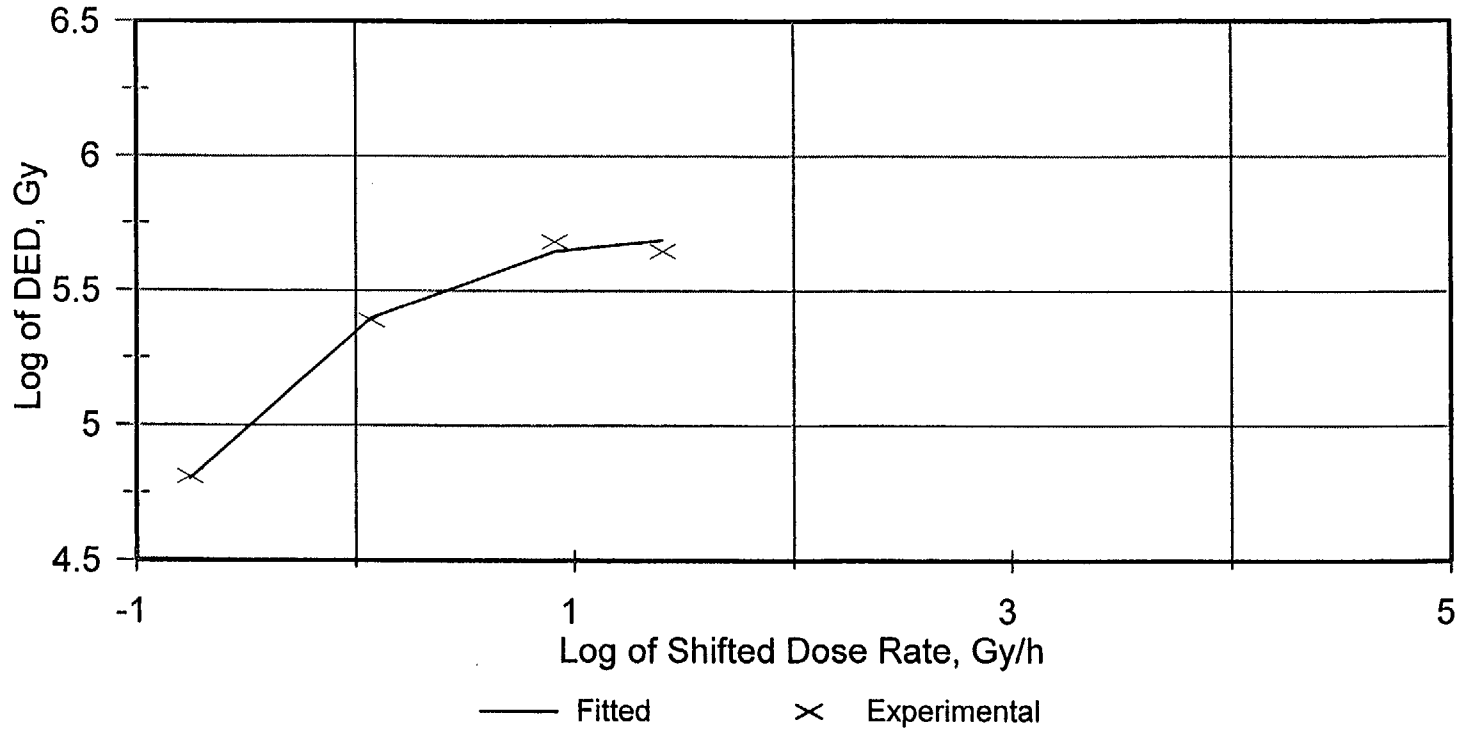


Figure A.3.5a Predicted DED vs D Curve - Rockbestos CSPE Jacket C-11 (60% Relative EAB)

Rockbestos CSPE Jacket C-11, 100% EAB

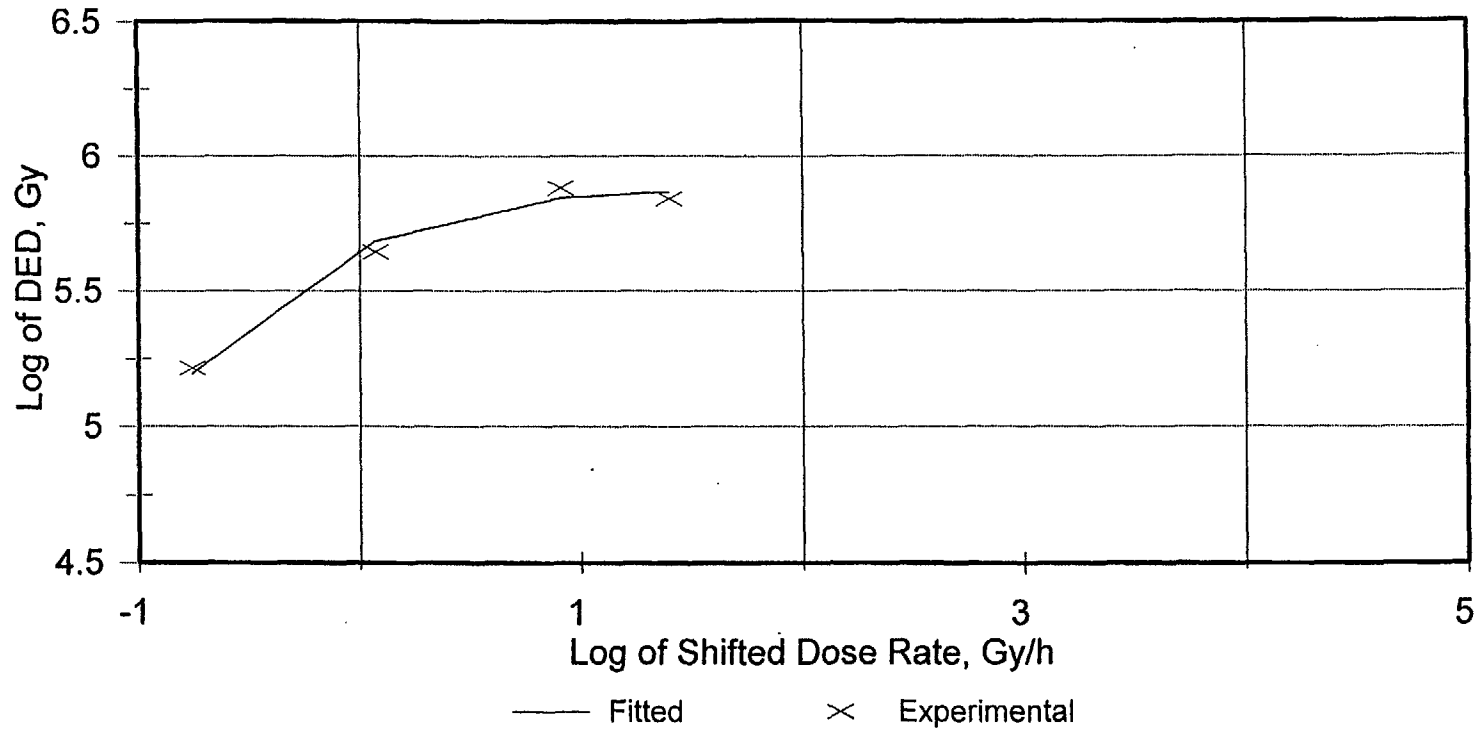


Figure A.3.5b Predicted DED vs D Curve - Rockbestos CSPE Jacket C-11 (100% EAB)

Eaton CSPE C-5, 60% Relative EAB

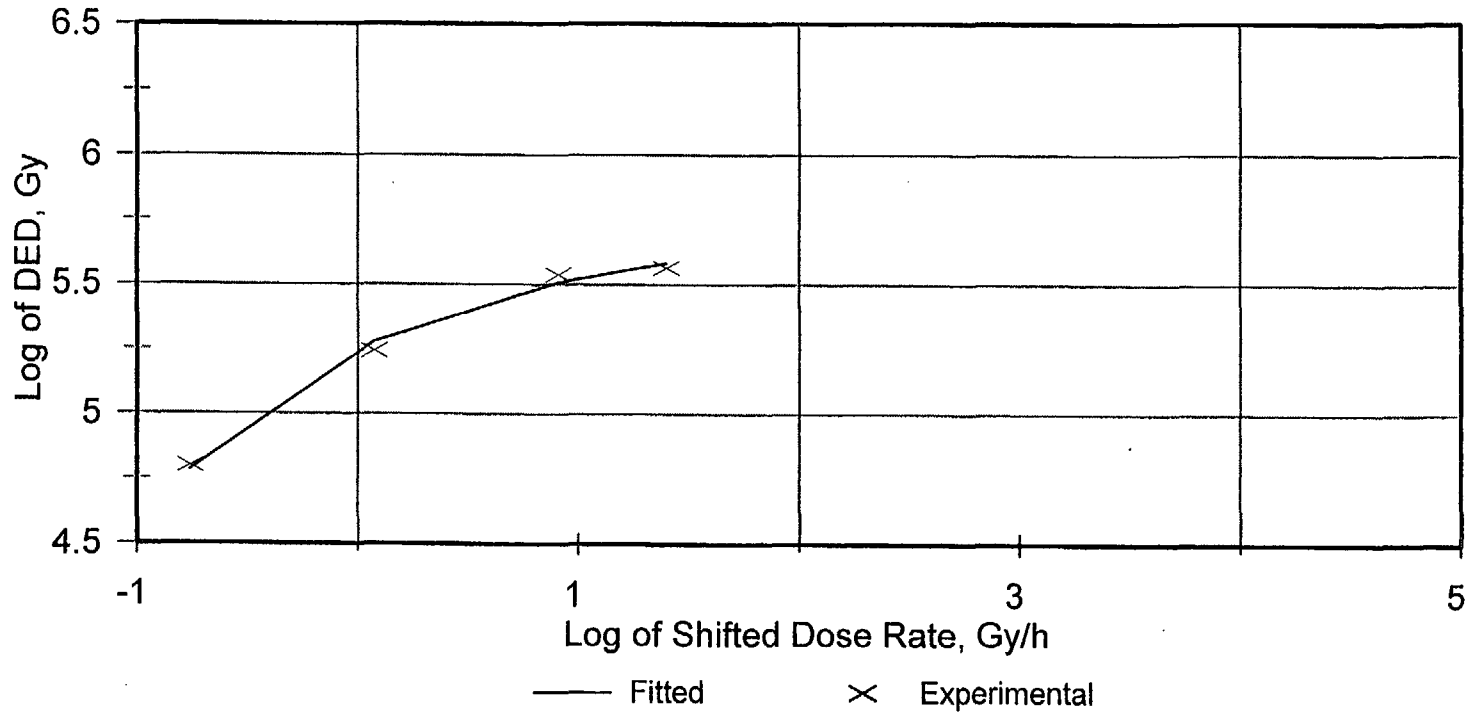


Figure A.3.6a Predicted DED vs D Curve - Eaton CSPE C-5 (60% Relative EAB)

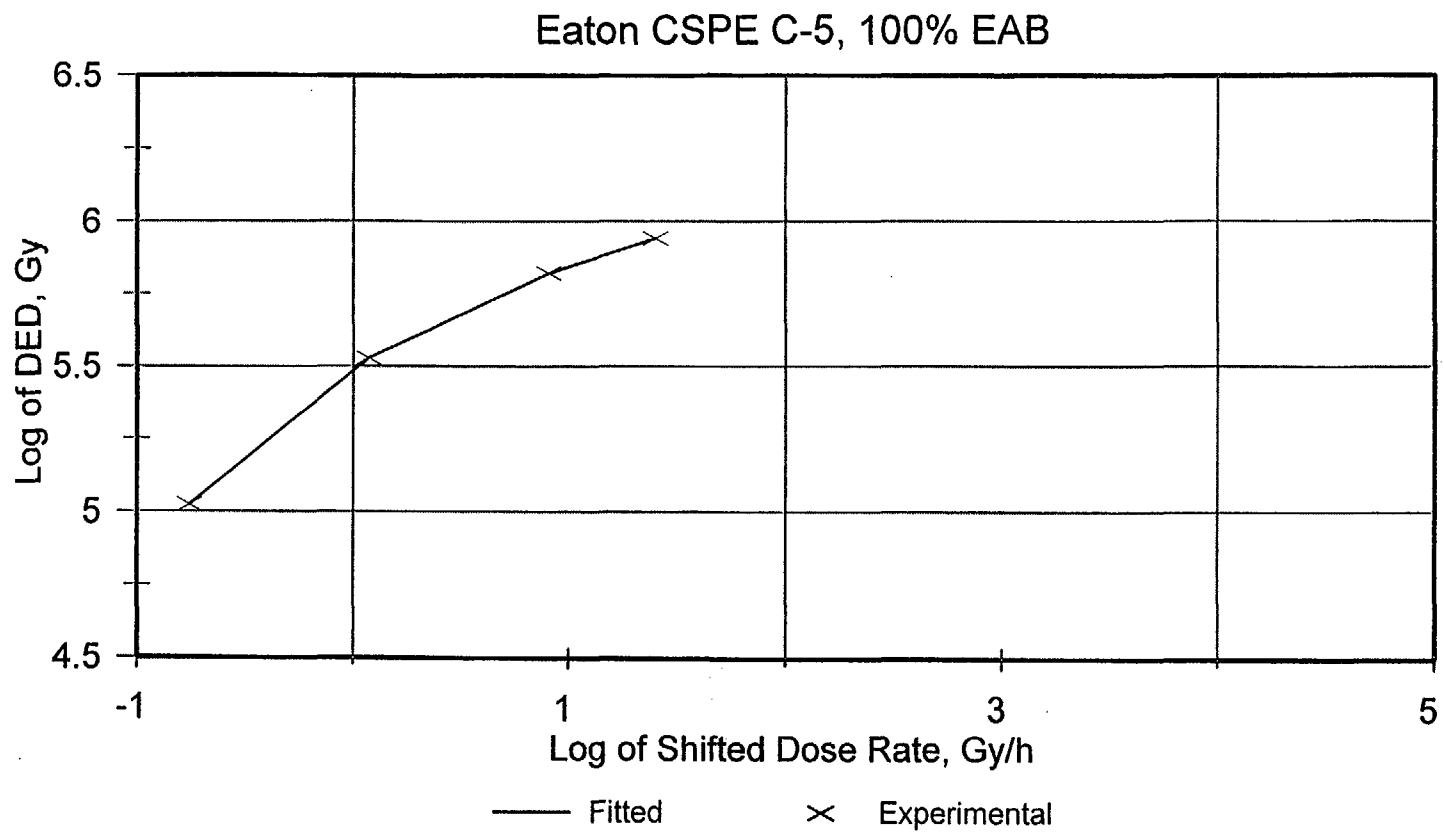


Figure A.3.6b Predicted DED vs D Curve - Eaton CSPE C-5 (100% EAB)

Anaconda EPR C-14, 100% EAB

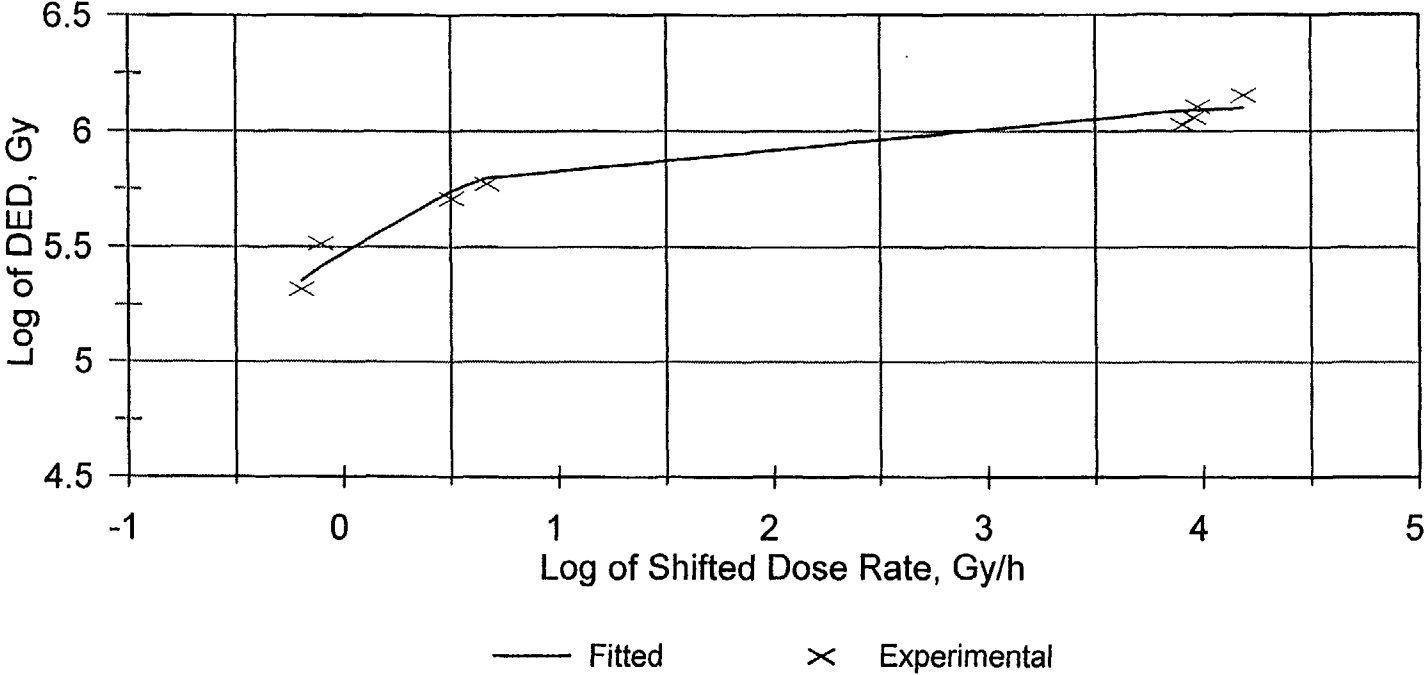


Figure A.3.7a Predicted DED vs D Curve - Anaconda EPR C-14 (100% EAB)

Anaconda EPR C-14, 150% EAB

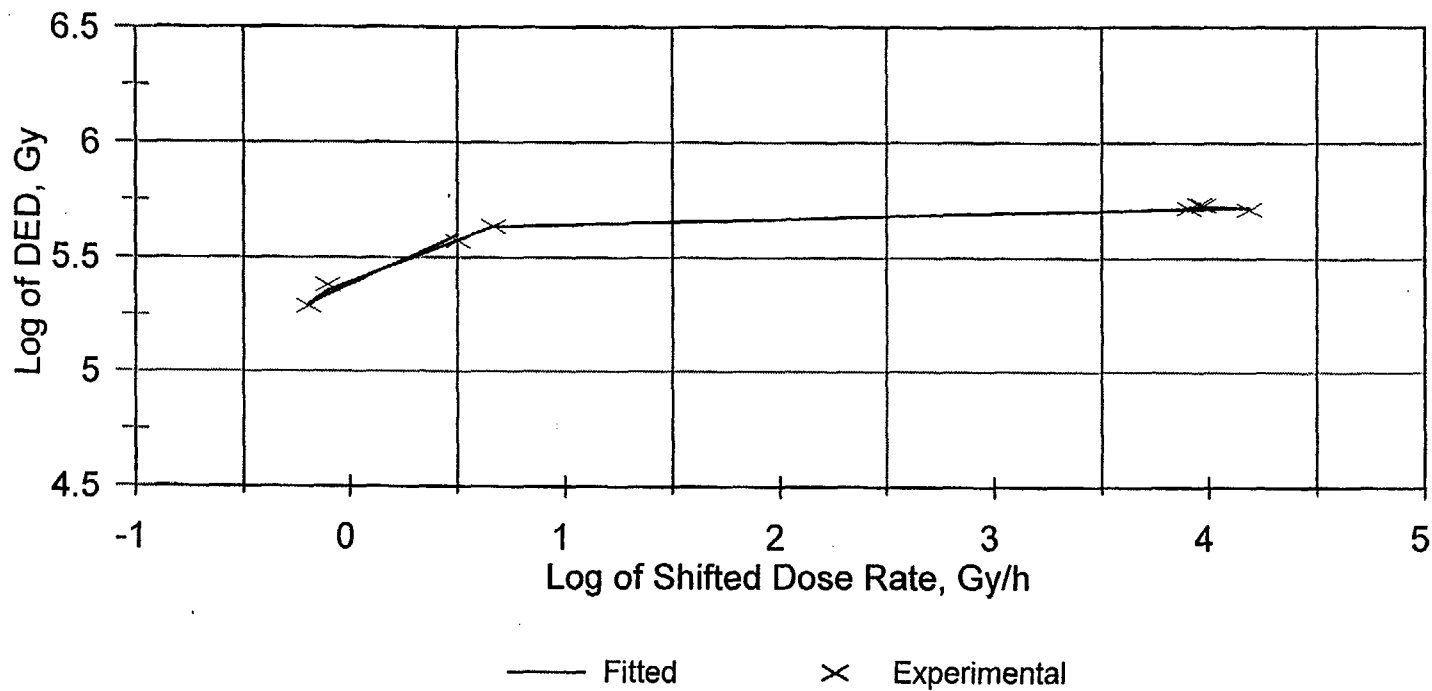


Figure A.3.7b Predicted DED vs D Curve - Anaconda EPR C-14 (150% EAB)

Anaconda EPR FR-EP C-2, 100% EAB

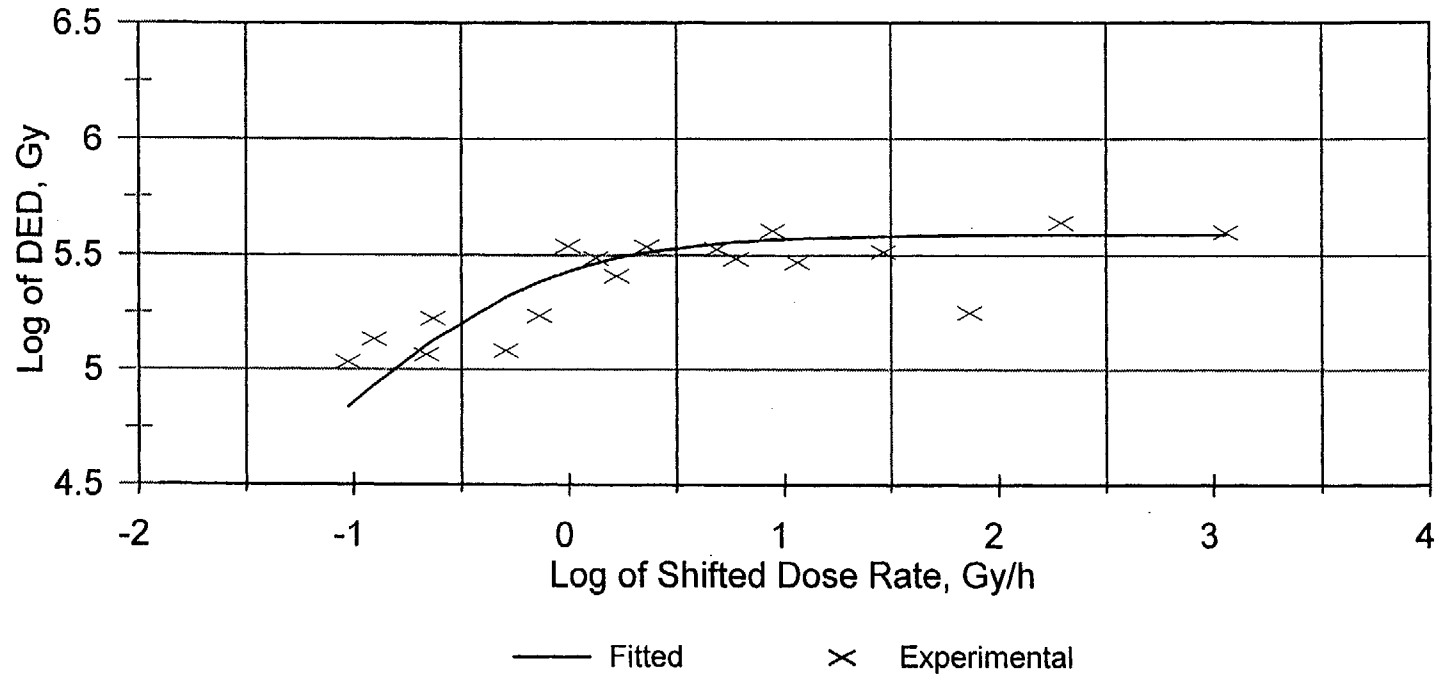


Figure A.3.8 Predicted DED vs D Curve - Anaconda EPR FR-EP C-2 (100% EAB)

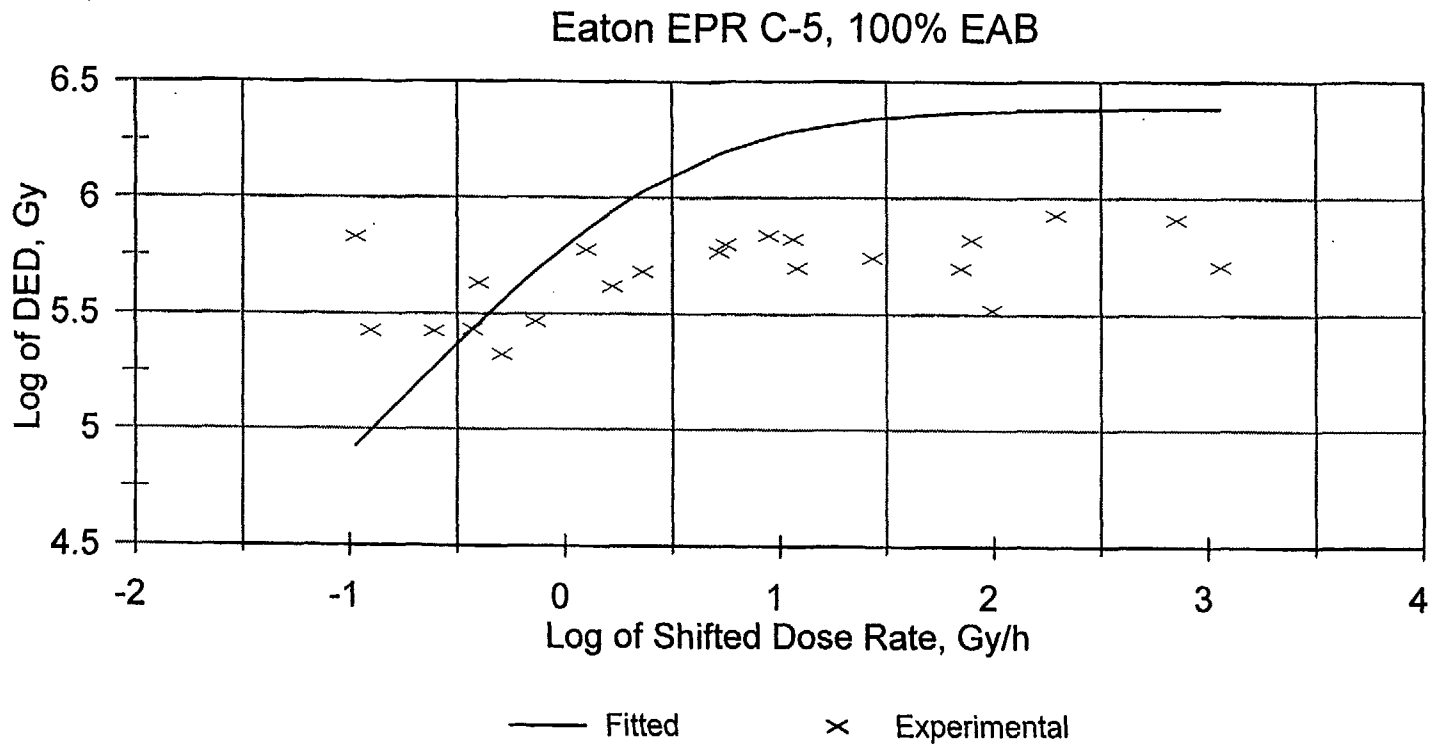


Figure A.3.9 Predicted DED vs D Curve - Eaton EPR C-5 (100% EAB)

Rockbestos Silicone Rubber C-7,
50% Relative EAB

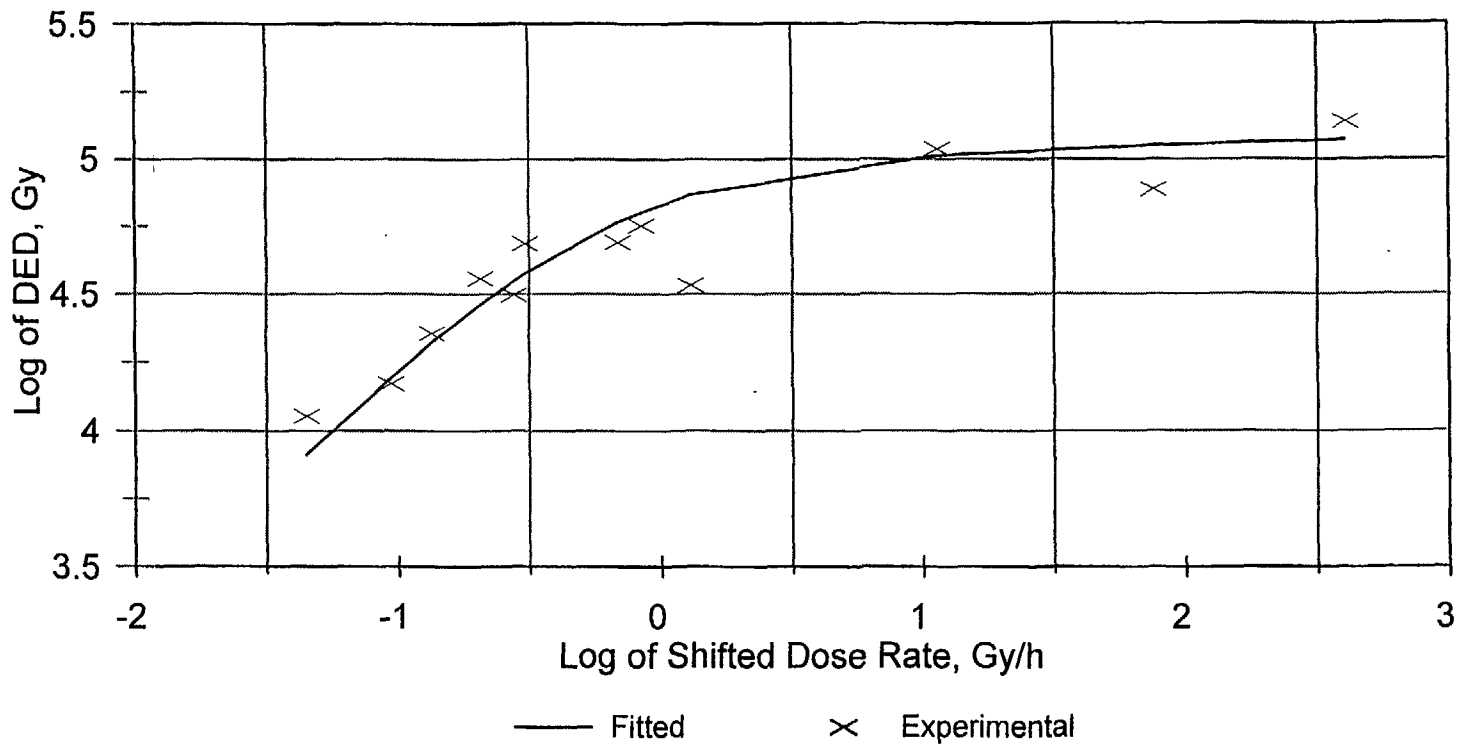


Figure A.3.10a Predicted DED vs D Curve - Rockbestos Silicone Rubber C-7 (50% Relative EAB)

Rockbestos Silicone Rubber C-7,
100% EAB

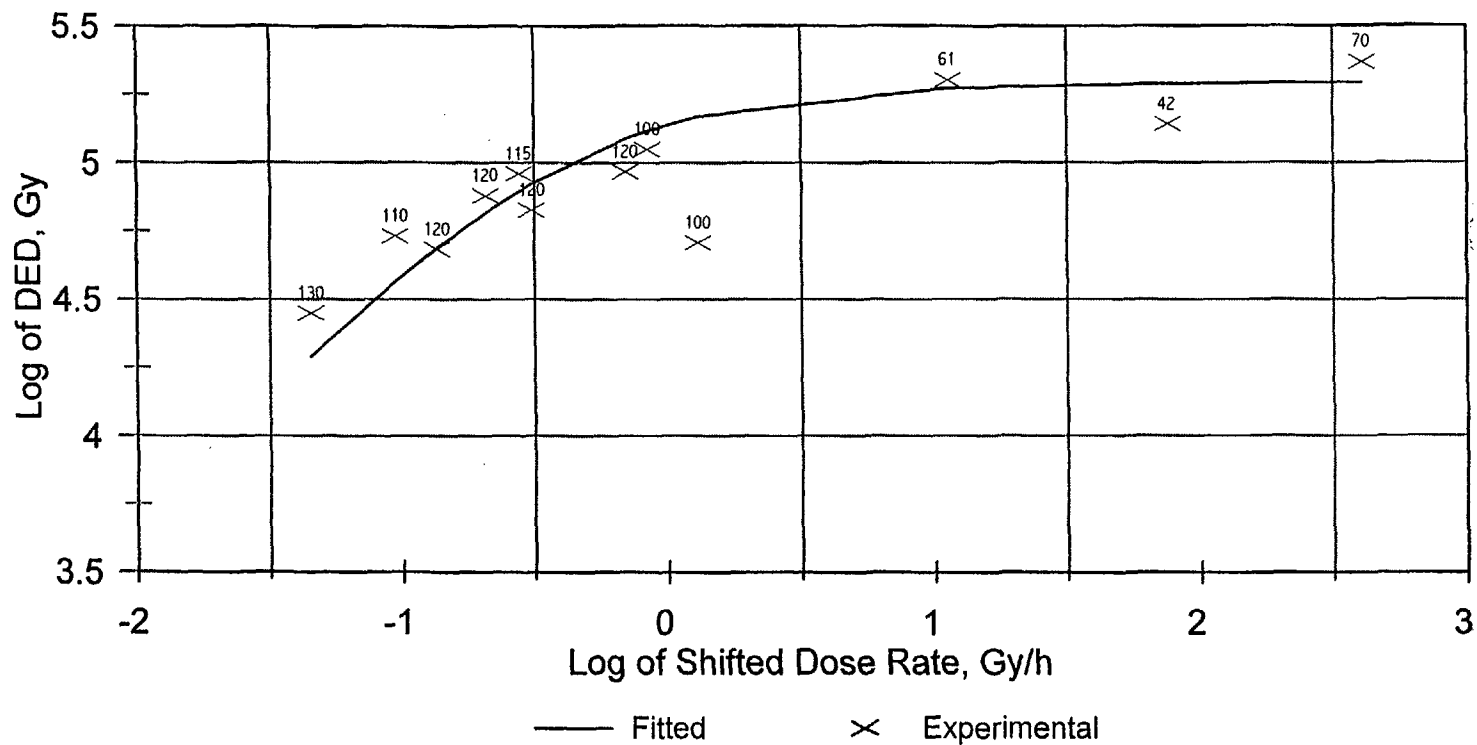


Figure A.3.10b Predicted DED vs D Curve - Rockbestos Silicone Rubber C-7 (100% EAB)

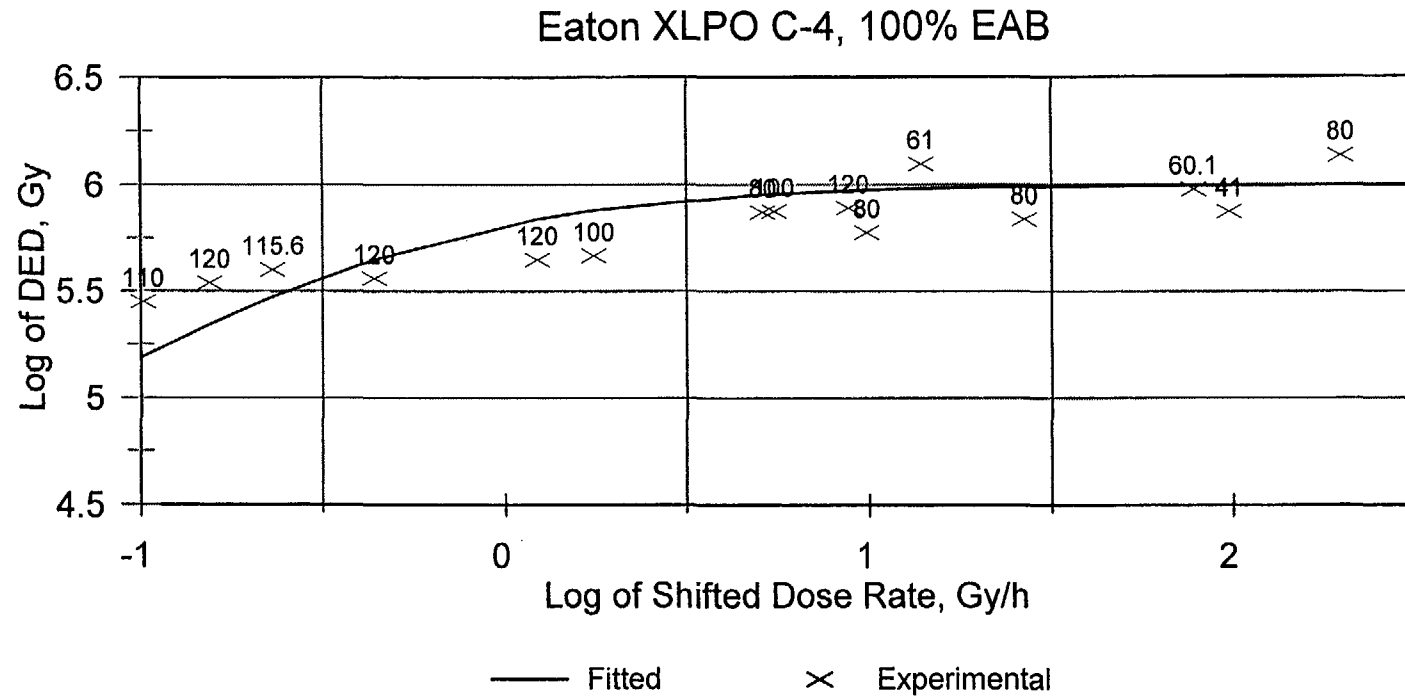


Figure A.3.11 Predicted DED vs D Curve - Eaton XLPO C-4 (100% EAB)

Okonite Neoprene C-17 Air, 100% EAB

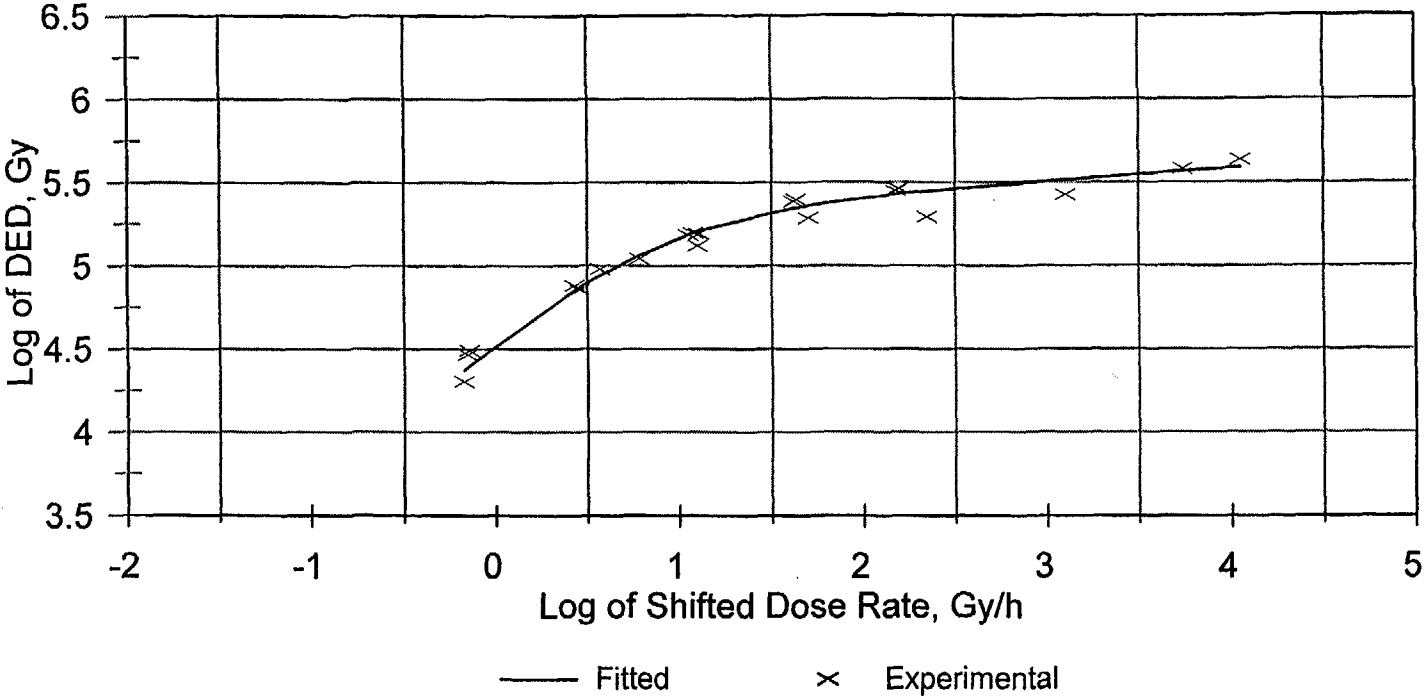


Figure A.3.12 Predicted DED vs D Curve - Okonite Neoprene C-17 Air (100% EAB)

Kerite Proprietary Insulation C-6,
100% EAB

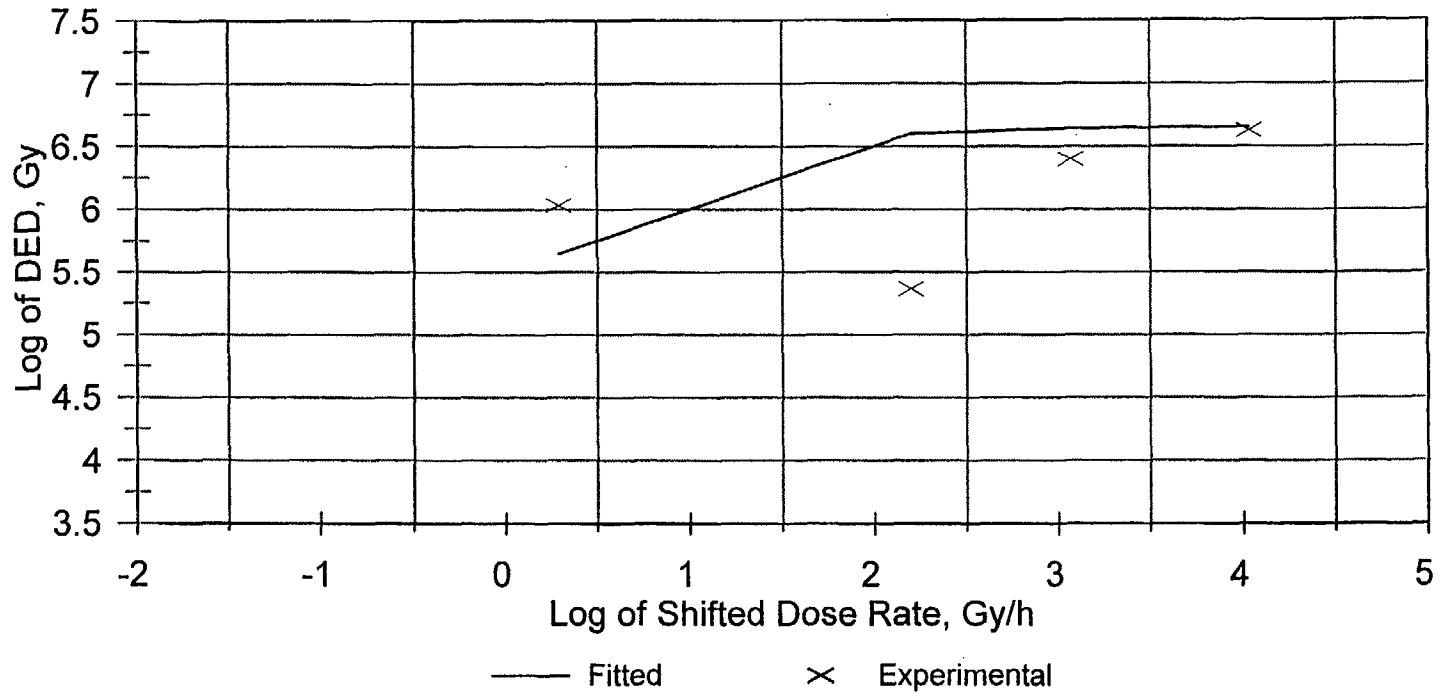


Figure A.3.13 Predicted DED vs D Curve - Kerite Proprietary Insulation C-6 (100% EAB)

A.4 REFERENCES

- A1. Gillen, K.T, and Clough, R.L., "Predictive Aging Results for Cable Materials in Nuclear Power Plants," Sandia National Laboratories, SAND90-2009, November 1990.
- A2. Gillen, K.T., Celina, M., Clough, R.L., and Bernstein, R., "Review of Several Improved Modeling Approaches for Predicting the Lifetimes of Cable Materials," Proceedings of the International Conference on Wire System Aging," U.S. Nuclear Regulatory Commission, Office of Nuclear Regulatory Research, NUREG/CP-0179, November 2002.
- A3. Lofaro, R., Grove, E., Villaran, M., Soo, P., and Hsu, F., "Assessment of Environmental Qualification Practices and Condition Monitoring Techniques for Low-Voltage Electric Cable, Condition Monitoring Test Results," NUREG/CR-6704, Volumes. 1 and 2, February 2001.
- A4. Gillen, K.T., and Clough, R. L., "Aging Predictions in Nuclear Power Plants- Crosslinked Polyolefin and EPR Cable Insulation Materials," Sandia National Laboratories, SAND91-0822, June 1991.

BIBLIOGRAPHIC DATA SHEET

(See instructions on the reverse)

NUREG/CR-6869
BNL-NUREG-73676-2005

2. TITLE AND SUBTITLE

A Reliability Physics Model for Aging of Cable Insulation Materials

3. DATE REPORT PUBLISHED

MONTH | YEAR

March | 2005

4. FIN OR GRANT NUMBER

JCN Y-6371

5. AUTHOR(S)

A. J. Buslik*, T.-L. Chu, M. Subudhi, and J. Lehner

6. TYPE OF REPORT

Technical

*U.S. Nuclear Regulatory Commission

7. PERIOD COVERED (Inclusive Dates)

March 1, 2002 –

March 31, 2005

8. PERFORMING ORGANIZATION - NAME AND ADDRESS (if NRC, provide Division, Office or Region, U.S. Nuclear Regulatory Commission, and mailing address; if contractor, provide name and mailing address.)

Energy Sciences and Technology Department
Brookhaven National Laboratory
Upton, NY 11973-5000

9. SPONSORING ORGANIZATION - NAME AND ADDRESS (if NRC, type "Same as above"; if contractor, provide NRC Division, Office or Region, U.S. Nuclear Regulatory Commission, and mailing address.)

Division of Risk Analysis and Applications
Office of Nuclear Regulatory Research
U.S. Nuclear Regulatory Commission
Washington, DC 20555-0001

10. SUPPLEMENTARY NOTES

A. J. Buslik, NRC Project Manager

11. ABSTRACT (200 words or less)

This report presents a method for predicting the probability that the insulation of an aged instrumentation or control cable inside of containment will reach a critical level of embrittlement. The critical level of embrittlement can be used to support an assessment of the probability that the cable will fail to perform its function if exposed to a loss of coolant accident (LOCA). However, there are instances where cables with severely embrittled insulation have performed their function, in tests. The method predicts the probability distribution for the time it takes for the insulation of a cable subjected to a constant dose rate and temperature to reach a critical level of embrittlement. The embrittlement level is measured by the elongation at break (EAB), a condition of the cable, the greater the EAB the less the embrittlement. In order to incorporate the results in a probabilistic risk assessment, it would be necessary to estimate the probability that a cable which has reached a critical level of embrittlement would fail to perform its intended function in a LOCA.

12 KEY WORDS/DESCRIPTORS (List words or phrases that will assist researchers in locating the report.)

Cable insulation, aging, reliability physics, elongation at break, Arrhenius equation, activation energy, time-temperature superposition, time-temperature-dose-rate superposition, uncertainty, loss of coolant accident (LOCA), probabilistic risk assessment (PRA)

13. AVAILABILITY STATEMENT

unlimited

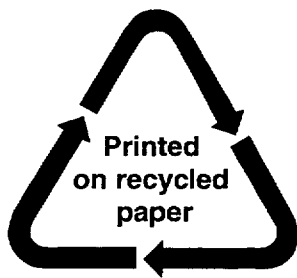
14. SECURITY CLASSIFICATION

(This Page)

unclassified

15. NUMBER OF PAGES

16. PRICE



Federal Recycling Program

UNITED STATES
NUCLEAR REGULATORY COMMISSION
WASHINGTON, DC 20555-0001

OFFICIAL BUSINESS